Designed to fit

The use of 3D anthropometric data of children's heads and faces in mask design

Goto, L.

DOI
10.4233/uuid:31ea7d92-e9d9-4029-8637-e36fa0ff2d6c

Publication date
2023

Document Version
Final published version

Citation (APA)
Goto, L. (2023). *Designed to fit: The use of 3D anthropometric data of children's heads and faces in mask design*. [Dissertation (TU Delft), Delft University of Technology]. https://doi.org/10.4233/uuid:31ea7d92-e9d9-4029-8637-e36fa0ff2d6c

DESIGNED TO FIT

The use of 3D anthropometric data
of children's heads and faces in mask design

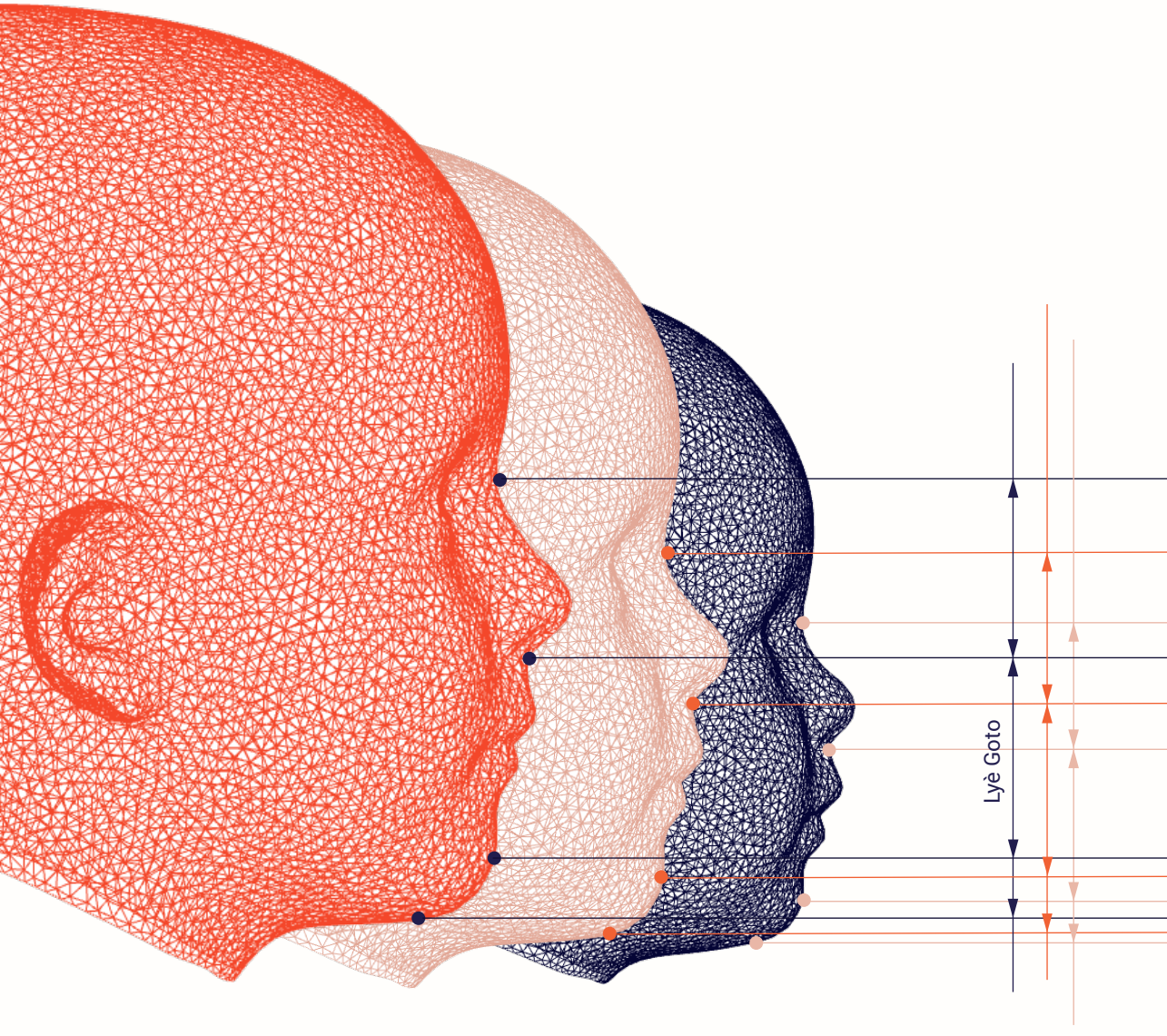

DESIGNED TO FIT

The use of 3D anthropometric data of children's heads and faces in mask design

Dissertation
for the purpose of obtaining the degree of doctor
at Delft University of Technology
by the authority of the Rector Magnificus, Prof.dr.ir. T.H.J.J. van der Hagen,
chair of the Board for Doctorates
to be defended publicly on
Wednesday 22 November 2023 at 12:30 o'clock

By

Lyè GOTO
Master of Science in Industrial Design Engineering, Delft University of Technology,
The Netherlands
born in The Hague, The Netherlands

This dissertation has been approved by the promotors.

Composition of the doctoral committee:

Rector Magnificus	Chairperson
Prof.dr.ir. R.H.M. Goossens	Delft University of Technology, promotor
Dr. ir. J.F.M. Molenbroek	Delft University of Technology, copromotor

Independent members:

Prof.dr. H. You	Pohang University, South Korea
Dr. R.A. Bem	Emma Children's Hospital, Academic Medical Centers, Amsterdam, The Netherlands
Prof.dr. P.J. Clarkson	Delft University of Technology
Prof.dr. T.J.M. van der Cammen	Delft University of Technology

Other members:

Dr. T. Huysmans	Delft University of Technology

Reserve member:

Prof.ir. D.J. van Eijk	Delft University of Technology

Dr. T. Huysmans and Dr. Wonsup Lee have contributed greatly to the research presented in this dissertation.

This research was funded by the Prinses Beatrix Spierfonds.

Keywords: 3D anthropometry, Dutch children, head and face, representative face model, parametric design, virtual fit testing, mask design

Cover and Layout Design: Alexander van der Kleij & Lyè Goto
Editing: Alexander van der Kleij
Printed by: IPSKAMP printing

ISBN 978-94-6384-507-6

TABLE OF CONTENTS

LIST OF ABBREVIATIONS

Acronym	Description
1D	One-dimensional
2D	Two-dimensional
3D	Three-dimensional
AL	Alare
CAD	Computer-Aided Design
CAESAR	Civilian American and European Surface Anthropometry
CBS	Centraal Bureau voor de Statistiek (Statistics Netherlands)
CH	Chelion
CV	Coefficient of variation
EN	Endocanthion
EU	Eurion
EX	Exocanthion
G	Glabella
GA	Genetic algorithm
GO	Gonion
ICU	Intensive Care Unit
ISO	International Organization for Standardization
M	Mean
MAD	Mean absolute distance
ME	Mention
MF	Maxillofrontal
MRI	Magnetic Resonance Imaging
N	Number of Participants
NIV	Non-Invasive Ventilation
PC	Principal Component
PCA	Principal Component Analysis
PG	Pogonion
PICU	Paediatric Intensive Care Unit
PRO	Pronasale
RM	Representative Model
RFM	Representative Face Model
RHM	Representative Head Model
ROI	Region of Interest
RQ	Research question
S	Sellion
SD	Standard Deviation
SL	Subnasale
SN	Sublabiale
WHO	World Health Organization
ZY	Zygion

SUMMARY

INTRODUCTION

When designing products like bicycle helmets or oxygen masks, achieving a good fit is crucial for optimal functioning, usability, safety, and comfort. Integrating anthropometric data in the development and design of products, workplaces, and environments whilst understanding the variations in anthropometric measurements amongst users will improve the usability, comfort, efficiency and interaction of products, subsequently enhancing the overall user experience.

Thus, accurate and detailed measurements of the human body shape in general and for a specific target population in particular, are essential for designing products that require a close fit. Therefore, designers should integrate relevant properties of the body, especially anthropometric dimensions in their design process to optimize the fit between the product and the relevant body part. Recent advancements in 3D imaging technologies have made it possible to collect anthropometric data faster, with higher accuracy and reproducibility. This has led to the increasing use of 3D imaging technologies in anthropometric surveys worldwide, providing detailed anthropometric information for the design of products that closely conform to the human body.

Although various anthropometric tools are available, both in 2D and 3D, designers often rely on traditional 1D anthropometric information when designing and sizing products due to familiarity, ease of use, and cost-efficiency of these tools. However, traditional anthropometric information may not provide sufficient details about the human body shape required for developing products with an optimal fit. While there are advantages to using 3D anthropometric data, there are challenges in integrating it into the design process. The complexity and large quantity of data, making it challenging to sort and analyse both quantitatively and qualitatively. Additionally, there is a lack of established procedures on how to effectively use 3D anthropometric data in product sizing, and limited research has been conducted on its application in the design process and the needs of designers themselves.

AIM OF THIS THESIS

The aim of this thesis is to provide knowledge and insights on how to analyse, interpret, and integrate 3D anthropometric data for design purposes, particularly for products that require a close fit. The goal is to support designers by offering insights into the collection and use of 3D anthropometric data, providing an overview of how it can be integrated into product sizing. The thesis involves developing an approach to extract relevant

information from 3D anthropometric data for design applications and developing a method for designers to visualize and utilize these complex data sets.

In order to develop the proposed approach, a case study was conducted focusing on the importance of fit of ventilation masks in non-invasive ventilation (NIV) for children. NIV is commonly used to provide respiratory support to children in both home and acute care settings. The effectiveness of NIV therapy depends heavily on the proper fit of mask interfaces. However, commercially available masks have limited shapes and sizes, making it challenging to accommodate the diverse facial features of young children and those with cranial facial anomalies. An improper fit can cause patient discomfort, skin damage, air leakage, and even facial deformation, leading to treatment failure. Therefore, detailed anthropometric data on the heads and faces of children is necessary to develop appropriately sized ventilation masks.

The case study forms the practical basis for the theoretical part of this thesis, which is divided into three levels: the anthropometric level, the design level, and the product level. Each level addresses different research questions (RQs) related to the integration and application of 3D anthropometric data in product design and sizing.

At the anthropometric level, the thesis focuses on collecting, processing, analysing, and presenting 3D anthropometric data of children's heads and faces for design purposes.

RQ 1: How to collect, process, analyse and present 3D anthropometric data of children’s heads and faces for design purposes?

On the design level, the thesis explores the relevant information from 3D anthropometric data that is useful for designing products with critical fit. It investigates approaches for integrating 3D anthropometric data in the development of sizing systems for head-related products.

RQ 2: What are approaches/methods to integrate the use of 3D anthropometric data of the head and face in developing sizing systems of head related products?

At the product level, the thesis applies the 3D anthropometric dataset of children's heads and faces to the design and sizing of a ventilation mask. It generates a computational design model of the mask based on representative models developed from the children's dataset. A virtual fit test method is developed to evaluate the fit of the masks, and the effect of increasing the number of representative models and mask designs on the fit results is investigated.

RQ 3: How can 3D anthropometric data be implemented in product design and sizing?

OVERVIEW OF THE CHAPTERS

With the research objective established and the current lack of detailed 3D anthropometric data for children's heads and faces, the first step is to gather 3D data from the target group. This is the focus of **Chapter 2** whereby the objective was to collect data to create a high-quality dataset that will serve as a foundation for the research conducted in the subsequent chapters. Chapter 2 outlines the acquisition, processing, and analysis of both traditional measurements and 3D scan data. Descriptive statistics of measurements of children's heads and faces in the Dutch population were presented. The study demonstrated that 3D photogrammetry is an effective technology for capturing quick and accurate 3D scans of infants and young children. Additionally, the data processing steps involved in extracting relevant 1D measurements from the 3D data were discussed, which included data cleaning, alignment, and virtual landmarking. Subsequently, the traditional measurements were compared to the most recent dataset of Dutch children, and a more detailed comparison was made with a dataset of North American children. This comparative analysis served to validate and cross-reference the results obtained in this study.

In chapter 2, the focus was primarily on 1D measurements, while **Chapter 3** shifted towards analysing the 3D shape variation of Dutch children's faces using the same set of 3D scans. Both dimension-based principal component analysis (PCA) and shape-based PCA were conducted and visually represented to explore the variation in face shape among Dutch children across different age groups. The objective of this study was to map the size and shape variation of Dutch children's heads and faces and examine its potential implications for designing a ventilation mask. First a dimension based PCA was conducted for which 9 mask relevant dimensions served as input. Results showed that first principal component explains the variation for overall size. Furthermore, the length related measurements have the strongest influence on PC1 and contribute the most to the overall variation in facial features captured by PC1. The second principal component revealed variations related to facial width. A second principal component analysis was conducted on the point coordinates. This shape based PCA offers an even more detailed way of investigating face shapes. By conducting a PCA on the 3D location of the vertices of each 3D face area, the face shape variation of the dataset could be revealed in a more visual way. The dimension-based principal component analysis (PCA) provides insights into how specific dimensions of a product influence the variation in face shape and to what extent. This helps designers understand the relationship between product dimensions and the variability of children's face shapes in

the dataset. On the other hand, the shape-based PCA allows designers to visually understand the variation in face shapes and provides face-scape modes that can assist in designing face-related products in a Computer-Aided Design (CAD) environment. Both analysis methods are useful and complementary for designers of head and face-related products, as they help organize and present complex 3D data.

Chapter 4 provides an overview of the current state of defining sizing systems for product development based on 3D data, specifically focusing on head and face data and the design of related products. It explores various approaches and considerations involved in developing a sizing system using 3D anthropometric data. The review highlights the need for tailored methods for developing sizing systems that incorporate shape information. Shape models are generated to represent different sizing categories, taking into account the unique requirements of diverse products for different body regions. The flexibility of 3D data allows for the adoption of these varied approaches. Shape-oriented sizing, relying on shape rather than key dimensions, requires statistical knowledge, computer proficiency, and data science expertise.

In the previous chapter, it was discussed how sizing systems often rely on traditional anthropometric data and typically consider the variation of one or two key body dimensions that directly relate to the product. However, for products requiring a close fit to specific body parts, it becomes relevant to incorporate multiple key dimensions or shape in the sizing process. In order to integrate 3D body shape into product sizing, representative (design) models (RMs) are commonly used to visualize the variability of the target population. Despite the increased development and use of RMs, there is limited research on how the type of anthropometric data used for RM development affects the representativeness, particularly for children. Within the context of mask sizing, **Chapter 5**, compared representative face models (RFMs) of 3D faces and their mask contours through a bivariate, multivariate, and shape-based analysis of the 3D children's head and face dataset. Initial visual inspection of the results showed relatively similar RFMs for each cluster regardless of the method, but further analysis revealed subtle differences in shape and size. The bivariate method displayed a larger variation in mouth width between clusters. Incorporating more information in the analysis resulted in smaller differences, suggesting that shape-based RFMs are more representative for their respective clusters. Mask contour analysis exhibited similar variation patterns within clusters when more information was incorporated. This implies that designing a mask based on shape-based RFMs has the potential to result in a better-fitting product.

While chapter 5 compared representative face models (RFM) and demonstrated that the shape based RFMs represent the dataset best, **Chapter 6** examines how to generate a

design based on these representative models and to subsequently virtually evaluate the fit with the target population. The 3D dataset of children's heads and faces was randomly divided into a training dataset and a testing dataset. A cluster analysis was done to cluster face shapes with similar shapes and dimensions. Representative face models (RFM) were generated based on each cluster. Based on the training dataset a representative face model (RFM) was generated and a parametric design of a ventilation mask was developed through visual programming, making the process more accessible for designers. Subsequently, this design was fit tested virtually with the testing dataset. The number of clusters was increased with n+1 to investigate the effect of the number of RFM's and the fit. Results showed that with the increase of clusters the overall fit improved but with n>3 clusters there were no significant improvements. Visual inspections indicated poor fits around the eyes and mouth within one, two, or three clusters, however, fit issues around in the nose bridge region were found in all clusters potentially due to the higher geometric complexity and thus greater variance.

Finally, **Chapter 7** looks back at the project and describes the responses to the research questions. It provides an overview of main insights generated throughout the research, limitations of this research and provides recommendations for future research in relation to the anthropometric, design and product levels.

SAMENVATTING

INTRODUCTIE

Bij het ontwerpen van producten zoals fietshelmen of zuurstofmaskers is een goede pasvorm cruciaal voor het functioneren, bruikbaarheid, veiligheid en comfort. Het integreren van antropometrische gegevens in het ontwikkelen en het ontwerpen van producten, werkplekken en omgevingen, met oog voor de variaties in antropometrische afmetingen van gebruikers, zal bruikbaarheid, comfort, efficiëntie, de interactie van producten, en daarmee de algehele gebruikerservaring verbeteren.

Nauwkeurige en gedetailleerde afmetingen van lichaamsvormen van de mens in het algemeen en voor een specifieke doelgroep in het bijzonder, zijn daarom essentieel voor het ontwerpen van producten die een nauwsluitende pasvorm vereisen. Om de juiste pasvorm tussen het product en het specifieke lichaamsdeel te verkrijgen moeten ontwerpers relevante antropometrische afmetingen integreren in hun ontwerpproces. Recente ontwikkelingen in 3D-beeldvormingstechnologieën hebben het mogelijk gemaakt om antropometrische gegevens sneller, met een hogere nauwkeurigheid en reproduceerbaarheid te verzamelen. Dit heeft geleid tot een toenemend gebruik van 3D-beeldvormingstechnologieën in antropometrische enquêtes wereldwijd, waardoor gedetailleerde antropometrische informatie beschikbaar is voor het ontwerpen van producten die nauw moeten aansluiten op het menselijk lichaam.

Hoewel verschillende antropometrische hulpmiddelen beschikbaar zijn, zowel in 2D als 3D, vertrouwen ontwerpers toch vaak op traditionele 1D-antropometrische informatie bij het ontwerpen en dimensioneren van producten. Dit is vaak een gevolg van het gebruiksgemak, de kostenefficiëntie en hun bekendheid met deze hulpmiddelen. Traditionele antropometrische informatie biedt echter mogelijk niet voldoende details over de lichaamsvorm die vaak nodig zijn voor het ontwikkelen van producten met nauwsluitende pasvorm vereisen. Hoewel er voordelen zijn aan het gebruik van 3D-antropometrische gegevens, zijn er uitdagingen bij het integreren ervan in het ontwerpproces. De complexiteit en grote hoeveelheid gegevens maken het moeilijk om zowel kwantitatief als kwalitatief te sorteren en te analyseren. Bovendien ontbreken er standaard procedures voor het effectief gebruik van 3D-antropometrische gegevens bij het ontwikkelen van maatsystemen en het dimensioneren van producten. Bovendien is er nog beperkt onderzoek gedaan naar de toepassing ervan in het ontwerpproces en de behoeften van ontwerpers zelf.

HET DOEL VAN DIT PROEFSCHRIFT

Het doel van dit proefschrift is kennis en inzicht te verschaffen over hoe 3D-antropometrische gegevens kunnen worden geanalyseerd, geïnterpreteerd en geïntegreerd voor ontwerpdoeleinden, met name voor producten die een nauwsluitende pasvorm te vereisen. Het is bedoeld om ontwerpers te ondersteunen door inzicht te bieden in het verzamelen en gebruiken van 3D-antropometrische gegevens, en een overzicht te geven van hoe het kan worden geïntegreerd in productdimensionering. Het proefschrift omvat het ontwikkelen van een aanpak om relevante informatie te extraheren uit 3D-antropometrische gegevens voor ontwerptoepassingen en het ontwikkelen van een methode voor ontwerpers om deze complexe datasets te visualiseren en te benutten.

De voorgestelde aanpak werd ontwikkeld middels een casestudy die zich richtte op het belang van de juiste pasvorm van beademingsmaskers bij niet-invasieve ventilatie (NIV) voor kinderen. NIV wordt vaak gebruikt om ademhalingsondersteuning te bieden aan kinderen in zowel thuis- als acute zorg. De effectiviteit van NIV-therapie is sterk afhankelijk van de juiste pasvorm van het beademingsmasker. Commercieel verkrijgbare maskers zijn vaak niet toereikend om jonge kinderen met verschillende gezichtskenmerken en degenen met craniofaciale afwijkingen te voorzien van een goed passend masker vanwege beperkte beschikbaarheid in vormen en maten. Een onjuiste pasvorm kan ongemak, huidbeschadiging, luchtlekkage en zelfs gezichtsvervorming veroorzaken, wat kan leiden tot behandelfalen. Om goed passende beademingsmaskers te ontwikkelen zijn daarom gedetailleerde antropometrische gegevens van de hoofden en gezichten van kinderen noodzakelijk.

De casestudy vormt de praktische basis voor het theoretische deel van dit proefschrift die is onderverdeeld in drie niveaus: het antropometrische niveau, het ontwerpniveau en het productniveau. Elk niveau behandelt verschillende onderzoeksvragen (RQ's) met betrekking tot de integratie en toepassing van 3D-antropometrische gegevens in productontwerp en dimensionering.

Op het antropometrische niveau richt het proefschrift zich op het verzamelen, verwerken, analyseren en presenteren van 3D-antropometrische gegevens van hoofden en gezichten van kinderen voor ontwerpdoeleinden.

RQ 1: Hoe kunnen 3D-antropometrische gegevens van hoofden en gezichten van kinderen worden verzameld, verwerkt, geanalyseerd en gepresenteerd voor ontwerpdoeleinden?

Op het ontwerpniveau onderzoekt het proefschrift de relevante informatie uit 3D-antropometrische gegevens die nuttig zijn voor het ontwerpen van producten met een nauwsluitende pasvorm. Het onderzoekt verschillende methoden voor het integreren van 3D-antropometrische gegevens in de ontwikkeling van maatsystemen voor producten die betrekking hebben op het hoofd.

RQ 2: Wat zijn methoden om het gebruik van 3D-antropometrische gegevens van het hoofd en gezicht te integreren in het ontwikkelen van maatsystemen voor producten gerelateerd aan het hoofd?

Op het productniveau past het proefschrift de 3D-antropometrische dataset van kinderen toe op het ontwerp en de dimensionering van een ventilatiemasker. Het genereert een computationeel ontwerpmodel van het masker op basis van representatieve modellen die zijn ontwikkeld vanuit de dataset van kinderen. Een virtuele pasvormtestmethode werd ontwikkeld om de pasvorm van de maskers te evalueren. Ook werd het effect van een toenemend aantal representatieve modellen en maskerontwerpen op de pasvormresultaten onderzocht.

RQ 3: Hoe kunnen 3D-antropometrische gegevens worden geïmplementeerd in productontwerp en dimensionering?

OVERZICHT VAN DE HOOFDSTUKKEN

Met het vastgestelde onderzoeksdoel en het huidige gebrek aan gedetailleerde 3D-antropometrische gegevens van hoofden en gezichten van kinderen, is de eerste stap om 3D-gegevens te verzamelen van de doelgroep. Dit is het focuspunt van **Hoofdstuk 2**, waarbij het doel was om gegevens te verzamelen om een hoogwaardige dataset te creëren die dient als basis voor het onderzoek dat wordt uitgevoerd in de daaropvolgende hoofdstukken. Hoofdstuk 2 beschrijft de verwerving, verwerking en analyse van zowel traditionele metingen als 3D-scan-gegevens. Er werden beschrijvende statistieken gepresenteerd van metingen van hoofden en gezichten van kinderen uit de Nederlandse bevolking. De studie toonde aan dat 3D-fotogrammetrie een effectieve technologie is voor het snel vastleggen nauwkeurige 3D-scans van baby's en jonge kinderen. Daarnaast werden de stappen in gegevensverwerking besproken om relevante 1D-metingen uit de 3D-gegevens te extraheren, inclusief gegevensreiniging, uitlijning en virtuele herkenningspunten. Vervolgens werden de traditionele metingen vergeleken met de meest recente dataset van Nederlandse kinderen, en werd een meer gedetailleerde vergelijking gemaakt met een dataset van Noord-Amerikaanse kinderen. Deze

vergelijkende analyse diende om de resultaten die in deze studie zijn verkregen te valideren en te kruisverwijzen.

In hoofdstuk 2 lag de focus voornamelijk op 1D-metingen, terwijl **Hoofdstuk 3** zich richtte op de analyse van de 3D-vormvariatie van de gezichten van Nederlandse kinderen met behulp van dezelfde reeks 3D-scans. Zowel dimensionele principal component analyse (PCA) als vorm-gebaseerde PCA werden uitgevoerd en visueel weergegeven om de variatie in gezichtsvormen te onderzoeken bij Nederlandse kinderen in verschillende leeftijdsgroepen. Het doel van deze studie was om de grootte- en vormvariatie van de hoofden en gezichten van Nederlandse kinderen in kaart te brengen en de mogelijke implicaties ervan voor het ontwerpen van een ventilatiemasker te onderzoeken. Eerst werd een dimensionele PCA uitgevoerd waarbij 9 masker-relevante dimensies als input dienden. De resultaten toonden aan dat de eerste hoofdcomponent de variatie in algemene grootte verklaart. Verder hebben metingen gerelateerd aan gezichtslengte de sterkste invloed op PC1 en dragen ze het meeste bij aan de algehele variatie in gelaatstrekken die door PC1 werden vastgelegd. De tweede hoofdcomponent onthulde variaties met betrekking tot de breedte van het gezicht. Er werd ook een tweede PCA uitgevoerd op de puntcoördinaten. Deze vormgebaseerde PCA biedt een nog gedetailleerdere manier om gezichtsvormen te onderzoeken. Door een PCA uit te voeren op de 3D-locatie van de vertexen van elk 3D-gezicht, kon de gezichtsvormvariatie van de dataset op een meer visuele manier worden onthuld. De dimensionele PCA biedt inzicht in hoe specifieke dimensies van een product de variatie in gezichtsvorm beïnvloeden en in welke mate. Dit helpt ontwerpers begrijpen hoe de productafmetingen samenhangen met de variabiliteit van gezichtsvormen bij kinderen in de dataset. Aan de andere kant stelt de vormgebaseerde PCA ontwerpers in staat om visueel inzicht te krijgen in de variatie in gezichtsvormen en biedt het modi voor gezichtsvormen die kunnen helpen bij het ontwerpen van producten die verband houden met het gezicht in een Computer-Aided Design (CAD) -omgeving. Beide analysemethoden zijn nuttig en complementair voor ontwerpers van producten gerelateerd aan hoofd en gezicht, omdat ze helpen complexe 3D-gegevens te structureren en te presenteren.

Hoofdstuk 4 geeft een overzicht van de huidige stand van zaken van het definiëren van maatsystemen op basis van 3D-gegevens van met name hoofd- en gezichtsgegevens en het ontwerp van gerelateerde producten. Het verkent verschillende methodes en overwegingen die toegepast worden bij het ontwikkelen van een maatsysteem met behulp van 3D-antropometrische gegevens. De review benadrukt de noodzaak van specifieke methoden voor het ontwikkelen van maatsystemen die vorminformatie bevatten. Rekening houdend met de unieke eisen van verschillende producten voor diverse lichaamsdelen, worden vaak representatieve vormmodellen gegenereerd om

verschillende maatcategorieën te vertegenwoordigen. De flexibiliteit van 3D-gegevens maakt deze gevarieerde benaderingen mogelijk. Vormgebaseerd dimensioneren, dat steunt op vorm in plaats van 1D afmetingen, vereist statistische kennis, computervaardigheid en expertise in gegevenswetenschap.

In het vorige hoofdstuk werd besproken hoe maatsystemen vaak gebaseerd zijn op traditionele antropometrische gegevens en meestal de variatie van één of twee belangrijke lichaamsafmetingen in acht nemen, die direct verband houden met het product. Voor producten die een nauwsluitende pasvorm vereisen voor specifieke lichaamsdelen wordt het echter relevant om meerdere belangrijke afmetingen of vormen in het dimensioneringsproces op te nemen. Om 3D-lichaamsvormen te integreren in het dimensioneren van producten, worden vaak representatieve (ontwerp)modellen (RMs) gebruikt om de variabiliteit van de doelgroep te visualiseren. Ondanks de toegenomen ontwikkeling en het gebruik van RMs is er beperkt onderzoek naar hoe het type antropometrische gegevens dat wordt gebruikt voor de ontwikkeling van RMs, de representativiteit beïnvloedt, met name voor kinderen. In de context van maskerafmetingen vergeleek **Hoofdstuk 5** representatieve gezichtsmodellen (RFM's) van 3D-gezichten en hun maskercontouren door middel van een bivariate, multivariate en vormgebaseerde analyse van de 3D-dataset van kinderhoofden en -gezichten. Een initiële visuele inspectie van de resultaten toonde relatief vergelijkbare RFM's voor elke cluster, ongeacht de methode, maar verder onderzoek onthulde subtiele verschillen in vorm en grootte. De bivariate methode toonde een grotere variatie in mondbreedte tussen clusters. Het opnemen van meer informatie in de analyse resulteerde in kleinere verschillen, wat suggereert dat op vorm gebaseerde RFM's representatiever zijn voor hun respectievelijke clusters. De analyse van maskercontouren vertoonde vergelijkbare variatiepatronen binnen clusters wanneer meer informatie werd opgenomen. Dit impliceert dat het ontwerpen van een masker op basis van vormgebaseerde RFM's het potentieel heeft om te resulteren in een beter passend product.

Terwijl hoofdstuk 5 representatieve gezichtsmodellen (RFM) vergeleek en aantoonde dat de op vorm gebaseerde RFM's de dataset het beste vertegenwoordigen, wordt in **Hoofdstuk 6** onderzocht hoe een ontwerp wordt gegenereerd op basis van deze representatieve modellen en vervolgens virtueel wordt geëvalueerd op pasvorm bij de doelgroep. De 3D-dataset van kinderhoofden en -gezichten werd willekeurig verdeeld in een trainingsdataset en een testdataset. Er werd een clusteranalyse uitgevoerd om gezichtsvormen met vergelijkbare vormen en afmetingen te clusteren. Op basis van elk cluster werden representatieve gezichtsmodellen (RFM's) gegenereerd. Op basis van de trainingsdataset werd een representatief gezichtsmodel (RFM) gegenereerd en via visuele programmering werd een parametrisch ontwerp van een ventilatiemasker

ontwikkeld, waardoor het proces toegankelijker werd voor ontwerpers. Vervolgens werd dit ontwerp virtueel getest op pasvorm met de testdataset. Het aantal clusters werd verhoogd met n+1 om het effect van het aantal RFM's en de pasvorm te onderzoeken. De resultaten toonden aan dat met de toename van clusters de algehele pasvorm verbeterde, maar met n>3 clusters waren er geen significante verbeteringen. Visuele inspecties toonden slechte pasvormen rond de ogen en mond binnen één, twee of drie clusters, maar pasvormproblemen rond het neusbruggebied werden gevonden in alle clusters, mogelijk als gevolg van de hogere geometrische complexiteit en dus grotere variabiliteit.

Ten slotte kijkt **Hoofdstuk 7** terug op het project en beschrijft de antwoorden op de onderzoeksvragen. Het geeft een overzicht van de belangrijkste inzichten die zijn gegenereerd tijdens het onderzoek, beperkingen van dit onderzoek en aanbevelingen voor toekomstig onderzoek met betrekking tot de antropometrische, ontwerp- en productniveaus.

1

GENERAL INTRODUCTION

This chapter provides an overview of the research topic, the research focus, the connected research questions, as well as the outline of the thesis.

Chapter has been partly adapted from:

Goto, L., Molenbroek, J.F.M., Goossens, R.H.M., 2013. 3D Anthropometric data set of the head and face of children aged 0.5-7 years for design applications. In N D'Apuzzo (Ed.), Proceedings of the 4th international conference on 3D body scanning technologies Ascona, Switzerland: Hometrica Consulting. 157–165.

1.1 INTRODUCTION

For many products, such as a bicycle helmet or oxygen masks, a good fit is essential to achieve optimal functioning, usability, safety and comfort. If the helmet does not fit properly, this could have severe consequences for the safety of the cyclist wearing the helmet, because the helmet could shift or even fall off when the cyclist has an accident. For example, Rivara et al. (1999) reported that a poor fit of a child's bicycle helmet considerably reduces their protective effect and doubles the risk of head or brain injuries. In addition, when a helmet does have a good fit, it results in increased comfort and lesser complaints when wearing the helmet for a longer period of time. More importantly, this will result in an increased tendency for people to use their helmet more often leading to a decrease in severe trauma or fatalities (Piotrowski et al., 2020; van den Brand et al., 2020).

There are numerous other examples that illustrate the importance of a good fit. A proper fit is especially important in protective gear such as the above-mentioned helmet, as well as medical products as the fit of these products could have a direct impact on the wearer's health and safety (Barker et al., 2018; Hsiao, 2013; W. Lee, Yang, et al., 2018; Ma et al., 2018). For instance, an ill-fitting respirator for firefighters could lead to life threatening situations when hazardous gasses penetrate the mask due to leakage along the sides of the mask (Butler, 2007). Another example is a ventilation mask that is used to support a patient with respiratory failure at the intensive care unit (ICU), whereby the lack of sealing due to an improper fit of the mask can result into too much air leakage which reduces the mask's effectiveness (Hovenier et al., 2022).

Precise measurements of the shape of the human body are therefore essential when it comes to the design of products that need a close fit. Therefore, designers should integrate relevant properties of the body, especially anthropometric dimensions in their design process to optimize the fit between the product and the relevant body part. In order for a designer to achieve these objectives, to develop these products and achieve a good fit, detailed anthropometric information of the correct target population is needed.

1.1.1 ANTHROPOMETRY

The term anthropometry derives from the Greek word (άνθρωπος) anthropos, which means human, and metron (μετρό), meaning to measure. It refers to the science of measuring, comparing and interpreting the variability of different proportions of the human body but also its strength, mobility and flexibility (Martin, 1914; Pheasant & Haslegrave, 2006). More than 200 years ago anthropometry, as part of the field of

anthropology, was used to study the physical differences amongst races and ethnic groups and in medical diagnoses (Roebuck et al., 1975). From thereon it developed into a discipline that is used to assess and predict performance, health and survival of individuals and to investigate the economic and social wellbeing of populations (World Health Organisation, 1995).

The field of anthropometry can be divided into two parts; static and dynamic anthropometry. Static anthropometry is the measurement of the human body in a static, defined posture. Whereas functional, or dynamic anthropometry, deals with the body in motion or under the influence of external forces like gravity. The focus of this research will be on static anthropometry. In traditional anthropometry, measurements are obtained by measuring distances between so-called landmarks (Figure 1 and 2). Landmarks are anatomical predefined points on the human body that serve as anchor points for the measuring equipment and to assure accuracy and consistency of the data (Martin, 1914). Some of these landmarks are defined by the underlying bone structure which makes it necessary to palpate its location. Accuracy herein relies very much on the experience and skill of the examiner (Farkas, 1996; Seth M. Weinberg, MA, 2008). These landmarks are used to determine linear and circumferential dimensions. Linear dimensions describe the shortest distance between two points on the body, whereas circumferential dimensions indicate the distance between two points along the surface of the body or returning to the same point resulting in a perimeter.

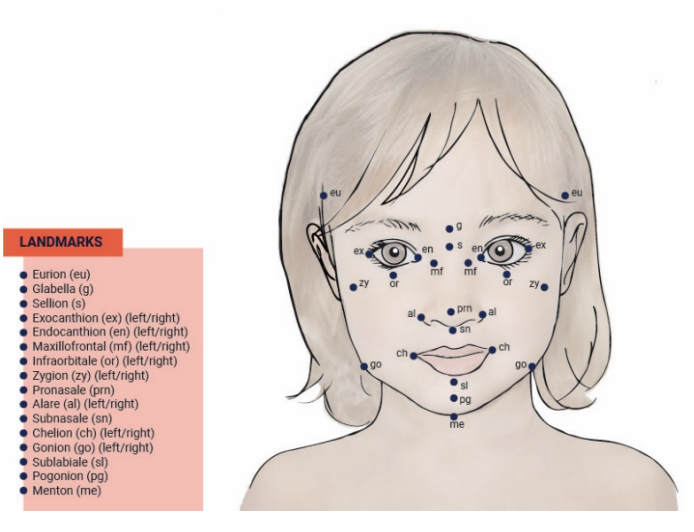

Figure 1 Traditional anthropometric landmarks of the face.

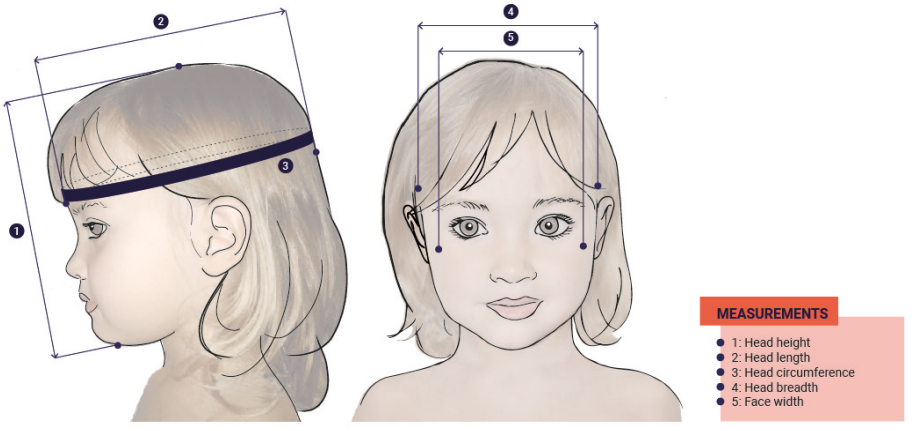

Figure 2 Basic measurements of the head.

There are a great number of measuring devices for performing anthropometric measurements. These devices include: anthropometers (to measure height), callipers (to measure linear distances), tape measures (to measure circumferences) and weight scales (to measure weight). This wide variety of measuring tools involved, in combination with the need to locate a large number of landmarks by hand and for each individual participant, makes the collecting of anthropometric data time consuming and expensive. Traditional anthropometric data is often presented in tables. These consist of numerical values of body dimensions often combined with demographic information of the sample, including some vital statistics such as means, standard deviations and percentiles. This makes the data easy to understand and therefore also easy to compare and analyse. Tables presenting anthropometric data are a common resource used for finding relevant measurements used in product design and ergonomics (Meunier et al., 2009; Veitch et al., 2009). For the designer, the advantages of using tables are that it is readily accessible and a relatively easy and quick way to evaluate product dimensions. However, it does not provide any information about the potential relationship between these different dimensions and, more importantly, it does not provide any information on how the human body is shaped.

1.1.2 ANTHROPOMETRY AND PRODUCT DESIGN

The methods and tools used within anthropometry also find their application in ergonomics and design, whereby the human-product interaction plays a central role. In user centred design it is the designer's task to find the best possible fit between the product and the user given the task to be performed (Figure 3). Here, understanding the anthropometric variability of users plays a key role. By integrating this anthropometric

data in the development and design of products, workplaces and environments, the interaction with the user is optimized in terms of usability, safety, comfort and efficiency (ISO 7250-1, 2010; Molenbroek, 1994; Pheasant & Haslegrave, 2006).

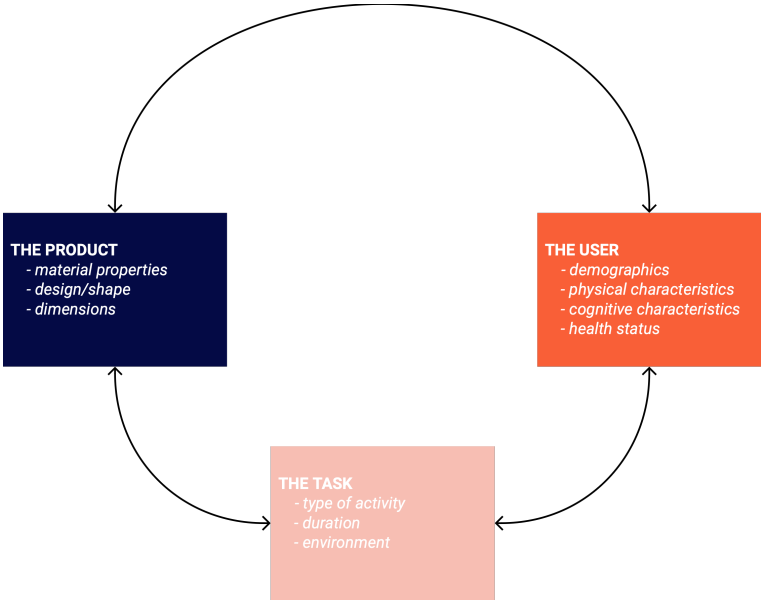

Figure 3 Adaptations of figure 1.1 from Pheasant & Haslegrave (2006, p. 6) and figure 2.1 from Gupta (2014, p. 37) shows that in user centred design, the interrelation between the product, the user and the task play a key role.

When designing (physical) products, designers integrate the use of anthropometric data in their design process to optimize the usability of the product and interaction with the product. In order to design a product, the designer applies an iterative design process in which they are constantly seeking for a balance between product and user requirements as well as the commercial aspect. There are different design approaches by which anthropometric data of a certain target population is considered and applied in the design and sizing of products (Dirken, 1999; Gupta, 2014; Molenbroek J.F.M. & De Bruin, 2006). An overview of possible approaches is presented in figure 4. The starting point of each approach is considering the anthropometric accommodation one wants to achieve for a certain product. The overall aim of user centred design is to try and accommodate as many people within the target group as possible but the choice for a certain strategy also depends on the type of product, the target population, cost-benefit ratio, safety, technical considerations etc. (Gupta, 2014; Hsiao, 2013; A. Luximon et al., 2012).

Figure 4 A selection of different anthropometric design approaches for product design and respective normal distributions (left) (Dirken, 1999; Molenbroek J.F.M. & De Bruin, 2006).

This iterative process and the role of anthropometry can be summarized in the following steps based on the anthropometric design approach as described by Hsiao et al. (2013) and the ergonomic design process as described by Dainoff et al. (2004) and in the Delft Design Guide (van Boeijen et al., 2020)

1. First the problem definition and body dimensions that are essential to the product to be designed are determined.
2. Then the target population needs to be identified.
3. The designer now needs to identify an anthropometric database that contains relevant body dimensions of the target population or, if the data is not available, collect the data themselves.
4. The accommodation percentage is determined.
5. The anthropometric data is analysed.

6. And finally, an anthropometric design approach is selected resulting into product features, product dimensions or a sizing system.

1.1.3 3D ANTHROPOMETRY

Advances in 3D imaging technologies have resulted in new developments in the field of anthropometry (Daanen & Ter Haar, 2013; Hsiao, 2013). With the commercially available 3D scanners it is now possible to collect anthropometric data faster, with a higher degree of accuracy and reproducibility. 3D imaging technologies are increasingly being used in anthropometric surveys around the world (Ball et al., 2010; Ball & Molenbroek, 2008; Robinette et al., 1999, 2002; Zhuang & Bradtmiller, 2005). These datasets provide detailed anthropometric information for the development of products that need to closely fit the human body.

There are many advantages in using 3D imaging in anthropometric studies. In traditional anthropometry the measuring process is often time consuming, such that when an experienced examiner measures 30 dimensions for one subject this will typically take about 15 minutes. When considering that large scale anthropometric surveys can include an average of 100 traditional measurements (Blackwell et al., 2002; Hotzman et al., 2011; Robinette et al., 2002), the participant is asked to keep his/her posture for quite some time. With the use of 3D technology, it is possible to capture a complete 3D image of the whole body in a matter of seconds, making the whole process less invasive and especially suitable for, for example, children, elderly and physically impaired persons.

Anthropometric measurements can then be derived from the 3D data and results in a higher and efficient throughput during a survey. The types of measurements, information on geometry and other variables, which are extracted from the stored 3D image files, are limitless, can be recalled when necessary and do not need to be completely determined beforehand. Another great advantage of 3D anthropometric data is that where traditional anthropometric data offers information about 1D body dimensions like arm length and head circumference, 3D anthropometric data has the potential to also provide information about the shape, volume and geometry of the body.

1.1.4 APPLICATION OF 3D ANTHROPOMETRY IN DESIGN

In spite of the wide variety of available anthropometric tools, designers most commonly use traditional (1D) anthropometric information when designing and sizing products because it is a familiar resource, is easy to use and cost efficient (Hsiao, 2013; Y. Luximon et al., 2016; Meunier et al., 2009; Molenbroek & Bruin, 2005). However, traditional anthropometric information has shown not to provide sufficient information

for most design problems (Veitch & Robinette, 2006). The main drawback is that it does not offer the detailed information of the human body shape that is required to develop a product with an optimal fit, which is specifically the case in wearable products. 3D anthropometric data however, offers great opportunities when it comes to designing products whereby detailed information of human body shape is needed. Also, 3D anthropometric data is convertible to different formats, making it possible to import a 3D scan into CAD (Computer Aided Design) programmes. In this way designers can easily integrate 3D anthropometric information into their design process. Based on the 3D data, statistical shape models that show shape variation can be generated, where instances of the shape model are called representative models, design models or mannequins (Huysmans et al., 2020; Wuhrer et al., 2012; Zhuang, Benson, et al., 2010). By using these representative models (RM's) to simulate product fit or evaluating their product in a virtual environment, designers are able to gain a better insight into proportions and filter out design problems (for example that concern the fit) at any stage in the design process, but especially in early stages without having to resort to physical models or products. In this way designers can increase quality, efficiency and save time.

The rapid developments in the field of 3D scanning and printing technologies have resulted in a paradigm shift in the field of design (Minnoye et al., 2022). 3D printing and 3D scanning are technologies that are closely linked. With the emerging of mass customization or product personalisation, it is now possible to, for example, scan a face and print a fully customized ventilation mask (Wu et al., 2018). Here, only a couple of 3D scans of one person are needed in order to develop a personalised product.

Although there are many advantages in using 3D anthropometric data, there are still a number of drawbacks when integrating it into the design process. As a result of the complexity and large quantity of the data, the required computational steps in the process is high, making it difficult to sort and analyse (Godil, 2007; Y. Luximon et al., 2012; Niu, Li, & Xu, 2009). For raw 3D scans to be of use, they need to be processed, converted, analysed and tailored to its design application. Despite the steadily growing availability of 3D anthropometric data, there is no overview of procedures on how 3D anthropometric data can be used in product sizing to inform designers (Hsiao, 2013; Niu & Li, 2012). Moreover, little research has been done on how 3D anthropometric data is currently applied in the design process nor into the needs of the designers themselves (Ball, 2009; Lacko, Huysmans, et al., 2017; Sims et al., 2012).

1.2 AIM OF THIS THESIS

The aim of this thesis is therefore to provide knowledge on how to analyse, interpret and integrate 3D anthropometric data for design purposes and specifically, for products for which a close fit is an important requirement. The goal is to provide insight into the process of the collecting and use of 3D anthropometric data. And ultimately supporting designers who consider its use by providing an overview of how 3D anthropometric information can be integrated in the sizing of a product in general and especially in which fit is important. This involves developing an approach to extract relevant information from 3D anthropometric data for design applications and developing a method for designers to visualize and utilize these complex data sets. In order to develop such an approach, the decision was made to do so according to a case study in which fit was of paramount importance so as to evaluate the developed approach and provide further practical feedback.

1.2.1 RESEARCH CONTEXT: VENTILATION MASKS FOR CHILDREN

Over the last decades, non-invasive ventilation (NIV) has been increasingly utilized to provide children with respiratory support, both in a home setting as well as in acute settings at paediatric intensive care units (PICU) (Castro-Codesal et al., 2019; Hovenier et al., 2022; Mortamet et al., 2017; Nørregaard, 2002). NIV is a way to provide breathing support through a mask interface as opposed to the alternative called invasive mechanical ventilation where a tube is inserted into the airway. NIV is a good alternative to invasive ventilation, because it minimizes infections, there is a reduced need for sedation and patients can therefore, depending on their condition, still talk, eat or drink while being treated by NIV.

In home ventilation, the nasal mask (covering only the nose) is the most commonly used interface, however, nasal ventilation can be ineffective in some children, for instance when they sleep with their mouths open resulting in too much air leakage, when they show intolerance towards the nasal mask or when complications occur (Castro-Codesal et al., 2019). For example, this can occur because of a nasal obstruction caused by polyps or in small children where a small displacement of the mask could result in obstruction of air flow (Mortamet et al., 2017; Nørregaard, 2002). In this case a face mask or oronasal mask (covering the mouth and nose) can be an alternative option (Castro-Codesal et al., 2019). This face mask is also the most common mask used in PICU's, for instance in patients with acute respiratory failure (Barker et al., 2018; Mortamet et al., 2017).

The effectiveness of NIV therapy in both settings is however highly dependent on the proper fit of the mask interfaces. Achieving a good fit is currently challenging because commercially available masks come in limited shapes and sizes and do not serve the variation of faces of children that change during their growth, particularly the very young children (younger than four years old) or children with cranial facial anomalies (Amirav et al., 2013; Barker et al., 2018; Castro-Codesal et al., 2019; Ramirez et al., 2012). An improper fit can lead to patient discomfort because of skin damage such as pressure sores, eye infections caused by air leakage or even facial deformation (Fauroux et al., 2005; Nørregaard, 2002). As a result, the treatment can ultimately fail (Hovenier et al., 2022). Therefore, detailed anthropometric data of the heads and faces of children is required to be able to develop a ventilation mask that is correctly sized and suitable for young children.

1.2.2 THESIS OUTLINE AND RESEARCH QUESTIONS

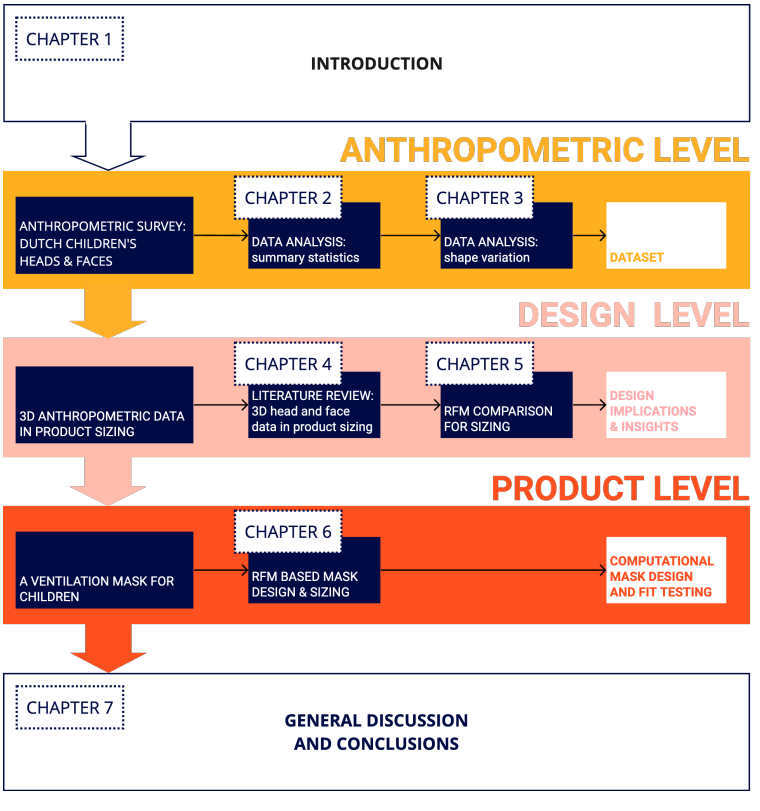

Figure 5 Visual outline of this thesis.

The scope of this thesis was subdivided into three levels namely, the anthropometric level, the design level and the product level. In each of these levels we address different research questions (RQs). The following paragraphs provide a description of each level and how the related research questions are addressed within the context of the research. The three levels are visualised in figure 5. which displays the visual outline of this thesis.

1.2.2.1 Anthropometric level

In order to understand the head and facial variation of children and to be able to conduct an anthropometric analysis, 3D Anthropometric data of 302 children's heads and faces were collected by means of 3D photogrammetric imaging as well as by traditional methods. In chapter 2, these detailed head and face dimensions of Dutch children are presented and the traditional measurements were compared with the most recent dataset of Dutch children. The more detailed facial measurements were compared with a dataset of North American children as a reference and to investigate differences or trends. Subsequently, in chapter 3, from a designer's point of view, the shape variation of a children's head and face was retrieved by analysing the 3D data and possible implications for the design of a ventilation mask were investigated.

RQ 1: How to collect, process, analyse and present 3D anthropometric data of children's heads and faces for design purposes?

Sub questions:

- What is the facial (shape) variation of children aged 0-6 years?
- How can the facial shape variation be presented to designers?

1.2.2.2 Design level

On a design level the type of information of the 3D anthropometric data that is relevant to designers was determined when designing products with critical fit. As a result, insights were gained into how sizing systems based on 3D anthropometric data are developed for these products. The literature review in chapter 4 provided an overview of approaches of how 3D anthropometric data of heads and faces is used in the process of sizing head and face related products. One promising direction is the development of representative models (RM's) based on a 3D anthropometric dataset. In chapter 5 RM's of the children's dataset were generated based on different commonly used analysis methods in sizing system development processes. The resulting RM's were compared and the mask contours that were subsequently projected on the RM's were analysed to determine possible implications for mask design. This provided answers to the following research question and sub questions:

RQ 2: What are approaches/methods to integrate the use of 3D anthropometric data of the head and face in developing sizing systems of head related products?
Sub questions:

- What type of data is used and how is it processed?
- What information of the 3D head /face data is used in the sizing system development process?
- What considerations from a product development perspective are taken into account?
- How do representative models, that are developed based on different sizing analysis methods, differ and what are implications for the design and sizing of a ventilation mask?

1.2.2.3 Product level

On this level, the 3D heads and face dataset of children were used in the design and sizing of a ventilation mask. In chapter 6, a computational design model of the ventilation mask was generated based on the RM's that were generated based on the children's dataset. Subsequently, a virtual fit test method was developed in order to evaluate the fit of these masks. Finally, the number of RMs and respective mask designs were increased to investigate its effect on the fit results.

RQ 3: How can 3D anthropometric data be implemented in product design and sizing?
Sub questions:

- How can 3D face data of children be implemented in the design and sizing of ventilation masks?
- How does a ventilation mask, designed based on 3D representative face models (RFM's), fit the target population?

Finally, the general discussion (chapter 7) reflects on the knowledge gained during the research and translate it to a more generic level. This chapter summarises and discusses results of the work as well as some of the limitations encountered during the project and provide a starting point for future research and further recommendations.

1.2.3 READING GUIDE AND PUBLICATIONS PART OF THIS THESIS

The chapters of this thesis have been partially published and based on these publications. Therefore, overlap in text might have occurred. Chapter 1 is partly adapted from a manuscript published in conference proceedings. Chapter 2 and 3 are adapted from manuscripts published in both conference proceedings and academic journals. Chapter

4 is based on a manuscript that is to be submitted to a journal and chapter 5 is based on a manuscript published in conference proceedings. Chapter 6 is also based on a manuscript to be submitted to a journal. Table.1 presents an overview of the publications that are part of this thesis.

Table 1 Overview of publications that are part of this dissertation.

Chapter	Article title	Journal	Status
1/2	3D anthropometric dataset of the head and face of children aged 0.5 – 7 years for design applications	*Conference paper* International conference on 3D body scanning technologies	Published
2	Traditional and 3D scan extracted measurements of the heads and faces of Dutch children	International Journal of Industrial Ergonomics	Published
3	Analysis of a 3D anthropometric data set of children for design applications	*Conference paper* IEA	Published
3	The variation in 3D face shapes of Dutch children for design applications	Applied Sciences "Novel Approaches and Applications in Ergonomic Design"	Published
4	A review of approaches in the use of 3D anthropometric head/face data in product sizing: a design perspective		To be submitted
5	A comparison between representative 3D faces based on bi- and multi-variate and shape-based analysis	*Conference paper* IEA	Published
6	Development and evaluation of 3D representative face models of children for mask design and sizing		To be submitted

2

TRADITIONAL AND 3D SCAN EXTRACTED MEASUREMENTS OF THE HEADS AND FACES OF DUTCH CHILDREN

Given the research objective outlined in the previous chapter and the fact that detailed 3D anthropometric data of children heads and faces is still lacking, the first step is to collect 3D data from the target group in order to develop a high-quality dataset in order to provide a basis for the research conducted in the upcoming chapters. This chapter presents up to date descriptive statistics of detailed measurements made of heads and faces of Dutch children. For the purpose of developing ergonomic head and face wear for children, an anthropometric survey was conducted, whereby children aged 6 months to 7 years were measured, utilising both traditional anthropometric measurement techniques and 3D image derived measurements. The traditional measurements were subsequently compared with the most recent dataset of Dutch children and, on a more detailed level, with a dataset of North American children in order to compare and verify the results of this analysis.

This chapter is based on Goto, L., Lee, W., Molenbroek, J.F., Cabo, A.J., Goossens, R.H. (2019). Traditional and 3D scan extracted measurements of the heads and faces of Dutch children. International Journal of Industrial Ergonomics, volume 73.

2.1 INTRODUCTION

Anthropometry plays an important role in product design. Designers utilise anthropometric information during the product development process to optimise the usability and fit of the product. The required type of anthropometric information highly depends on the product that needs to be developed. Currently, traditional anthropometric data is being used extensively in product development, but it lacks the level of detail that is essential in products that need to closely fit the human body.

3D anthropometry has created a significant opportunity for designers to improve fit by offering detailed information regarding the shape of the human body. Advances in 3D imaging technologies have resulted in new developments and applications in the field of anthropometry. Collecting 3D body scan data is thus increasingly being incorporated in anthropometric surveys (Ball, 2011; Ballester et al., 2015; HQL, 1997; Robinette et al., 2002; Zhuang, Benson, et al., 2010). The use of 3D scanning technologies facilitates the collection of measurements and shape information, and because of their high capturing speed, it makes the whole process less time consuming. Moreover, 3D scanners offer the opportunity to gather anthropometric data in a less invasive way and is therefore more suitable for elderly, physically impaired persons, and children (Conkle et al., 2019; Kau et al., 2004).

3D anthropometric information can be especially important for the development of head- and face-related products, such as oxygen masks, helmets, and goggles (Y. Luximon et al., 2016; Wuhrer et al., 2012). These products need to fit well, to ensure functionality, safety, and comfort. Various researchers have shown the benefit of using 3D anthropometric data in the development or evaluation of head related products (Alemany et al., 2012; Ellena et al., 2016; Lacko, Vleugels, et al., 2017; H. Liu et al., 2008; Schreinemakers et al., 2013; Skals et al., 2016; Stavrakos & Ahmed-Kristensen, 2016; Verwulgen et al., 2018). In medical products, a proper fit can have an immediate impact on the health of the patient. For instance, in a ventilation mask, an improper fit could result in eye infections, pressure sores and, for young children, it may even affect the growth of the face (Fauroux et al., 2005; Nørregaard, 2002).

Currently, there is no suitable full face ventilation mask (covering the nose and mouth) available for young children (younger than 6 years old) who suffer from, for example, muscular diseases, obstructive sleep apnea syndrome or who have a cranial facial disorder. Most of the existing paediatric masks are nasal masks which cover only the nose. However, nasal ventilation is not always effective. For example, with children who sleep with their mouth open (Amin et al., 2016). Because of this deficiency, some

hospitals have chosen to make their own custom-made masks (Fauroux et al., 2005; Mellies et al., 2003; Nørregaard, 2002) or modify nasal masks for adults in order to use it as a full-face mask for children (Samuels & Boit, 2007; Simonds et al., 2000). However, this is only an intermediate solution. In order to improve the comfort of the patient and the functionality a ventilation mask, designed specifically for children is required.

Anthropometric data of the head and face is necessary in order to develop a ventilation mask for young children. According to Farkas et al. (1992) cross-sectional anthropometric studies involving growing children have provided valuable data for quantitatively evaluating face and head development. Most traditional anthropometric surveys of children include only a select number of head dimensions such as head circumference, head length and head breadth (Fryar et al., 2012; Steenbekkers, 1993). Growth studies typically only include head circumference (Schönbeck & van Buuren, 2010; WHO Multicentre Growth Reference Study Group, 2009). Only a select number of studies provide anthropometric data of children specifically for product design and safety (Steenbekkers, 1993; Steenbekkers & Molenbroek, 1990) and only two of these studies include the more detailed dimensions of the head and face (Schneider et al., 1986; Snyder et al., 1977). Other studies that provide detailed data of head and face related dimensions are often from the medical field, e.g., orthodontics or plastic surgery (Bugaighis et al., 2013; Farkas, 1994; Meyer-Marcotty et al., 2014; Tutkuviene et al., 2015). Medical studies are a potential source of information but not fine-tuned to design and often focus on specific (facial) areas. Nevertheless, there is no detailed anthropometric information currently available of heads and faces of Dutch children. Moreover, there are no 3D anthropometric studies of young children, which evaluate the form and shape variation of the head and face. This is especially important in the development of a mask that must follow the contours of the face in order to achieve a good fit.

The aim of the present study was to provide data for detailed head and face dimensions of Dutch children employing 3D scanning techniques. In this study, 303 Dutch children aged 6 months to 7 years were measured for the purpose of designing head and face wear for children and as a first step in the development of a methodology for using 3D data in the sizing and design of a ventilation mask for children (Goto et al., 2013). The measurements of this dataset were analysed and compared with the most recent dataset of Dutch children (Steenbekkers, 1993) to identify anthropometric differences or trends. Steenbekkers measured 2421 Dutch children aged 0–12 years to obtain data of physical and psychomotor characteristics for the development of safer daily-life products for children. The survey included five head dimensions (breadth, height, length,

circumference, and chin to crown length). However, because of the lack of data regarding the more detailed facial dimensions in this study and since there is no reference data of the more detailed facial measurements of Dutch children, detailed measurements of current dataset were compared to that of North American children (Farkas, 1994). Farkas measured the heads and faces of around 1590 North American Caucasian children aged 1–18 years as part of research in craniofacial anthropometry with applications in medicine and genetics and this dataset is still, up until now one of the most extensive normative databases of the head and face available.

2.2 METHODS

2.2.1 PARTICIPANTS AND RECRUITMENT

The participants were Dutch children aged 6 months to 7 years old of mixed ethnicity. In this sample 17.8% (N=54) were of non-native Dutch origin. A child was considered to be of non-native Dutch origin when the country of origin of either one or both parents was not the Netherlands. They were sampled by age and gender. A total of 302 children (128 females 174 males) were recruited. According to ISO 15535 (2007), which describes the general requirements for establishing anthropometric databases age categories should be divided as follows: individual age for age group 1 is 0.50 to 1.49 years; for age group 2, it is 1.50 to 2.49; and, for age group 3, it is 2.50 to 3.49, etc. However, in order to conduct the comparison with the Steenbekkers and Farkas dataset the age categories were calculated to match their categorisation. This was done as follows. The age of each child was calculated by determining the difference between the date of measurement and the date of birth. It was then rounded to the nearest decimal and categorised in age groups (e.g., children aged 3.00–3.99 were categorised as 3-year-olds). The total numbers of children per age and gender are presented in Table 2.

Potential participants were recruited through primary schools and health centres in the Delft, Rijswijk and Leidschendam-Voorburg municipalities in the Province of South-Holland and through the Delft University of Technology. When schools were willing to cooperate, an information package was sent to the parents of the children providing them with information about the purpose of the research and the protocol of the survey. Parents could indicate whether they wanted to cooperate and give permission for their child(ren) to participate in the survey by signing a consent form and filling in a brief demographic questionnaire. Recruitment at the health centres took place on site by approaching the parents personally. University staff was contacted through newsletters. Ethical approval for the survey was gained from the Human Research Ethics Committee of the Delft University of Technology.

Table 2 Sample size by age and gender, including age range, average age and standard deviation (SD).

Age group	Age range	Average age and SD	Gender	N
0	0.5 - 0.9	0.8 +/- 0.2	Male	10
			Female	7
1	1.0 - 1.9	1.4 +/- 0.2	Male	21
			Female	8
2	2.0 - 2.9	2.5 +/- 0.3	Male	12
			Female	11
3	3.0 - 3.9	3.3 +/- 0.2	Male	17
			Female	15
4	4.0 - 4.9	4.6 +/- 0.2	Male	39
			Female	15
5	5.0 - 5.9	5.5 +/- 0.3	Male	34
			Female	30
6	6.0 - 6.9	6.48 +/- 0.3	Male	32
			Female	34
7	7.0 - 7.9	7.2 +/- 0.2	Male	9
			Female	8
			Total	302

2.2.2 DATA COLLECTION

In the survey a combination of traditional anthropometric measurement techniques as well as 3D image derived measurements were used.

2.2.2.1 Measuring and image capture

After explaining the purpose of the study and the protocol, the anthropometric data form was filled out and a reference number was assigned to the participant. Traditional anthropometric measurements were then recorded. These included 5 head and face measurements (Figure 6) and stature and weight. Children less than 24 months old were weighed using a baby scale, children older than 24 months were weighed with a standing scale. Children less than 24 months old who were not able to stand up by themselves were measured lying down (recumbent length) with a horizontal length scale, while older children were measured with a stadiometer. The head circumference was measured with a measuring tape and head and facial dimensions were recorded with an anthropometer and a spreading calliper. These head measurements were measured traditionally because they are more difficult to extract from 3D images since the landmarks rely primarily on palpation and not only on visual inspection.

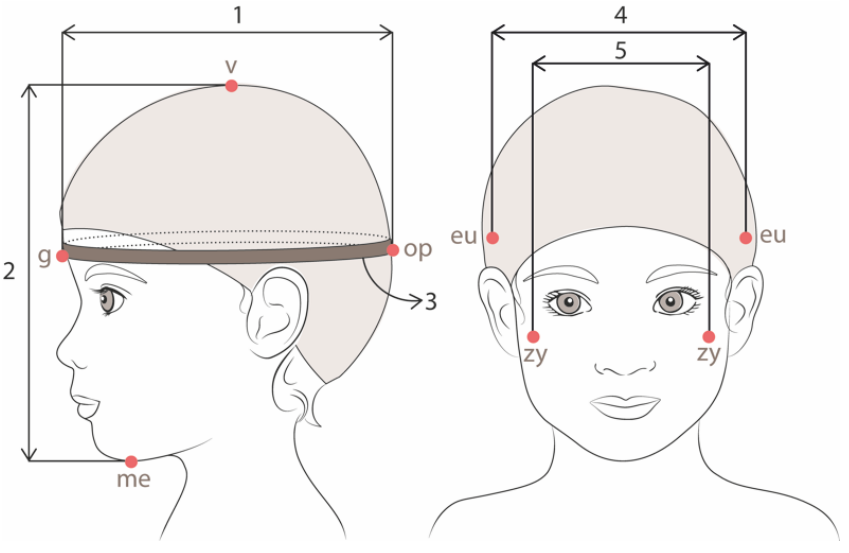

Dimension	Description
1	Head length (g-op)
2	Head height (v-me)
3	Head circumference
4	Head breadth (eu - eu)
5	Face width (zy - zy)

Figure 6 Traditional measurements (eu: eurion, g: glabella, me: menton, op: opisthocranion, v: vertex, and zy: zygion).

Lastly, the 3D images were obtained using the 3dMD Face system (3dMD Ltd., London, UK). 3D photogrammetry was used because of its accuracy (geometric accuracy of 0.2 root mean square) and high capturing speed (1.5 ms) (Lübbers et al., 2010; Wong et al., 2008). The imaging set-up was as presented in figures 7 and 8. Before photographing, each participant was provided with a nylon wig cap to capture the shape of the head and to avoid noise or holes in the 3D data caused by hair. A total of 4 images of the participant were taken from the front, 45 degrees to the left, 45 degrees to the right and from the back. The child was positioned on a highchair that was mounted on a plateau on wheels (Figure 8) in order to be able to rotate the child in the respective angels.

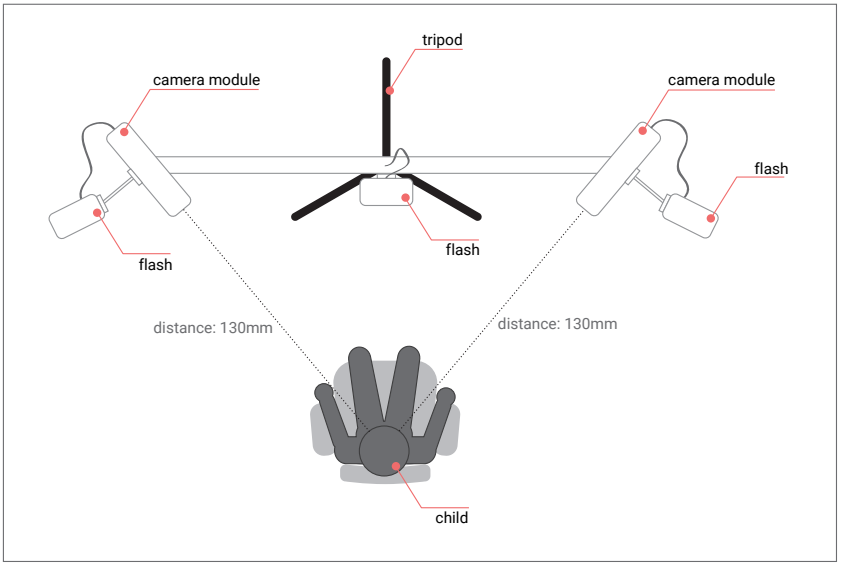

Figure 7 Floor footprint of the imaging system.

Figure 8 3D imaging setup with a 3-year-old girl (left) and with a 1-year-old girl sitting on the highchair mounted on the wheeled plateau (right).

2.2.2.2 Data process and alignment

The four 3D images that were captured were combined in ArtecStudio 9 software (Artec group, Luxembourg) to obtain a complete 3Dimage of the participant (figure 9).

Subsequently, remaining holes in the image were repaired in Geomagic Studio 2013 software (3D Systems, Rock Hill, SC, USA). The 3D images and landmark coordinates are not directly comparable, as the position of each participant and the orientation of the head relative to the 3D imaging system varied. All images were aligned with MATLAB™ 2015a software (The MathWorks,Inc., Natick, MA, USA) according to the Frankfort horizontal plane and the sellion landmark. The Frankfort plane, which is a commonly used anthropometric reference plane, runs through the right infraorbitale and the left and right tragion landmarks (Martin & Knussmann, 1988). The sellion landmark was set as the origin point (0, 0, 0) and subsequently, the 3D image of the face was rotated around the x, y, and z axes until a line through the landmarks was parallel to either the x, y or z axis. For example, the face was rotated around the y-axis until the line passing through the left and right infra-orbitale landmarks was parallel to the z axis. In this way, all the 3D faces were aligned so when they are superimposed, they are all oriented according to the same coordinate system.

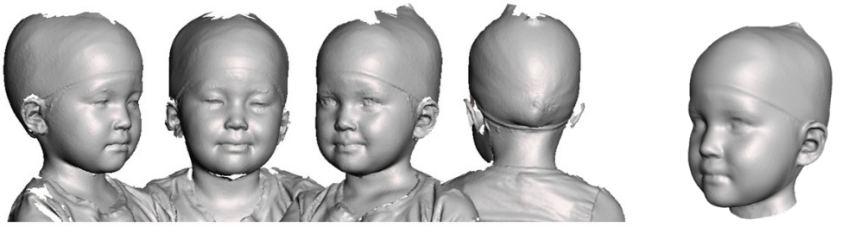

Figure 9 Four images were combined into a complete 3D image of the head (From left to right; image 45° from the right, from the front, 45° from the left, the back and the merged complete 3D head).

2.2.2.3 Landmarking and measurement extraction

The 3D images were manually landmarked using 3dMDvultus 2.1 software (3dMD Ltd., London, UK). A total of 15 landmarks were selected in order to obtain information of the facial area relevant to the design of ventilation mask. The landmarks included in this study could be located on the 3D image without the use of palpation and were based on identifiable facial features (figure 10). Landmark descriptions were defined based on previous research (Facebase, 2013; Martin & Knussmann, 1988; Zhuang, Slice, et al., 2010). The landmarks included in this study were glabella, sellion, endocanthion (left/right), nasal root point(left/right), pronasale, alare (left/right), subnasale, cheilion (left/right), sublabiale, pogonion and menton. Facial measurements were extracted from the 3D images by calculating the Euclidian distances between these landmarks with a programme developed in MATLAB™ (figure 11).

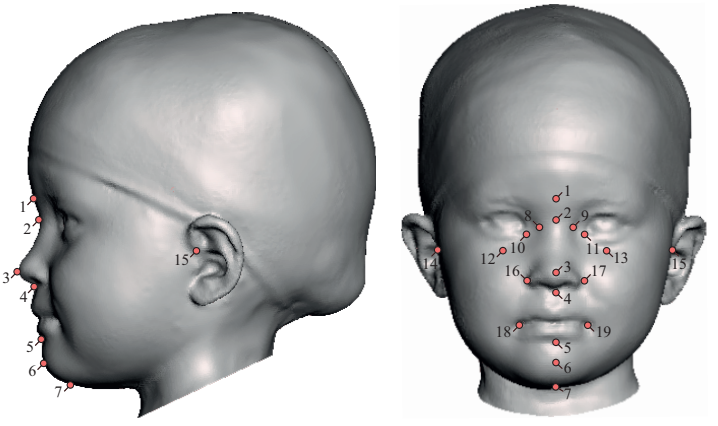

No.	Landmark	Definition
1	Glabella (g)	The most prominent point in the median sagittal plane between the eyebrow ridges.
2	Sellion (s)	The deepest point of the nasalfrontal angle.
3	Pronasale (prn)	The most protrusive point on the nasal tip in the midline of the face.
4	Subnasale (sn)	The junction the lower border of the nasal septum, the partition that divides the nostrils, and the cutaneous portion of the upper lip in the midline.
5	Sublabiale (sl)	The deepest point of the labiomental groove at the midline.
6	Pogonion (pg)	The most anterior point in the middle of the soft tissue chin.
7	Menton (me)	The lowest point in the midline on the lower border of the chin.
8/9	Nasal root point (nrp) (right/left)	The point on the side of the nasal root halfway between endocanthion and the midline of the nasal bridge.
10/11	Endocanthion (en) (right/left)	Bilateral landmark located at the inner corner of the eye where the upper and lower eyelids meet.
12/13	Infraorbitale (or) (right/left)	Lowest point on the inferior margin of the left and right orbit, directly inferior to the pupil.
14/15	Tragion (t) (right/left)	Bilateral landmark located at the most anterior point of the small notch just above the tragus where the cartilage meets the face.
16/17	Alare (al) (right/left)	Bilateral landmark defined by the most lateral point on the nasal ala.
18/19	Cheilion (ch) (right/left)	The outer corner of the mouth where the outer edges of the upper and lower vermilions meet.

Figure 10 Landmark locations and definitions.

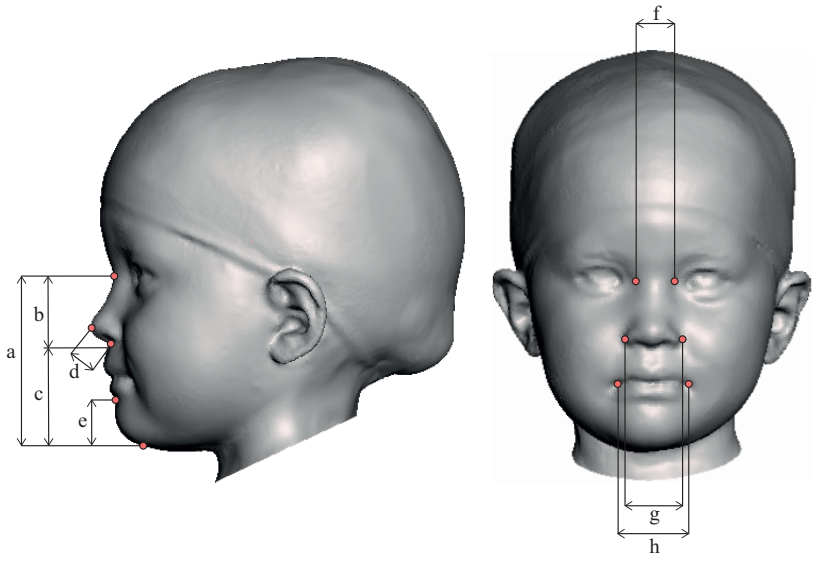

	Description
a	Face height (s-me)
b	Nose length (s-sn)
c	Lower face height (sn-me)
d	Nasal tip protrusion (sn-prn)
e	Chin height (sl-me)
f	Nasal root breadth(nrp-nrp)
g	Nose width (al-al)
h	Mouth width (ch-ch)

Figure 11 3D image extracted measurements.

2.2.2.4 Reliability of the measurements

Measuring the participants and landmarking the 3D images was all done by one investigator. The reliability of the consistency of both measuring methods was also evaluated. The reliability of the traditional head measurements was tested by measuring the same single participant five times with an interval of at least 24 hours to reduce memory bias. The magnitude of the intra-observer variation in standard variation was equal or less than 2 mm for four out of five dimensions. This is within the allowable error as defined by Gordon et al. (2014). One dimension showed greater differences than the allowable error (2.45 mm), namely the length of the head; hair volume might have influenced these measurements.

In order to test the reliability of the 3D image extracted measurements, a 3D scanned head of one and the same participant was landmarked by the investigator on five separate occasions with at least 24 hours in between. The Euclidean distance between two landmark pairs was calculated in order to extract the face measurements. The intra-

observer variation in standard deviation were all less than 1 mm. Also, the coefficient of variation (CV) was calculated for each dimension which resulted in scores less then 1% for 4 dimensions and less then 3% for the remaining 4. This translates to a very good (CV=1%–3.9%) to excellent (CV=1% or less) precision as stated by Weinberg et al. (2004).

2.2.3 DATA ANALYSIS AND COMPARISON

The data was analysed using descriptive statistics and scatter plots. Two-dimensional scatterplots were generated by pairing age with all dimensions, outliers were checked for data entry errors or incorrect landmarking and corrected or eliminated if necessary. The number of participants (N) varies per dimension because specific measurements of some children were eliminated because of an unwanted facial expression that influenced the measurement (e.g. smiling, open mouth). But also, because for some participants it was not possible to take any (N=10) or some direct measurements because they were either too scared or emotional. This happened mostly within age group 1 to 3, when measuring head dimensions with the anthropometer. For instance, in age group 1, head height is missing for all except one female participant. Capturing a 3D image, however, was in all cases possible. A statistical analysis of traditional measurements and scan-derived measurements was conducted for all age groups using SPSS Statistics 22 software (IBM, New York, NY, USA). Mean values and standard deviations of all measurements were calculated for each gender and age group. In addition, for each dimension the maximum and minimum values were determined. Also, summary statistics of the gender combined data are calculated. Gender combined data can often be more useful for design applications (Bradtmiller, 1996). Additionally, the mean values (MG) of the traditional measurements of the current dataset were compared with the mean values (MS) of Dutch children of Steenbekkers' dataset. Steenbekkers' dataset consisted of five head dimensions (breadth, height, length, circumference and chin to crown length) of which the latter not was not included in this study. Furthermore, these dimensions, including the more detailed facial measurements of current dataset, were also compared with mean values (MF) of the facial measurements of North American children collected by Farkas. A t-test (α=0.05) was conducted to determine the significance of the differences between each mean value of each dimension of this dataset and that of Steenbekkers' and Farkas' dataset. The dimensions that were included in all three datasets were head circumference, head breadth, head height and head length.

2.3 RESULTS

2.3.1 DESCRIPTIVE STATISTICS

The results of the traditional anthropometric measurements and 3D scan extracted measurements are presented in Table 3. The mean and standard deviation for each dimension are presented for each age group and gender. The summery statistics of the gender combined data can be found in Appendix 2.1 and charts showing the mean value and standard deviation of a selection of measurements per age group are presented in Appendix 2.2.

2.3.2 COMPARISON OF THIS DATASET WITH STEENBEKKERS' DATASET

A selection of traditional measurements of this dataset was compared to the corresponding dimensions of Steenbekkers' dataset by calculating the difference between the mean values (MG – MS). The number of participants included in Steenbekkers' study, mean and standard deviation are presented per age group for each dimension in Table 4. Of the total of 88 comparisons between mean values, 44 (50%) cases showed significant differences (21 among male versus 23 among female). In 57 (65%) comparisons (28 male and 29 female), significant and non-significant, the values of current dataset were smaller than Steenbekkers' dataset. A more visual way of the comparison between datasets can be found in Appendix 2.3 in the form of cross-sectional growth curves.

The differences were distributed throughout all age groups and different dimensions. Just a couple of significant differences between the datasets were found for weight and stature. Only one significant difference was observed for weight and stature for the male participants. For the females, one value showed a significant difference for weight and two for stature. Significant differences were found in all age groups except two for head circumference, for both male and female. In all instances, current dataset showed smaller values (MG – MS = -15.4 ~ -7.0 mm) than Steenbekkers' dataset. Head length was found to be significantly different for males in all age groups and for female all except one (MG – MS = -12.6 ~ -3.7 mm). For head height, only significant differences were observed for female (MG – MS = -9.5 – 2.5 mm) and not for male whereas for head breadth, more differences (all except one) were observed in the male population (MG – MS = 3.8 – 9.5 mm). The only dimension for which current dataset showed bigger values than Steenbekkers' dataset throughout almost all age groups for both male and female (all except age group 4), was head breadth.

Table 3 Summary statistics of face and head measurements (Mean and Standard Deviation) of Dutch children of six months to seven years of age. Traditional measurements and *3D image derived measurements (mm).

	Stature						Weight (Kg)					
	Male			*Female*			*Male*			*Female*		
Age	**N**	**Mean**	**SD**	**N**	**Mean**	**SD**	**N**	**Mean**	**SD**	**N**	**Mean**	**SD**
0	10	736.0	47.9	7	721.6	26.6	10	8.8	1.1	7	8.8	0.9
1	21	827.2	43.0	7	805.4	51.9	21	11.2	1.2	7	10.1	1.8
2	12	942.0	66.6	11	934.5	86.8	12	14.0	1.8	11	13.5	2.1
3	17	1005.3	35.2	15	1002.2	47.2	17	15.7	1.1	15	15.3	2.1
4	39	1088.6	43.6	15	1108.6	30.8	39	19.0	2.4	15	18.7	2.5
5	34	1160.3	59.1	30	1147.2	50.6	34	21.3	3.1	30	20.5	2.1
6	32	1218.8	57.2	34	1216.9	44.0	32	22.9	2.8	34	22.6	2.6
7	9	1260.3	50.9	8	1240.1	43.7	9	24.8	2.5	8	24.3	2.4

	Head Breadth						Head Height					
	Male			*Female*			*Male*			*Female*		
Age	**N**	**Mean**	**SD**	**N**	**Mean**	**SD**	**N**	**Mean**	**SD**	**N**	**Mean**	**SD**
0	8	124.9	5.6	7	123.1	4.8	8	155.8	9.7	5	162.0	9.9
1	18	133.2	8.2	2	123.5	7.8	15	168.5	7.8	-	-	-
2	11	138.0	6.6	11	133.4	7.2	11	175.3	15.0	11	174.5	11.1
3	17	139.9	4.8	15	135.3	7.0	17	185.1	12.5	15	177.7	11.9
4	39	141.8	5.2	15	135.6	4.7	39	189.6	10.0	15	183.9	9.4
5	34	143.4	5.9	30	139.9	7.3	34	194.4	9.4	30	187.0	7.9
6	32	145.5	6.3	34	142.6	8.0	32	195.7	10.0	34	192.0	10.5
7	9	148.2	8.4	8	142.5	3.9	9	199.6	8.6	8	186.5	4.8

	Face Width						*Face Height					
	Male			*Female*			*Male*			*Female*		
Age	**N**	**Mean**	**SD**	**N**	**Mean**	**SD**	**N**	**Mean**	**SD**	**N**	**Mean**	**SD**
0	8	100.4	6.2	7	98.7	3.6	10	75.0	3.6	7	74.2	4.6
1	19	103.9	7.3	2	96.0	5.7	21	80.7	4.1	8	78.2	3.7
2	11	104.5	4.4	11	102.8	6.7	12	84.8	3.2	11	82.5	4.2
3	17	108.4	4.4	15	104.6	4.4	17	88.4	3.3	15	87.3	4.0
4	39	108.8	6.0	15	106.2	3.4	39	93.2	4.2	15	92.4	3.3
5	34	108.9	5.4	30	108.2	6.2	34	96.0	5.0	30	93.7	4.3
6	32	110.5	7.0	34	110.9	6.8	32	97.4	4.4	34	95.1	4.2
7	9	109.8	8.5	8	112.4	4.4	9	99.5	3.1	8	96.0	6.1

	*Height of Chin						*Nasal Root Breadth					
	Male			*Female*			*Male*			*Female*		
Age	**N**	**Mean**	**SD**	**N**	**Mean**	**SD**	**N**	**Mean**	**SD**	**N**	**Mean**	**SD**
0	10	16.8	2.1	7	18.1	2.1	10	19.7	1.5	7	19.0	1.2
1	21	20.0	2.8	8	19.6	1.8	21	20.1	2.0	8	17.5	1.8
2	12	21.3	1.7	11	21.9	2.9	12	19.7	2.0	11	19.8	2.0
3	17	24.4	3.2	15	24.0	2.8	17	21.0	1.1	15	20.4	1.5
4	39	25.3	3.0	15	23.9	2.1	39	21.4	2.0	15	21.2	1.3
5	34	25.4	2.4	30	25.1	2.5	34	21.2	1.4	30	21.0	2.0
6	32	26.2	2.8	34	26.1	2.3	32	21.5	2.0	34	21.4	1.7
7	9	26.8	2.3	8	24.8	2.7	9	21.6	2.8	8	21.8	1.1

Table 3 (continued).

	Head Circumference						*Nasal Tip Protrusion					
	Male			*Female*			*Male*			*Female*		
Age	**N**	**Mean**	**SD**	**N**	**Mean**	**SD**	**N**	**Mean**	**SD**	**N**	**Mean**	**SD**
0	10	458.2	13.2	7	446.7	12.4	10	11.5	1.0	7	11.4	1.0
1	20	478.7	12.4	7	459.7	17.0	21	11.8	0.9	8	11.4	1.0
2	11	492.6	12.1	11	483.4	8.8	12	12.4	1.5	11	12.5	1.7
3	17	506.9	13.1	15	498.8	26.6	17	13.4	1.3	15	13.1	1.5
4	39	511.0	13.5	15	502.2	9.7	39	14.1	1.2	15	14.6	1.0
5	34	513.7	11.6	30	507.1	15.6	34	15.0	1.2	30	14.4	1.1
6	32	517.6	14.9	34	508.8	15.9	32	15.5	1.4	34	15.0	1.1
7	9	517.6	15.7	8	511.5	11.7	9	15.0	0.9	8	15.8	1.6

	Head Length						*Nose width					
	Male			*Female*			*Male*			*Female*		
Age	**N**	**Mean**	**SD**	**N**	**Mean**	**SD**	**N**	**Mean**	**SD**	**N**	**Mean**	**SD**
0	8	152.4	8.8	5	150.6	6.9	10	25.6	1.6	7	24.8	0.7
1	17	162.7	7.8	3	163.3	9.9	21	26.5	1.8	8	25.4	1.2
2	11	164.4	12.0	11	166.6	9.2	12	27.4	2.2	11	26.4	1.6
3	17	173.6	6.2	15	170.4	9.1	17	28.4	2.1	15	27.4	2.3
4	39	176.1	7.1	15	175.3	5.4	39	28.4	1.7	15	27.3	1.1
5	34	179.4	6.6	30	176.1	6.8	34	28.7	1.6	30	27.9	1.3
6	32	180.3	7.7	34	175.5	7.8	32	29.4	1.4	34	28.5	1.7
7	9	179.7	7.6	8	177.4	7.5	9	29.4	1.6	8	29.5	1.2

	*Lower Face Height						*Mouth width					
	Male			*Female*			*Male*			*Female*		
Age	**N**	**Mean**	**SD**	**N**	**Mean**	**SD**	**N**	**Mean**	**SD**	**N**	**Mean**	**SD**
0	10	47.3	3.0	7	46.7	3.6	9	34.4	3.8	7	30.5	2.5
1	21	51.0	2.9	8	49.9	3.2	20	34.2	2.9	8	34.1	1.3
2	12	53.2	1.9	11	51.6	3.0	11	35.7	2.0	11	35.4	2.6
3	17	55.1	2.7	15	54.1	3.7	17	37.6	2.8	15	35.6	2.8
4	39	57.8	3.7	15	56.0	3.3	39	37.8	2.7	15	36.3	3.0
5	34	58.7	3.7	30	57.8	3.7	34	39.3	3.5	30	37.9	3.3
6	32	59.0	3.9	34	58.0	2.8	32	39.9	2.9	34	39.6	3.3
7	9	60.9	2.1	8	57.0	4.3	9	40.6	3.4	8	41.4	3.7

	*Nose Length					
	Male			*Female*		
Age	**N**	**Mean**	**SD**	**N**	**Mean**	**SD**
0	10	27.7	2.0	7	27.5	1.8
1	21	29.7	1.8	8	28.3	1.4
2	12	31.5	2.5	11	30.9	3.0
3	17	33.3	2.0	15	33.2	2.5
4	39	35.3	2.1	15	36.3	1.9
5	34	37.3	2.3	30	35.8	2.2
6	32	38.4	2.5	34	37.2	2.6
7	9	38.6	1.9	8	38.9	3.4

Table 4 Summary statistics of L.P.A. Steenbekkers (1993) and a comparison between mean values (MG-MS) (mm). Mean values of this dataset (MG) are all based on traditional measurements.

	Weight (kg)							
	Male				*Female*			
Age**	**N**	**Mean**	**SD**	**M_G-M_S**	**N**	**Mean**	**SD**	**M_G-M_S**
6.0-11.9 mo.	35	8.9	0.9	-0.1	30	8.6	1.1	0.2
12.0-17.9 mo.	17	10.8	1.0	0.3	28	9.6	1.3	0.0
2	81	14.5	1.9	-0.5	92	14.1	1.6	-0.6
3	97	17.0	2.0	-1.3*	86	16.0	1.8	-0.7
4	85	18.6	2.0	0.4	79	18.4	2.1	0.3
5	86	21.6	2.8	-0.3	94	21.0	3.0	-0.5
6	98	23.5	2.5	-0.6	92	23.6	2.6	-1.0
7	106	26.4	3.6	-1.6	93	26.9	4.3	-2.6*
	Head Circumference							
	Male				*Female*			
Age	**N**	**Mean**	**SD**	**M_G-M_S**	**N**	**Mean**	**SD**	**M_G-M_S**
6.0-11.9 mo.	35	455.7	11.4	2.5	30	450.5	13.7	-3.8
12.0-17.9 mo.	17	480.5	13.9	-0.9	28	466.1	13.1	-12.3*
2	81	508.0	13.0	-15.4*	92	493.0	15.0	-9.6*
3	97	515.0	14.0	-8.1*	86	504.0	15.0	-5.2
4	85	518.0	12.0	-7.0*	79	510.0	13.0	-7.8*
5	86	524.0	13.0	-10.3*	94	516.0	14.0	-8.9*
6	98	529.0	14.0	-11.4*	92	522.0	13.0	-13.2*
7	106	531.0	12.0	-13.4*	93	524.0	14.0	-12.5*
	Head Height* **							
	Male				*Female*			
Age	**N**	**Mean**	**SD**	**M_G-M_S**	**N**	**Mean**	**SD**	**M_G-M_S**
2	81	176.0	11.0	-0.7	92	172	12.0	2.5
3	97	185.0	11.0	0.1	86	178	11.0	-0.3
4	85	190.0	11.0	-0.4	79	186	11.0	-2.1
5	86	198.0	11.0	-3.6	94	193	10.0	-6.0*
6	98	199.0	11.0	-3.3	92	193	10.0	-1.0
7	106	204.0	11.0	-4.4	93	196	10.0	-9.5*

Table 4 (continued).

Stature							
Male				*Female*			
N	**Mean**	**SD**	**M_G-M_S**	**N**	**Mean**	**SD**	**M_G-M_S**
35	728.0	35.6	8.0	30	715.4	37.0	6.2
17	787.1	36.2	31.3*	28	772.6	43.0	20.4
81	939.0	45.0	3.0	92	929.0	46.0	5.5
97	1021.0	44.0	-15.7	86	1004.0	45.0	-1.8
85	1085.0	47.0	3.0	79	1082.0	40.0	26.6*
86	1170.0	48.0	-9.7	94	1159.0	49.0	-11.8
98	1225.0	47.0	-6.2	92	1227.0	49.0	-10.1
106	1287.0	53.0	-26.7	93	1286.0	57.0	-45.9*
Head Breadth							
Male				*Female*			
N	**Mean**	**SD**	**M_G-M_S**	**N**	**Mean**	**SD**	**M_G-M_S**
35	118.0	4.7	6.9*	30	116.6	5.8	6.5*
17	123.9	4.8	9.5*	28	121.3	5.8	2.2
81	134.0	4.0	4.0	92	130.0	5.0	3.4
97	136.0	5.0	3.9*	86	133.0	5.0	2.3
85	138.0	5.0	3.8*	79	136.0	4.0	-0.4
86	139.0	5.0	4.4*	94	137.0	5.0	2.9*
98	141.0	5.0	4.5*	92	138.0	4.0	4.6*
106	142.0	5.0	6.2*	93	140.0	5.0	2.5
Head Length* **							
Male				*Female*			
N	**Mean**	**SD**	**M_G-M_S**	**N**	**Mean**	**SD**	**M_G-M_S**
81	177.0	6.0	-12.6*	92	172.0	7.0	-5.4
97	180.0	7.0	-6.4*	86	176.0	7.0	-5.6*
85	182.0	7.0	-5.9*	79	179.0	6.0	-3.7*
86	185.0	7.0	-5.6*	94	182.0	6.0	-5.9*
98	185.0	7.0	-4.7*	92	184.0	6.0	-8.5*
106	187.0	6.0	-7.3*	93	184.0	6.0	-6.6*

* Significantly different; $p < 0.05$

** Steenbekkers categorized age group 0 and 1 per three months. In order to compare the datasets, the mean and standard deviation were calculated per six months and N was adjusted accordingly.

*** Steenbekkers did not include age group 0 and 1 for the dimensions Head Height and Head Length.

2.3.3 COMPARISON OF THIS DATASET WITH FARKAS' DATASET

The head dimensions and the more detailed facial dimensions were compared with the corresponding dimensions of Farkas' dataset. In Table 5, the number of participants included in Farkas' study, mean and standard deviation are presented per age group for each dimension. Out of the total of 160 comparisons between mean values, 71 (44%) cases showed significant differences (38 among male and 33 among female). In 86 (53%) cases (44 male and 42 female), significant and non-significant, the values of current dataset were smaller than Farkas' dataset. A comparison of the mean values (MG - MF) for head breadth indicated that the children in this dataset have significantly broader heads in comparison with Farkas' dataset. Face width (MG - MF=-6.2 – -2.9mm for age groups 5, 6 and 7 and MG - MF=5.6–7.2mm for age groups 1, 2 and 3), nose length (MG - MF=-1.6 – -4.2 mm) and nasal tip protrusion (MG -MF=1.1–2.4 mm) for the male participants were significantly different for most of the age groups. A few significant differences were found for head height and head length. For head height, one significant difference was found in one age group for male and in two age groups for female. A significant difference was observed for head length in only one of the age groups for both male and female. A more visual way of the comparison between datasets can be found in Appendix 2.4 in the form of cross-sectional growth curves.

Table 5 Summary statistics of L.G. Farkas (1994) and a comparison between mean values (MG-MF) (mm)). Mean values of this dataset are based on traditional measurements (MG) and 3D scan derived measurements (MG*).

Head Circumference

	Male				*Female*			
Age	**N**	**Mean**	**SD**	**M_G-M_F**	**N**	**Mean**	**SD**	**M_G-M_F**
6-12 mo.	20	452.6	14.1	5.6	8	451.6	16.3	-4.9
1	18	490.9	11.1	-12.2*	28	475.5	16.8	-15.8*
2	31	500.8	14.5	-8.2	30	490.7	10.5	-7.3*
3	30	508.8	12.9	-1.9	30	502.2	12.8	-3.4
4	30	518.4	14.7	-7.4*	30	508.9	10.3	-6.7*
5	30	520.0	11.9	-6.3*	30	516.7	9.4	-9.6*
6	50	518.6	14.3	-1.0	49	507.4	12.1	1.4
7	50	521.2	14.2	-3.6	50	515.4	14.4	-3.9

Head Height

	Male				*Female*			
Age	**N**	**Mean**	**SD**	**M_G-M_F**	**N**	**Mean**	**SD**	**M_G-M_F**
6-12 mo.	-	-	-	-	-	-	-	-
1	17	177.5	7.1	-9.0*	28	173.8	6.2	-
2	31	182.5	8.6	-7.2	32	179.3	6.5	-4.8
3	30	187.4	7.1	-2.3	30	181.6	7.0	-3.9
4	30	193.0	7.1	-3.4	30	188.1	5.9	-4.2
5	30	193.0	6.1	1.4	30	190.9	6.6	-3.9*
6	50	198.2	9.9	-2.5	50	194.0	9.8	-2.0
7	50	201.1	10.7	-1.5	50	199.0	9.4	-12.5*

*Significantly different; p< 0.05 two tailed

Table 5 (continued).

Face Width

	Male				*Female*			
Age	**N**	**Mean**	**SD**	**M_G*-M_F**	**N**	**Mean**	**SD**	**M_G*-M_F**
6-12 mo.	20	97.8	5.2	2.6	8	94.6	4.6	4.1
1	18	96.7	3.3	7.2*	27	95.6	4.3	0.4
2	31	98.9	4.9	5.6*	32	97.9	3.0	4.9*
3	30	101.4	5.0	7.0*	30	101.2	4.2	3.4*
4	30	110.2	5.4	-1.4	30	106.8	4.6	-0.6
5	30	111.8	5.1	-2.9*	30	109.4	3.6	-1.2
6	50	114.9	5.3	-4.4*	50	113.4	5.1	-2.5
7	50	116.0	5.8	-6.2*	50	115.8	4.6	-3.4*

Nose Length

	Male				*Female*			
Age	**N**	**Mean**	**SD**	**M_G*-M_F**	**N**	**Mean**	**SD**	**M_G*-M_F**
6-12 mo.	20	27.0	1.7	0.7	8	26.9	1.6	0.6
1	18	30.9	1.9	-1.2	20	29.2	2.6	-0.9
2	31	33.7	2.7	-2.2*	31	32.6	2.6	-1.7
3	30	35.3	2.6	-2.0*	30	34.6	2.3	-1.4
4	30	39.5	1.9	-4.2*	30	37.8	1.9	-1.5*
5	30	38.9	2.7	-1.6*	30	39.3	2.1	-3.5*
6	50	40.1	2.6	-1.7*	50	39.3	2.7	-2.1*
7	50	41.4	1.9	-2.8*	50	40.7	2.7	-1.8

Nose Width

	Male				*Female*			
Age	**N**	**Mean**	**SD**	**M_G*-M_F**	**N**	**Mean**	**SD**	**M_G*-M_F**
6-12 mo.	20	26.5	1.4	-0.9	8	1.5	25.4	-0.6
1	18	26.5	1.5	0	21	1.4	25.9	-0.5
2	31	25.6	1.4	1.8*	31	1.2	26.1	0.3
3	30	26.1	1.5	2.3*	30	1.1	25.9	1.5*
4	30	28.4	1.7	0	30	1.3	27.8	-0.5
5	30	28.9	1.5	-0.2	30	1.5	28.5	-0.6
6	50	28.6	1.6	0.8*	50	1.3	27.8	0.7*
7	50	28.8	1.9	0.6	50	1.7	28.6	0.9

Head Breadth

	Male				*Female*			
Age	**N**	**Mean**	**SD**	**M_G-M_F**	**N**	**Mean**	**SD**	**M_G-M_F**
6-12 mo.	20	116.8	6.2	8.1*	8	115.7	4.9	7.4*
1	18	125.5	5.6	7.7*	28	122.0	6.0	1.5
2	30	130.5	5.5	7.5*	32	127.8	3.7	5.6*
3	30	133.7	4.0	6.2*	30	130.8	4.0	4.5*
4	30	136.4	4.7	5.4*	30	135.8	3.8	-0.2
5	30	138.2	4.0	5.2*	30	135.4	3.8	4.5*
6	50	139.8	4.8	5.7*	50	136.8	4.6	5.8*
7	50	140.8	5.3	7.4*	50	137.6	4.6	4.9*

Table 5 (continued).

Head Length

	Male				*Female*			
Age	**N**	**Mean**	**SD**	**M_G-M_F**	**N**	**Mean**	**SD**	**M_G-M_F**
6-12 mo.	20	151.9	5.3	0.5	8	158.3	3.9	-7.7*
1	18	166.7	6.2	-4.0	28	162.0	7.9	1.3
2	30	170.5	12.4	-6.1	32	168.6	5.7	-2.0
3	30	177.5	6.7	-3.9	30	173.7	6.3	-3.3
4	30	181.5	6.2	-5.4*	30	175.2	5.2	0.1
5	30	180.5	6.2	-1.1	30	178.8	5.2	-2.7
6	50	183.2	7.6	-2.9	50	177.7	5.8	-2.2
7	50	184.0	7.7	-4.3	50	180.8	6.4	-3.4

Face Height

	Male				*Female*			
Age	**N**	**Mean**	**SD**	**M_G*-M_F**	**N**	**Mean**	**SD**	**M_G*-M_F**
6-12 mo.	20	70.5	4.8	4.5*	8	68.0	4.4	6.2*
1	18	80.6	4.8	0.1	19	72.7	4.9	5.5*
2	31	87.5	3.5	-2.7*	31	77.2	3.9	5.3*
3	30	88.5	3.5	-0.1	30	83.8	2.4	3.5*
4	30	96.4	4.3	-3.2*	30	86.9	3.6	5.5*
5	30	96.7	3.5	-0.7	30	92.6	4.6	1.1
6	50	98.5	5	-1.1	50	96.5	4.4	-1.4
7	50	99.5	5	0	50	95.7	3.7	0.3

Nasal Tip Protrusion

	Male				*Female*			
Age	**N**	**Mean**	**SD**	**M_G*-M_F**	**N**	**Mean**	**SD**	**M_G*-M_F**
6-12 mo.	20	9.1	1.2	2.4*	8	9.7	0.8	1.7*
1	18	10.1	1.5	1.7*	20	10.2	1.4	1.2*
2	31	11.3	1.5	1.1*	31	11.5	1.4	1.0
3	30	12.1	1.4	1.3*	30	12.4	1.8	0.7
4	30	13.0	1.1	1.1*	30	12.3	1.1	2.3*
5	30	13.3	0.8	1.7*	30	13.1	1.2	1.3*
6	50	15.1	1.5	0.4	50	14.8	1.2	0.2
7	50	15.3	1.3	-0.3	50	15.5	1.1	0.3

Mouth width

	Male				*Female*			
Age	**N**	**Mean**	**SD**	**M_G*-M_F**	**N**	**Mean**	**SD**	**M_G*-M_F**
6-12 mo.	20	33.1	2.2	1.3	8	1.6	33.0	-2.5*
1	18	34.8	2.6	-0.6	28	2.5	33.3	0.8
2	31	35.2	2.6	0.5	31	1.8	35.0	0.4
3	30	36.7	2.4	0.9	30	2.5	36.3	-0.7
4	30	38.9	2.5	-1.1	30	2.2	37.9	-1.6
5	30	40.7	2.4	-1.4	30	2.7	39.5	-1.6*
6	50	41.7	2.8	-1.8*	50	2.9	41.2	-1.6*
7	50	42.7	2.7	-2.1	50	2.2	42.4	-1.0

*Significantly different; p< 0.05 two tailed

2.4 DISCUSSION

This paper presents the descriptive statistics of traditional and 3D scan extracted measurements of children's heads and faces based on an anthropometric survey conducted amongst Dutch children. Considering the relatively small sample size in some age categories and the imbalance between genders, this dataset may not considered to be representative of the entire Dutch child population. Therefore, a comparison with existing child datasets was conducted in order to discover whether the measurements of this dataset align with those from the larger datasets. And by studying similarities and differences between the datasets, potential hypothesis for further investigations could be formulated. The cross-sectional growth curves of the three datasets are presented in appendix 2.3 showing the differences in a more visual way.

Current survey took place in the Province of South-Holland which represents only a part of the Dutch population of 0.5 to 7-year-old children. Although there are no studies to determine how representative these children are for the entire population of 0.5 to 7-year-old Dutch children when it comes to head and facial measurements, research conducted by Steenbekkers (1993) found that when measuring children in all Provinces of the Netherlands, there were no significant differences for head circumference, despite differences for stature, weight and popliteal height based on geographical region/location. The question is whether this is also the case for other head dimensions and the more detailed facial measurements and if these differences would influence design decisions.

When comparing this dataset to that of Steenbekkers', with regard to traditional measurements, a number of significant differences were found. These differences could be observed throughout different age groups, for different measurements and for both male and female. However, considerably less significant differences were found for weight as well as for stature. Besides the traditionally measured head dimensions, the scan extracted, more detailed facial measurements were compared with Farkas' dataset. Significant differences were found for various dimensions throughout different age groups, for both male and female. Overall, the results of both comparisons showed no clear trend. When comparing the mean values of the dimensions that were included in all three dataset (head circumference, head breadth, head height and head length) the difference is generally smaller between Steenbekkers' and Farkas' datasets than compared to values of this dataset. This is true for all except head breadth, for which the current dataset is closer to Steenbekkers' dataset for both male and female in all age groups.

These observed differences between the datasets could be potentially explained by a number of factors, including age composition, ethnicity, secular growth changes and measuring protocols.

Firstly, the age composition within each age category could differ for each dataset which could influence the results. The dimensions of the face experience the most growth of the entire head, with rapid growth phases occurring mostly between the ages of 6 months and 4 years (Burdi et al., 1969; Farkas et al., 1992). As a result, having more children with an age between 12 and 18 months in age group 1 (that runs from 12 months to 24 months), for example, could result in smaller average values. Comparing these measurements with the same age group of a different dataset with a different composition would thus result in larger differences between the mean values. For future studies, it could therefore be important to mention the average age of the age group.

Moreover, in product design, it may be more appropriate to concentrate on other variables, rather than age (Lueder & Berg Rice, 2008; Steenbekkers, 1993), especially given that adjacent age groups often show great overlap for a variety of dimensions. In product sizing, often a number of easy to measure dimensions is used to group individuals of the target population. These so-called key dimensions are often also predictive of other dimensions. A number of studies have identified key dimensions related to mask design for adults (W. Lee, Lee, et al., 2018; Oestenstad & Perkins, 1992; Zhuang et al., 2005). For children, Amirav et al. (2013) suggest that width of the mouth and sellion-promentale length are relevant dimensions for the sizing of aerosol masks. And interestingly, Ramirez et al. (2012) assign ventilation masks to young patients not only based on age but primarily on weight. Weight is a common way to define product sizes for children as for instance in car seats and diapers. Determining the key dimensions, investigating the variability of these dimensions and how to translate these into product sizes for face mask design will be subject of further study.

Secondly, the current dataset consists of different ethnicities and ethnicity is known to influence growth (Churchill et al., 1978; Farkas et al., 2005). Indeed, the anthropometric dimensions of children with native Dutch parents tend to be larger than the dimensions of children whose parents are not native Dutch, implying a difference in growth (Steenbekkers, 1993). For this sample, 18% (55 out of 302 children) were considered of non-native Dutch origin of which 39 had one parent that was native Dutch. The country of origin of one or both parents varied considerably (30 different countries). Steenbekkers' data was based on a Dutch population including children of non-Dutch origin (4%) and Farkas' study was conducted amongst the North American population and was exclusively Caucasian. A comparison between the datasets however, did not

show any trend that could be explained by differences in the composition of the datasets in terms of ethnicity. Moreover, analysing the effect of ethnicity on the variance of the dimensions in this dataset would have been complex because of the sample size and the diverse composition of the group that was considered non-Dutch. However, ethnicity and ethnic composition of a country is important and due to globalization, interpreting anthropometric data becomes more complex. For example, the distribution of Dutch and non-Dutch citizens in the Netherlands was 22.6% on January1st, 2017 (Statistics Netherlands (CBS), 2017).

Thirdly, given that Steenbekkers' survey was conducted in/before1993 and Farkas' study was conducted around 1992 it is likely that secular growth changes have taken place in the last 20 years. Recent studies have shown an increase in Dutch children that are overweight but they have stopped growing taller ever since 1997 (Schönbeck et al., 2011, 2013). Even though the comparison between the datasets did not directly show these trends, these growth shifts could also affect the more detailed dimensions of, for example, the face.

Differences between datasets could also be caused by differences in measuring protocols. For instance, Steenbekkers measured head height, length and breadth with an automated anthropometer whereas in this study we used an anthropometer for height and length and for head breadth we used a spreading calliper as according to Kolar and Salter (1997). The measuring protocol for Farkas' study is unknown given that the study only shows the landmarks that define the dimensions. It is therefore not possible to come to a valid comparison between the results.

Finally, scan derived measurements from the current dataset were compared with traditional measurements of Farkas' dataset. When a dimension is measured directly, one has to palpate the bony structure underneath the skin and one can easily impress the skin with the measuring device which could influence the measurement. Although a 3D image derived measurement is always based on the actual dimensions of the face, landmarking is sometimes more challenging because of the difficulty of recognizing the difference between soft and hard tissue without palpation. Previous studies have shown the accuracy and reliability of using 3D images of the 3dMD face system (Hong et al., 2017; Lübbers et al., 2010; Wong et al., 2008) and other 3D imaging systems in anthropometry (Fourie et al., 2011; W. Lee, Yang, et al., 2017; Weinberg et al., 2004) by comparing traditional measurements with scan extracted measurements. However, the identified differences between the two approaches still do not indicate which of the measurements are more accurate and it does not deliver a verdict on which of the measurements represent the population better.

A clear advantage of including 3D imaging in an anthropometric survey is that it facilitates the collection of data of young children for whom a direct anthropometric examination is often too intense for they cannot sit still for long periods of time (Farkas, 1996). Ball et al. (2011) scanned 400 children for the Size China survey but the rejection rate under the age of five was close to 100% because of the slow capturing speed of the scanner they used at the time. During the current survey, we observed that taking traditional, direct measurements was in some cases not possible (especially in the younger age categories 0–3 years) whereas taking a 3D image of children, who initially refused to cooperate during the direct measurements, was still possible mainly because of the fast-capturing speed. And even though some challenges still remain (Sims et al., 2012), this 3D scanning technology seems to be promising also for collecting data of physical impaired persons or elderly.

Furthermore, the added value of this dataset lies in the fact that beside the statistical information of facial measurements of children, the collection of 3D images provides richer, more detailed information. In addition, the 3D dataset can be accessed whenever needed and relevant, new information can be extracted depending on the application without re-inviting participants. But most importantly the data also provides valuable information about the shape of the face (Goto et al., 2015; Zhuang et al., 2013) for product designers. But, before it can be integrated into the design process, the data first needs to be processed, analysed and tailored to a certain design application such that this shape information can be presented to and utilized by designers.

2.5 CONCLUSION

This chapter presented up to date descriptive statistics of detailed measurements made of heads and faces of Dutch children. But also, a 3D dataset which can be referenced in the future for different purposes and to study face and head shapes of children. Collecting anthropometric data of very young children is time consuming when done by hand. This study shows that 3D photogrammetry offers an efficient way to scan babies and young children and facilitates this process because of its quick acquisition speed. This anthropometric dataset is an addition to the traditional anthropometric information of Dutch children that currently is available and the first study providing information that is richer and more up to date.

3

THE VARIATION IN 3D FACE SHAPES OF DUTCH CHILDREN FOR MASK DESIGN

In the previous chapter the summary statistics of the 3D dataset were presented. However, 3D anthropometric data is more versatile and richer because it also contains shape information. The use of 3D anthropometric data of children's heads and faces therefore has great potential in the development of protective gear and medical products that need to provide a close fit in order to function well. In this study, the children's head and face dataset consisting of traditional measurements and 3D scans were analysed. A principal component analysis (PCA) of the facial measurements was performed to map the variation of the children's face shapes. The results showed that the first principal component describes the overall size, whilst the second principal component captures the more width related variation of the face. After establishing a homology between the 3D scanned face shapes, a second principal component analysis was done on the point coordinates, revealing the most prominent variations in 3D face shape within the sample.

This chapter is based on Goto, L., Lee,W., Huysmans, T., Molenbroek, J.F.M., Goossens, R.H.M. (2021). The Variation in 3D Face Shapes of Dutch Children for Mask Design. Applied Sciences, 11, 6843.

3.1 INTRODUCTION

Anthropometric information is commonly used in the design and evaluation of numerous applications such as workplaces, tools, clothing and wearables. Designers look to translate key body dimensions to relevant product shape and size in order to achieve a good fit. Traditional 1D anthropometric measurements are not able to capture the shape of the human body. However, this morphological information is becoming more important in the development of products such as apparel, backpacks, orthoses and headwear that need to closely fit a part of the body.

In headwear, a good fit is often required in order for the product to function properly. This is especially important in protective gear or medical products as the fit of these products could have a direct impact on the wearer's health and safety (Barker et al., 2018; Hsiao, 2013; W. Lee, Yang, et al., 2018; Ma et al., 2018). Thus, anthropometric information of the head and face is necessary to describe the variation in size and shape in order to develop a product that fits the user. Previous research has demonstrated the benefit of using 3D anthropometric data in order to understand the morphological variation of the head and face as well as in the improvement of product fit. Various researchers have studied the anthropometric variation of heads and faces based on 3D head scan data (Lacko et al., 2015; Y. Luximon et al., 2012; Zhuang, Slice, et al., 2010) in order to develop new sizing systems (Bolkart et al., 2015; Kouchi & Mochimaru, 2004; W. Lee, Lee, et al., 2018), in order to generate representative models (Ellena et al., 2017; W. Lee, Lee, et al., 2018; Yu et al., 2011; Zhuang, Benson, et al., 2010) or to improve the fit of certain products (Chu et al., 2015; Lacko, Vleugels, et al., 2017; W. Lee et al., 2013; H. Liu et al., 2008).

Previous studies all focus on adults, but relatively few studies have been carried out on 3D scan data for children using similar forms of analysis. In addition, the availability of 3D anthropometric data of children's heads and faces for designers is limited. Anthropometric surveys targeting children are a necessity as it has already been determined that children cannot be considered small adults, and thus that one cannot simply downsize a product designed for adults because body proportions are different especially in early childhood (Bogin, 1988; The Canadian Institute of Child Health, 2007). Detailed head and facial anthropometric data of children enable designers to create products with a better fit and by doing so, increasing safety and comfort of, for example, helmets (Bradtmiller, 1996), dust masks (Kim et al., 2016), oxygen masks (Young, 1966) and other medical devices (Amirav et al., 2019). Furthermore, the anthropometric data of children also give insights in age related differences or growth, which is essential for designers when designing a product for children (Lueder & Berg

Rice, 2008). For example, Bradtmiller (1996) conducted a 3D anthropometric study of children (n = 1035) for the development of better fitting helmets for American children aged 2 to 18. Based on the (3D) anthropometric data, he defined a new sizing system and subsequently generated head forms representing each size for helmet design. More recently, researchers have gathered 3D scans of children in order to analyse and extract shape information for the design of facial masks for both medical and commercial applications (Amirav et al., 2013; Goto, Lee, et al., 2019; W. Lee, Goto, Molenbroek, Goossens, et al., 2017; Seo et al., 2016).

After collecting the 3D scanned data, one of the challenges a designer encounters is to try to accommodate the variation in shape. This is especially true when developing a product that needs to closely fit a certain part of the body (A. Luximon et al., 2012). In order to do so, anthropometric information is translated into a sizing system and/or product dimensions. A common way of determining this is by identifying one or two key dimensions (or sizing parameters) that can be translated into product dimensions (Hsiao, 2013; W. Lee et al., 2016; A. Luximon et al., 2012). However, with a product that needs a close fit, such as a ventilation mask, two dimensions are not sufficient to describe the shape variation of the face (Hsiao, 2013; W. Lee et al., 2016). One way of incorporating more dimensions into the design or a sizing system is by mapping the variation of multiple key-dimensions by means of a principal component analysis (PCA) (A. Luximon et al., 2012; Zhuang et al., 2007). PCA is a technique to increase interpretability of large datasets that consist of a high number of interrelated variables by dimensionality reduction. It generates a new set of uncorrelated (orthogonal) variables to describe the dataset while preserving as much of the variation present in the dataset. Studies have shown that a multivariate approach results in a more accurate representation of the variation compared to bivariate analysis for applications in sizing system development (Hsiao, 2013; Lacko, Huysmans, et al., 2017; A. Luximon et al., 2012; Zhuang et al., 2007).

Currently, PCA remains the most commonly used form of analysis of 3D anthropometric data sets. PCA has been used to study shape variation or extract relevant information for the development of fit test panels, defining sizing systems, or determining product dimensions (A. Luximon et al., 2012; Meunier et al., 2009; Xi & Shu, 2009). In addition, PCA has been conducted in order to study body shape differences in children (Medialdea et al., 2019). The input variables for a PCA can vary from measurements, landmark locations or point-cloud data/3D geometric models (W. Chen et al., 2009; Hsiao, 2013; Y. Luximon et al., 2010, 2012; Zhuang, Benson, et al., 2010; Zhuang et al., 2013). The outcome of a PCA is not widely used in design practice because of its complexity (Y.

Luximon et al., 2016), and it is not directly applicable in the design process for it does not offer an intuitive description of the shape (Lacko et al., 2015). Nevertheless, it does offer a method to present a complex and rich data set in a more understandable way. In order for the designers to be able to use this information in the design process, representative or average shape models that represent the variance of the target population are usually generated based on these analyses (Y. Luximon et al., 2012; Zhuang et al., 2013). Designers can then use these representative 3D face models to adapt their designs to the target group. In this way, protective equipment of medical products that needs to fit a children's head or face can be developed.

Therefore, the aim of this study is to present and analyse the shape variation of Dutch children's faces, and, more specifically, the area relevant for the design of a ventilation mask, by conducting both a measurement based PCA and shape based PCA. In addition, this paper investigates possible implications for the design of the ventilation mask and discusses the applicability for designers of both PCAs.

3.2 METHOD

3.2.1 PARTICIPANTS AND DATA COLLECTION

A survey was conducted in order to collect anthropometric data of children's heads and faces (Goto et al., 2013; Goto, Lee, et al., 2019). A total of 302 Dutch children (128 females, 174 males) aged 6 months to 7 years were recruited through health centres, primary schools, and the university. Of the total population, 17.8% (n = 54) children were considered to be of non-native Dutch origin. This was defined as when the country of origin of either one or both of the child's parents was not the Netherlands. The anthropometric survey was approved by the Human Research Ethics Committee (HREC) of the Delft University of Technology in December 2012. Because at that time the HREC did not provide an ethical approval code, the application was re-submitted on the 20th of July 2021 and approved. The study was provided with approval number 1736. Informed consent was obtained from all participants involved in the study. Age categorisation was done according to ISO 15535 (2007), which describes the general requirements for establishing anthropometric databases. Age groups were divided as follows: individual age for age group 1 is 0.50 to 1.49 years; for age group 2, it is 1.50 to 2.49; and, for age group 3, it is 2.50 to 3.49, etc.

In the survey, both traditional anthropometric measurements as well as 3D image derived measurements were collected as described in Goto et al. (2019) through a five-step procedure. First, the following traditional anthropometric head and face dimensions

were recorded; head circumference, head length, head height, head width, and face width, as well as more general measurements such as stature and weight. Second, four 3D images captured from different directions per participant were collected using the 3dMD Face system (3dMD Ltd., London, UK). All children were scanned with a neutral face expression. These images were then combined into a 360 degree 3D image of the head. using Artec Studio 9 software (Artec Group, Luxembourg) and the remaining holes in the image were repaired in Geomagic Studio 2013 software (3D Systems, Rock Hill, SC, USA). After that, a total of nineteen landmarks were marked on each 3D face with 3dMD Vultus 2.1 software (3dMD Ltd., London, UK) as shown in Figure 12. The landmarks that were included in the survey could be identified on the 3D image without palpation. The definitions of these landmark locations can be found in (Goto, Lee, et al., 2019). Finally, eight facial dimensions were measured and extracted after the 3D images were aligned according to the Frankfort horizontal plane (Martin and Knussmann, 1988) using MATLAB^{TM} software (The MathWorks, Inc., Natick, MA, USA). An overview of the full procedure is illustrated in Figure 13. Table 6 shows the summarized information of the data including mean and standard deviations for each dimension per age group, males and females combined.

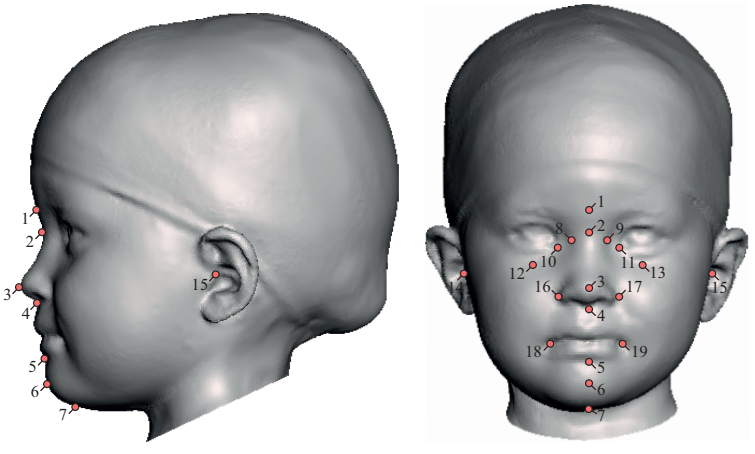

Figure 12 The landmarks included in this study; 1. glabella, 2. sellion, 3. pronasale, 4. subnasale, 5. Sublabiale, 6. Pogonion, 7. menton, 8/9. nasal root point, (right/left), 10/11. endocanthion (right/left), 12/13. infraorbitale (right/left), 14/15. tragion (right/left), 16/17. alare (right/left) and 18/19. cheilion (right/left) (Goto, Lee, et al., 2019).

Table 6 Mean and standard deviation for each dimension (mm) per age group where age group 1 consists of children aged 0.50 to 1.49 years, age group 2 consists of children aged 1.50 to 2.49, etc.

	Age Group 1 (*n* = 33)		Age Group 2 (*n* = 28)		Age Group 3 (*n* = 29)		Age Group 4 (*n* = 32)	
	Mean	**SD**	**Mean**	**SD**	**Mean**	**SD**	**Mean**	**SD**
Stature *	768.7	55.8	875.3	65.1	994.9	50.6	1068.6	53.6
Weight *	9.6	1.4	12.4	1.9	15.1	1.8	18.2	2.8
Head circumference *	460.9	17.5	484.0	12.7	497.6	18.9	509.4	16.9
Head width *	126.8	8.2	135.0	7.5	136.3	6.3	140.2	5.4
Head length *	154.3	8.0	167.1	7.0	169.6	11.2	175.0	7.3
Head height *	160.8	9.5	173.1	10.6	178.8	14.2	186.7	10.5
Face width *	100.9	6.0	103.2	6.9	105.4	4.6	108.6	5.3
Face length	90.6	4.8	96.5	5.3	100.2	4.4	104.3	5.7
Sellion-menton length	76.9	4.6	81.8	3.9	86.9	3.4	91.6	4.7
Lower face length	48.8	3.6	51.3	2.9	54.1	2.8	57.0	4.0
Intercanthal width	29.3	2.4	30.4	2.2	31.3	2.4	31.9	2.1
Nasal root breadth	19.3	1.9	19.6	2.1	20.5	1.5	21.1	1.7
Nose length	28.1	1.8	30.4	2.4	32.8	2.2	34.6	2.1
Nose bridge length	18.9	1.8	20.6	2.2	22.4	1.7	23.6	2.2
Nasal tip protrusion	11.5	0.9	12.0	1.3	13.0	1.6	13.8	1.2
Nose width	25.7	1.5	26.5	1.9	27.8	2.2	27.8	1.9
Mouth width	34.3	4.7	34.9	3.0	36.7	2.9	37.0	2.9
Chin height	18.1	2.2	20.9	2.3	23.7	2.3	24.9	3.3
Sellion-sublabiale length	58.8	4.5	60.9	3.4	63.3	3.0	66.7	3.6
Sellion-pogonion length	67.2	4.9	69.9	3.7	73.7	4.2	76.4	3.8
Inter-pupillary distance	50.4	2.8	52.5	2.5	53.4	2.7	54.9	2.8

* Dimensions measured by the traditional measurement method.

Table 6 (continued).

Age Group 5 (*n* = 67)		Age Group 6 (*n* = 65)		Age Group 7 (*n* = 48)	
Mean	**SD**	**Mean**	**SD**	**Mean**	**SD**
1116.4	51.9	1195.9	53.3	1230.5	53.3
19.5	2.5	22.1	2.9	23.4	2.5
509.4	13.5	511.3	15.7	513.2	14.1
140.5	6.8	143.5	6.5	144.4	7.4
177.3	7.0	177.1	7.3	177.8	7.9
189.0	9.9	192.0	10.6	194.6	8.8
107.9	5.5	109.7	6.3	111.4	6.8
107.0	5.5	109.7	5.6	111.2	4.8
93.3	4.1	96.2	4.6	96.9	4.5
57.4	3.5	58.5	3.7	58.7	3.4
32.2	2.1	32.5	2.4	32.8	2.4
21.2	1.7	21.4	1.9	21.5	1.8
35.9	2.0	37.6	2.5	38.1	2.6
24.3	2.0	25.7	2.2	25.9	2.8
14.5	1.1	15.0	1.4	15.3	1.1
28.2	1.5	28.7	1.6	29.1	1.5
38.0	3.0	39.2	3.3	40.4	3.2
24.9	2.7	25.7	2.4	26.2	2.5
68.3	3.5	70.5	3.9	70.7	3.8
78.5	3.9	80.4	4.3	80.7	4.2
55.3	2.3	56.0	2.9	57.1	3.0

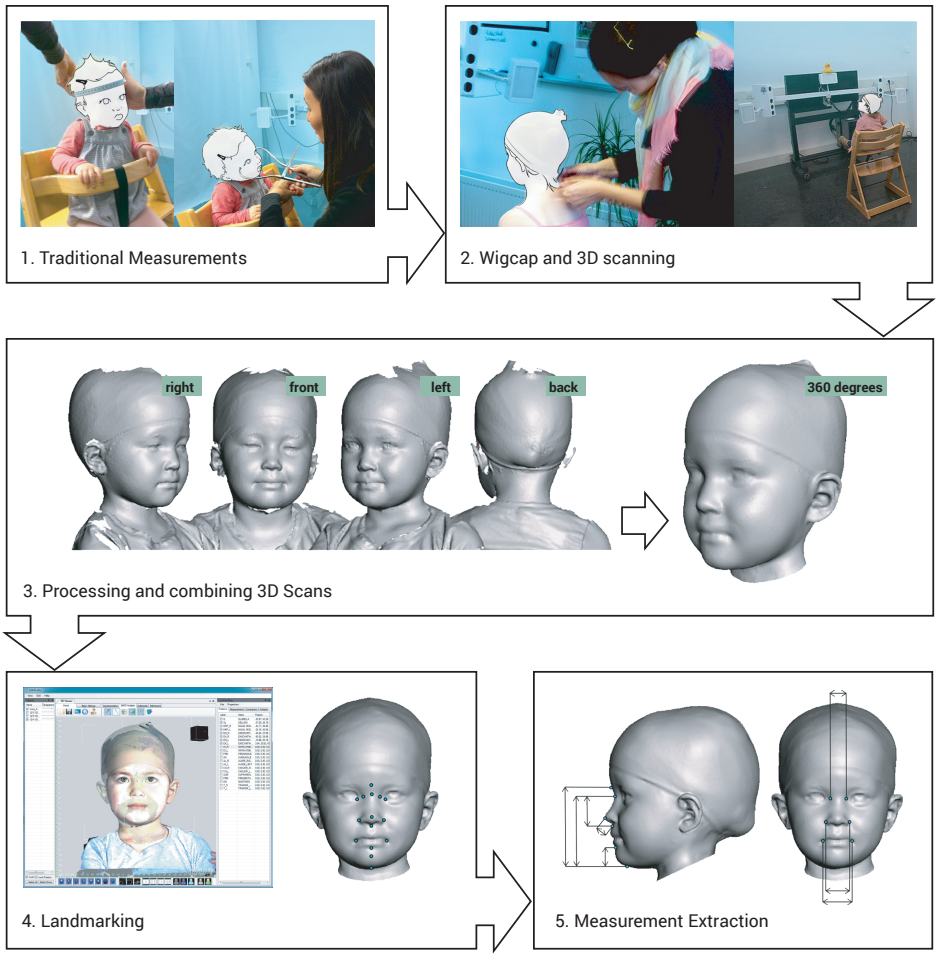

Figure 13 Data collection and processing of the 3D scan images; an overview of the steps (print screen: 3dMD Vultus software).

3.2.2 DATA ANALYSIS PROCEDURE

3.2.2.1 Comparison between Genders

First, an independent t-test was performed to investigate similarities between gender for each dimension per age group. As opposed to anthropometric data of adults, male and female data of children can sometimes be combined depending on the application (Bradtmiller, 1996). When considering a product that needs to fit a certain age range of children, the variability of relevant dimensions has to be taken into account in the design. Because the variability of dimensions of children's heads and faces due to age is greater

than the variability due to gender, it is often valid to combine the data of the different genders (Bradtmiller, 1996). A total of 21 dimensions served as input for the t-test. A multiple comparisons correction was applied by employing the Benjamini–Hochberg procedure (Benjamini & Hochberg, 1995). When multiple statistical tests are performed simultaneously, such as comparing 21 dimensions, there's an increased risk of obtaining false-positive results. To address this issue the Benjamini–Hochberg procedure controls the false discovery rate (FDR). The FDR is the proportion of false positives among all the significant results which is often close to 5% when there is no significant difference (Benjamini & Hochberg, 1995). By setting an FDR threshold, the rate at which false discoveries are accepted can be controlled. The FDR was set at 0.05. MATLAB™ was used for statistical analysis.

3.2.2.2 Measurement Based Analysis of Face Variation

The PCA was performed to find important factors that explain the variation of the children's faces (MATLAB™). The input variables for the PCA in this study were chosen based on a review of previous studies and through discussion in a panel consisting of four anthropometry experts and ergonomists. The input variables for the PCA were considered relevant to mask design and the selection was based on the method proposed in two previous studies by Zhuang et al. (2007) and Amirav et al. (2013). Zhuang et al. (2007) identified 10 dimensions that were considered related to respirator fit in a study focussing on respirators for the adult civilian workforce namely, minimum frontal breadth, face width, bigonial breadth, face length, inter-pupillary distance, head breadth, nose protrusion, nose breadth, nasal root breadth and subnasale-sellion length. Amirav et al. (2013) considered two facial dimensions relevant in the development of aerosol masks for children, namely, the width of the mouth and sellion-pogonion length. To our knowledge, similar information about dimensions related to fit does not exist for ventilation masks for children. As a result, PCA was applied to the following 9 measurements that were chosen for this study: face length, sellion-pogonion length, nose bridge length, mouth width, nose tip protrusion, nasal root breadth, nose breadth, inter-pupillary distance and face width. The definition of each measurement can be found in Table 7. The principal component (PC) loadings were calculated (MATLAB™) to give insight into the influence of different dimensions on the variation.

Table 7 Definitions of the nine selected measurements for the measurements based PCA.

Measurement	Definition
Face length	Straight-line distance between the sellion (s) and menton (me) landmarks
Sellion-pogonion length	Straight-line distance between the sellion (s) and pogonion (pg) landmarks
Nose bridge length	Straight-line distance between the sellion (s) to pronasale (prn) landmarks
Mouth width	Straight-line distance between the left and right chelion landmarks (ch-ch)
Nose tip protrusion	Straight-line distance between the subnasale (sn) and the pronasale (prn) landmarks
Nasal root breadth	The horizontal breadth of the nosals root spanning from the left nasal root point to the right (nrp-nrp)
Nose breadth	Straight line distance between the left and right alare landmarks (al-al)
Inter-pupillary distance	The straight-line distance between the centre of the left and the centre of the right pupil
Face width	Horizontal breadth between the left and right zygion landmarks (zy-zy)

3.2.2.3 3D Shape Based Analysis of Face Variation

In order to analyse the shape variation of the 3D face images, a morphological correspondence between each individual face image needs to be realized. Meshes of individual scans contain a varying amount of 3D data points that are distributed in different ways, which makes it impossible to compare them directly. By creating a correspondence, meshes are converted in such a way that the data points are approximately uniformly distributed over the shape, creating meshes that have the same number of data points and connectivity (triangles), with comparable landmark locations. This is referred to as homologous meshes. In this study, the so-called non-rigid template registration method (Dyke et al., 2020) is used using Wrap 3.4 software (Russian3dscanner, Moscow). First, a high-quality individual scan was selected to serve as the template mesh. This scan was then processed to be topologically equivalent to a disc (no surface handles and a single boundary at the neck) and with a uniform distribution of vertices. The obtained template was then used to create these homologous meshes by deforming the template mesh towards each individual face scan (target scan) as is illustrated in Figure 14. The annotated landmarks were used to steer the registration by forcing an exact match. Finally, the homologous meshes were spatially aligned (limited to translation and rotation) via Generalized Procrustes Analysis (Gower, 1975).

A PCA was then conducted on the 3D coordinates of the homologous meshes in order to analyse and visualize the 3D shape variation of the children's faces. The principal component analysis was conducted on the x-, y-, and z-values of each vertex of the 3D

mesh data using a custom script in Python. The average head mesh was processed in ParaView to extract the relevant facial area through clipping with two interactively positioned planes. The resulting facial region of interest of the average shape was then warped to each individual face through the homology, effectively resulting in corresponding regions of interest for all subjects in the database, forming the input for the facial PCA analysis. Face shape modes that represent the shape variation are visualized along the first 7 Principal Components (PC's).

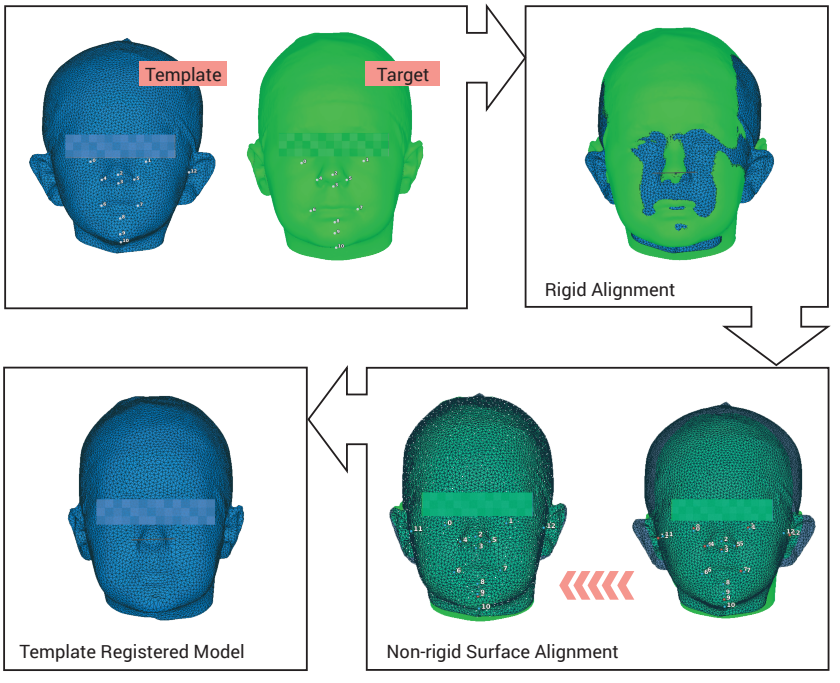

Figure 14 The template registration process.

3.3 RESULTS

3.3.1 GENDER COMPARISON

The differences in dimensions between gender for each age group are shown in Table 8. Overall, the mean head and face measurements for the male participants were larger than the female participants (120 out of 133 comparisons (90%) throughout all the age categories). However, only some incidental significant differences could be observed (7/133). They were scattered throughout different age groups and related to different dimensions. Therefore, for the remainder of this study, we work with a combined dataset in terms of gender.

Table 8 Independent t-test between boys and girls for each age group (mean difference in mm).

	Age Group 1		Age Group 2		Age Group 3		Age Group 4	
	Mean Diff	*p*	Mean Diff	*p*	Mean Diff	*p*	Mean Diff	*p*
Stature	21.00	0.33	−8.17	0.76	−21.56	0.27	52.85	0.01 *
Weight	0.70	0.18	−0.06	0.94	0.36	0.60	1.96	0.09
Head circumference	19.90	0.00 **	2.54	0.63	12.03	0.09	3.38	0.63
Head width	5.65	0.10	3.50	0.29	3.43	0.15	5.08	0.02 *
Head length	1.51	0.69	−1.26	0.67	0.15	0.97	5.67	0.05
Head height	−4.13	0.39	2.63	0.58	−1.57	0.77	9.88	0.02 *
Face width	4.24	0.09	2.38	0.44	3.32	0.05	1.75	0.43
Face length	1.32	0.45	3.51	0.10	1.21	0.47	3.52	0.13
Sellion-menton length	1.74	0.30	1.96	0.21	0.70	0.59	3.02	0.12
Lower face length	1.02	0.43	1.36	0.24	0.50	0.64	3.03	0.06
Intercanthal width	1.89	0.02 *	−0.09	0.92	0.97	0.29	1.41	0.10
Nasal root breadth	1.70	0.01 *	0.44	0.60	0.54	0.35	0.73	0.30
Nose length	0.72	0.27	0.60	0.54	0.20	0.81	−0.02	0.99
Nose bridge length	0.45	0.48	0.96	0.28	0.38	0.56	0.01	0.99
Nasal tip protrusion	0.22	0.49	−0.27	0.60	0.15	0.81	0.12	0.82
Nose width	0.73	0.17	1.20	0.12	0.83	0.32	0.77	0.34
Mouth width	3.38	0.04 *	0.45	0.72	1.00	0.36	1.72	0.15
Chin height	−0.69	0.39	0.01	0.99	−0.67	0.44	2.12	0.12
Sellion-sublabiale length	2.43	0.13	1.95	0.15	1.37	0.23	0.89	0.55
Sellion-pogonion length	2.55	0.14	1.41	0.34	1.81	0.26	2.78	0.07
Inter-pupillary distance	2.32	0.02 *	0.65	0.52	0.56	0.58	1.93	0.09

* $p < 0.05$. ** significant with FDR correction set at 0.05.

3.3.2 FACE VARIATION

A PCA was conducted with the following dimensions: face length, sellion-pogonion length, nose bridge length, mouth width, nose tip protrusion, nasal root breadth, nose breadth, inter-pupillary distance and face width. The plot in Figure 15 shows the cumulative variance explained of each component. The threshold of the cumulative variance was set at 90% with each individual PC explaining at least 5% of the variance, resulting in the five PC's that are presented in Table 9. The first five PC's account for 90.39% of the total variation of the sample. The PC loadings of the first principal component (PC1) are all positive and relatively high. This means that each dimension contributes considerably to PC1 and thus captures the overall size and shape of the face.

Table 8 (continued).

Age Group 5		Age Group 6		Age Group 7	
Mean Diff	*p*	Mean Diff	*p*	Mean Diff	*p*
−5.95	0.65	15.04	0.26	2.49	0.87
0.31	0.62	1.04	0.14	−0.36	0.62
7.51	0.03 *	7.00	0.07	7.42	0.06
4.50	0.01 **	6.88	0.11	5.18	0.01 *
3.07	0.08	2.35	0.20	3.40	0.13
7.95	0.00 **	4.78	0.07	7.04	0.00 **
1.90	0.17	−0.37	0.82	−0.42	0.83
2.82	0.02 *	1.39	0.32	2.38	0.08
1.94	0.06	1.52	0.19	3.35	0.01 *
1.83	0.03 *	0.10	0.91	2.10	0.03 *
0.43	0.41	0.02	0.98	0.46	0.50
0.27	0.52	−0.01	0.99	0.13	0.80
0.10	0.84	1.42	0.02 *	1.25	0.10
−0.07	0.89	0.55	0.32	1.49	0.06
0.03	0.91	0.77	0.03 *	−0.05	0.87
1.31	0.00 **	0.78	0.06	0.59	0.18
2.59	0.00 **	0.15	0.86	−0.08	0.93
1.21	0.07	0.09	0.88	0.21	0.77
0.72	0.41	1.43	0.15	3.14	0.00 **
0.61	0.53	2.10	0.05	2.23	0.06
0.69	0.23	−0.01	0.99	0.69	0.43

PC1 explains 56.94% of the variation. The PC loadings of the length related dimensions are all negative for the second principal component. This means that 12.22% of the variation is more width related, varying from broader shorter faces with less protruded noses (high PC 2 loading) to longer narrow faces with more protruded noses (low PC 2 loading). The general loadings of PC 2 to 5 are relatively low, which indicates that the differences in face shape are smaller.

Table 9 PC loadings resulting from the dimension based PCA.

Component Matrix					
Face Dimensions	**PC1**	**PC2**	**PC3**	**PC4**	**PC5**
Face width	0.62	0.31	0.28	0.62	0.17
Face Length	0.91	−0.32	−0.01	0.06	−0.01
Sellion-pogonion length	0.85	−0.39	0.07	0.07	−0.09
Inter-pupillary distance	0.82	0.30	−0.31	−0.07	−0.15
Nasal root width	0.64	0.47	−0.56	−0.05	−0.04
Nasal bridge length	0.77	−0.46	−0.07	−0.08	−0.12
Nasal tip protrusion	0.75	−0.19	−0.13	−0.27	0.48
Nose width	0.73	0.17	0.36	−0.28	−0.36
Width of mouth	0.65	0.41	0.42	−0.28	0.18
Variance explained (%)	56.94	12.22	9.00	7.07	5.16
Cumulative variance explained (%)	56.94	69.16	78.16	85.23	90.39

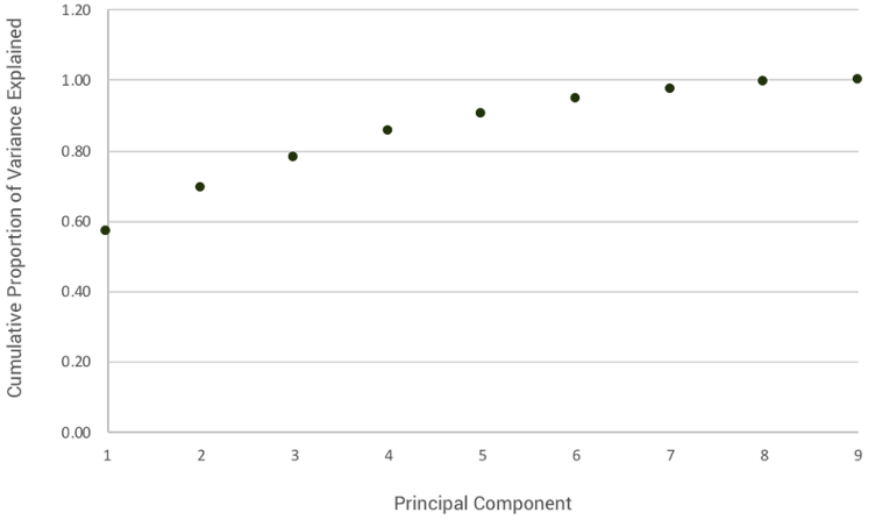

Figure 15 Plot showing the cumulative proportion of the variance explained for each PC. The first 5 PC's account for 90.39% of the total variance.

The first and second principal components' scores are calculated with the eigenvalues for each component for each participant as follows:

PC1 = 0.62 × (face width) + 0.91 × (face length) + 0.85 × (sellion-pogonion length) + 0.82 × (inter-pupillary distance) + 0.64 × (nasal root width) + 0.77 × (nasal bridge length) + 0.75 × (nasal tip protrusion) + 0.73 × (nose width) + 0.65 × (width of mouth).

PC2 = 0.31 × (face width) + −0.32 × (face length) + −0.39 × (sellion-pogonion length) + 0.30 × (inter-pupillary distance) + 0.47 × (nasal root width) + −0.46 × (nasal bridge length) + −0.19 × (nasal tip protrusion) + 0.17 × (nose width) + 0.41× (width of mouth).

3.3.3 FACE SHAPE VARIATION

A second PCA was conducted on the face area in order to investigate the shape variation of the children's faces. The PCA was conducted on the vertices of the mesh of the face area. The first seven principal component scores were extracted, which explained at least 90% of the variation of the face shapes of the sample (see Figure 16 for the cumulative proportion of the explained variance). The PC based face shape modes are visualised in Figure 17, together with the colour map, projected on the mean, which visualises the magnitude of displacement for the shape mode per PC.

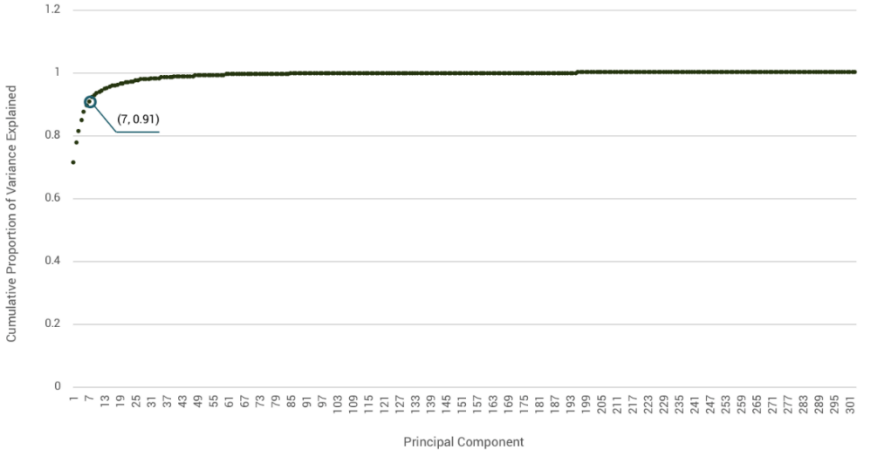

Figure 16 Plot showing the cumulative proportion of the variance explained. The first 7 PC's explain 91% of the variance.

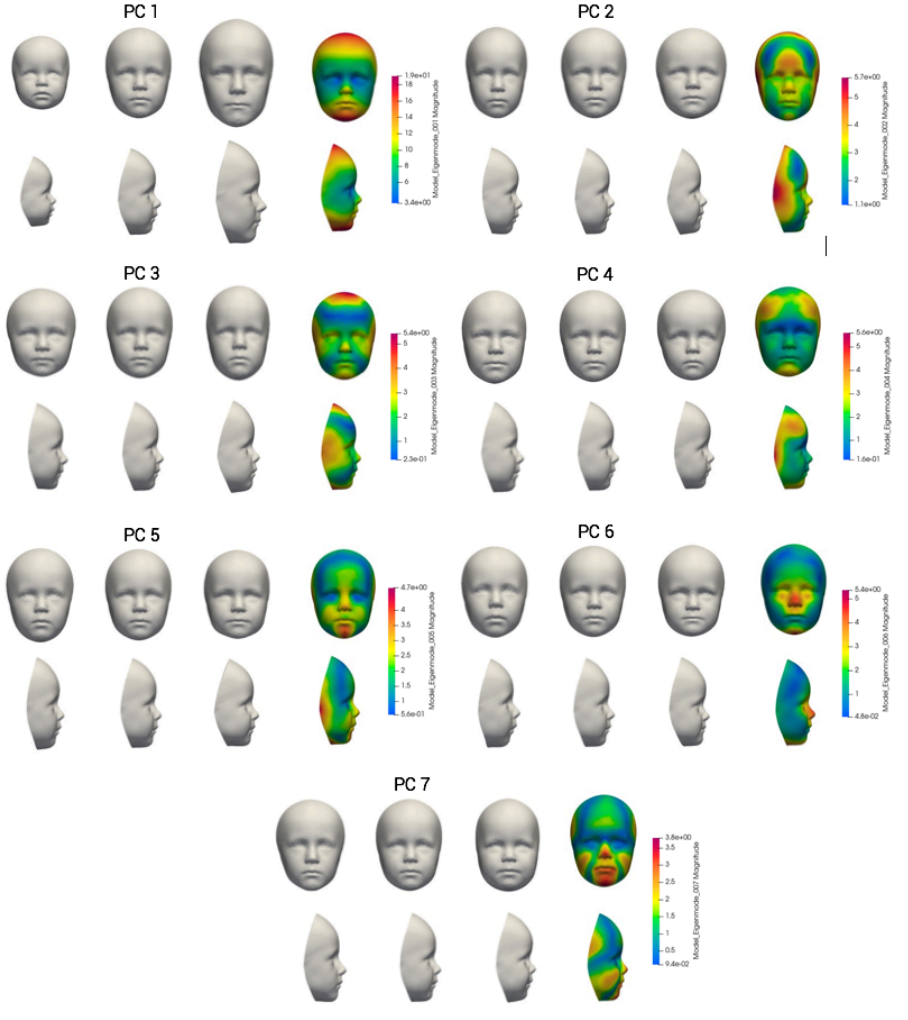

Figure 17 Visualisation of the first seven principal components. Each principal component is shown as the mean, −3 (left) and +3 (right) standard deviations together with the colour map of the magnitude of displacement (projected on the mean) of the respective principal component.

The first PC describes the variation of the overall size of the face, changing from small to large and accounts for 72% of the total variation. The second PC is related to the width of the face, varying from narrow to wide faces. The third PC is more related to the width of the forehead and the length and angle of the chin whilst the fourth PC shows the

variation of the shape of the forehead related to the shape of the jaw. The fifth component shows the variation of the shape of the jaw and the depth of the face and, for the sixth PC, the variation represents the ratio between the lower face height and the head height and variance in nasal tip protrusion. Finally, the seventh PC shows the variation in face and jaw shape and the nose and lip protrusion. The second to seventh PC respectively account for 6%, 4%, 3%, 3%, 2%, and 1% of the variability. Figure 18 shows the scatter plot of the sample along the first and second PC's including the different shape modes.

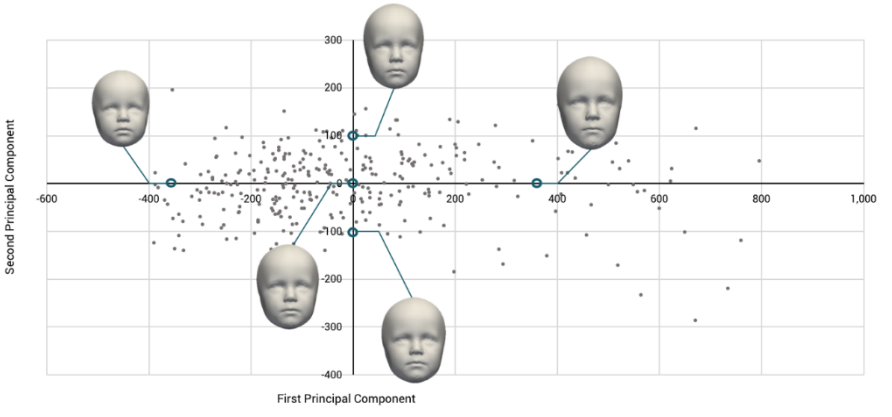

Figure 18 Scatterplot of shape based PCA including shape modes (−1.5 and +1.5 standard deviations).

3.4 DISCUSSION

3D anthropometric data of children's faces are necessary in order to develop head and face gear with a proper fit. However, detailed (3D) anthropometric data of children's heads and faces are still lacking, even though there is a clear demand from the industry (Solves et al., 2017). The aim of this study was to map the variation of the size and shape of children's faces, with a focus on the area relevant to mask design, by a multivariate and shape-based approach. An independent t-test was conducted in order to compare differences between gender. Given the relatively limited sample sizes within some age categories, the generalizability of these findings may be limited. However, efforts were made to identify noticeable patterns when examining these differences, but no significant trends were found. The results showed that only 20 out of the 252 comparisons were considered significantly different, and these differences appeared to be distributed among the dimensions. When considering anthropometric data of children of a certain age range for applications in product design, genders can often be combined because of the greater variability of different dimensions compared to the variability due

to gender (Bradtmiller, 1996). Therefore, the PCA was conducted without differentiating between gender.

In addition, the children's dataset was not classified in age groups for the PCA. When designing a product for children within a certain age range, it is often more appropriate to investigate the variability of relevant dimensions irrespective of age (Lueder & Berg Rice, 2008; Steenbekkers, 1993). There is a large variation in size amongst children within the same age group, which results in an overlap between successive age groups for most of the body dimensions (Goto, Lee, et al., 2019). In addition, the mean values and standard deviations of these body dimensions increase with age, which indicates an increasing differentiation among age groups. The differences in body shape between children of the same age will become larger and larger (Steenbekkers, 1993). Indeed, the scatterplot of the PC scores (Figure 19) shows that colours representing each age group are scattered throughout the graph, which illustrates the overlap between different age groups for multiple face dimensions.

A PCA was conducted on a selection of relevant dimensions for mask design, in an attempt to describe the morphological trend in the dataset to be used in the development of a ventilation mask. The result of the PCA describes the morphological distribution of the children's faces over an age span of 0.5 to 7 years. The first principal component describes the variation in the overall size of the face. While the PC1 score increases, the overall size of the face also increases. The second component describes the width of the face. Children with a relatively high PC 2 score have short and broad faces, whereas children with a low PC 2 score have longer and narrower faces. The findings of this study are in agreement with the study of Seo et al. (2016) who studied facial dimensions of Korean children for respirator design, where face length and face width were also found to influence the variation the strongest. Interestingly, Zhuang et al. (2007) use a similar description for the size categories of adults based on a PCA as part of his study for the development of a new fit test panel for respirators—namely, small, medium, large, short-wide and long-narrow. This suggests that the overall characteristics that describe the face variation are similar for adults; however, there is one clear difference. The relatively high scores for PC 1 in this dataset (0.623–0.907) compared to the PC 1 scores for adults (0.194–0.426) indicate that the overall size of the face varies more in children. This can be due to age differences, resulting in a relatively larger difference between the smallest face and the largest face in the children's dataset.

A shape based PCA offers an even more detailed way of investigating face shapes. By conducting a PCA on the 3D location of the vertices of each 3D face area, the face shape

variation of the dataset could be revealed. In this study, the first seven PC's were selected in order to investigate the shape variation. When determining the number of relevant principal components, a selection of components needs to be made that explain a cumulative percentage of the population. In this study, these seven PC's explain 91% of the total variation and, for most applications, a threshold between 70% and 90% is considered sufficient (Jollife & Cadima, 2016; Lacko, Huysmans, et al., 2017). The shape variation along each PC is visualized through the shape modes that were generated for the average, +3 and −3 standard deviations. Similar to the measurement based PCA, the first PC describes the variation in the overall size of the face and the second PC describes the variation in the width of the face that resembles the results of the shape based PCA conducted by Zhuang et al. (2013) and A. Luximon et al. (2012) for their study of face shape variations of U.S. civilian workers and Chinese adults, respectively. The shape variations in the remaining PC's are more subtle and contribute less to the overall variation.

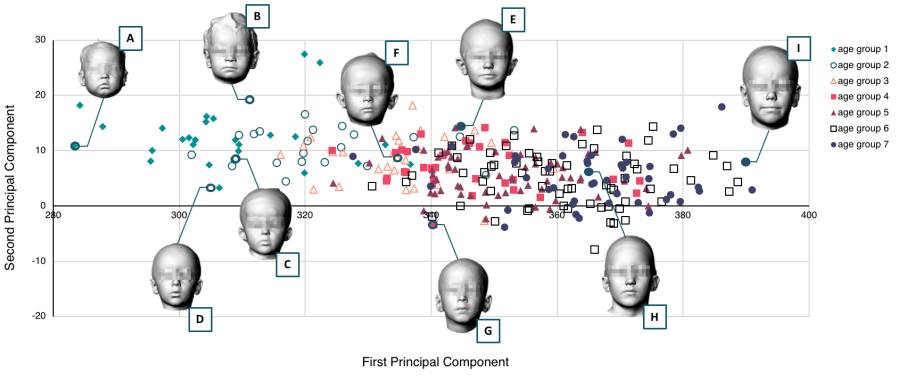

Figure 19 Scatterplot of the measurements based principal component scores including examples of different face shapes.

Apart from the shape modes that are previously presented in Figure 17 and 18, and in order to illustrate the face variation of real participants, Figure 19 shows the measurement-based PC scatterplot with a preliminary selection of 3D face scans of eight participants. A selection was made of five faces that were distributed among the PC 1-axis, including a small (A), close to average (F) and a large (I) face. Secondly, for B and C, two additional faces were selected to illustrate the differences along the PC2 axis. Next, to illustrate the variation in shape and the possible implications for the design of a ventilation mask, contours were projected on each of these faces (Rhinoceros□). Each contour passes the sellion, pogonion and approximately 10 mm distance from the left

and right cheillion landmarks. They were then aligned at the sellion landmark. These points were selected because they could represent the preliminary contour of the rim of the ventilation mask. This illustration shows that the contours indeed not only vary in size but also in shape (Figure 20). When analysing the contours from the front, we observe that, as the contour size increases, the shape varies but this does not necessarily scale proportionally. From the side, we observe that, as the contour increases in height, the depth of the contour also increases. This suggests that, when developing ventilation masks for children, one should take into account the facial characteristics as well as the size in order to achieve a good fit—for instance, by using a parametric design that is adjusted to different face shapes rather than simply scaling a product to different sizes.

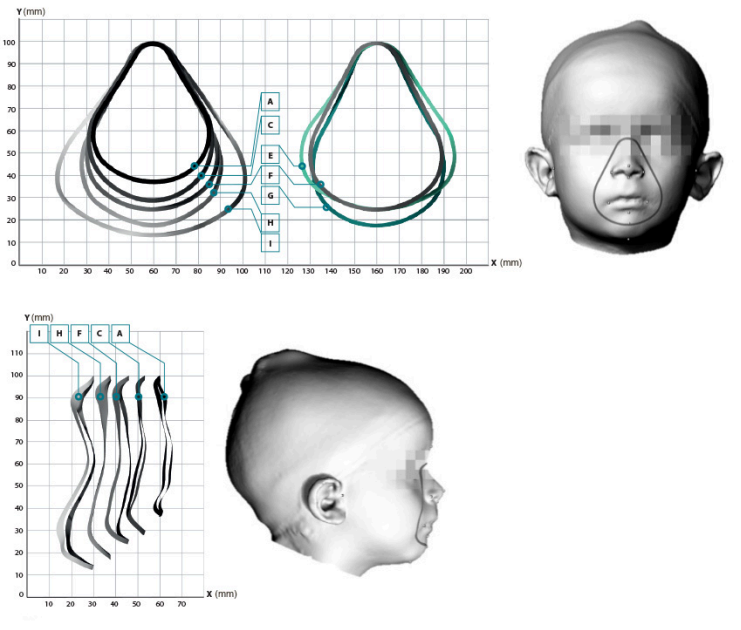

Figure 20 A comparison between contours of a facemask of children with different face shapes and sizes (mm). Lettering refers to the face examples as shown in Figure 19. Front view (top) and side view (below) and an example of a 3D scan with the contour projection (face example F).

Both the dimension and shape based PCA give insight into how the face shape of Dutch children of different age groups varies. Each method reveals this information concerning the variation in face shapes in a different way. The dimension based PCA gives insight into which product relevant dimension influences the variation of face shape and to which extent. This helps the designer to understand the relationship between the product

relevant dimensions and the face shape variation of the children in the dataset. The shape based PCA helps the designer to understand shape variation in a more visual way and shows how the face-scapes vary. The shape modes that are generated based on the analysis can facilitate the design of face related products in a Computer Aided Design (CAD) environment. For a designer of head and face related products, both analysis methods can be useful and are complementary because they facilitate in organising and presenting the complex 3D data.

However, in order for the designer to be able to conduct a PCA and get the most out of the data, they need advanced knowledge of statistics, the ability to apply custom algorithms for data processing and to translate the results of these analysis to generate shape modes and specific 3D modelling skills to be able to visualize this data. These are not necessarily all in a designer's repertoire. Nevertheless, the richness of 3D anthropometric data is an advantage when it comes to its versatility in applications, and it can therefore be applied in different phases of the product development process and for different purposes, from product design and sizing to the virtual evaluation of a product's fit using actual face scans of individuals. This shows that, despite the usefulness of 3D anthropometric data for product design, designers are faced with a dilemma. Either they have to go through the complex process of processing, analyzing, translating and visualizing data alone or with experts in order to utilize the richness that 3D Data can provide, or they have to rely on available tools whose functionality may not always align with the designers' objectives. Thus, there is a clear need to provide designers with an intuitive way to access and explore body shape variation related to their product design. One step has been made by presenting current data via the so-called Mannequin tool of the DINED platform, which is accessible through https://dined.io.tudelft.nl/en (15 May 2021) (Huysmans et al., 2020). This tool implements a regression model relating the 1D measurements to the 3D PCA scores and thus provides a means to generate and explore the variation of children's 3D head shapes.

3.5 CONCLUSION

In conclusion, the shape based PCA employed in this study offered an approach to investigate face shapes in more detail. The dimension-based PCA complemented the analysis by revealing the influence of product-relevant dimensions. The visualization of shape modes and mask contours demonstrated the variability, emphasizing the importance of considering both size and shape of the face when designing ventilation masks for children. Both analysis methods can potentially be useful for designers of head and face-related products, as they facilitate data organization, interpretation, and visualization. However, conducting a PCA and fully utilizing 3D anthropometric data requires advanced statistical knowledge, custom algorithms, and 3D modelling skills,

which may not be readily available to designers. Future research should invest in the development of anthropometric tool that allows designers to access and explore 3D body shape data for their designs.

4

A REVIEW OF APPROACHES IN THE USE OF 3D ANTHROPOMETRIC HEAD/FACE DATA IN PRODUCT SIZING: A DESIGN PERSPECTIVE

As a result of the collection and analysis of the 3D anthropometric data in the previous chapter, a deeper understanding has been created regarding the variation of children's face shapes. Nevertheless, the question remains, how is this data currently used in the development of head and face related products? And how can this information be utilized by researchers and designers as input in the sizing of a product? This chapter presents the state of the art of defining sizing systems based on a review of literature on 3D data.

4.1 INTRODUCTION

In user centred design it is essential to consider and find the right balance regarding the product, user and functional requirements. In some products a close fit is essential because the proper functioning relies on it. This means that the product size and shape need to be tailored to the user or the body part for which the product is to be designed. Anthropometric data of the target population is needed to establish this close fit between the product and the user, which is then used as input for the design and sizing of the product. In order to accommodate this target population, and for practical and economic reasons, multiple-sized products are required. Such a sizing system consists of a number of product versions that are designed based on anthropometric measurements of the target population and ideally accommodates everyone that falls within this group, trying to capture the variation in human body shape by individual sizes (A. Luximon et al., 2012).

4.1.1 ANTHROPOMETRY AND SIZING SYSTEMS

For the development of a sizing system, it is common to start with a search for existing body measurements, or when necessary, collecting new body measurements of the target population. The designer identifies which body dimensions are relevant for a specific design problem or product and conducts an anthropometric analysis to understand the ranges and variations of these dimensions within the desired sample population (Dainoff et al., 2004; Gupta, 2014; W. Lee et al., 2022). In many design problems, product dimensions often depend on several interrelated measurements of the target population. These so-called key dimensions are then used to divide the sample into groups of individuals with similar key body dimensions. Subsequently, accommodation percentage, number of sizes, size increments etc, are considered and will form the basis for determining the new sizing system (B. Lee et al., 2019).

Traditionally, anthropometric data is presented in a tabulated form, combining various body measurements and demographics of a specific sample population. Even today, most of the available anthropometric data is presented in this way. As a consequence, sizing systems are generally developed based on one or two linear measurements. The acquisition of this data is not only a time-consuming process, but it also provides the design with very limited information regarding the actual shape of the human body (W. Lee et al., 2021). This can have a negative effect in achieving a good fit which is essential for a great number of products (A. Luximon et al., 2012; Niu & Li, 2012)

4.1.2 3D ANTHROPOMETRIC DATA FOR HEAD AND FACE RELATED PRODUCTS

One category of products for which a good fit is of great importance are products designed for the head and face. The head contains some of the most important features of the human body namely the brain, eyes for vision, the nose for smell/scent, mouth for taste and ears for hearing. Products such as helmets, goggles and (protective) glasses, (protective) headphones and hearing aids, ventilation masks and respirators, all have an important purpose namely to protect, amplify, or to support one or more of these senses. These products particularly need to have a close fit to serve their purpose, as well as to be comfortable and provide safety while wearing. This close fit often comes with a challenge; detailed anthropometric data of the head and face is needed to develop a good fit and an accurate sizing system for these types of products (Bradtmiller, 2022).

With the developments in 3D scanning technologies, it is now possible to collect detailed 3D body data in an efficient way and as a result is increasingly incorporated in anthropometric surveys (Ball, 2011; Robinette et al., 1999; Zhuang & Bradtmiller, 2005). This allows designers to integrate this information in the design process by extracting relevant measurements and shape information from the 3D scans and use this as input in the sizing of the product. Three-dimensional anthropometric data of heads and faces offers the possibility to improve the existing sizing systems of head-mounted products and improve the fit and comfort. Previous research has shown that the use of 3D anthropometric data of the target population results in a more accurate and complete documentation of face and head geometry (Assessment of the NIOSH Head-and-Face Anthropometric Survey of U.S. respirator users, 2007) and its use in het sizing process leads to better fitting products (A. Luximon et al., 2012). Indeed, over the past years, literature shows an increase in use of 3D anthropometric data for the development and sizing of head and face related products. Also, the same type of 3D data has resulted in an increase in the research and development of customized products such as medical masks, helmets, helmet liners and glasses (Chu et al., 2015, 2017; Cui et al., 2022; Hovenier et al., 2022; Wu et al., 2018; Zhang et al., 2022). However, customised products might result in better fit with higher comfort, they are still more expensive in terms of production and hence it is not (yet) suited for mass production (Lacko, Huysmans, et al., 2017; A. Luximon et al., 2012). This is why the development of sizing systems remains a desirable solution for many products and it is thus essential to continue optimizing these size systems to achieve the right balance between number of sizes and optimal fit.

4.1.3 ADVANTAGES OF 3D ANTHROPOMETRIC DATA FOR PRODUCT SIZING AND DESIGN

Because of the rich nature of 3D anthropometric data, it can offer many opportunities in terms of usage and application. One advantage is that it offers the opportunity to provide information whenever needed, long after the initial data acquisition has taken place. Meaning that once the 3D anthropometric data has been collected and documented, one can revisit and reanalyse the data for different purposes at any time for the sizing or design of different products (W. Lee, Yang, et al., 2017). For instance, when design specifications change, or additional information is needed. This can be any of the traditional anthropometric measures, but also relevant shape information related to a specific product, or even new forms of measurements such as arcs, contours or 3D areas (W. Lee, Goto, Molenbroek, & Goossens, 2017). With 3D data it is possible to focus the analysis on a product related area, which results in a more complete representation of head and face geometry.

Another advantage is that the format of 3D data allows easy conversion to different formats making it easy to import in different Computer aided design (CAD) programs where it can be used to, for example, simulate product fit. So called representative models (RM's) can be generated and used in different stages of the product development process to evaluate the fit and assess sizing systems in an objective way. The advantage that 3D data offers is that 3D representative models offer a way to virtually evaluate and optimize a product and its sizing system in an early stage of the design process, before fit testing with actual people, making the design process potentially more efficient. This richness and versatility that this type of data offers, allows the designer to tailor the data to their needs which matches the innovative and visual style of thinking that designers have.

4.1.4 RATIONALE

Unlike traditional anthropometric data which is relatively simple in its use and familiar to designers, 3D data comes with some challenges. 3D data is complex and cannot be used directly as input for the design (Gupta, 2014; Lacko, Huysmans, et al., 2017; Meunier et al., 2009). The 3D scans consist of a large number of data points which need processing and proper analysis. Therefore, the integration and use of 3D anthropometric data can have a significant impact on the design process and ultimately the sizing methods. There are multiple strategies to process, analyse, extract relevant information from 3D data and use it for design and product sizing. In addition, there is no clear standard for sizing in general and companies and researchers tend to develop their own sizing systems because of that (A. Luximon et al., 2012). Moreover, sizing systems based on 3D anthropometric data results in even more methods for sizing system

development. Even though there are similarities, some of the practical approaches are different compared to the traditional sizing methods with which designers and ergonomists are familiar with. This large variety of strategies and potential outcomes can lead to an ambiguity which makes it difficult for designers to apply 3D data in their current design practices.

Currently, to the author's knowledge, there is no overview of approaches for developing sizing systems based on 3D anthropometric data. And there remains a gap between 3D anthropometric data and the application in the design process (Ball, 2009; Dianat et al., 2018; Gupta, 2014; W. Lee et al., 2021; Y. Luximon et al., 2012; Niu & Li, 2012). In order to provide an overview of methodologies and approaches, a review has been conducted by Dianat et al. (2018) on the use of anthropometry in the design of products and environments in general. And Shah and Y. Luximon (2018) explain and analyse techniques and methods that are used in the development of 3D head and face models for product design in their literature review. But none have investigated the different approaches used in the application of 3D head and face data in product sizing. And therefore, the purpose of this paper is to provide a comprehensive overview of the current state of defining sizing systems for product development based on 3D data, specifically focusing on 3D head and face data. The paper aims to provide an overview of the different approaches used and the practical and statistical considerations made in the development of a sizing system based on 3D anthropometric data for product design.

4.2 METHOD

4.2.1 SEARCH STRATEGY

The literature search was performed in the electronic databases PubMed and Scopus. In order to identify potentially relevant articles the following sets of terms were searched for in the article title, key words and abstract (exact search terms between brackets): Anthropometry (Anthropometry or Anthropometric or "morphological variation" or morphology), 3D (3D or "three-dimensional"), Product Design (design or product or "product design" or equipment or "protective devices"), Sizing (size or sizing or cluster or "fit mapping") with a focus on head and face related products (head or face). The last search was conducted on February 8, 2023.

4.2.2 INCLUSION CRITERIA

Articles that were included in this review met the following criteria:

1. The paper describes a study with a head/face related product design application with the aim of product sizing excluding studies focussing on customized, personalized, or tailor-made head and face related products.

2. The data that is studied in the paper is acquired through 3D scanning technologies.
3. The paper describes the application of 3D anthropometric head/face data in product design or sizing system development rather than the presentation, processing, analysis, and descriptive statistics of 3D anthropometric head/face data only.
4. The paper is available, written in English and published after 1995.

Two researchers reviewed the abstracts independently in order improve the objectivity and accuracy of the selection process of the studies. Differences in opinion were discussed and in case of doubt the paper was included for full text review.

4.3 RESULTS

Search results from Scopus and PubMed databases resulted in a total of 379 records (145 from Scopus and 234 from PubMed) of which 52 studies were selected as potentially relevant; of these, 17 studies met the inclusion criteria and another 5 were added from reference screening resulting in a total of 22 selected articles that were included in the review (figure 21). The selected studies are summarized in Table 10.

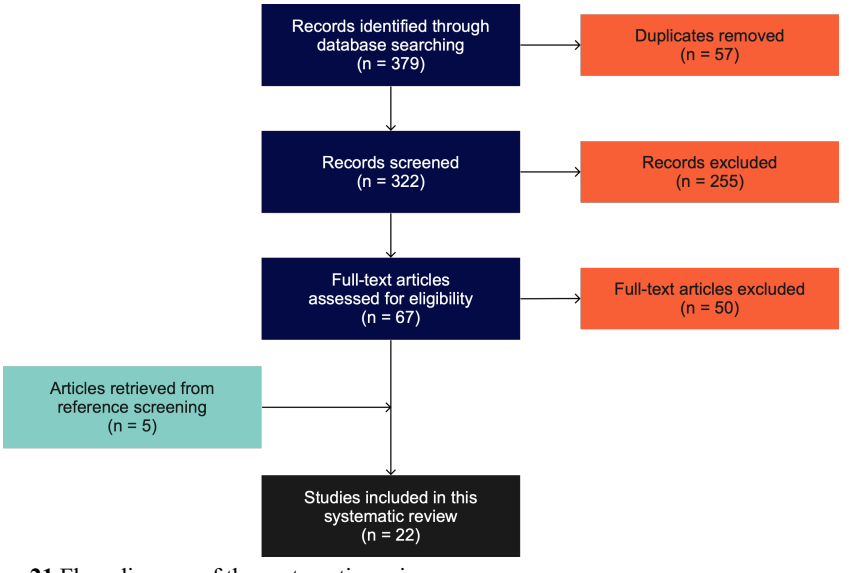

Figure 21 Flow diagram of the systematic review.

This review identified different approaches in the development of a sizing system based on 3D anthropometric head or face data. And in each approach roughly six steps could be identified that relate to the six-step paradigm for anthropometric design described by

Hsiao (2013). The sequence of the activities has been adjusted to align them with how they are presented in most of the studies and are as follows.

1. Determine the target population.
2. Collect or get access to relevant anthropometric data of the target population.
3. Determine the body dimensions that are essential for the design.
4. Determine the accommodation percentage of the target population.
5. Compute or analyse the data.
6. Product dimensioning/sizing system development.

The results have been organized following this structure and can be described as follows. First the 3D anthropometric data of the target population that are used in the different studies and how they are collected and processed is discussed in section 4.3.1 (step 1 & 2), followed by which and how product relevant information was selected from the 3D data and analysed for sizing (section 4.3.2) (step 3, 4 & 5). Then, section 4.3.3 presents how this product relevant information is used for product sizing (section 4.3.4) (step 6). Often, when 3D anthropometric data is used in the sizing process, so-called, representative models (RM's) or mannequins are generated. In section 4.3.4, these models, that were presented or generated as part of some of the included studies is presented. Finally, the different approaches are discussed from a design point of view, gaps are identified and opportunities for further research are presented. A summary of these steps and how they are organised in this chapter are depicted in the flowchart in figure 22.

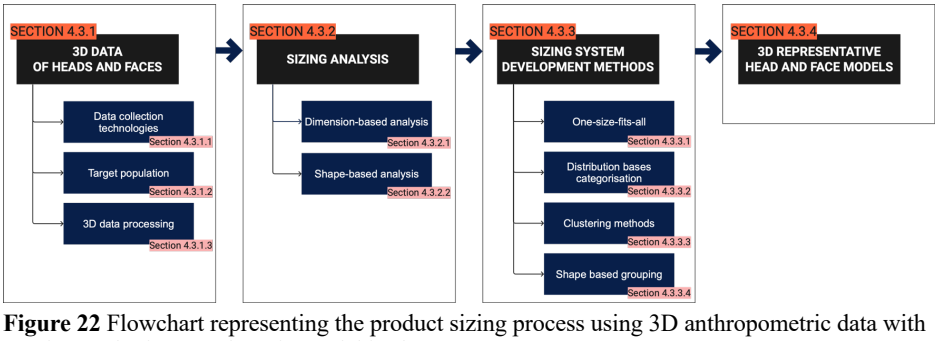

Figure 22 Flowchart representing the product sizing process using 3D anthropometric data with numbers referring to subsections of this chapter.

Table 10 Overview of studies that use 3D anthropometric head/face data in product sizing.

Study	Design application	Target population	Sample size (N)	Nationality	Age range	3D technology
Bradtmiller (1996)	Bicycle helmet	Children	1035	US	2y – 18y	3D scanning
Kouchi and Mochimaru (2004)	Spectacle frames	Adults	56	JP	18y – 35y	Plaster model + 3D digitizer, 3D scanning
Godil (2009)	Head and face related products	Adults	200	US/EUR	18y – 65y	3D scanning
Meunier et al. (2009)	Helmets	Military	611	CA	-	3D scanning
Niu, et al. (2009)	Head and face related products	Adult	378	CN	19y – 23y	CT scanning
Zhuang, Benson and Viscusi (2010)	Respirator (half and full face)	Working population	1013	US	18y – 66y	3D scanning
Hsiao (2013)	Respirator (full face)	Fire fighters	951	US	18y – 65y	3D scanning
Yu et al. (2012)	Respirator (half/full face)	Working population	350	CN	18y – 66y	3D scanning
Wuhrer, Shu and Bose (2013)	Glasses	Adults	50	US/EUR	18y – 65y	3D scanning
	Helmets	Adults	1500	US/EUR	18y – 65y	3D scanning
Amirav et al. (2014)	Face mask (half face)	Children	271	Western	1m – 4y	3D scanning
Bolkart et al. (2015)	Face mask (half face)	Adults	101	Various ethnicities	-	Dynamic 3D scanning
Y. Luximon, Ball and Chow (2016)	Head and face related products	Adults	144	CN	18y – 30y	3D scanning
Seo et al. (2016)	Respirators (half face)	Children	144	KR	5y – 13y	3D scanning
Skals et al. (2016)	Bicycle helmet liner	Adults	122	AU/NZ/ EU/AS	24y – 47y	3D scanning
Ellena, et al. (2017)	Helmets	Adults (Cyclists)	117	AU/EU/ AS/other	18y – 65y	3D scanning
Lacko et al. (2017)	EEG headset	Adults	100	Western	20y – 30y	MRI
Lacko et al. (2017)	Head related products	Adults	100	Western	20y – 30y	MRI
Lee et al. (2018)	Head and face related products	Adults	2299	US/EUR	18y – 65y	3D scanning
Amirav et al. (2019)	Medical devices (Respimometer)	Children	287	CD	5m – 5.5y	3D scanning
Goto et al. (2019)	Ventilation Mask	Children	302	NL	6m – 7.5y	3D scanning
Kuo et al. (2020)	Head and face related products	Adults	1010	TWN	18-33y	3D scanning
Lee et al. (2022)	Face mask	Adults	336	KR	-	3D scanner

Table 10 (continued).

3D Data	Extracted data for sizing	Sizing Analysis	Sizing method
Head and face	Measurements (2)	Bivariate distribution analysis	Bivariate based grouping
3D models of the face	3D face area	MDS	MDS grouping
Full body scans (CAESAR)	3D Face area	PCA	K-means clustering
Head and face scans	3D head/face shape, measurements (2)	PCA	Bivariate/PC-based
Head and face scans	3D head shape, measurements (2)	Bivariate, PCA, other	K-means clustering
Head and face scans	Measurements (10)	PCA	Fit test panel based
Head and face scans	Measurements (2)	Bivariate distribution	Fit test panel based
Head and face scans	Measurements (10)	PCA	Fit test panel based
Face scans (CAESAR)	Measurements (2)	Bivariate	Other (greedy covering algorithm
Head scans (CAESAR)	Measurements (3)	Multivariate	Other (greedy covering algorithm
Face scans	Measurements (2)	Bivariate	K-means clustering
3D motion database of faces	Measurements (2-6)	Bivariate and multivariate	Other (Box stabbing technique)
Head and face (SizeChina)	Measurements (1)	Univariate	Percentile selection
Face scans	Measurements (16)	Multivariate	Hierarchical clustering
Head and face scans	37 landmarks	Shape	Other
Head and face scans	Head shape area	Shape	Modified hierarchical clustering
MRI head scans	Landmarks	PCA	Other
MRI head scans	Measurements (10), Shape model	PCA	K-medoids clustering
Head and face (CAESAR)	Measurements (1/2)	Univariate, bivariate	K-means clustering
Face scans	Measurements (2)	Bivariate	K-means clustering
Head and face	Measurements (2, 9) and 3D face area	Bivariate, multivariate and shape	K-means clustering
Head and face	Measurements (40)	PCA	K-means clustering
Face scans	Measurements (2)	Bivariate distribution analysis	Bivariate based grouping

4.3.1 3D DATA OF HEADS AND FACES

Depending on the application, both full head scans (including both the head and face) (Bradtmiller, 1996; Goto et al., 2021; Hsiao, 2013; Kuo et al., 2020; Lacko, Huysmans, et al., 2017; W. Lee, Lee, et al., 2018; Meunier et al., 2009; Niu, Li, & Salvendy, 2009b; Yu et al., 2011; Zhuang, Benson, et al., 2010) and face scans (Amirav et al., 2013, 2019; Coblentz et al., 1991; Kouchi & Mochimaru, 2004; W. Lee et al., 2022; Seo et al., 2016) are collected or used in the different studies. In one study, 3D face scans with different facial expressions were included in a study for the development of a face mask (Bolkart et al., 2015). Depending on the target population, the application/product, required quality, available budget, different scanning techniques are used to collect the head and face data.

4.3.1.1 Data collection technologies

Collecting 3D anthropometric data of heads and faces can be accomplished in different ways and has increasingly become part of anthropometric surveys and product development processes. Often, studies combine traditional techniques and 3D scanning technologies to acquire anthropometric data (Bradtmiller, 1996; Coblentz et al., 1991; Kouchi & Mochimaru, 2004; Y. Luximon et al., 2016; Yu et al., 2011; Zhuang, Benson, et al., 2010). 3D data collection is conducted using different techniques such as, 3D laser scanning technologies (Godil, 2009; Kuo et al., 2020), 3D photogrammetry (Goto, Lee, et al., 2019), structured light technologies (Amirav et al., 2013, 2019; Seo et al., 2016), Medical Computerized Tomography (CT) (Niu, Li, & Salvendy, 2009b) and Magnetic Resonance Imaging (MRI) (Lacko, Huysmans, et al., 2017; Lacko, Vleugels, et al., 2017). Kouchi and Mochimaru (2004) used a 3D digitizer to scan plaster models of the faces of participants in their study. Bolkart et al. (2015) used a dataset with 3D faces including facial expressions that were captured employing a so-called dynamic 3D scanning technique. With this technique multiple scans are taken of the face while the scanned person follows a sequence of facial expressions.

4.3.1.2 Target population

The type of 3D anthropometric data that is used in the studies varies in terms of the target population that is included in the survey and whether the researcher collected their own data or made use of existing datasets. Depending on the applications and the target population of the product to be developed, one can search for available and suitable 3D anthropometric datasets, or a survey needs to be set up to gather data. Common factors to take into account when defining the target population for a specific design purpose are gender, age, nationality (ethnicity) and occupation (Pheasant & Haslegrave, 2006).

Gender

In the reviewed papers most of the surveys included both male and female participants (Amirav et al., 2013, 2019; Bradtmiller, 1996; Ellena et al., 2018; Goto, Huysmans, et al., 2019; Hsiao, 2013; Lacko, Huysmans, et al., 2017; Lacko, Vleugels, et al., 2017; W. Lee, Lee, et al., 2018; Y. Luximon et al., 2016; Meunier et al., 2009; Seo et al., 2016; Skals et al., 2016; Yu et al., 2011; Zhuang, Benson, et al., 2010). In some however, only male participants were recruited (Kouchi & Mochimaru, 2004; Kuo et al., 2020; Niu, Li, & Salvendy, 2009b) or no gender specification was mentioned at all (Bolkart & Wuhrer, 2013; Godil, 2009; Wuhrer et al., 2012).

Age

In anthropometric surveys, age specification of the participants is an essential part of the presented demographics. As many of the reviewed papers focus on adults or the working population, participants within the age range of 18 – 66 years are often included in the studies. The remaining studies focus on children, describing an age range anywhere between 5 months – 18 years. Two studies did not specify the age range of the dataset they used (Bolkart et al., 2015; Meunier et al., 2009).

Nationality/ethnicity

Apart from gender and age, ethnicity has a significant effect on the variation of head and face shape too (Ball et al., 2010; Farkas et al., 2005; Zhuang, Landsittel, et al., 2010). For some products it might be relevant to distinguish between ethnicities or map differences between different ethnicities for product design. For instance, in helmet design, the shape of the helmet that is developed for Caucasians, who generally have an oval shaped head, will often not properly fit an Asian person who has a rounder head shape (Ball et al., 2010).

General (civilian) population

Previously, detailed extensive anthropometric surveys were conducted by the military who would have the recourses and the urgency to collect this data for the development of protective gear. Anthropometric data of the general population however is still not largely available and varies per country and target population. Developments in the field of 3D scanning technologies offers a more efficient way of collecting anthropometric data. More and more large- and small-scale surveys that incorporate 3D scanning technologies are initiated worldwide to collect data of the general population.

Adults

The data that is collected as part of the CAESAR (Civilian American and European Surface Anthropometry Resource) project is used in many studies (Godil, 2009; W. Lee et al., 2015; W. Lee, Lee, et al., 2018; Robinette et al., 1999, 2002; Wuhrer et al., 2012).

This CAESAR project was the first survey that collected anthropometric information including 3D full body scans, in three different postures, of all participants (N=4431) on a large scale, targeting civilian populations of the Unites States of America, The Netherlands and Italy. Depending on the application, the head (W. Lee et al., 2015; W. Lee, Lee, et al., 2018) or face area (Godil, 2009; Wuhrer et al., 2012) is separated from the full body scan before analysis.

A database of more than 2000 head scans of Chinese adults was set up as part of a large-scale 3D anthropometric survey named SizeChina (Ball & Molenbroek, 2008). Y. Luximon et al. (2016) developed 3D head templates of Chinese men and women for designers based on this dataset to be used for the development of better fitting head and face related products.

Data is collected on a smaller scale whenever specific data of a target population is not readily available or when there is a need for a detailed scans of a specific area of the body. One example is the study by Kouchi and Mochimaru (2004) for which they generated 3D face models of Japanese adult men (N= 56) with a focus on the upper face for spectacle design. In another study, MRI scans that were obtained from the International Consortium for Brain Mapping (ICBM) database (Capetillo-Cunliffe, 2007) were used as input for the studies that Lacko et al. (Lacko, Huysmans, et al., 2017; 2017) conducted. In another study, Kuo et al. (2020) collected 3D head data of 1010 Taiwanese male adults for their study to establish an anthropometric database for the Taiwanese population. In some cases, facial expression might be relevant to be included in a study. For instance, to analyse the effect of facial expressions on mask sizing. This is what Bolkart et al. (2015) investigated in their study for which they used the motion data of the so-called BU-4DFE database (Yin et al., 2006), which contained 100 participants performing seven expressions (neutral, happiness, disgust, fear, anger, surprise and sadness) in four levels of intensity, resulting in 2500 shape models.

Children

In general 3D anthropometric data is becoming more available but the availability of 3D anthropometric data of children is still limited. Bradtmiller (1996) collected 3D full head scans of 1035 children aged 2 to 18 years to define a sizing system for bicycle helmets. Amirav et al. (2013) collected face scans of 271 children aged 1 month to 4 years for the design of an aerosol face masks, and in another study (Amirav et al., 2019) he analysed the face scans of 287 Congolese children aged 1 month to 5.5 years for the development of medical devices. The faces of 144 Korean children aged 5 to 13 years were scanned by Seo et al. (2016) in order to develop respirators. Goto et al. (2019) collected 3D full head scans of 302 Dutch children aged 6 moths to 7 years old to analyse face shape variation for the design of ventilation masks for children.

By Occupation

Army personnel

As mentioned, many of the first large scale anthropometric surveys focused on army personnel for the development and sizing of their clothing and equipment (Gordon et al., 2014; Gupta, 2014). Meunier et al. (2009) incorporated 3D head scans in their study that were collected as part of the Anthropometric survey of Canadian land forces (N=708). The survey was conducted in 1997 (Chamberland et al., 1997) for which a subset of 611 individuals (243 females, 465 males) underwent a 3D head scan. 3D head data of young male Chinese soldiers (N=378) (all male) were acquired through CT scanning technology in order to size military helmets by (X. Chen et al., 2002). This same data was analysed by Niu et al. (2009b) as part of a study in which they develop a new sizing method that can be used in the development of head and face related products.

Working population

Another large-scale anthropometric study that incorporated 3D scanning, was initiated by NIOSH's (National Institute for Occupational Safety and Health) National Personal Protective Technology Laboratory. The goal of this survey was to develop an anthropometric database of heads and faces representing civilian respirator users such as, fire fighters, people in law enforcement and health care workers (N=1013). Next to traditional measurements, 3D scans were collected of a subset that included 1013 participants (Zhuang & Bradtmiller, 2005). Zhuang et al. (2010) used these 360º scans of the heads and faces representing the U.S. working population of respirator users in his study. A similar study for NIOSH, involving only firefighters, was initiated by Hsiao et al. (2013; 2014). In order to improve firefighters' protective equipment such as respirators, 951 (88 females, 863 males) U.S. firefighters participated in a survey to collect anthropometric data including facial dimensions that were extracted from head and face scans. The extracted facial dimensions were studied in order to investigate the need to revise the existing NIOSH respirator test panels and respirator sizing schemes to improve fit. Yu et al. (2011) used 3D head and face data of 350 Chinese workers that were collected as a subset of an anthropometric survey (Du et al., 2008) employing traditional measuring techniques (N=3000) in his study to analyse sizing categories for half and full-face respirators.

Sports

The data that were used in both Ellena et al. (2018) and Skals et al. (2016) studies were part of the 2014 "3D anthropometric Database of Australian Cyclists" (N=222) (46 females, 176 males) (Perret-Ellena et al., 2015) from which 200 participants were

included in Ellena's study and 122 (101 males, 21 females) were included in Skals et al. research for the optimization of helmet design and fit.

4.3.1.3 3D DATA PROCESSING

Once the 3D scans are obtained, the data needs to be cleaned, aligned and in some cases a surface correspondence needs to be established. This often depends on the 3D scanning technology that is used, the scanning set-up and the quality of the scans. Each 3D face/head scan will be acquired and saved in the form of a point cloud. This original 3D human scan data (point cloud) commonly consists of unwanted data points (noise) or missing data points (holes) and needs to be processed. These processing steps are needed before the data can be used for product sizing. Each processing step will be explained in the following sections and is illustrated by the studies that are included in the review.

Point-cloud and mesh processing

Processing of the data often consists of registration (combining point cloud data resulting from a 3D scanner that consists of two or more cameras from different angles), merging (combining scans), and removing noise. Noise can be the result of scanned clothes, part of the chair the participant is sitting on or any other unwanted part of the scan. In addition, holes often appear in regions that are not properly captured because of the scanning range or angle (e.g., top of the head, ear region, nostrils) or the presence of hair. Finally for visualisation and further processing, each point (vertex) in the point cloud is connected to form the 3D surface or so-called mesh which is built up out of triangular faces (figure 23). This surface often still consists of holes or irregularities and so may require post processing such as hole filling and smoothing. This is often done by hand (Niu, Li, & Salvendy, 2009a) by reviewing each individual scan and can be a time-consuming exercise (W. Lee et al., 2015). However, automated algorithms that fill the data points by extrapolating the curvature continuity of a template mesh around the missing area (Ellena et al., 2018) is becoming increasingly common and can be provided by 3D data processing software. Hair bumps and fabric folds can be corrected by decreasing the angles between individual polygons (Skals et al., 2016) and surfaces sometimes need smoothing after, for example, when merging multiple scans. Finally, depending on the application, the 3D area of interest needs to be separated from the rest of the 3D scan (Godil, 2009; W. Lee, Lee, et al., 2018; Niu, Li, & Salvendy, 2009b; Wuhrer et al., 2012).

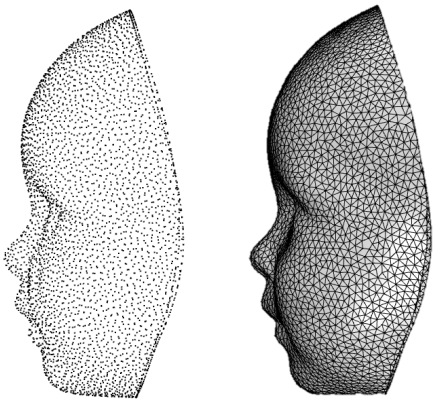

Figure 23 Example of point-cloud (vertices) (left) and meshed surface consisting of triangular faces (right)

Alignment of mesh coordinates

In order to extract, compare and analyse relevant data, individual scans sometimes need to be aligned to a common coordinate system. Often, 3D scans have different orientations caused by the variation in posture or positioning of the participant related to the 3D scanner. Aligning the 3D head scans can be done in various ways depending on the type of data and its purpose. For instance, in some studies the data is aligned according to the design application, others use more general anthropometric features to align the data. The various approaches that were identified in the studies are described here.

Reference plane

If the 3D scan data needs to be aligned, this is often done through the use of a reference plane. For example, the Frankfurt plane is often used to align head data (Kuo et al., 2020; Y. Luximon et al., 2016; Zhuang, Benson, et al., 2010). The Frankfurt horizontal plane passes through three landmarks; left infra orbitale and left and right tragions (figure 24.). Zhuang et al. (2010) and Yu et al. (2011) use the Frankfurt plane combined with a vertical symmetry plane for alignment. However, they aligned the scans after the sizing system development for the purpose of developing head models that represent each size category. Others make use of a plane which is related to the product to be designed. Such as in the case of Bradtmiller et al. (1996) who uses a segmentation plane that represents the bottom edge of a standard bicycle helmet in order to analyse and compare the head shapes. Skals et al. (2016) use three planes spanning key dimensions of the head that are considered relevant to helmet design, to align their head scans to a generic axis system.

The three planes they used were the head circumference-plane, saggital arc-plane and the bi-tragion coronal arc-plane.

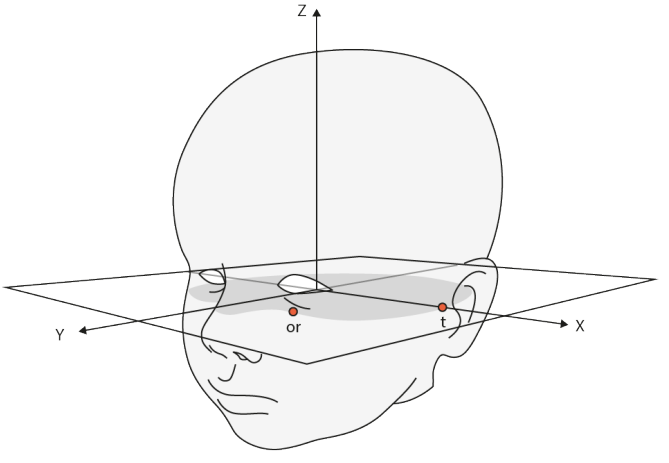

Figure 24 Frankfurt plane with landmarks depicted: infra orbitale (or) and tragion (t).

Landmarks

Another way of aligning the scans is through multiple landmarks. For instance, Godil et al. (2009) makes use of four landmarks located on the face to position and align the 200 face scans for his study. Wuhrer et al. use the 73 landmarks (whole body) that were manually placed and recorded on the 3D scans of each participant of the CAESAR database for their alignment process. Kouchi et al. (2004) employ the homologous shape modelling method of which you could say that it is a step towards data parametrization (see section “data parametrization”). Here the goal is that each body part is represented by the same number of data points of the same topology for each individual 3D scan and each data point is based on a specific (anatomical) landmark. Here Kouchi et al. (2004) developed a so-called homologous model based on both anatomical landmarks and landmarks that are related to the product to be designed, in this case spectacle frames resulting in a total 61 landmarks. Subsequently, virtual landmarks (also called pseudo or mathematical landmark) were added between each two landmarks in order to describe the shape, resulting in a total of 211 data points covering each face model. A similar approach was employed by Y. Luximon et al. (2016) using both 54 anatomical landmarks and 130 virtual landmarks to create full correspondence between each individual scan (Y. Luximon et al., 2012).

Head/facial features

In other cases, facial features such as the nose and mouth, that are recognizable by its location and distinct shape in all face scans serve as a good reference for the alignment

of 3D face scans. Other studies employ an algorithm called iterative closest point (ICP) to align the scanned meshes. The algorithm iteratively matches the orientation of the geometric structure of each 3D face or head based on facial features such as eyes, nose and mouth (Amirav et al., 2013, 2019) or a proportion of the head (Ellena et al., 2018) and minimizes the alignment error or distance between each mesh. It is a so-called rigid transformation method which means that the meshes and vertex locations remain the same and only adjusts the orientation (rotation, translation in 3D space) of each 3D face scan. In another study, (Niu, Li, & Salvendy, 2009b) the centre of mass, combined with an anatomical feature (nose tip) is used as a starting point to align all scans. First the centre of mass of each head was calculated, then the 3D scans were aligned by translating the centres of mass to the origin in a cartesian coordinate system. This coordinate system was defined by the Z-axis pointing towards the top of the head, the y-axis pointing from centre to the nose and finally, a vector on the X-Y plane running through the centre and pointing towards the nose-tip.

Other

In some cases, often when shape information is initially not considered, the 3D scans do not need to be aligned because the data that is used for the analysis and sizing system development are extracted from the scans directly. In other cases, the measurements that are selected and used as input for the analysis and sizing are directly extracted from the scans (Hsiao, 2013; W. Lee, Lee, et al., 2018; Seo et al., 2016; Yu et al., 2011; Zhuang, Benson, et al., 2010). In this case, the alignment of the scans is not a necessity. Or in other cases, the alignment step is completely skipped and the correspondence procedure (see next paragraph) is directly initiated.

Data parametrization

After the alignment of the data and before any statistical shape analysis or comparison can be made within the 3D dataset, a surface correspondence needs to be established between each individual 3D scan because the heads and faces of the scanned individuals vary in size and shape. As a result, each scan consists of varying amounts of data points (vertices) that are distributed in different ways. The goal of creating correspondence is that data points in the point cloud or in the mesh structure (triangles) of the scan are evenly distributed, that the amount of data points are the same and that they are located at corresponding anatomical locations. After this remeshing process, vertices located in the same landmark locations have corresponding indices which will facilitate the analysis. There are different approaches in achieving this topological correspondence.

Parameterization based correspondence

Lacko et al. (Lacko, Huysmans, et al., 2017; Lacko, Vleugels, et al., 2017) use a so-called group-wise correspondence optimization procedure to process their dataset of 100

head surfaces that were obtained from MRI scans (Huysmans et al., 2010; Lacko et al., 2015). This is done by, after achieving initial correspondence and optimizing the correspondence through a non-rigid transformation, calculating an average head with 10000 points evenly distributed over its surface. This average head is subsequently used to achieve full correspondence resulting in 100 head surfaces with uniformly distributed point sets of 10000 points at corresponding locations.

Template Model Registration

After an initial alignment through landmarks, Meunier et al. (2009) and Wuhrer et al. (2012) use a template model and additional automatically generated virtual landmarks to parameterize the 3D scans by using the approach as described by Xi et al. (2007). A similar approach called hybrid template registration method (W. Lee, Goto, Molenbroek, & Goossens, 2017) is used by Goto et al. (2019). A template model or generic model is a representative (average) 3D model that resembles the dataset and consists of a reasonable number of vertices and is oriented in the required position. A mesh deformation algorithm is employed to align each individual scan to this template model and subsequently a 3D image registration technique is used to achieve full correspondence by deforming the template model for each scan. The non-rigid Iterative Closest Point (ICP) is such a registration algorithm and is used by a number of studies in this review (Amirav et al., 2019; Ellena et al., 2018).

4.3.2 SIZING ANALYSIS

There are different strategies to size a product. And even though in all studies 3D data was used with the purpose to size a product, 3D (shape) information was not always used. Traditionally sizing systems are defined by determining product related key dimensions and studying the variation of these key dimensions. Depending on the product and its complexity, the number and type of key dimensions is determined based on previous sizing systems, studies in literature or ergonomic and product development experience. The type of key dimensions that are selected are often related to its relevance to the design but has a practical application. Namely, when selecting the appropriate size of a certain product, it is beneficial to select dimensions that are easy to measure to make sure that they provide a good reference to, for instance, the shop owner to assign a person to the appropriate sizing category.

In order to translate the extracted data into a sizing system or product dimensions, the relevant data in the form of key dimensions or shape information needs to be analysed to understand the variation of key dimensions or surface area of the target population. The analysis of the anthropometric data and the sizing system development method often depend on the type of data that is taken into consideration and the determined accommodation percentage. The different methods can be categorised under dimension-

based analysis methods which focus on the analysis of the variation of product related key dimensions and shape-based analysis methods that focus on the shape variation of the body part or area of interest. These different approaches will be explained next.

4.3.2.1 Dimensions-based analysis

Univariate analysis using a single key dimension

Traditionally, sizing systems are based on a few key dimensions (Wuhrer et al., 2012). And for some design problems even a single key body dimension might be sufficient. When one single anthropometric measurement is considered as relevant for a certain design, means, standard deviation and histogram are studied to determine the distribution and variation of this key dimension. Y. Luximon et al. (2016) selected face width as a single key dimension for determining size categories for mask design (figure 25). In this study, one dimension was considered sufficient since the dimensions of the human head are positively correlated, and the largest variation exists in general head size. Here the dimensions are extracted from the 3D data by calculating the distance between predefined landmarks or vertices. They then study the frequency distribution graph of the face width of Chinese people. In the sizing tool developed by Lee et al. (2018) the user can select one or more key dimensions in order to study the frequency or distribution of the dimension(s) before creating a sizing system.

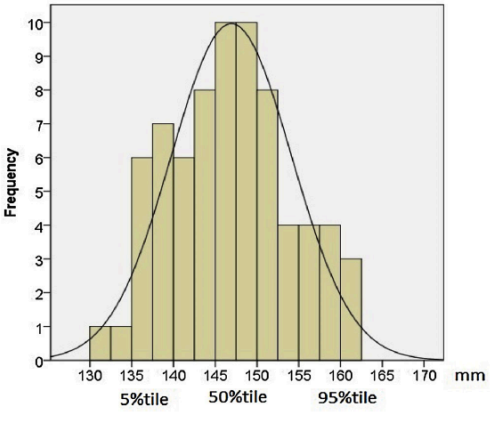

Figure 25 Frequency distribution of face width of female participants (Y. Luximon et al., 2016)

Bivariate analysis using two key dimensions

When two dimensions are deemed relevant for product sizing, distribution analysis with the two key dimensions along the two axes are studied. Often, the selection of key dimensions is based on previous research on the sizing or fit analysis of the same or a similar product, or existing sizing systems are combined with the (ergonomic) design

experience of the researchers, or the input of experts is included in the study. For example, in the sizing tool that Lee et al. (2018) developed, a designer can select one or two key dimensions to study the distribution and determine the sizing categories depending on the product to be designed. Indeed, developing a sizing system based on two product related key dimensions is a more common practice. For the development of products such as helmets, full face and half face respirators, considering two key dimensions as input for the analysis is common. Based on available literature, expert advice and/or experience from the field, key dimensions are determined. These key dimensions often encompass the width and length of the wearable to be designed.

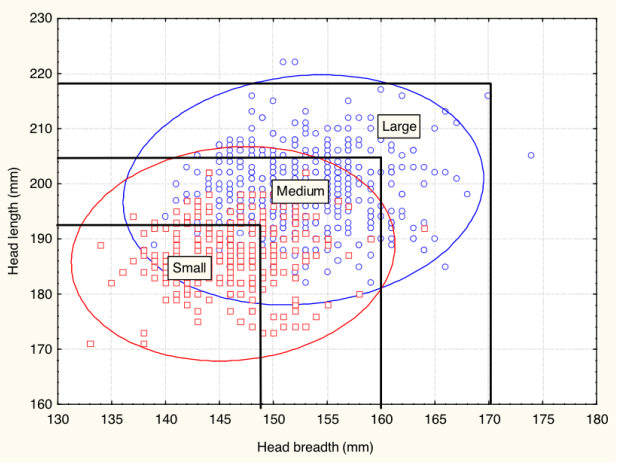

Figure 26 Example of bivariate plot of a proposed helmet sizing system for both male (blue) and female (red) populations based on head breadth and head length (Meunier et al., 2009).

Bradtmiller (1996) for instance, uses head length and head breadth in the development of a sizing system for helmets for children. According to the author these dimensions are good predictors of the variability of other head dimensions as well. Meunier et al. (2009) and Niu et al. (2009b) use these same two key dimensions as the basis for the development of a helmet sizing system for adults (figure 26). Hsiao (2013) analysed face length and width to update the sizing system for firefighter masks. Lee et al. (2022) used the bivariate distribution of sellion-to-supramentale length and lip width as a starting point for their sizing system for face masks for pilots. In their research on the sizing of medical aerosol masks for children, Amirav et al. (2013) identified two key dimensions: the distance between the nose bridge and the tip of the chin, and the width of the mouth. They concluded that these dimensions were strong predictors of whether the mask would create a proper seal on the face. Additionally, the length between the nose bridge and chin tip varies significantly during early life due to the impact of growth,

which further emphasizes the importance of these dimensions in determining the appropriate fit of the mask. Similarly, Goto et al. (2019) selected mouth width and sellion-pogonion length as input for the analysis of face mask sizing. Bolkart et al. (2015), used these same dimensions as input for his study to explore the dynamic movement and sizing system for a face mask. For a study involving sizing glasses, Wuhrer et al. (2012) looked into the variation of the dimensions, width of face and width of nose bridge, in order to develop and evaluate the representative 3D face model for their sizing categories.

Multivariate analysis using three or more key dimensions

Often, multiple body dimensions are relevant for the functioning or fit of a product. Wuhrer et al. (2012) developed a new method for developing sizing categories for helmet design. They used 3 key dimensions based on previous research by Meunier et al. (2009) namely, head width, head depth and face height. They organised the 3D head shapes in a 3-dimensional parameter space based on those three key dimensions resulting in a 3D scatterplot. For the development of respirators, six (Bolkart et al., 2015), ten (Yu et al., 2011; Zhuang, Benson, et al., 2010) or even sixteen (Seo et al., 2016) facial dimensions are included in their study to develop a sizing system. Bolkart et al. (2015) uses a 6-dimensional parameter space to include the top six of the 22 facial measurements for the design of an oxygen mask as classified according to their importance in a previous study by Lee et al. (2013) for the development of an oxygen mask for Korean pilots.

Zhuang et al. (2010) determined the 10 dimensions for their study based on a combination of literature analysis and expert opinions. Experts who were approached for the study were members of the International Organization of Standardization (ISO) Technical Committee working on Respiratory Protective devises. They considered 10 facial dimensions important, and this was subsequently backed up by the literature study that covered various studies determining the critical dimensions for respirator design, or studies into the relationship between facial dimensions and respirator fit. The selected dimensions were considered because they were directly related to respirator fit, they can be measured consistently and have a correlation with other facial dimensions. Yu et al. (2011) based the protocol of their study on Zhuang's work (2010) and therefore in their development of a new respirator, included the same 10 facial dimensions for the development of the face size categories that were representative of the Chinese workers.

For the analysis of Korean children's faces, Seo et al. (2016) included 16 facial dimensions based on a previous study of the face shape variation of the Chinese and Greek population (Y. Liu et al., 2013; Y. Luximon et al., 2012). Kuo et al. (2020) included 40 dimensions in the study they conducted based on the ISO 7250 standard

(ISO 7250-1, 2010) that describes body measurements and landmark definitions for technological design.

Measurements based PCA

Principal component analysis (PCA) is a statistical analysis method that is often used for shape analysis and multivariate approaches in sizing. The input variables for this type of analysis are a selection of dimensions that are either relevant for the product to be designed or located in the area on the body that is relevant for the product fit. By conducting a PCA one can discover the variation of body(part) size and proportion of the product relevant area and discover which measurements influence the variation in the 3D data the most. These are summarized and described in so-called components. Both Zhuang et al. (2010) and Yu et al. (2011) used 10 key dimensions as input for a principal component analysis to map face shape variation of the US workforce and Chinese workers respectively (figure 27). Based on previous studies, 9 facial dimensions that were considered relevant for mask design, were selected as input for the PCA conducted by Goto et al. (2019). In other cases, all available dimensions can be included in the analysis. A total of 40 anthropometric dimensions served as input for the PCA that Kuo at al. (2020) conducted to map the variation of Taiwanese males.

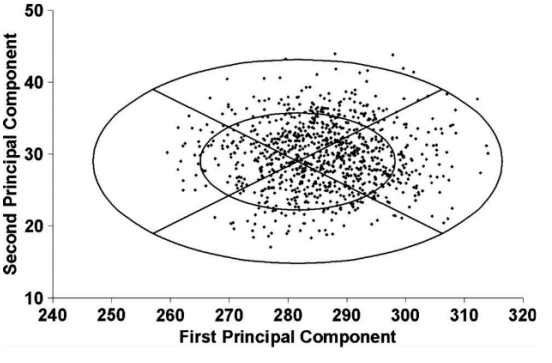

Figure 27 Participant distribution of the first and second principal component scores based on dimensions including regression values for head breadth, face width and bigonial breadth (Zhuang, Benson, et al., 2010).

4.3.2.2 Shape-based analysis

Because 3D anthropometric data contains information of shape of the face and head, it is logical to include this information in the analysis for product sizing to realise a better fit. It provides an opportunity to map the shape variation of the area of interest for the product to be designed (figure 28). Various studies have proposed methods to include 3D shape information in the sizing of helmets and their liners (Ellena et al., 2018; Niu,

Li, & Salvendy, 2009b; Skals et al., 2016). Ellena et al. (2018) defined a boundary edge that defines an area of the head that should be protected by a helmet and all the vertices of the 3D scan head mesh above this boundary are used in the analysis for shape variation. Skals et al. (2016) defined 37 points on 3D head surface located on the head circumference and above for the analysis of head shape variation for the design of bicycle helmet liners. Another product that requires a critical fit to the head is an EEG headset. In the case of a one-size-fits-all EEG headset that Lacko et al. (2017) designed, the analysis of the scalp shape variation combined with four anatomical landmarks that are essential for electrode positioning were used as input in the analysis. In a follow up study, Lacko et al (2017) explored shape-based sizing methods based on 100 3D shape models of the scalp. Each shape model consisting of 10.000 uniformly distributed 3D points distributed over the scalp, served as input for the shape analysis. For this analysis, they conducted a shape based PCA, that besides the previously mentioned measurements based PCA, is also being used to study shape variation of 3D scan data (Godil, 2009; Niu et al., 2009a). Godil (2009) focuses on the face shape variation for the development of sizing systems for face related products. For their study, the 3D facial grid was separated from the CEASAR full body scans and subsequently a PCA on these 3D surfaces is conducted. Niu et al. (2009b) uses the 3D surfaces of the heads and faces divided into patches and their representative vectors as input for a shape-based PCA.

Kouchi and Mochimaru (2004) study the morphological face variation focusing on the area relevant for spectacle frame design. The 3D facial region was defined based on traditional landmarks and newly defined landmarks based on the relationship between the spectacle frame and the face. Often the area of interest for product sizing with shape information is determined based on contact area and/or on product functioning and does not rely on previous studies on sizing of similar products. They use a shape analysis technique called Multi-Dimensional Scaling (MDS). This technique is used to analyse the face shape area relevant for spectacle frames. This is done by calculating the distance between each face shape model in the form of the sum of the distances between corresponding data points which consist of predefined landmarks on each surface. This is done for each pair of subjects resulting in a distance matrix for the whole dataset. Subsequently, the morphological variations of these face shapes are calculated and analysed. A similar approach is used by Amirav et al. (2019) who studied the variation of face shapes of young children. In this face related study, that involved the development of a device to measure respiratory rate in children, Amirav et al. (2019) zoomed into a specific area of interest of the face by cropping the 3D face image to the product relevant nose-mouth area, then the Euclidean distances between each face shape model were calculated resulting in a distance matrix.

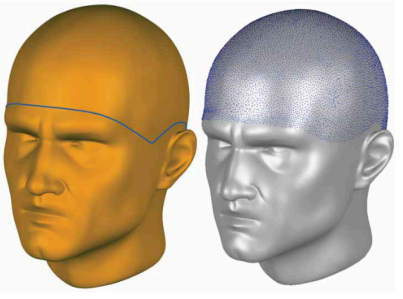

(a)

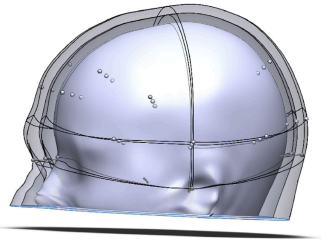

(b)

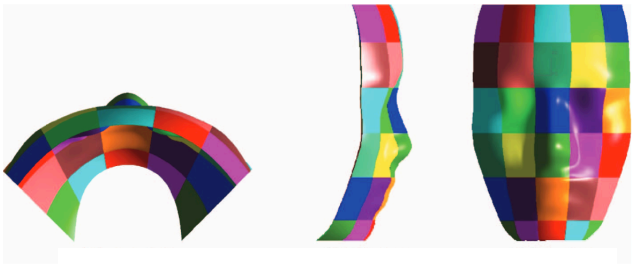

(c)

Figure 28 Some examples of visualizations of shape areas used as input for analysis. (a) Curve (blue) on the 3D head model (left) and the Head Covering Points (HCP) (right) for helmet sizing used in the clustering algorithm (Ellena et al., 2018), (b) Electrode positions visualized on the smallest, average, and largest design mannequin for EEG headset (Lacko, Huysmans, et al., 2017), (c) Block division of a face model for face mask sizing (Niu, Li, & Salvendy, 2009b).

4.3.3 SIZING SYSTEM DEVELOPMENT METHODS

After analysing the product relevant data, the output needs to be translated into a sizing system, product dimensions or product shape. Sizing systems are determined based on the analysis of the distribution and variation of one or multiple key dimensions and subsequently dividing the selected anthropometric data into categories or groups of individuals with similar (key) body dimensions or body shape. These are then translated into product dimensions representing each size. There are different approaches for this division into groups or sizing categories which are described here.

4.3.3.1 One-size-fits-all

In one size fits all design, the adjustability or material properties allow the product to be used or worn by a large part of the target population. This means that there is only one size category. This approach was explored by Lacko et al. (2017) in their development of a one size fit all EEG headset for western adults. The design was based on the calculation and visualisation of the PCA based average head surface, the smallest head

surfaces (based on the PC weights minus three times the standard deviation) and the largest head surface (based on the PC weights plus three times the standard deviation), including electrode locations. After aligning these surfaces according to the Frankfurt plane, the variation of the electrode positions on each head surface served as input for the frame design and positioning of the sliding electrode mounts resulting in the one size fits all EEG headset.

4.3.3.2 Distribution based categorisation

For the sizing of a helmet for children, Bradtmiller (1996) defines four size categories based on the distribution of two key dimensions namely, head breadth and head length. They chose four sizes to cover the variation within each category by taking the elasticity of the foam padding into account which is used to line the bicycle helmet with.

In another study on helmets for adults by Meunier et al. (2009) the size categories were based on the bivariate distribution of the same key dimensions by looking at it as an upper bound problem. Which means that a head that is larger than a certain value will not fit, whereas a smaller head will. While considering a retention system to cover this variation, they divide the population in three sizes, indicating 3 upper boundaries.

Kouchi and Mochimaru (2004) classified their sample population into four groups based on the distribution of the first and second scale of MDS where the first scale represented primarily the variation in the depth of the face and the second scale is related to the breadth of the mid face. The determining of the number of sizes was not a theoretical one but was based on a combination of the following factors. First, the number of spectacle frame styles to ensure profit. Second, the production number of each style should be the same. And lastly, the range of variation in face morphology that each spectacle frame should cover.

In Wurher's paper (2012), the range of the fit along each dimension is determined based on the type of product, the stretch or adjustability in the respective direction. In the case of glasses, the adjustability for the first key dimension (width of face) is set at 2.67 cm and the second key dimension (width of nose bridge) is set at 0.19 cm. This defines each of the 3 sizing categories.

For the development of a sizing system of half face masks that incorporates motion data of the face, Bolkart et al. (2015) incorporate the variation of the measurements due to motion along the two axes of key dimensions and for the size of the boxes (size categories) the tolerance for each dimension is determined based on the amount of stretch of the gear or material of the mask to the face.

To develop a sizing system for face masks for Korean pilots, a bivariate distribution of sellion-to-supramentale length and lip width was analysed. Based on the fit tolerance of each mask, the total accommodation percentage, and the number of sizes required, this distribution was divided into four sizes. For determining the number of sizes, an existing sizing system for US pilots was used as a reference point.

Percentiles

Percentile values in anthropometry refer to a certain percentage below which a percentage of the data falls and it refers to the location of the cumulative frequency of a certain measurement (Robinette & Hudson, 2006). For example, at the 95th percentile of head circumference, 95% of the population have a smaller head circumference and 5% have a larger value. Y. Luximon et al. (2016) used the 5th, 50th and 95th percentiles of the reference dimension face width, for both male and female as representatives for six sizing categories to generate 3D head templates for helmet design.

Fit test panels

Fit test panels are used in the research, design, testing and certification of respiratory protective devices (W. Chen et al., 2009; Zhuang, Benson, et al., 2010). These panels consist of individuals that represent a certain target population that is relevant for a specific product. The selection of these panels is based on the data collected through an anthropometric survey. The variation and correlation of relevant key dimensions is studied, and the data is divided into categories or cells. For each cell representative individuals (individuals with that have the same measurements as determined within the cell) are recruited to be part of the fit test panel.

For instance, for the development of a fit test panel for a full-face respirator, the fit test panel was based on a bivariate distribution of face length and face width (Zhuang et al., 2007) with the upper and lower limit set by the mean value of the male population plus two standard deviations and the mean value for the female population minus two standard deviations, respectively. The data was then divided into categories based on a 10 mm face length and 9 mm face width increment while the boundaries of the cells are defined in such a way that the population is distributed as uniformly among cells as possible. This resulted in a 10-cell panel, including at least 91% of the target population. The eventual fit test panel consisted of 25 participants based on the number of individuals per cell varying from two to five individuals/models per cell.

These fit test panels are often used as a starting point for new sizing schemes (Hsiao, 2013; Yu et al., 2011; Zhuang, Benson, et al., 2010). By combining cells one can test different sizing schemes. For example, for a two-size system (e.g., small-medium, medium-large), the sizes are tested on the test panel that is divided in two groups (cells

1 through 6 and cells 5 through 10) and for a three-size system (small, medium, large) the test panel is divided in to three groups (cells 1 through 4, 4 through 7 and 7 through 10) (Hsiao, 2013). The fit test panel can be used to optimize the fit of a certain product or to update/improve a sizing system in two ways. (1) The design and sizing of the product can be adjusted according to the fit testing with the test panel and (2) the sizing scheme or test panel can be adjusted based on research into the accommodation rate or applicability of an existing fit test panel for the same product to another (similar or more recent) data set of the target population.

4.3.3.3 Clustering methods

A common way of determining sizing categories based on grouping the available anthropometric information is clustering. Cluster analysis is a way to group the 3D anthropometric data into clusters that are composed of individuals with similar measurements or head/face shapes. For each cluster group a product size is determined based on the range of specific dimensions or the representative model that is developed based on the clusters.

K-means

K-means clustering is an iterative clustering algorithm that divides the dataset into clusters based on the distance between each data point of an individual scan and the mean of each of the clusters. The input variables for the k-means clustering can be dimensions (Amirav et al., 2019; Goto, Huysmans, et al., 2019; Niu, Li, & Salvendy, 2009b; Seo et al., 2016), principal component scores (Amirav et al., 2019; Goto, Huysmans, et al., 2019; Kuo et al., 2020; Niu, Li, & Salvendy, 2009b), vectors (Niu, Li, & Salvendy, 2009b) or 3D shapes models (Godil, 2009; Lacko, Huysmans, et al., 2017). The number of clusters are required to be determined beforehand. Different arguments are given in each study for determining the number of clusters.

For dimension-based clusters Seo et al. (2016) determined the required number of clusters by conducting a hierarchical clustering of the 144 facial anthropometric values and studying the resulting dendogram. Subsequently a k-means clustering was performed to classify the faces into three clusters each represented by a 3D face shape.

Amirav et al. (2013, 2019) divided the bivariate distribution (nose bridge and the tip of the chin and mouth width) through k-means clustering in three sizes. This was done based on “economical and practical reasons for providing suitable masks for infants and children” and by doing that they state that, “to achieve their design aims (for the aerosol mask) while providing appropriate convenience for the prescribing physician/pharmacist” (Amirav et al., 2013). The same key dimensions served as input in the study by Goto et al. (2019).

Kuo et al. (2020) conducted k-means clustering in two ways namely, two stage clustering and two-level Self-Organising Map (SOM) and compared the resulting sizing systems. In order to determine the number of clusters for the two-stage clustering, a scree plot was generated based on the PCA indicating that four components explain over 85% of the variance and thus using four clusters as input. Then a k-means clustering was performed to classify the head shapes into groups. Subsequently, each head shape type was classified into size subgroups based on control dimensions (head circumference, head length, head breadth) and size intervals as stated in the Chinese Standard for protective helmets for motor cyclists (CNS 2396) (Chinese Standard Institution, 2007). This resulted in 12 sizes with an accommodation rate of 84.33%. The two-level SOM resulted in 3 head shape types which were subsequently classified into 9 size groups with an accommodation rate of 86.63% concluding that the two-level SOM generates better results.

Niu et al. (2009b) used head breadth and head length to divide a sample of 3D upper head and face scans in to seven clusters through k-means clustering. The number of clusters used in their study was seven in order to be able to compare the results with a previous study with the same target population, in this case Chinese male soldiers. In order to compare the outcome and the effect of the input data, a vector-based approach was also performed. A PCA was conducted on the vectors and subsequently, a k-means clustering was done both on the vectors itself and on the top five PC's resulting from the PCA. The results showed no significant difference between the vector-based clustering with and without PCA. However, comparison with the 'traditional' dimension-based clustering indicated that the shape-based clustering method showed better results.

Similarly, Amirav et al. (2019) conducted a shape based, age based and measurement-based k-means cluster analysis. For this study, the sample was divided into three groups, and they then compared the results by calculating the distance between each individual face model to the average model of the cluster it belonged to. Results showed that the shape similarity within the shape-based clusters was highest (lowest distance) and therefor used as input for the design of the medical device. The argumentation to develop three sizes was not presented in the? current study and is most likely to be the same as in their previous study (Amirav et al., 2013). A similar comparison was made by Goto et al. (2019) who conducted a dimension based, PCA based and shape-based k-means clustering. A Shape based clustering was also conducted by Godil (2009). In this study a k-means clustering was done with 200 face shapes to develop different sizes for a sizing system for products that need to be worn on the face. In this preliminary study they selected four clusters to develop the sizing categories but no (product related) motivation is provided for this number.

K-medoids

A similar approach to k-means clustering is the k-medoids clustering method conducted by (Lacko, Huysmans, et al., 2017) to analyse sizing strategies. The medoid within a cluster is the individual face shape within the dataset that is closest to the mathematical mean shape of the cluster. In k-medoids clustering the clustering is done based on the distance between each surface and the medoid of each cluster instead of the mean as is done in k-means clustering. Lacko et al. (2017) modified the clustering algorithm by constraining the clustering by product related dimensions to make it more applicable for product design. The clustering was done with 2 to 10 clusters, and they suggest that for setting the right number of sizes for a specific product, the designer should set some boundaries based on, for example, manufacturing constraints, material properties and experience. In their example for the sizing of an EEG headset, three sizes were chosen but the fit was not optimal, which indicated that one supplemental size was needed.

Other

Ellena et al. (2018) use a novel modified hierarchical clustering method that is tailored for their study purposes. In this method, clusters are created one after the other instead of simultaneously as in regular clustering methods resulting in a smaller number of clusters and a higher level of intra-cluster similarity. For the clustering they made sure that the maximum distance between any individual head scan within a cluster was 20 mm and that each cluster contained at least 5% of the participants from the initial sample. This resulted in four clusters each represented by a mean head shape. This method offers an objective way of determining the number of clusters or size categories, but it is a complex method which is not (yet) suitable for large datasets (N>1000) (Ellena et al., 2018).

There are a few studies that incorporate both traditional data and 3D shape information in their study to compare clustering results (Amirav et al., 2019; Goto, Huysmans, et al., 2019; Lacko, Huysmans, et al., 2017; Niu, Li, & Salvendy, 2009b). These studies show that clustering based on shape information result in better cluster quality which means higher shape similarity within each cluster.

4.3.3.4 Shape based approach

Based on head shape similarity and with a focus on the area relevant for helmet fitting, Skals et al. (2016) computed 16 subgroups within his sample of head scans, potentially representing different size groups. They subsequently used one subgroup consisting of 30 participants for the sizing and design of a helmet liner. This was done by combining the outside surface of each head mesh and using this combined shape as input for the helmet liner design. And even though they did not take a one size fit all approach, they use a similar design method as used by Lacko et al. (2017) by using the variation of the

3D surfaces as input for the design, in this case, the shape and thickness of the helmet liner material.

3D Representative head and face models

In many of the studies that incorporate 3D anthropometric data, besides the development of a sizing system, 3D representative models (RM's) are a common outcome (table 11). These models are often also called mannequins, design forms or design models. These models include information on dimensions, landmark coordinates, and most importantly, 3D shape information of a specific target population (Kouchi & Mochimaru, 2004). Depending on the application, these models can be represented as an entire head or focus only the region of the face. In 3D anthropometry, 3D models can serve different purposes. By generating 3D models based on a 3D dataset one can visualise the variation of a certain sample population in 3D space. Often 3D RM's are generated to represent sizing categories (Bradtmiller, 1996; B. Lee et al., 2019; W. Lee et al., 2022). They can be 3D scans of (a selection of) individuals (W. Lee et al., 2022), or more often, they are generated based on calculating the mean shape of each sizing category (Amirav et al., 2013; Bolkart et al., 2015; Y. Luximon et al., 2016; Wuhrer et al., 2012) or percentile values of a certain key dimension (Y. Luximon et al., 2016; Meunier et al., 2009). Some RM's are generated to present the variability of the target population such as the head forms that were explored for helmet design in the study of Meunier et al. (2009) or the ones that were developed by Zhuang et al. (2010) and Yu et al. (2011) for respirator research and design. In other studies, that employ cluster analysis for sizing system development, RM's are generated to represent each cluster. These RM's are often based on the mean head/face shape (Amirav et al., 2019; Ellena et al., 2018; Goto, Huysmans, et al., 2019; Lacko, Huysmans, et al., 2017; Niu, Li, & Salvendy, 2009b; Seo et al., 2016; Skals et al., 2016) of each cluster and sometimes the minimum and maximum shapes are also included (Lacko, Huysmans, et al., 2017; Lacko, Vleugels, et al., 2017). RM's can be both physical and digital and can therefore be used as input in different phases of the design process. By using these RM's designers can easily shift between virtual and real world by iterating the design through virtual and physical prototyping, evaluate the fit, optimize the design and adjust number of sizing categories accordingly (Y. Luximon et al., 2016; Wuhrer et al., 2012). In figure 29 some examples of RMs are visualised.

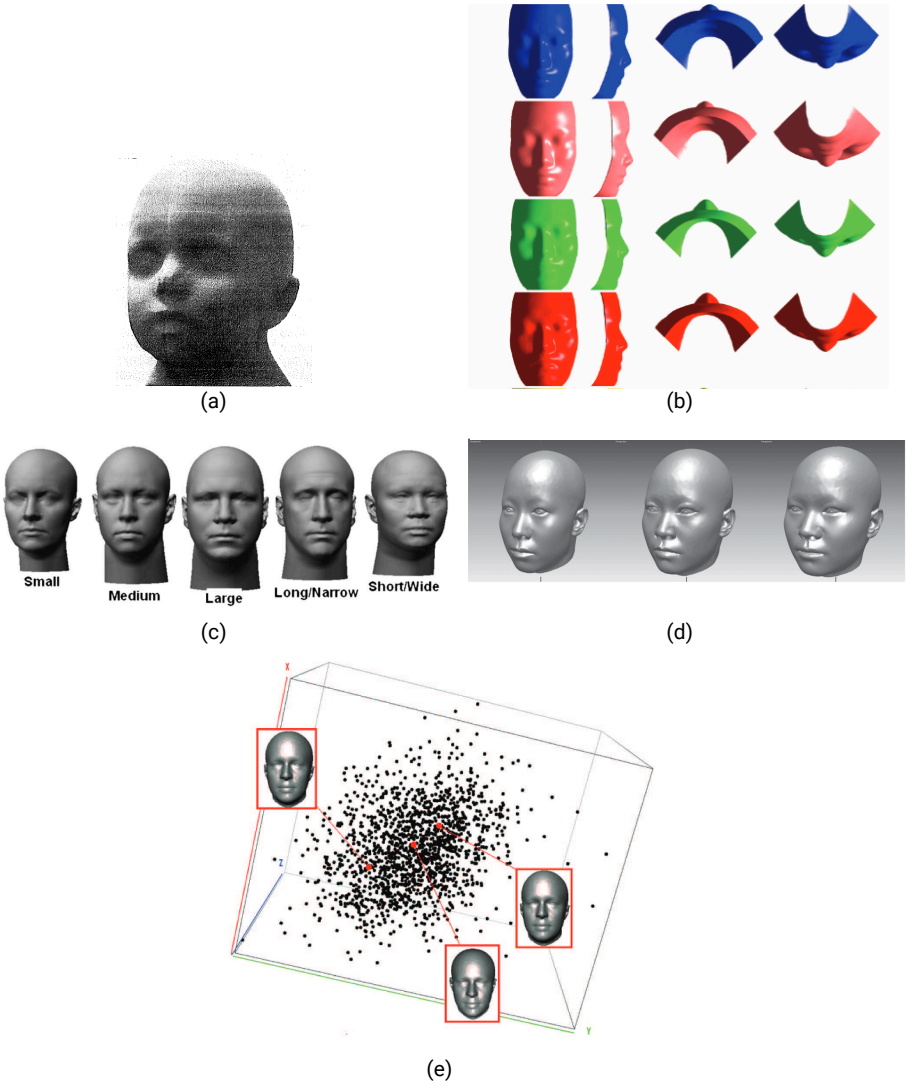

Figure 29 Examples of RFMs: (a) Physical RFM of child's head for helmet design (Bradtmiller, 1996) (b) Average faces of PCA based clusters (Niu, Li, & Salvendy, 2009b) RFM of US respirator users (Zhuang, Benson, et al., 2010) (d) 3D head models of Chinese females (Y. Luximon et al., 2016) (e) Design models for helmet design (Wuhrer et al., 2012)

Table 11 An overview of studies with RM's as outcome.

Study	**RM type Physical/digital**	**RM based on** (number of sizes)	**Design application**
Bradtmiller (1996)	Physical	For each size (4), the largest value of head length and head breadth was used to summarize the 3D data in each head form.	Helmets for children
Kouchi and Mochimaru (2004)	Physical/digital	Average face forms were calculated for each shape group (4).	Spectacle frames
Meunier et al. (2009)	Digital	Design head forms that represent the upper bounds of each helmet size category (3).	Helmets
Niu et al. (2009)	Digital	For each cluster (7) an average face and upper head shape was generated.	Head and face wear
Zhuang et al. (2010a)	Digital	3D head forms that represent face size categories (5)	Respirator design
Yu et al. (2011)	Digital	3D head forms that represent face size categories (5)	Respirator design
Wuhrer et al. (2012)	Digital	3D face forms and head forms that represent the shape for different sizes for different products	Glasses and helmets
Amirav et al. (2014)	Digital	Average face models based on size categories (3)	Medical soother mask for children
Bolkart et al. (2015)	Digital	Representative 3D shape model for each size	Mask design
Y. Luximon et al. (2016)	Digital	3D head templates representing each percentile (5%tile, 50 %tile and 95%tile for face width for both female and male) (6)	Head and face wear
Skals et al. (2016)	Digital	Mean head shapes representing each cluster (4)	Helmet liner
Seo et al. (2016)	Digital	3D face shapes representing each cluster (3)	Respirators
Lacko et al. (2017)	Digital	- Minimum and maximum shapes for each of the clusters. - Average head form for each of the clusters (3)	Head based products
Lacko et al. (2017)	Digital	Statistical shape model representing average, smallest and largest of the head shape (3)	EEG headset
Ellena et al. (2018)	Digital	Mean head shapes based on computed clusters (4)	Head and facial gear
Lee et al. (2018)	Digital	Representative 3D heads based on 7 types of products x 5 ethnic groups x 3 gender groups (105)	Head and face wear
Amirav et al. (2019)	Digital	Average face models representing each cluster (3)	Medical devices for children
Goto et al. (2019)	Digital	Average face models representing each cluster (4)	Ventilation mask
Lee et al. (2022)	Digital	Selected 3D face scans of individual representing a sizing category	Face mask

4.4 DISCUSSION

The purpose of this review was to investigate the various approaches found in literature, that are used in the application of 3D anthropometric data in the development of sizing systems for head and face related products. This review presented a broad range of approaches with a variety of target populations across the world. In this chapter, the main findings of this review are discussed from a design point of view, whereby certain gaps have been identified and opportunities for further research are presented.

4.4.1 THE AVAILABILITY AND ACCESSIBILITY OF 3D ANTHROPOMETRIC DATA OF THE TARGET POPULATION

For the design and sizing of a product, the first step is to evaluate whether relevant datasets of the target population are available. Initial large-scale surveys focussed mainly on the military population and the general workforce, making these target populations well represented. Over the past years more surveys were initiated that included the more general population and children. But even though there has been a slight increase in availability of 3D anthropometric data over the years, publicly available datasets are still limited. This makes it challenging for designers to access such data for their specific design task (Dianat et al., 2018; Lacko, Huysmans, et al., 2017; Veitch et al., 2009). Whilst datasets focusing on elderly, children or other specific target groups remain scarce.

4.4.2 3D DATA COLLECTION, PROCESS AND ANALYSIS

Because of the developments in the field of 3D scanning technologies there is a lower threshold to collect own data for specific (product development) projects in the form of small-scale tailored surveys. Advances in 3D technologies and reduced costs of 3D scanning devices, make the process faster and more accessible for both researchers and designers. This review showcases both the large-scale anthropometric data surveys and the small-scale surveys (N<150) that are set up for specific design or research applications.

However, the relative easiness to collect 3D data nowadays is followed by the more challenging task of processing and analysing the data before it can be used in the sizing process. When extracting relevant data, be it in the form of 1D key dimensions or shape information, one is reliant on having a certain knowledge in the field of computer science and/or statistics. This review also illustrates that there are multiple ways of processing the generated data. Standards that give guidance and structure to this process are currently under development. The collection, processing, and analysis of 3D anthropometric data for sizing and design can be seen as a multi-disciplinary effort considering the different areas of expertise that are required, which not only include

statistics, computer science, as mentioned previously but also product design and ergonomics.

In addition, to the process itself, some form of automation might be required to make the process more efficient. Efforts have been made in the form of platforms that provide access to anthropometric data and allow designers to interact with the data, but data entry is still not automated, and a computer/data scientist is required to prepare the data and to make it accessible through the platform or tool (Huysmans et al., 2020; B. Lee et al., 2019)

4.4.3 SHIFT FROM KEY BODY DIMENSIONS TOWARDS BODY SHAPE VARIATION

Over the years there has been an increase in the incorporation of 3D shape information in the development of sizing systems, but 3D data is not always used to its full potential. This review shows that 10 out of 22 studies incorporate 3D shape information in their sizing approach, meaning the use of the 3D surface data in determining sizing categories instead of only the body dimensions. Thus, the sizing systems in the majority of the reviewed studies are still based on 1D measurements.

It is important to note that in recent years, there have been considerable advances in 3D data processing techniques making the integration of 3D data less daunting (Zhang et al., 2023). Thus, studies that started more than five years ago, might not have had the advantage of these developments. Of the studies that started more than five years ago (n=14) a considerable amount (n=10) did not use shape information in their sizing system development process.

Apart from the technological advances, some products, such as oxygen masks and helmets which are developed for the military, have a long history in sizing system development and optimization. And naturally, these initially used traditional anthropometric data and fit test panels as a starting point in the optimisation of these sizing systems built upon this knowledge (Zhuang 2008).

In general, despite the technological advances in the use of 3D anthropometry in some cases designers and/or researchers prefer to use 1D data for practical or historical reasons. For example, for some designers, traditional 1D data (tables with summery statistics, percentiles etc.) can be sufficient depending on the design problem and experience. Using this type of data has a low threshold because of its simplicity, ease of use and the fact that most designers are familiar with this process (Meunier et al., 2009). Another example is that in some products, such as oxygen masks and helmets which are developed for the military, have a long history in sizing system development and

optimization based on traditional data. In this case researchers use traditional anthropometric data and fit test panels as a starting point in the optimisation of these sizing systems and revert back to the 1D data for the sake of effective comparison (W. Lee et al., 2022; Zhuang et al., 2007).

But for many products, especially protective gear or medical products that are presented in this review, which are often products that need a close fit, or that need to be worn over a long period of time or under critical circumstances, 3D anthropometric data seems beneficial. More comparative studies are needed to show benefits of different types of data for different types of products.

4.4.4 SIZING SYSTEM DEVELOPMENT

Whether utilizing a traditional or 3D data-based sizing system, determining the number of sizes is typically a subjective decision influenced by the designer's experience, input from ergonomics specialists, or previous sizing systems for the product (Ellena et al., 2018; Lacko, Huysmans, et al., 2017). The studies reviewed in this analysis commonly begin with 3 or 4 sizes, sometimes lacking a clear rationale. Selecting the appropriate number of sizes for a specific product involves balancing cost and fit and is heavily influenced by factors such as the target market, population, product complexity, and materials utilized (A. Luximon et al., 2012). For example, products designed for children may require more sizes to accommodate growth, compared to the same product designed for adults. However, fewer sizes are desirable to minimize costs. The number of required sizes also increases for products that require a more precise fit, to cater to the target population (A. Luximon et al., 2012). Ideally, designers strive to follow inclusive design principles to accommodate the greatest number of potential users. Although optimal methods exist for determining the ideal number of sizes, the results may not be favourable for all design applications, making it too expensive for certain products, but worthwhile for others, such as medical products (Lacko, Huysmans, et al., 2017).

4.4.5 RECOMMENDATIONS FOR FUTURE RESEARCH

The findings of this review lead to the following recommendations for future research to support the development of 3D anthropometric included sizing.

- Conduct comparative studies to demonstrate the advantages of using different anthropometric data types (1D, 2D, 3D) for various product types.
- Research is needed to explore which sizing methodologies are most effective for different product categories and how they impact fit quality.
- Research is needed to investigate methods and tools for supporting designers in processing, analysing and the application of 3D anthropometric data.

4.5 CONCLUSION

This chapter presents an overview of the current state of defining sizing systems for product development based on 3D data, with a specific focus on head and face data and the design and development of related products. It provides an overview of various approaches and practical and statistical considerations that are taken into account in the development of a sizing system based on 3D anthropometric data for product design. This review showed that incorporating shape information in sizing requires tailored sizing system development methods. In this context, shape models are generated to specifically represent various sizing categories. Diverse products designed for different body regions require distinct analysis techniques and visualizations. The flexibility of 3D data enables the adoption of these varied approaches. Shape-oriented sizing can be viewed as an alternative method for determining sizes, one that relies solely on shape rather than key dimensions. This necessitates a different set of skills, including statistical knowledge, computer proficiency, and expertise in data science.

As 3D data becomes more widely available and utilized in product design, it is important to continue exploring and refining sizing systems development methods based on this technology. This will contribute to making the use of 3D data more accessible for designers and, consequently, result in the creation of better-fitting products.

5

A COMPARISON BETWEEN REPRESENTATIVE 3D FACES OF CHILDREN FOR MASK DESIGN

The previous chapter demonstrated that sizing systems are still often based on traditional anthropometric data and generally use the variation of one or two key body dimensions directly related to the product. For products that need to closely fit a certain part of the body it is relevant to incorporate multiple key dimensions or shapes in the sizing process. In order to integrate the use of 3D body shape in product sizing, representative models (RM's) for design are often used to visualize the variability of the target population. But despite the increased development and use of RM's, there is little research into how the type of anthropometric data used for RM development effects the representativeness of the target population, especially for children. For the development of a ventilation mask for children, this study compares RM's of 3D faces and their mask contours based on a bivariate, multivariate, and shape-based analysis of the 3D children's dataset. The results are discussed with regard to the implication for the sizing and design of the mask and more generally the added value of these methods for designers.

This chapter is based on Goto, L., Huysmans, T., Lee,W., Molenbroek, J.F.M., Goossens, R.H.M. (2018). A comparison between representative 3D faces based on bi- and multi-variate and shape based analysis, in: Proceedings of the 20th Congress of the International Ergonomics Association (IEA 2018) Volume VII. pp. 1355–1364.

5.1 INTRODUCTION

One of the challenges a designer faces when designing product series for people where a good fit is essential, is translating anthropometric data of the target population into product dimensions or a sizing system. Currently, sizing systems are often based on traditional anthropometric data and generally use the variation of one or two key body dimensions directly related to the product (Dainoff et al., 2004; Hsiao, 2013). This information is usually presented in tables or scatterplots but rarely represents the complexity of the human form.

For products that need to closely fit a certain part of the body it is relevant to incorporate multiple key dimensions. This can be realized by a multi variate approach which maps the variation in these dimensions in order to generate a sizing system. The most common approach is conducting a principal component analysis (PCA). A PCA is often used to analyse anthropometric datasets in order to discover trends in the variation of multiple dimensions (Goto et al., 2015; Hsiao, 2013; Y. Luximon et al., 2012; Zhuang et al., 2007).

Recent developments in the field of 3D imaging have resulted in an increase in the incorporation of 3D scans in anthropometric surveys (Ball, 2011; Ballester et al., 2015). The richness of 3D data makes it possible to visualize complex results from anthropometric analysis. By generating 3D models, that represent the variability of the target population, this information becomes more understandable for designers (Wuhrer et al., 2012). In addition, designers can then easily utilize these sets of 3D models in their design process, especially with the use of computer aided design (CAD) programs.

In order to develop a ventilation mask for children, the aim of this study is to compare representative models of 3D faces based on bivariate, multivariate and shape based analysis of 303 children's faces, aged 6 months to 7 years. Mask contours are projected on each face model to simulate the contact area of the mask and the differences of the contours of each cluster related to the representative face models (RFM's) are analysed. These results are discussed with regard to the implication for the sizing and design of the mask and more generally the added value of these methods for designers.

5.2 METHOD

5.2.1 CHILDREN'S HEADS AN FACE DATASET

The analysis was based on the existing dataset of 303 children's head and faces. The dataset was acquired by combining traditional and 3D scan extracted anthropometric information (Goto, Lee, et al., 2019). Participants were Dutch children aged from 6

months to 7 years old and included 174 males and 128 females of mixed ethnicity. The heads and faces of the children were captured from four angles (front, 45 □ degrees to the left and right, and the back) using a 3dMD face scanner (3dMD Ltd., London UK). The scans were subsequently combined into a 3D scan of the complete head with Artec Studio 9 software (Artec group, Inc., Luxemburg). 19 anthropometric landmarks were defined on the scan and based on these landmarks, 13 facial dimensions were extracted (Figure 30) by calculating the Euclidian distances between the landmarks (MATLAB™).

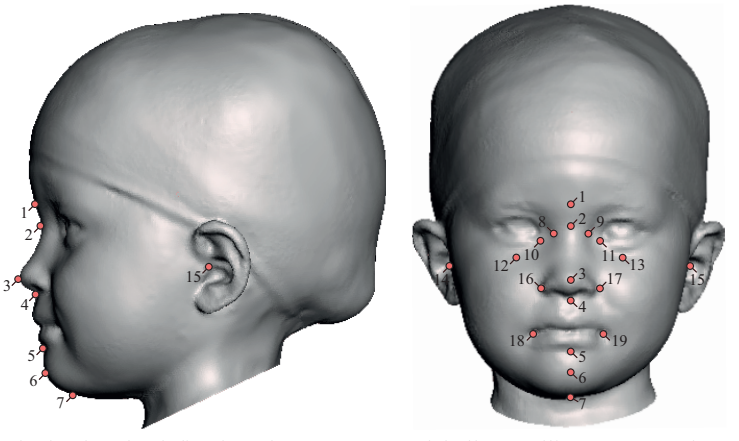

Figure 30 The landmarks defined on the 3D scan; 1. glabella 2. sellion 3. pronasale 4. subnasale 5. Sublabiale 6. Pogonion 7. Menton 8/9. Nasal root point (right/left) 10/11. Endocanthion (right/left) 12/13. Infraorbitale (right/left) 14/15. Tragion (right/left) 16/17. Alare (right/left) 18/19. Cheilion (right/left) (Goto et al., 2019b).

5.2.2 TEMPLATE REGISTRATION

In order to develop representative models based on the sample, the individual 3D scans needed to be registered. This means that each 3D scan needs to have the same number of vertices at corresponding anatomical locations and a consistent mesh topology. The 3D head scans were registered by using a hybrid template registration method. The template registration was conducted on the face area only according to the method as described in Lee et al. (2017).

5.2.3 DEVELOPMENT OF FACE MODELS WITH MASK CONTOURS

First, an average face was generated based on the complete set of template registered models as described in Huysmans et al. (Huysmans et al., 2020). This average face shape still contains information of each individual face of this dataset in terms of face shape variation based on principal component analysis (PCA) which contains the calculated differences between the average face and each individual face. It is therefore called

statistical shape model (SSM). Next, a mask contour was projected on the SSM. The contour was drawn using Rhinoceros 3D Version 6.35 (Robert McNeel & Associates) and passed through the sellion and pogonion landmark and both the left and right chellion landmark laterally with a 10 mm distance to give an approximation of the contact area of the face and mask. Finally, the contour was projected on each individual registered template through vertex correspondence (Python and Visualization toolkit (VTK), Kitware Inc.). The SSM and the curve served as input for the script in Python that ran this procedure. First the SSM is first split in three regions: the inside of the mask, the curve itself and the rest of the face region. The region inside the curve of the SSM is subsequently aligned to each individual face through vector displacement and vertex correspondence (figure 31.).

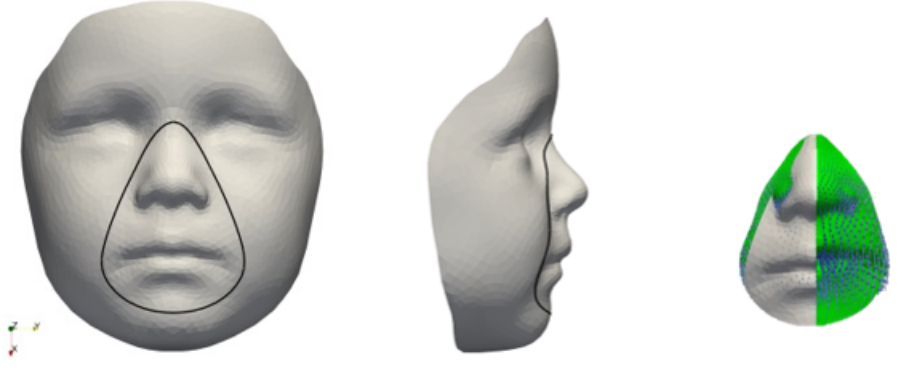

Figure 31 The template-registered statistical shape model (SSM) from the front and side respectively, with the mask contour projection and an individual mask contour with the region of the nose and mouth (green) including PC displacement vectors (blue arrows) mapped with the SSM mask region (grey) (right).

5.2.4 STATISTICAL ANALYSIS OF KEY DIMENSIONS

Traditionally, a sizing system is based on one or two relevant key dimensions of the targeted population that are directly related to product dimensions. In previous research, sellion-pogonion length and mouth width were considered to be related to the fit of a medical aerosol mask for children (Amirav et al., 2013). A scatterplot was generated based on sellion-pogonion length and mouth width in order analyse the distribution.

Multivariate approaches in sizing system development are often used to incorporate more than two relevant dimensions in order to get an even more representative distribution of the data. A principal component analysis was performed on 9 facial dimensions that were considered relevant to mask design based on previous research namely, face length, sellion-pogonion length, nose bridge length, mouth width, nose

protrusion, nasal root breadth, nose breadth, interpupillary distance and face width (Amirav et al., 2013; Goto et al., 2021; Zhuang et al., 2007). A scatterplot was generated based on the scores for the first and second principal component. The component scores were calculated as follows:

PC1 = 0.623 × (face width) + 0.907 × (face length) + 0.852 × (sellion pogonion length) + 0.818 × (interpupillary distance) + 0.636 × (nasal root width) + 0.773 × (nasal bridge length) + 0.754 × (nasal tip protrusion) + 0.728 × (nose width) + 0.647 × (width of mouth)

PC2 = 0.312 × (face width) + -0.323 × (face length) + -0.388 × (sellion pogonion length) + 0.289 × (interpupillary distance) + 0.466 × (nasal root width) + -0.459 × (nasal bridge length) + -0.188×(nasal tip protrusion) + 0.165 × (nose width) + 0.411×(width of mouth)

5.2.5 SHAPE BASED ANALYSIS

A principal component analysis was conducted on the face mask area in order to develop shape based representative face models (RFM's). The face mask area is the area of the template registered face that falls within the mask contour. The principal component analysis was conducted on the vertices of the mesh of the face mask area. The first and second principal component scores were extracted and plotted. The results of the shape based PCA are visualised in figure 32.

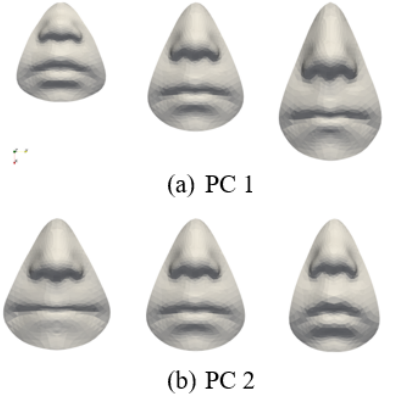

Figure 32 Visualization of the first two principal components showing the average (middle), -3 (left) and +3 (right) standard deviations of the respective PC.

5.2.6 CLUSTERING AND RFM DEVELOPMENT

Clustering methods have been used to determine product sizes in previous work (Amirav et al., 2013; Lacko, Huysmans, et al., 2017; Niu, Li, & Salvendy, 2009b). A K-means clustering method was utilized (SPSS version 22) in order to divide the sample into four clusters that represent the variation of the children's faces. Based on prior research that categorizes sizing systems for children's facial variations, four clusters were selected. These clusters encompass three age categories, originally designed for children aged 1 month to 4 years. Given our specific age range spanning from 6 months to 6 years, four sizes were selected as the initial startng point in this study. The clustering was both done for the bivariate and the multivariate distribution. For the bivariate distribution, the input variables were sellion-pogonion length and mouth width. The input variables for the multivariate and shape based distribution were the first and second principal component scores of the PCA. Finally, mean representative face models were generated for each cluster for each method (Python and Visualization toolkit (VTK), Kitware Inc.). This was done by conducting a generalized Procrustus alignment per cluster and subsequently, calculating the mean for each respective cluster. Figure 33 presents a visualization of a RFM (side view) and the individual faces (coloured contours) on which it is based.

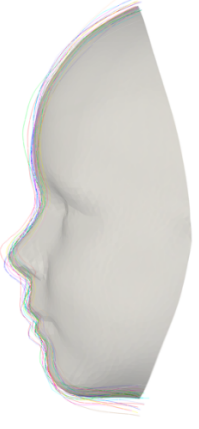

Figure 33 Visualization of the generated RFM (grey) and de contours of the individuals (coloured lines) within one cluster.

5.2.7 RFM COMPARISON

In order to analyse the representativeness of each RFM for each cluster and per method, the mean distance between the vertices of the RFM and all the members within the same cluster was calculated and subsequently visualized.

5.2.8 CONTOUR COMPARISON

For each method and cluster the local variation of the mask contour was quantified by the Frobenius norm of the landmark covariance matrix. This quantity was calculated for each landmark on the curve as follows. First, the average location of the landmark is calculated by averaging the corresponding points across the set of curves within the same cluster for this landmark, this corresponds with the landmark locations on the mask contour of the RFM for the respective cluster. Then, the set of corresponding points were centred around 0, by subtracting the average landmark position, and the 3 by 3 XYZ-covariance matrix of the centred points was calculated. This covariance matrix captures the main directions and extent of variation for this landmark. Finally, the Frobenius norm of the covariance matrix was calculated, as the square root of the sum of squared matrix elements, quantifying the extent of the variation in position of this landmark across the set of curves. The Frobenius norm could also be calculated as the square root of the three squared singular values (= the variances of the points in the three principal directions) of the covariance matrix and therefore is a measure of the size of the cloud of points in the set for this landmark. If the Frobenius norm is large, it means that the landmark on the curve varies a lot in its position across different individuals and if it is small, it means that the same landmark is close to all the others across the sample. This procedure was then repeated for each landmark on the curve and the resulting values were visualised through a colour map on the average curve for that set.

5.3 RESULTS

5.3.1 K-MEANS CLUSTERING AND RFM'S

The bivariate, multivariate and shape based distributions are shown in figures 34, 35 and 36. Within each distribution the clusters are indicated and the RFM's are displayed. Table 12 shows the number of participants assigned to each cluster per method.

Table 12 Number of individuals in each cluster based on two key dimensions, per PCA based cluster and per shape based PCA cluster.

Cluster	Number of Cluster Members		
	Bi-variate distribution	Multi-variate distribution	Shape based distribution
1	77	92	77
2	54	57	111
3	115	29	72
4	55	112	43
Total	301	290	303

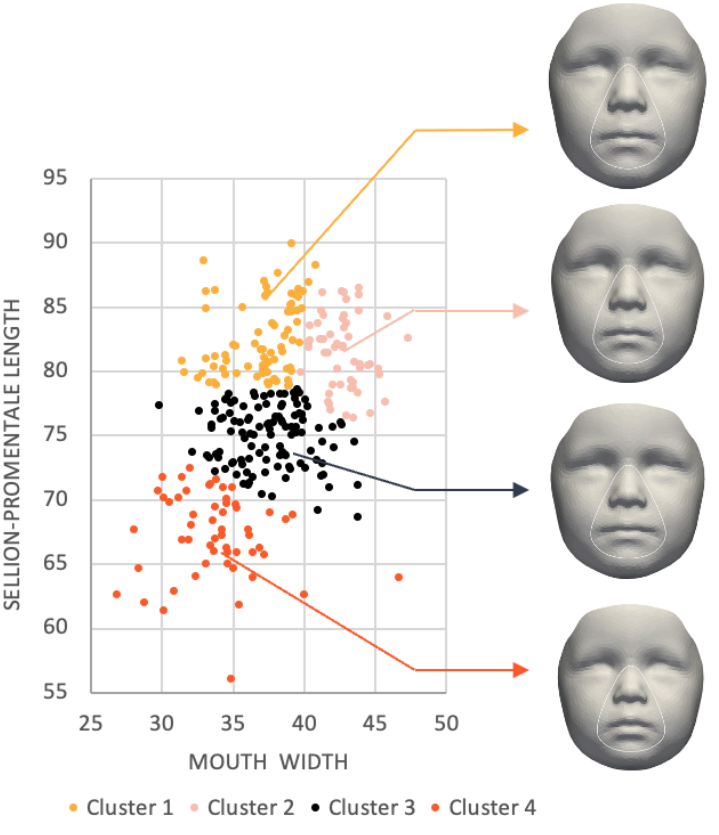

Figure 34 Scatterplot of mouth width against sellion-pogonion length divided into four clusters and the RFM's (bi-variate distribution).

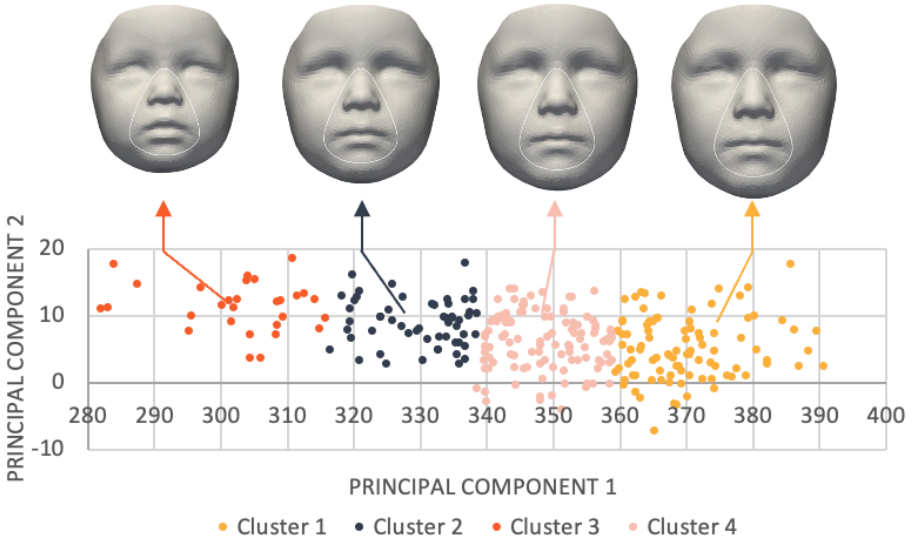

Figure 35 Scatterplot of key dimension based principal component 1 against principal component 2 divided into four clusters and the RFM's (multi-variate distribution).

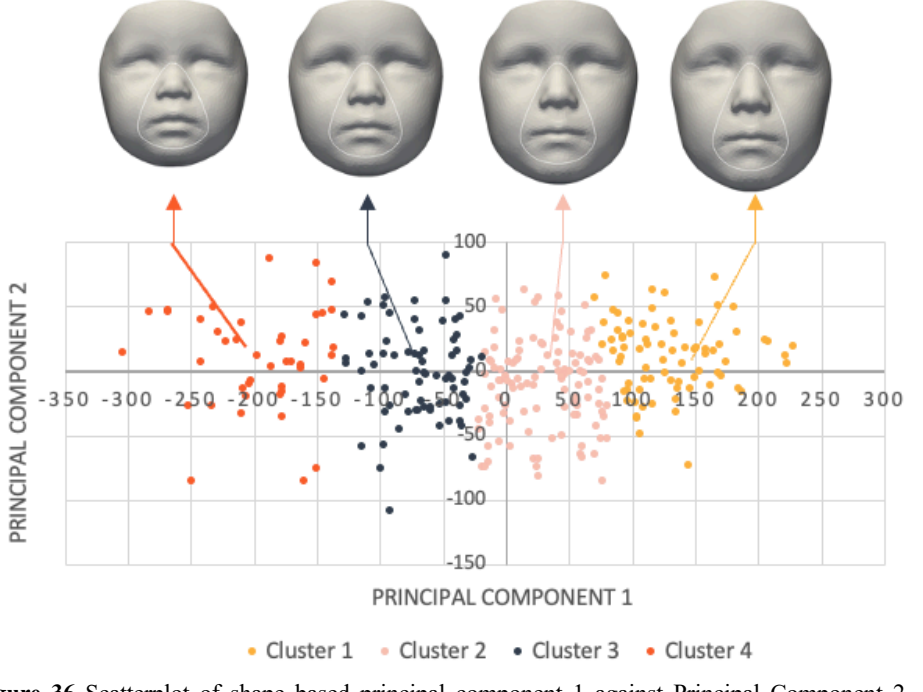

Figure 36 Scatterplot of shape based principal component 1 against Principal Component 2 divided into four clusters and the RFM's (shape based distribution).

5.3.2 MEAN DISTANCE TO RFM WITHIN EACH CLUSTER FOR EACH METHOD

Figure 37 shows the results of the comparison between the RFM and the cluster members. Less variation (blue) was observed in the area surrounding the sellion landmark (nose bridge area) because the template registered faces were aligned with the origin point at that landmark. Variation was the largest in the regions surrounding the chellion landmarks for the smallest RFM of all three methods. This is also reflected in table 15 where the mean distances were calculated between the vertices of each individual face and the respective RFM. The mean distance between the RFM and cluster members is largest for the bivariate approach and smallest for the shape based PCA.

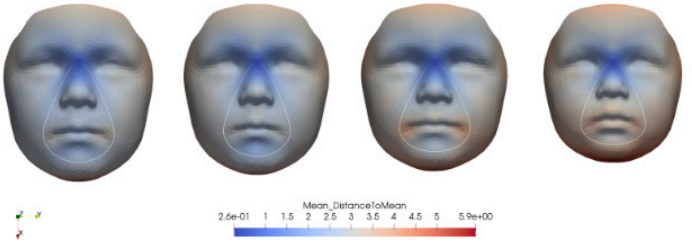

(a) Bivariate

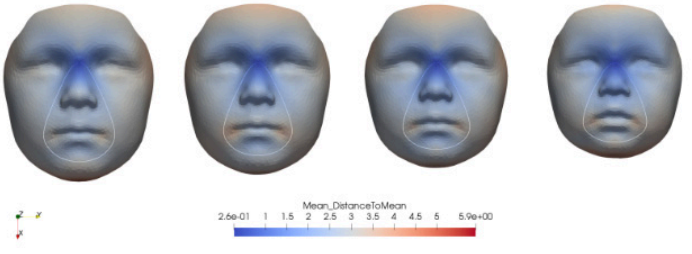

(b) PCA

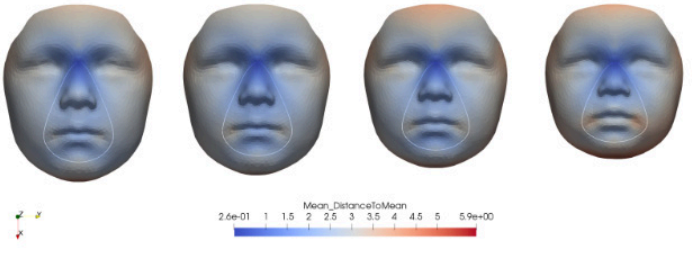

(c) Shape based PCA

Figure 37 Colour map of the mean distance to RFM (mm) per cluster. High variability is indicated by red and low variability by blue.

Table 13 Overview of the mean distance (mm) between the vertices of the RFM and the vertices of individual faces over the face mask area per method and per cluster.

		Cluster				Mean
		1	2	3	4	
Method	BIVARIATE	2.35	2.35	2.54	2.74	2.50
	PCA	2.36	2.30	2.16	2.16	2.25
	PCASHAPE	2.10	1.93	1.98	2.15	2.04

5.3.3 CONTOUR COMPARISON PER CLUSTER PER METHOD

Figure 38 and 39 show the average contours of the RFM's for each four clusters per method with a colour map indicting the local variation on the curve compared to the contours of the cluster members.

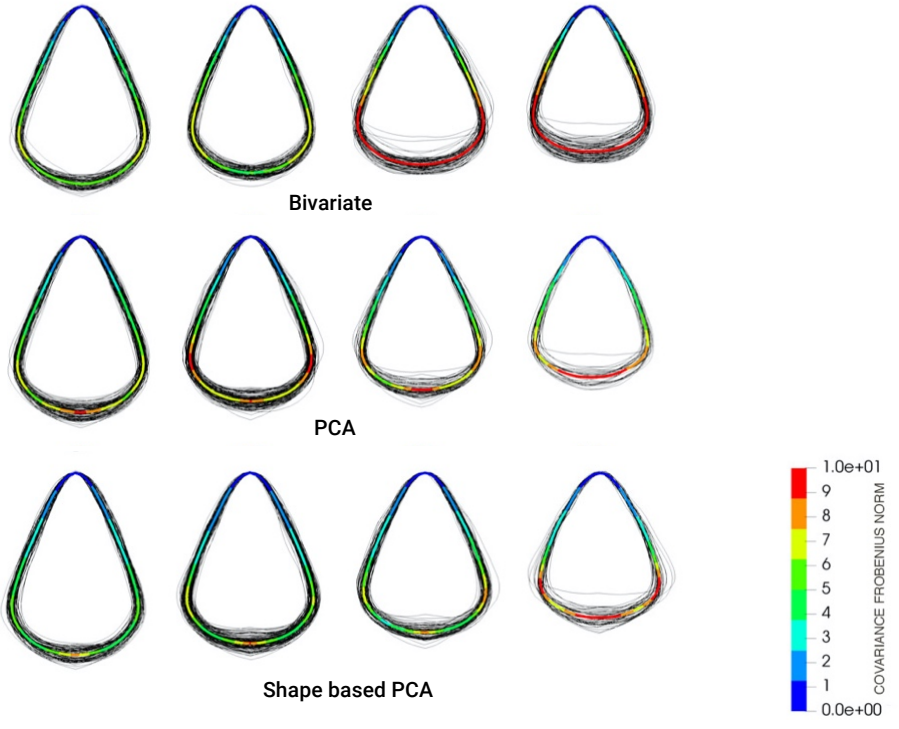

Figure 38 The contours per cluster compared to the average contour (front view) for each method. High variability is indicated by red and low variability by blue.

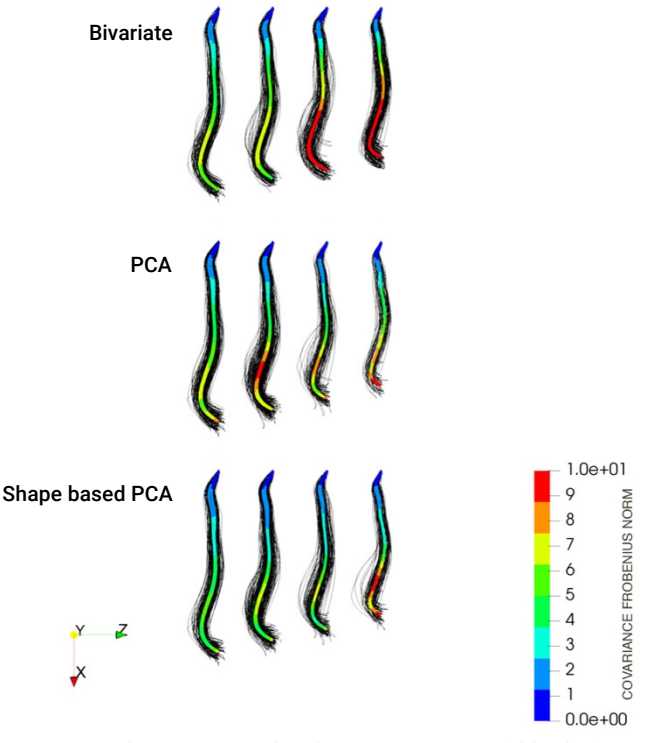

Figure 39 The contours per cluster compared to the average contour (side view) per method. High variability is indicated by red and low variability by blue.

5.4 DISCUSSION

Initial, visual inspection of the RFM's seem to indicate that for each cluster the RFM's are relatively similar to each other, regardless of the utilized method. When analysing the RFM's in further detail, small differences could be observed. For the multi-variate and shape based RFM's the overall shape and size changes gradually from smallest to largest. However, for the bivariate method there appears to be a jump in the width of the mouth from cluster 2 to 3, resulting in cluster 3 having a relatively larger mouth. This may be due to the fact that mouth width directly influences the RFM in the bivariate method whereas in both PCA's the first component described the variation in the overall size of the face and the second component was more related to the width of the face.

The comparison of each RFM to their cluster members shows that the largest variations were observed in each of the smallest RFM's, regardless of method. This could be explained by the rapid growth phases that occur mostly in the first few years of a child's life (Farkas et al., 1992) resulting in larger differences in the facial dimensions for children within these clusters. Interestingly, the mean inter-vertice distance between the

RFMs and its respective cluster members for each method (table 13), show that as more information is incorporated (i.e. more dimensions) in the analysis, the smaller the mean distance becomes. The mean distance is largest for the bivariate RFM and smallest for the shape based RFM's. This indicates that, for the latter, the shape based RFM's is more representative for its respective cluster.

Mask contours were projected on each RFM and subsequently analysed in order to determine the possible implications for mask design. The comparison of the average contours (RFM contour), with its cluster members, show that the largest variation was observed in the two smallest RFM contours for each method. This is reflected in the comparison of the RFMs, whereby the two smallest RFMs showed the largest differences in mean distance. In addition, the variation decreases within each cluster, just like in the RFMs, when using the methods that utilize more information. It is important to note that the RFM contours are currently presented as a specific curve whereas this does not take into account geometric tolerance (e.g. the top of the mask may align on the sellion landmark but could also sit 5 mm lower on the nose bridge), the elastic properties of materials (a part of the variation can be compensated by for instance an material with high elasticity) and biomechanical properties of the face.

Firstly, it is important to note that the number of individduals assigned to each cluster varied per method from N=2 to N=13, in part due to the method of clustering but also for practical reasons as described in previous research (Goto, Lee, et al., 2019). This often occurred in age groups one (aged 6 months to 1.5 years) and two (1.5 to 2.5 years) where some of the direct measurements were impossible to take. This will, to a certain extent, have influenced the generation of the PCA RFMs for the clusters that represent the smallest children.

Secondly, in this study, the distribution was divided into four clusters. Determining the number of clusters in order to develop a sizing system depends on the type of data, the required fit, cost-benefit, etc. and is often a combination of statistical and practical experience (Hsiao, 2013; Lacko et al., 2017a). Further research is needed in order to determine the ideal number of clusters (sizes) for the development of the mask or any other product for that matter. Considering that largest differences were observed in the smallest (youngest) cluster, this could indicate that an additional cluster might be desirable for mask design.

At present, sizing system development based on a bivariate distribution seems more intuitive for designers because there is a direct link between body dimensions and product dimensions. This approach is partially based on statistics but also practical

knowledge (material properties, etc.). It is important to note however, that all three methods use shape data to develop models rather than the classical anthropometric approach whereby anthropometric measurements are directly translated to product dimensions. The next step is to investigate to what extent the differences between the RFMs generated by the three methods have an actual and noticeable influence on the mask design.

Even though the multivariate approach incorporates multiple product relevant dimensions, the outcome is not directly translatable to product dimensions. More statistical knowledge from the designer's side is needed but the development of representative models offers a solution that can be incorporated in the design process. A solution would be to develop a software tool which allows for this approach without having detailed statistical knowledge.

5.5 CONCLUSION

In conclusion, this study compared three different methods of generating representative facial models for children in order to develop a sizing system for masks. While the initial visual inspection indicated relatively similar RFMs for each cluster regardless of method, further analysis revealed small differences in shape and size, with the bivariate method showing a larger jump in mouth width between clusters. The mean inter-vertice distance between the RFMs and the cluster members it represents, also showed that incorporating more information in the analysis resulted in smaller differences. And thus it can be concluded that the shape based RFMs is more representative for its respective cluster. Mask contour analysis showed similar patterns of variation within clusters when more information was incorporated, which indicates that when designing a mask based on the shape based RFMs, it will potentially result in a better fitting product.

6

A COMPUTATIONAL DESIGN AND EVALUATION METHOD FOR VENTILATION MASKS BASED ON 3D REPRESENTATIVE FACE MODELS OF CHILDREN

The previous chapter compared representative face models (RFM) and demonstrated that the shape based RFMs represent the dataset best. In this chapter these RFMs are used to design a ventilation mask for children, followed by a virtual fit test. The aim of this study was to examine how a mask design based on these RFM's fits the target population. After randomly dividing the 3D dataset of Dutch children's heads and faces into a training dataset and a testing dataset, the training data was subsequently clustered to represent different sizing categories. Then, a RFM was generated based on each cluster and a design of the ventilation mask was developed with respect to the shape of the contact area. Subsequently, this design was virtually fit tested on the testing dataset to evaluate the fit. Finally, the number of clusters and respective RFMs was increased from n=1 to n=6 to investigate the effect on the resulting fit.

6.1 INTRODUCTION

Detailed anthropometric data of the head and face are crucial for designing and sizing head and face related products. This is because the head and face contain some of the most important features of the human body. Products designed for these areas often serve critical purposes such as protection (helmets, goggles), communication (hearing aids, headphones), or support (ventilation masks). In these cases, a proper fit is vital as it directly affects the functioning, safety and comfort of the product.

In an ergonomic, user centred design process, anthropometric information is used to tailor a product to the body shape and size within the target population. Especially in products that need to fit closely to the human body, using detailed data can lead to a better fit and more comfort for the user. However, despite the advancements in industry and manufacturing techniques, achieving a perfect fit for each individual user is currently not feasible for most companies due to the high cost of personalised options (Lacko, Huysmans, et al., 2017; Minnoye et al., 2022). The development of personalised products often involves manual design work, specialised manufacturing techniques, more complicated logistics combined with low volumes. As a result, many companies rely on offering multiple sizes of a product to accommodate the target population.

Traditionally, sizing systems have been developed by considering several key dimensions that are relevant to the product. Anthropometric measurements are collected, analysed, and then grouped into sizing categories that ideally cover the complete target population. However, traditional anthropometric data is typically presented in tabulated form and does not provide shape information or subtle geometric transitions of the human shape, especially for the head and face. This can be particularly problematic when designing products that require a tight fit to function optimally. Additionally, dimensions related to the head and face have poor intercorrelation, making it even more challenging to design a series of products that can accommodate the varying sizes and shapes of different individuals (Bradtmiller, 2022; Hsiao, 2013).

To improve the design and sizing of head-related products, it is necessary to have models that provide insight into the variability of the head and face among the target population. Because of the increasing use of 3D data collection in anthropometric studies and the growing availability of 3D anthropometric datasets, it is now possible to generate these models. These models, known as representative models (RMs), are a collection of individuals or statistical shape models with specific dimensions (e.g. mean, percentile values). RMs are created based on 3D head and face datasets and provide insight in shape variation and details on the face, such as the nose bridge transition, ear location,

and other geometries that might be relevant for certain products (Ellena et al., 2017; Huysmans et al., 2020; Jung et al., 2010; Lacko et al., 2017b; Lee et al., 2019; Meunier et al., 2009; Wuhrer et al., 2012; Zhang et al., 2023a; Zhuang et al., 2010).

RMs can be a selection of individuals' 3D face scans as described in Lee et al. (2022) for the design of oxygen masks (figure 40a). However, more often, RMs are generated by calculating average head forms based on mathematical calculations or statistical analyses of a 3D head/face dataset or subset (figure 40b) (Wuhrer et al., 2012). For sizing system development, this involves for instance, calculating percentiles of key dimensions, conducting a principal component analysis, or cluster analysis (Ellena et al., 2017; Lacko, Huysmans, et al., 2017; Y. Luximon et al., 2012, 2016; Wuhrer et al., 2012; Zhuang, Benson, et al., 2010). To subsequently construct the 3D RMs, the individual scans must first be aligned, then a correspondence between each individual scan is established and finally, statistical modelling is conducted (Huysmans et al., 2020; Zhang et al., 2023b). RMs can be presented as both digital and physical models, allowing designers to use them in a CAD environment to virtually adjust their designs or to for example, verify virtual prototypes (Ball, 2009; Bradtmiller, 1996).

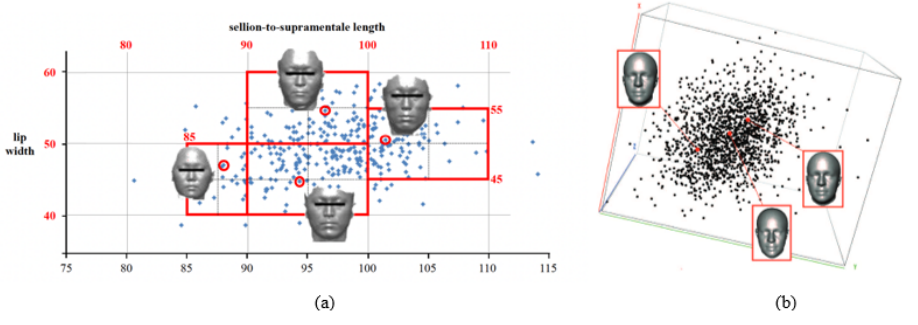

Figure 40 (a) RFMs for oxygen masks for Republic of Korea Air Force pilots and (b) 3D head forms for helmet design (Wuhrer et al., 2012).

Therefore, 3D models have significant potential, however, research into the application of Representative Face Models (RFMs) in the design and sizing of products for children is still lacking. This may be even more relevant for children since the variation of head and faces of children are affected by growth and can result in more variation within and over different age groups compared to adults (Goto et al., 2021; Zhang et al., 2023a). This presents a greater challenge when developing an effective sizing system to ultimately design face wear that offer a good fit.

Computational design has opened up new possibilities for quick adjustments and iterative design in a CAD environment. Computational design involves using computer algorithms and software tools to automate and enhance the design process. It enables faster iterations, problem-solving, and exploration of design possibilities. (Minnoye et al., 2022). By integrating RFMs in this design process, it becomes feasible to explore various designs and forecast the compatibility of mask designs during the early phases of product development. Visual programming, also known as graphical programming, offers an opportunity for designers to make programming more accessible. It allows designers to use a graphical interface to visually construct their design ideas and translate them into code without having to write complex scripts manually. This approach can make computational design more approachable for designers who may not have extensive coding experience, offering new possibilities for creativity and innovation.

In order to bridge this gap, this paper presents a method for creating mask designs for children using RFMs through visual programming. Firstly, RFMs are generated based on a 3D dataset of children's heads and faces. Next, a virtual fit test method was developed to evaluate the fit of each generated mask with the 3D face dataset. To determine the appropriate number of RFMs required to represent the variability of children's faces, this study investigates the impact of varying the number of generated RFMs on the fit quality. This information can be useful in determining the number of product sizes needed to accommodate children for mask design.

6.2 METHOD

A method was developed to generate a mask design based on RFMs representing a children's head and face dataset. Subsequently, these generated mask designs were virtually fit tested on 3D face dataset of the target population. The general workflow that was employed to conduct the current study consisted of the following steps. First, the relevant face area was separated from the full head data followed by splitting the dataset into a training set and testing set (section 6.2.1). Next, a weighted cluster analysis (section 6.2.2) that was conducted to group faces with similar size and shape and, subsequently, for each cluster an RFM was generated (section 6.2.3). These RFMs served as input for the parametric mask designs (section 6.2.4). Then each generated mask was fit tested with the individual faces that were assigned to the testing set (section 6.2.5) for that cluster. And finally, the fit test results were analysed and evaluated (section 6.2.6). The general workflow is presented in figure 41.

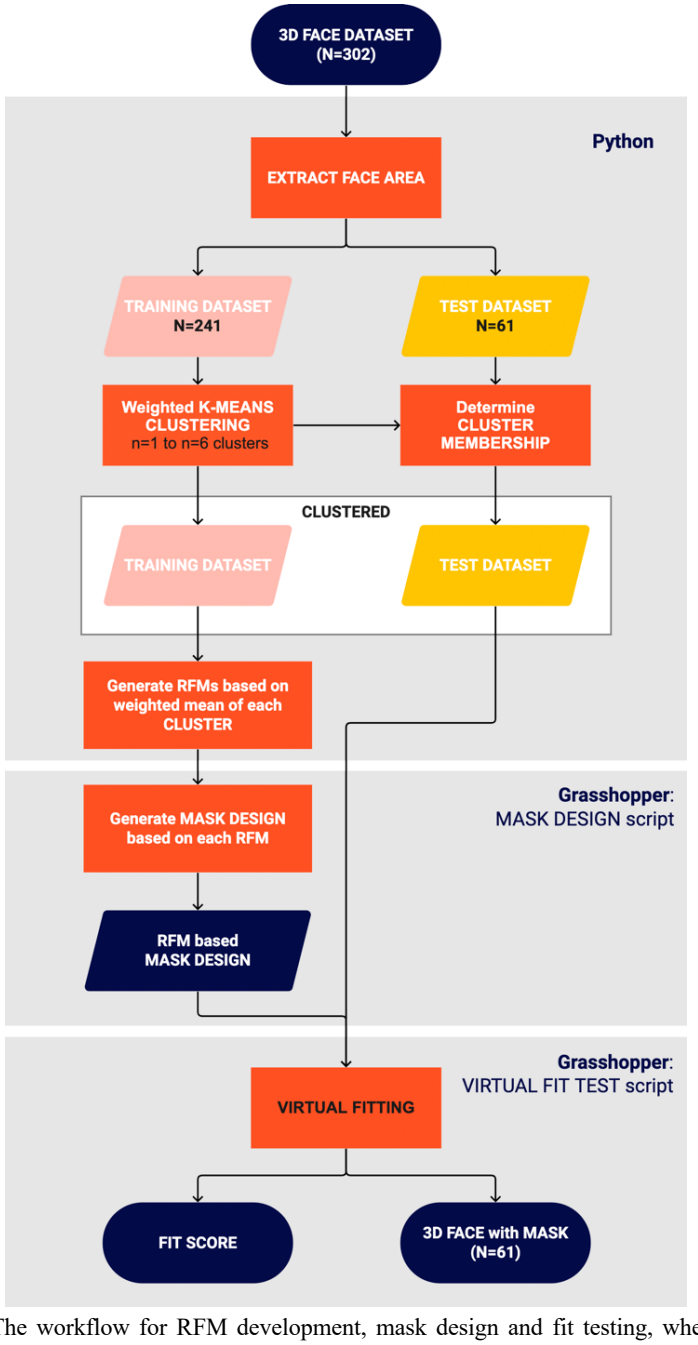

Figure 41 The workflow for RFM development, mask design and fit testing, where N is the number of individual 3D faces and n is the number of clusters which varied from n=1 to n=6.

6.2.1 3D HEAD AND FACE DATASET OF CHILDREN

For this study, the 3D head scan data of Dutch children aged 6 months to 7 years old were used as input to develop the representative face models and mask designs. The dataset consisted of 302 (128 females, 174 males) 3D head scan images and was generated as part of a previous study (Goto et al., 2021) employing both traditional anthropometric methods and 3D scanning techniques. A detailed description of the data collection, process, and analysis can be found in (Goto, Lee, et al., 2019). An overview of the age distribution and sample size can be found in table 14.

Table 14 Sample size by age, including age range (years), average age (years), and standard deviation (SD).

Age group	Age range	Average age and SD	N
1	0.50 - 1.49	1.0 +/- 0.3	33
2	1.50 – 2.49	2.0 +/- 0.4	28
3	2.50 -3.49	3.2 +/- 0.3	29
4	3.50 - 4.49	4.1 +/- 0.3	32
5	4.50 - 5.49	5.0 +/- 0.3	67
6	5.50 - 6.49	6.0 +/- 0.3	65
7	6.50 - 7.49	6.9 +/- 0.3	48
		Total:	302

6.2.1.1 3D Face data

To be able to conduct further analysis and generate RFM's based on the 3D head scan data of children there is a need to establish a correspondence between the individual scans. This action is necessary to make sure that the vertices that are part of the mesh of each scan are evenly distributed, are located at similar anatomical landmark locations, and have the same connectivity (Goto et al., 2021; Huysmans et al., 2020). A non-rigid template registration method (Dyke et al., 2020) is used to realize correspondence between each scan as is described in Goto et al. (2021). The following landmarks were used to steer the correspondence between the scans; tragion (right/left), infra-orbitale (right/left), pro-nasale, sub-nasale, alare (right/left), sub-labiale, promentale and menton. Next, the face area was separated from the head model because the focus of this study was on the face region where the ventilation mask is positioned and to focus the analysis on the geometry of this part of the 3D head scan. In order to do this, first, a template face was clipped to isolate the face region (figure 42). Then the selected region was mapped to the individual faces through the vertex correspondence between the template and individual faces, to clip the individual faces of the dataset, resulting in homologous meshes of the face. The objective was to generate meshes accurately

representing the facial shapes, while ensuring computational manageability for software like Grasshopper, resulting in face models consisting of 4072 vertices.

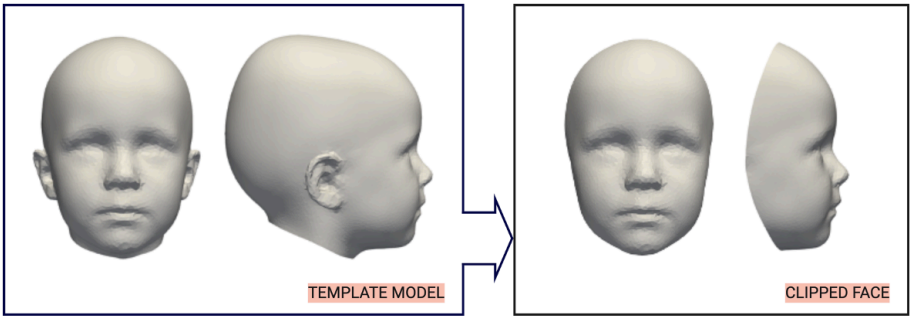

Figure 42 Template model, front and side view (left) and the clipped template model, front and side view (right).

6.2.1.2 Training and test data

The 3D face dataset was divided in a training dataset and a test dataset. The RFM's and the mask designs are generated based on the training dataset. Subsequently, the mask designs are fit tested with the test dataset to evaluate the mask designs and the representativeness of the RFM's. The 3D face dataset was randomly divided into 80% to 20% ratio, stratified over the age categories, to generate a training and test data set (Pedregosa et al., 2011). The training data consisted of 241 faces and the testing data consisted of 61 faces. The training data served as input for the generation of RFM's based on the cluster analysis.

6.2.2 CLUSTER ANALYSIS

Cluster analysis is a method to group subjects into clusters based on similarity between individuals. In anthropometry, clustering techniques are used to categorise individuals with similar body shape characteristics into groups which can then be used for sizing system development. K-means clustering is a clustering algorithm that divides the data into clusters based on the distance between each data point of an individual and the mean or centroid of each of the clusters. Clustering methods have been previously used to group 3D body shapes for product development and sizing (Baek & Lee, 2012; Lacko, Huysmans, et al., 2017).

6.2.2.1 Face shape clustering

A weighted k-means clustering method was performed on the 3D face shape models of the training dataset to divide the sample into n clusters that represent the number of sizing categories. The number of clusters varied from n=1 to n=6. A weighted clustering

was employed to prevent bias towards a certain age group because of differences in sample size per age category. Faces in a certain age category are assigned a weight equal to the ratio between the number of faces in the largest category (age group 5), effectively resulting in equal weight of the age categories during clustering (table 15).

Table 15 Clustering weights based on ratio between the largest age group (age group 5) and the other age groups.

Age group	Clustering weights
1	2.03
2	2.39
3	2.31
4	2.09
5	1
6	1.03
7	1.43

The maximum number of clusters was initially set at 6. For the clustering a region of interest (ROI, 1221 vertices) was selected in order to steer the clustering towards the relevant part of the face. This ROI is the area of the face which was considered as relevant for mask design and fit testing (figure 43). The clustering was done with the data points that fell within this region of the face. The k-means clustering used as feature vector the concatenation of the coordinates of all points of the ROI. The sum of the Euclidian distances of each individual face feature vector to the cluster centroids were iteratively assessed and subsequently assigned to different clusters. Subsequently, the cluster membership was determined for each 3D face shape in the test dataset. Finally, the number of cluster members per cluster were calculated, the average distance between each cluster member and the cluster mean was determined and the mean-to-mean distance between the clusters of the training and the test dataset were computed.

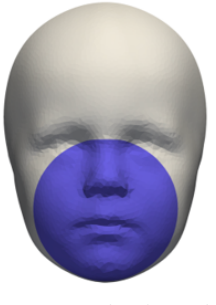

Figure 43 Region of interest (blue) that was used as input for the clustering of the face models.

6.2.3 RFM DEVELOPMENT

After clustering, representative face models (RFM's) were generated based on the training dataset for each cluster. Each RFM was constructed as the weighted mean of faces of each cluster, using a custom Paraview (https://www.paraview.org) filter, representing a sizing category for mask design. A more detailed explanation of the procedure can be found in chapter 5.2.6.

6.2.4 PARAMETRIC MASK DESIGN

Computational design has made it easier to quickly adjust and iterate designs within a CAD environment. When combined with RFMs it is possible to test different designs and predict the fit of masks designs in the early stages of product development. Cui et al. (2022) provides a stepwise approach for how mask designs can be generated based on RFMs. First, an initial design of the contact area that fits the RFM is determined, then, the contact area is refined through virtual or actual fit testing with a prototype. Finally, the design is optimized and the remaining parts, such as the connector to the oxygen supply system, is developed. This study focusses on the first step in RFM based design.

The mask design for this study was constructed using Rhinoceros 3D Version 6.35 (Robert McNeel & Associates) together with the integrated visual programming tool and environment, Grasshopper 3D (Robert McNeel & Associates). With the Grasshopper tool, one can build generative algorithms to generate 3D models. A parametric design method is utilised to generate the mask designs based on the RFM's. Parametric design allows to build up the design by using input parameters that use the 3D shape of the RFM and the predetermined vertex locations, which are the previously mentioned landmarks on the homological mesh, as a reference. This computational modelling allows for each mask design to automatically be generated for each RFM and would otherwise be time consuming when done manually. RhinoScript was used to apply the Grasshopper parametric design for all RFMs. Figure 44 presents the modelling workflow including how the parametric design is build up (Rhinoceros) and the respective Grasshopper algorithm. The following stages are depicted.

1. The mesh surface of the RFM is loaded into Rhino, Grasshopper.
2. 2D contour that passes through sellion, cheilion landmark (+16.5mm to the left and right) and the promentale landmark, is drawn.
3. 2D contour is projected on the RFM surface.
4. 2D contour and an 8 mm offset of this contour are projected on the RFM surface creating 2 3D curves. The projected curves are rebuilt to remove sharp corners.

5. These curves are then used to construct the contact area of the mask out of the mesh of the RFM surface. Curves are created between the inner and outer points of the mesh to replicate the exact surface of the mesh. A surface is created between the two curves, which is the base surface of the cushion: the 3D rim.

This is followed by the design of the remaining parts of the ventilation mask. For this study this part was only added for aesthetic/presentation purposes only. Based on the 3D rim the following parts are constructed:

1. The cushion.
2. The mask.
3. The connector.
4. Resulting in the final design.

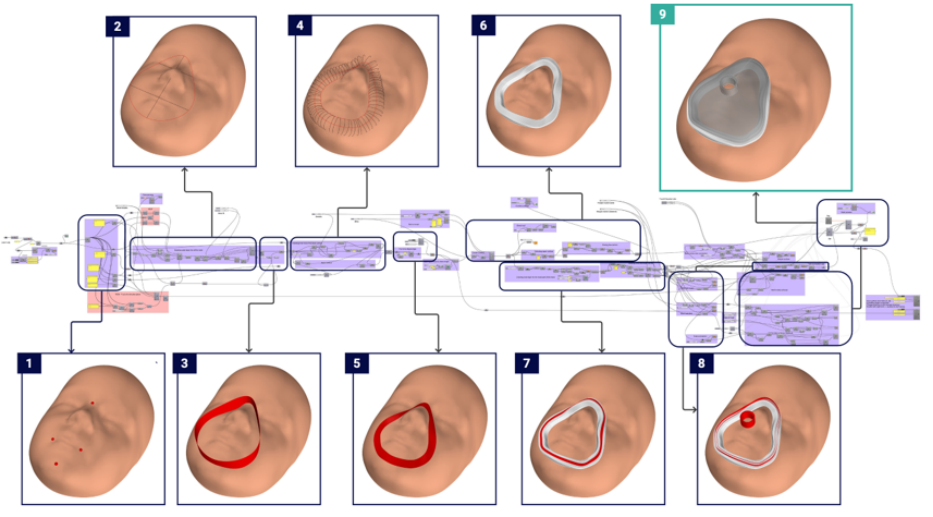

Figure 44 Modelling workflow for the parametric mask design depicting the following steps: (1) RFM is loading in Rhino. (2) Contour is drawn based on landmarks. (3) 2D contour is projected on the surface. (4) 2D contour and 8mm offset of contour are projected to create two 3D contours. (5) These two curves are used to create the contact area of the mask: the 3D rim. Based on the 3D rim the 3D cushion (6), the mask (7), the connector (8), are constructed. Resulting in the final design (9).

6.2.5 VIRTUAL FIT TESTING

Virtual fit testing is a method to simulate and evaluate the fit between the product design and the 3D body part for which it is designed in a virtual environment (Cui et al., 2022; W. Lee et al., 2021). A virtual fit test procedure was developed to analyse how each RFM based mask design fits on the individual 3D faces in the test dataset. This was done using Rhinoceros 3D Version 6.35 (Robert McNeel & Associates) together with Grasshopper 3D (Robert McNeel & Associates). Furthermore, because the fit testing needed to be executed multiple times, for each RFM based mask design, for each cluster and with each cluster member of the test dataset, a looping needed to be implemented to automate the process. For this, Phyton (version 2.7) was used. The procedure for the virtual fit testing of the RFM based mask design on each individual face within a cluster is visualised in figure 45 and consisted of the following steps:

1. The 3D face and the 3D rim are loaded into Rhino.
2. The 3D rim and face are moved into proximity by using an average line that connects the sellion landmark, tip of the nose and supramentale landmark and the y-axis of the rim as a reference. Subsequently, the 3D rim is moved until the point on the inner curve of the rim corresponds with the supramentale landmark on the 3D face.
    a. A genetic optimizer, called FroG (Framework for Optimization in Grasshopper) (Wortmann et al., 2023) was used to find the optimal fit between each individual 3D face and the rim.
    b. Different parameters (3 translational and 2 rotational degrees of freedom) served as input to find and optimize the positioning of the mask with respect to the 3D face. This procedure involves iteratively adjusting the transformation parameters of the mask to reduce the distance between mask and face. Each individual fit optimalisation ran for approximately 10 minutes.
    c. The fit test resulted in the final set of parameters based on the best fit option found. Based on that, the mean absolute distance (MAD) between the 3D face and rim were calculated. The best option was kept and saved as output.
3. Finally, the mask design is matched with the optimized rim location for visualisation purposes resulting in the final position of the fit tested mask on the 3D face.

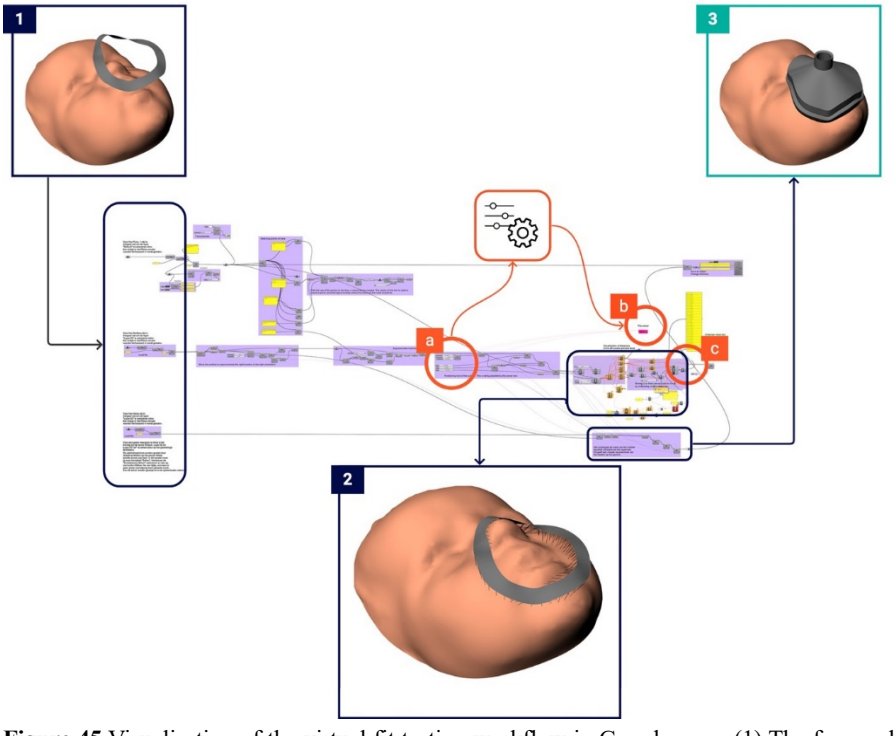

Figure 45 Visualisation of the virtual fit testing workflow in Grasshopper; (1) The face and rim are loaded in Rhino. (2) Virtual fit testing with (a) the input parameters, (b) the genetic optimizer (c) output distances and the best fit result. (3) Visualisation of the face and the fit tested mask.

6.2.5.1 Optimizing and quantifying the fit

The different parameters that served as input for the optimizer (point b. in the fit testing workflow) were (automatically) varied in order to find the optimal fit. These predetermined parameters affect the fitting procedure and can be summarised in the following formula:

$$D_{total} = \lambda_{distance} D_{distance} + \lambda_{gaps} D_{gaps} + \lambda_{asymmetry} D_{asymmetry} + \lambda_{nose\_asymmetry} D_{nose\_asymmetry}$$

with $\lambda_{distance} = 1.0$, $\lambda_{gaps} = 10000.0$, $\lambda_{asymmetry} = 5.0$, and $\lambda_{nose\_asymmetry} = 10.0$, which have been empirically obtained by multiple trials. Here, D_distance measures the sum of distances between mask points and the corresponding closest points on the face, for those points that are below the surface of the face. While D_gaps measures the sum of distances between mask points and the corresponding closest points on the face, but for those points that are above the surface of the face, i.e. air gaps. The former pushes the mask as close as possible to the face, while the latter term punishes

when air gaps appear during the fitting procedure. As shown, the factor for the gap term is high (10000) in order to avoid gaps in the final fit. These first two parameters, D_distance and D_gaps, formed the basis for the optimization process. The following parameters were added to refine the fitting procedure, with a specific focus on the nose bridge and symmetry. In order to make sure that the fit is symmetric, i.e. the left and right part of the mask are protruding the face similar amounts, two additional terms are included. The overall asymmetry of the fit, D_asymmetry, measures the difference in protrusion along the center of the rim between the left side and right side of the mask. We included a copy of this term that focussed on the nose part, named D_asymmetry, resulting in a stronger penalty for asymmetric fits in the nose area, due to the lower soft tissue thickness in that area. This ultimately results in the best fit found within the run time of the fit optimalisation.

6.2.6 FIT TEST EVALUATION

Based on the result, the fit test was evaluated both quantitatively and through a visual inspection. The quantitative analysis assesses the fit between a 3D face and mask rim design by calculating the distance between the mask and the face and subsequently visualizing the results in a heatmap. A visual inspection alongside quantitative analysis was necessary to evaluate the fit between a 3D face and the rim. The quantitative analysis provided measurements of the distance between the face and rim, which could indicate a good fit. However, the visual inspection was necessary to ensure that the rim itself was positioned correctly. It allowed to assess if the rim was too low or too high, or if it was too close to the mouth or eyes, despite seemingly good quantitative fit measurements. The visual inspection protocol encompassed several key criteria, namely, ensuring that there is no overlap with the eyes, ensuring that the corners of the mouth do not touch the rim, verifying that the rim did not penetrate the face by more than 8 mm, and confirming the absence of any gaps between the face and rim. 8 mm was chosen as to simulate impression of the rim of the mask as was done in (W. Lee et al., 2021). Each mask and face combination was first inspected based on overall fit and positioning and then closely inspected based on previously mentioned criteria. If one or more of these criteria were not met, the fit was considered a bad fit. These criteria allowed to assess qualitative aspects of fit that are important for comfort and functionality.

6.3 RESULTS

In this section, the clustering results are presented first (6.3.1), followed by the RFM's that were generated based on each cluster together with the respective mask designs (6.3.2). Finally, the virtual fit test results are presented (6.3.3).

6.3.1 ROI based face shape clusters

The result of the weighted k-means clustering that was performed on the 3D face shape models is visualised in figure 46 and summarised and presented in table 18. Figure 46 shows the cluster results in a 2D plot based on face length and face width and illustrates how the individual faces are distributed over the different clusters. The visualisations of the clustering results show that the clustering was largely based on overall face size in terms of width and length. However, when clustering into 5 or 6 cluster another variable influences the clustering of the smallest faces, namely the shape of the face or the upper and lower face ratio (cluster 5.1, 5.2, 6.1 and 6.2). Table 16 provides more detailed information about the number of cluster members per cluster, the average distance between each cluster member and the cluster mean as well as the mean to mean distance between the clusters of the training and the test dataset. It shows that the training dataset and the test dataset have a similar spread throughout the different clusters, but the test dataset clusters are in average more compact (the average distance and standard deviation of the distance to the cluster mean is smaller). But the distance between the means of both the training dataset and test dataset is typically quite small, except when the number of test subjects is low. This is subsequently visualised in figure 47, where the mean distance between the training cluster mean and cluster members per cluster for both the training dataset and the test dataset are visualised in a heat map. Here, the average distances of different locations within the region of interest can be observed. Prominent/distinguishing features of the face, such as the eyes, nose, and chin can be observed and show larger distances towards the mean of the cluster.

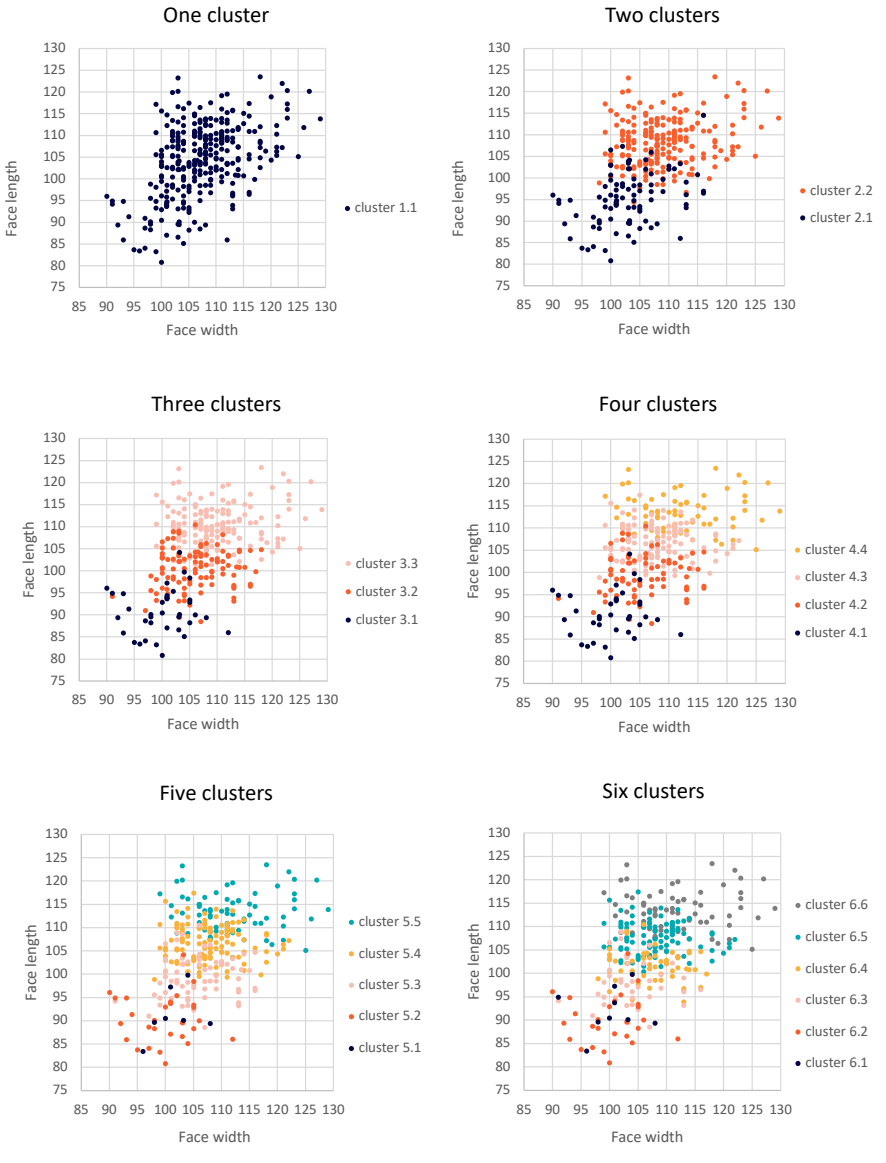

Figure 46 Clustering results of 301 3D faces presented in a 2D scatterplot of face width and face length.

Table 16 Number of cluster members (total and test dataset), member distribution (%), mean distance and standard deviation between cluster members and training cluster mean for both the training and test dataset, and the mean to mean distance between the training and test dataset (mm).

	Cluster number	Number of cluster members (Total)	Member distribution%	Number of cluster members (test dataset)
1	1.1	301	100	61
2	2.1	89	29.6	17
	2.2	212	70.4	44
3	3.1	37	12.3	6
	3.2	103	34.2	24
	3.3	161	53.5	31
4	4.1	73	24.2	13
	4.2	117	38.8	30
	4.3	37	12.3	6
	4.4	74	24.5	12
5	5.1	74	24.5	12
	5.2	29	9.6	5
	5.3	8	2.7	1
	5.4	117	38.8	30
	5.5	73	24.2	13
6	6.1	72	23.9	11
	6.2	27	9.0	5
	6.3	54	17.9	10
	6.4	39	13.0	10
	6.5	10	3.3	1
	6.6	99	32.9	24

Table 16 (continued).

Mean distance to cluster mean (training)	Std of distance to cluster mean (training)	Mean distance to cluster mean (test)	Std of distance to cluster mean (test)	Mean to mean distance (training - test)
3.6503	1.9812	3.3341	1.7304	0.5529
2.5652	0.7726	2.3857	0.4948	0.6783
3.3491	1.3414	2.9748	0.9564	0.6690
2.1880	0.5156	2.3045	0.4339	0.6895
3.1583	1.1141	2.2915	0.3563	0.9494
2.3684	0.6299	2.2282	0.3718	0.6811
2.1269	0.5028	2.2081	0.4471	0.9717
2.0420	0.4153	2.1086	0.3283	0.7102
3.1583	1.1141	2.2915	0.3563	0.9494
2.1613	0.5696	2.1737	0.2807	0.8156
2.1613	0.5696	2.1737	0.2807	0.8156
2.4593	0.6272	2.3330	0.6729	1.3486
3.0158	1.1226	2.4865	0.0000	2.4865
2.0420	0.4153	2.1086	0.3283	0.7102
2.1269	0.5028	2.2081	0.4471	0.9717
2.1572	0.5716	2.1200	0.2264	0.7964
2.4062	0.6331	2.4040	0.7271	1.5054
1.9659	0.5173	2.0625	0.3189	1.1833
1.9803	0.4799	2.0164	0.4653	0.9622
3.0860	0.9475	1.9276	0.0000	1.9276
2.0080	0.4303	2.0888	0.3237	0.6740

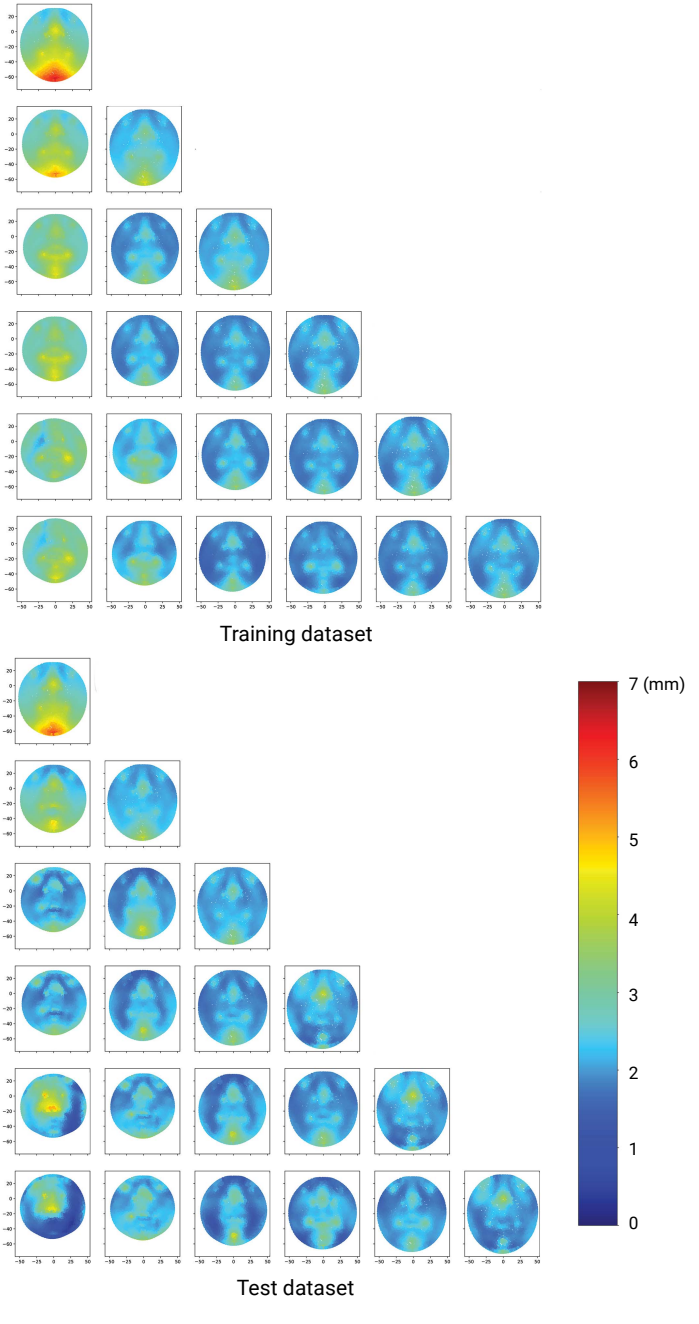

Figure 47 Visualisation of the mean distance (mm) between the mean and cluster members per cluster for both the training dataset (top) and the test dataset (bottom) in a heat map.

6.3.2 REPRESENTATIVE MODELS AND MASK DESIGN

Based on the training dataset members within each cluster a total of 21 RFMs were generated (figure 48). Subsequently, based on these RFMs the mask designs were generated. Both RFMs for all clusters and the respective mask designs are presented in figure 49.

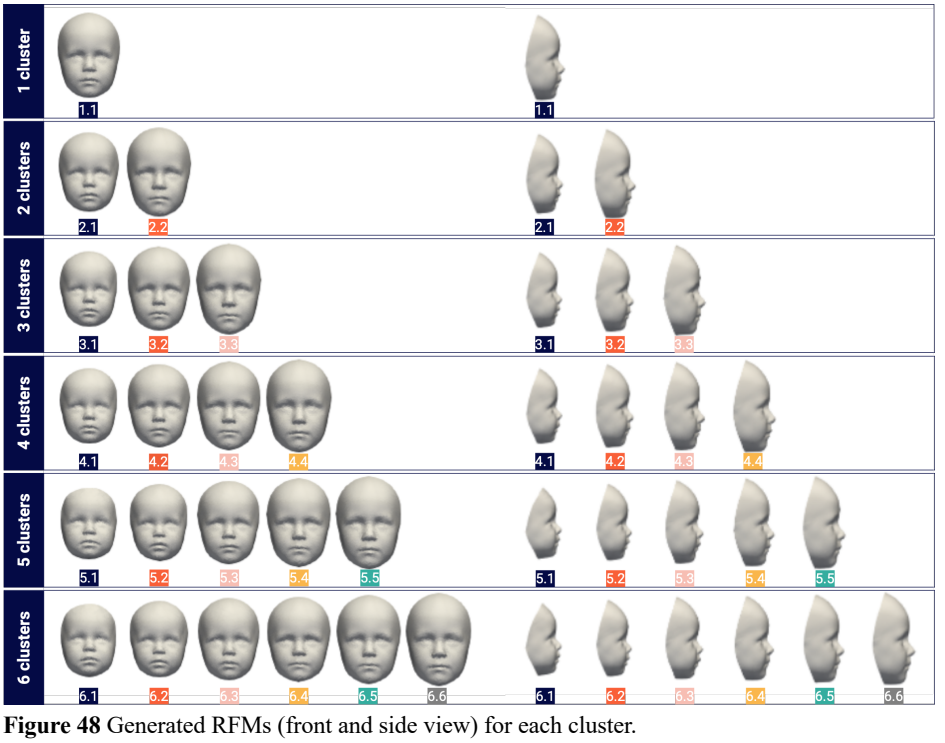

Figure 48 Generated RFMs (front and side view) for each cluster.

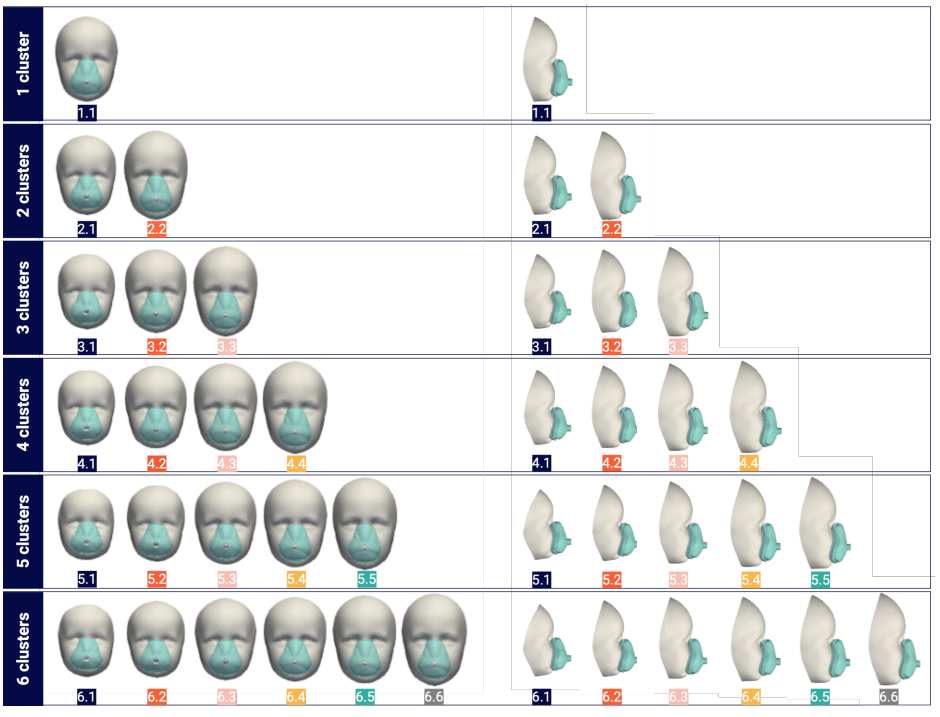

Figure 49 Generated RFM based mask designs (front and side view) for each cluster.

6.3.3 VIRTUAL FIT TEST RESULTS

The generated mask designs were virtually fit tested on the test dataset. Each mask design that was developed based on an RFM representing a certain cluster was fit tested on each respective cluster member that is part of the test dataset. The initial quantification of the fit was calculated based on the distance between the rim of the mask and the 3D face.

6.3.3.1 Quantified fit test results

Per cluster, the mean absolute distance (MAD) between the mask and each 3D face (test dataset) was calculated. Table 17 presents, the mean distance, standard deviation, and maximum distance for each cluster, together with the 25th, 50th and 75th percentile values of each distance. The mean distance decreases with the number of clusters but with four clusters and more, the is no clear trend. The virtual fit test results per cluster are also visualised through heat maps in figure 50.

Table 17 The mean absolute distance between each 3D test face and mask, calculated for each clustering, including, mean, standard deviation (std), minimum (min), maximum (max), and 25th, 50th ,75th, percentiles.

Number of clusters	MAD							
	Count	Mean	std	min	25%	50%	75%	max
1	61	2.56	0.90	1.33	1.97	2.44	2.82	6.67
2	61	2.31	0.66	1.18	1.86	2.20	2.59	4.18
3	61	2.24	0.61	1.10	1.82	2.17	2.60	4.11
4	61	2.39	0.79	0.99	1.92	2.21	2.73	5.19
5	61	2.36	0.80	1.05	1.87	2.26	2.70	5.63
6	61	2.25	0.74	1.04	1.72	2.18	2.73	4.22

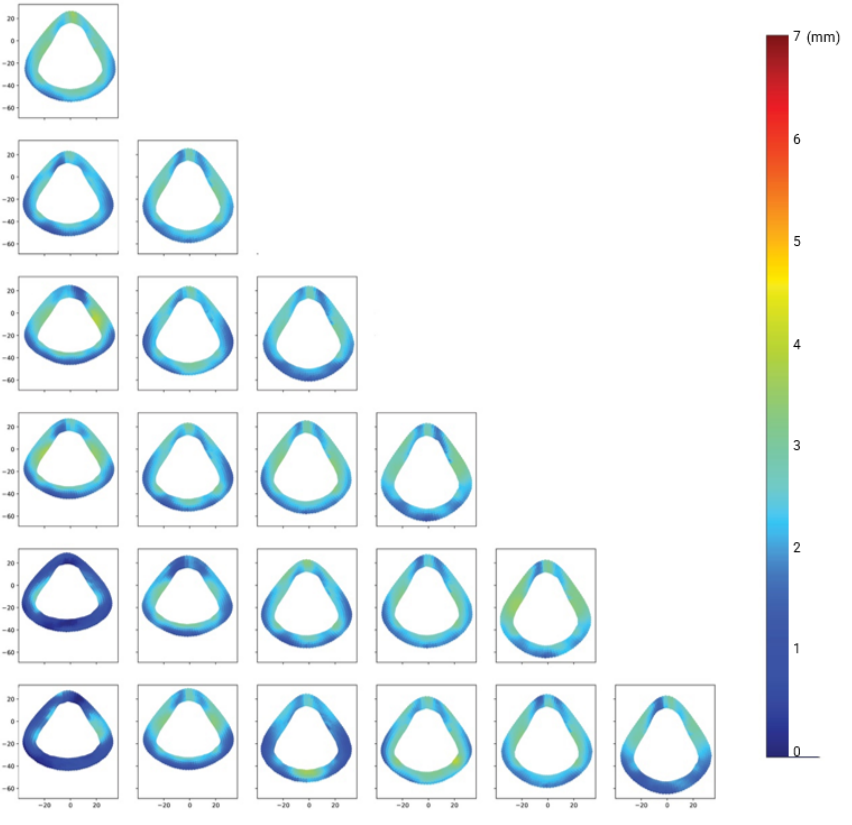

Figure 50 Visualisation of the fit test results per cluster in a heat map. The mean distance between the mask rim and the 3D faces in the test set, visualised through the range 0 mm (blue) to 7 mm (red). Mask rim dimensions are depicted in mm (horizontal and vertical axes).

6.3.3.2 Results of the visual inspection

Each 3D face and mask combination within each cluster was visually inspected based on predetermined criteria. The results can be found in table 18. The number of 3D faces and mask combinations that were considered a bad fit were recorded and the total number of bad fits per clustering were calculated. Furthermore, the type of bad fit was also recorded. The types of bad fits that were observed could be categorised as follows; the mask showed an overlap with the eye(s), there was a gap between the mask and the face (always in the nose bridge region), the mask was pushed too deep at the nose bridge, cheek(s) or chin, and finally, the mask rim was in close contact with the mouth, often in the breadth direction. These observations are presented in table 19 and examples of what were considered as a good fit and bad fist are depicted in figure 51.

Table 18 The number of visually identified bad fits per cluster.

Number of clusters	Cluster number	Number of bad fits per cluster total	Total number of bad fits	Percentage of total
1	1.1	30/61	30	49.%
2	2.1	6/17	23	38%
	2.2	17/44		
3	3.1	1/6	15	25%
	3.2	6/24		
	3.3	8/31		
4	4.1	1/13	10	16%
	4.2	5/30		
	4.3	1/6		
	4.4	4/12		
5	5.1	4/12	14	23%
	5.2	1/5		
	5.3	0/1		
	5.4	7/30		
	5.5	2/13		
6	6.1	4/11	12	20%
	6.2	0/5		
	6.3	1/10		
	6.4	1/10		
	6.5	0/1		
	6.6	6/24		

Table 19 Types of bad fits identified per clustering.

Number of clusters	Overlap Eye	Gap Nose	Too deep			Contact mouth/rim
			Nose (bridge)	cheek	chin	
1	4	3	6	3	1	13
2	6	2	4	2	1	8
3	4	0	6	2	0	3
4	1	1	4	1	2	1
5	0	6	6	0	1	1
6	0	6	4	2	0	0
Total:	15	18	30	10	5	26

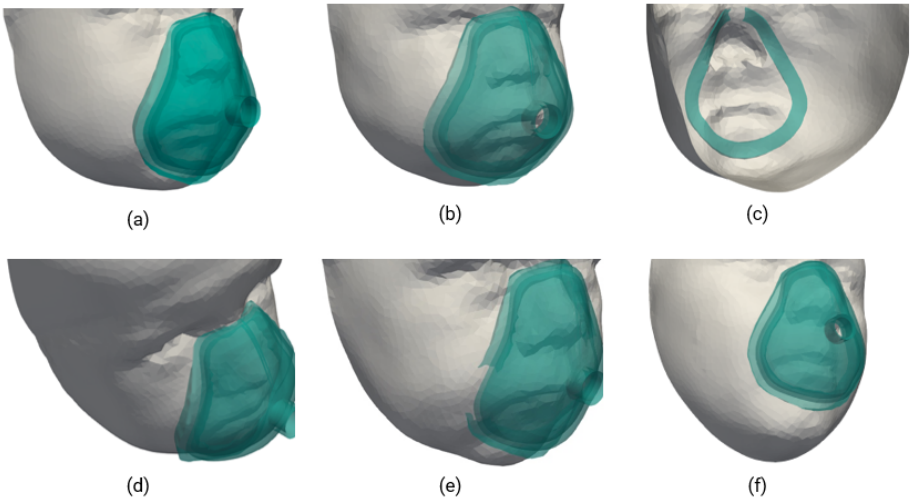

Figure 51 Examples of a fit that was identified as a good fit (a) and a bad fit, where the mask is too big and covers the eyes (b), shows a gap at the nose (posterior view) (c), too deep at the nose (d) or cheek (e) and contacts the mouth (f).

The frequency of bad fits per clustering decreased as the number of clusters increased. However, beyond 4 clusters there was no discernible trend in the reduction of bad fits. Among the clusters with the highest number of members, the occurrence of bad fits was most prevalent. Analysing the types of bad fits revealed a decrease in fitting issues around the eyes and mouth as the number of clusters increased. However, an increase in gaps around the nose was observed. Visual inspection further indicated that fitting problems around the nose bridge, specifically too deep, were consistently present across all clusters and accounted for most of the identified bad fits.

6.4 DISCUSSION

The aim of this study was to utilize RFMs to generate mask designs specifically for children. The research introduces a computational mask design method along with a virtual fit testing approach to evaluate the fit of these designs. The evaluation was conducted using a 3D face dataset, providing insights about the use and application of these methods and datasets in the development of masks for children. A specific effort was made to develop a method that is accessible for designers without coding skills by implementing the design and evaluation through visual programming.

RFMs were successfully employed to explore the potential use of RFMs in design. The utilization of RFMs offers the opportunity to incorporate more intricate anthropometric shape information into the design process, benefiting designers (Ball, 2009). The findings of this study underscore the potential of RFMs in optimizing the design and sizing of head-related products. Furthermore, by automating the process of tailoring mask designs to accommodate various facial shapes, specifically RFMs representing different clusters, it becomes possible to achieve swift iterations in the mask design process. Also, RFMs tailored for product design offer a privacy-conscious solution for designing products, particularly for vulnerable populations like children. These models capture average facial characteristics or variations within the target group, ensuring inclusivity and customization. By using RFMs instead of raw individual data, privacy concerns surrounding children's sensitive information can be addressed.

The study findings demonstrated that an increase in the number of RFMs resulted in an enhancement of the mask fit quality, as evidenced by the calculated MAD between the mask and face. However, it was observed that once a certain threshold of clusters (in this case, four) was reached, there were no substantial further improvements in the extent of fit. The variability in the quality within a particular cluster, transitioning from, for instance, three to four clusters, can be attributed to the fact that the mask fitting process does not consistently yield the most optimal outcome. Consequently, different runs of the same mask with the identical test set can yield variable results. On the other hand, the outcomes of the visual inspection provided clear indications that the bad fits identified within one, two, or three clusters primarily centred around the eyes and mouth, indicating instances where the mask was either too small or too big. These findings suggest that incorporating additional sizing categories would be necessary to adequately address the facial shape and size variations within this sample.

However, all clusters experienced fit issues in the nose-bridge region regardless of the number of clusters indicating that possibly the variation in this region is larger than for

the other regions or due to the difficulty for the algorithm to correctly position the mask. Nevertheless, if a more iterative process would be utilized whereby the feedback is incorporated into a second design iteration it would be possible to resolve specific fit issues, which were not obvious beforehand, on a more detailed level. This could be achieved in a number of ways including improving positioning of the mask, specific focus on problem areas in the face, incorporating local variations in the RFMs, or include low and high percentile RFMs to visualise overall variation, etc.

Furthermore, this study highlights the importance of performing a visual check in addition to the objective fit assessment. While the fit results may suggest a satisfactory objective fit, it is crucial to ensure that the mask does not obstruct the eyes or mouth and that there are no gaps between the 3D face and the mask rim. The visual check pointed out that integrating additional checks into future script iterations, such as identifying the angles of the eyes and mouth corners and penalizing any overlap with the mask rim, could effectively address this issue. By incorporating such considerations into the virtual fit testing process, a more comprehensive evaluation of mask fit can be achieved.

Due to time constraints, only a limited number of iterations was performed for the fit testing using the genetic algorithm (GA). Each fit optimization process took approximately 10 minutes with a maximum of 600 iterations of the genetic algorithm. It is important to note that the number of trials during the fit testing phase can have an impact on both the duration and the outcome, and using a genetic algorithm within a predefined time span may not always result in the best fit. Often the GA is started a few times (number of trials) and the best result is kept but within a specific time frame this does not guarantee that this will result in the best outcome. Future studies should allocate more time or computational resources to explore a wider range of iterations, allowing for a more comprehensive fit optimization process and potentially improving the quality of the mask fit. Additionally, various algorithms were tested, and the optimal algorithm and settings were empirically determined. In order to improve the computational efficiency of the Grasshopper script more systematic evaluation of different optimisation algorithms is advisable. For instance, using a Grasshopper optimizer component which is more efficient because it does not visualize every iteration, making it able to run more trials within the same time span.

One limitation of our study is the relatively small sample size of the 3D face dataset, which comprised 302 Dutch children. This dataset was randomly divided into a training dataset (n=241) and a testing dataset (n=61). While we used a significant portion of the dataset for training, the limited size of both the training and testing datasets may restrict the generalizability of our findings to the broader population. The smaller sample size

increases the risk of sampling bias and reduces the statistical power to detect subtle variations in face shapes and dimensions. To address this limitation, future research should aim to include larger samples, encompassing children from different age groups, ethnicities, and geographical regions. By increasing the sample size and diversity, the RFMs generated would better represent the variability of children's faces, enhancing the applicability of the findings in real-world scenarios and improving the accuracy of the fit evaluations.

The use of visual programming tools, such as Grasshopper and plug-ins, was preferred in this study to enhance accessibility for designers during the computational design process and fit testing. However, it is important to acknowledge that this choice comes with the drawback of increased time requirements compared to programming in Python or c++. In the Grasshopper environment, a notable issue arises with the overhead associated with visualizing the result after each iteration. Ideally, this overhead should be minimized since it consumes valuable processing time. In future research, alternative design platforms or automation techniques could be explored to find a balance between accessibility and efficiency, while still providing user-friendly interfaces for designers. Finding a suitable approach that optimizes both accessibility and computational efficiency would further enhance the usability and effectiveness of the mask design and fit testing process.

This study focused on generating a mask design using 3D anthropometric data and objectively assessing its fit. While in this study the fit is quantified, achieving an ideal, comfortable fit requires consideration of biomechanical factors like bony structures, fatty tissue, facial tissue sensitivity, and flexibility. Further research into these anatomical and biomechanical aspects, along with adjustments to design and materials, is needed. Additionally, product use and context, such as wearing the mask during sleep or in a hospital setting, can affect fit and comfort, necessitating further investigation for design optimization.

6.5 CONCLUSION

In conclusion, this study successfully utilized Representative Face Models (RFMs) to generate mask designs specifically for children. The implementation of a computational mask design method and virtual fit testing provided valuable insights into their use and application in the development of masks. The study highlighted the potential of visual programming in optimizing the design and sizing of head-related products, offering the opportunity to incorporate anthropometric shape information for designers without coding skills. By automating the process of tailoring mask designs to accommodate

different facial shapes represented by RFMs and subsequently virtual fit testing these masks, the study demonstrated the potential for quick iterations in the mask design process. The study findings emphasized the importance of visual inspection in addition to objective fit assessment. In addition, the study has identified areas for improvement within the use of RFMs in mask sizing and design, such as integrating additional checks into the fit testing process. Future research should aim to explore alternative design software platforms for improved efficiency, expansion of the algorithm to allow for a more iterative design process to optimize fit, expand the fit testing process to consider subjective measures and the effect of material properties or additional mask components. By addressing these aspects, the design and fit evaluation of masks can be enhanced to better meet user needs and preferences.

7

GENERAL DISCUSSION AND CONCLUSION

This final chapter reflects on this research project, discusses the answers to the research questions, provides general insights generated during the research and provides recommendations for further investigations.

7.1 INTRODUCTION

The overall objective of this thesis is to provide researchers and designers with specific knowledge on how to integrate 3D anthropometric data in the design process of products that need to closely fit the human body or part of the human body. This chapter summarises the results and conclusions of this thesis and reflects on the research as a whole by readdressing the research questions and by discussing the findings according to the research levels as presented in chapter 1; namely the anthropometric level, the design level and the product level. Subsequently the chapter will reflect on the contributions of the project, discuss the general limitations and finally identify opportunities for future research.

7.2 ANTHROPOMETRIC LEVEL

The starting point of this thesis is on the anthropometric level since this forms the basis for all the research activities that followed. The main research question was:

RQ 1: How to collect, process, analyse and present 3D anthropometric data of children's heads and faces for design purposes?

With the following sub questions.

- What is the facial (shape) variation of children aged 0-6 years?
- How can the facial shape variation be presented to designers?

Chapter 2 presented the process of acquiring, processing and analysing traditional measurements and 3D scan data. As a results, descriptive statistics of traditional and 3D scan extracted measurements of children's heads and faces of Dutch children were presented. The study showed that 3D photogrammetry is a suitable technology to collect 3D scans of babies and young children because of its high capturing speed and accuracy. It also showed that the data processing required in order to extract relevant 1D measurements from the 3D data requires multiple steps including data cleaning, aligning and virtual landmarking. While in chapter 2 the focus was on 1D measurements, in chapter 3 the 3D shape variation of Dutch children's faces were analysed based on the same 3D scans. Both a dimension based PCA and 3D shape based PCA were conducted and visualised to study the face shape variation, and thus provide insight into how the face shape of Dutch children throughout the different age groups varies.

The results revealed that the first principal component primarily captured the variation in overall face size, indicating that the morphological variation of the children's faces over an age span of 0.5 to 7 years varies most in overall size of the face. Additionally,

the length related measurements have the strongest influence within PC1 and contribute the most to the overall variation in facial features. The second component represented face width, with higher scores indicating short and broad faces and lower scores indicating longer and narrower faces. These findings were consistent with a study on facial dimensions of adults for respirator design. There was however a notable difference in the greater variation of overall face size among children compared to adults. This suggests that children's faces exhibit more diverse size differences, likely due to age-related factors. The shape variations in the remaining PC's are more subtle and contribute less to the overall variation.

The dimension based PCA gives insight into which product relevant dimension influences the variation of face shape and to which extent. The shape based PCA helps the designer to understand shape variation in a more visual way and shows how the face-shapes vary within the population. By subsequently projecting a product contour on the 3D face shapes, as was done in chapter 3, the product related shape variation can be visualised. For a designer of head and face related products, both analysis methods can be useful and are complementary because they facilitate in organising and presenting the complex 3D data in different ways whether it focusses on product specific dimensions or the dimensions of the faces as a whole.

During these two phases of the research additional insights were developed both with respect to the content generated and the underlying processes to develop this content as will be explained in the following sections.

7.2.1 COLLECTING 3D ANTHROPOMETRIC DATA

When relevant anthropometric data is not readily available, one of the options is to collect the data yourself. Setting up a survey and collecting anthropometric data is a time-consuming undertaking. An anthropometric survey of adults can include 100 to more than 1000 participants because it requires a considerate number of participants in order to get a representative sample (ISO 15535, 2007). Extensive (often full body) surveys can include more than 60 measurements per participant and could take more than an hour per session. If some of the traditional measurements were to be replaced by 3D scan extracted measurements through 3D scanning the participant, this may reduce the survey time. Therefore, the threshold for setting up a survey to collect relevant data may be lower than with traditional data. If that results in an increase of publicly available 3D anthropometric datasets, designers will be able to incorporate 3D anthropometric data more often, potentially leading to better fitting products (Li et al., 2022).

7.2.2 POTENTIAL OF 3D ANTHROPOMETRIC DATA

One of the important advantages of 3D data is its versatility and its (re-)accessibility once it has been obtained. The research that was conducted as part of this thesis shows some examples of how the 3D data can be analysed, visualised and used for design purposes related to the second sub question. The current dataset was studied and presented in the work of Lee et al. (2017). The dataset served as input to explore different analysis and visualisation methods to study the face shape variation within the current dataset. The analysis methods that were employed were based on, landmarks, vertex points and curvatures as presented in figure 52 to 55 respectively. The scatterplot in figure 52 shows how the landmarks locations vary through different age groups by assigning each landmark of each age group a different shade of red (bright red: 0.5-year-old; dark red: 7-year-old). Figure 53 and 54 show the result of a PCA conducted on landmark locations and vertex points respectively. Here the direction (red lines) of how each landmark or vertex varies throughout the age groups can be observed. The red lines in figure 53 represent the eigenvector × ± 10 standard deviations (SD) applied to each landmark point and eigenvector × ± 20 SD applied to each vertex point in figure 54. By zooming in on a specific product relevant area of the face (e.g., nose bridge for glasses) and visualising the contours, the designer can determine the shape and estimate the number of required sizes for a certain product by taking into account material margins, properties or adjustability of the design (W. Lee et al., 2016). Each method unveils the variation of the same dataset in a different way and can provide the researcher or designer with different insights. Close collaboration between for example a data scientist who can demonstrate what is possible in terms of visualizations and analysis methods can inspire designers to develop more creative solutions when designing better fitting products.

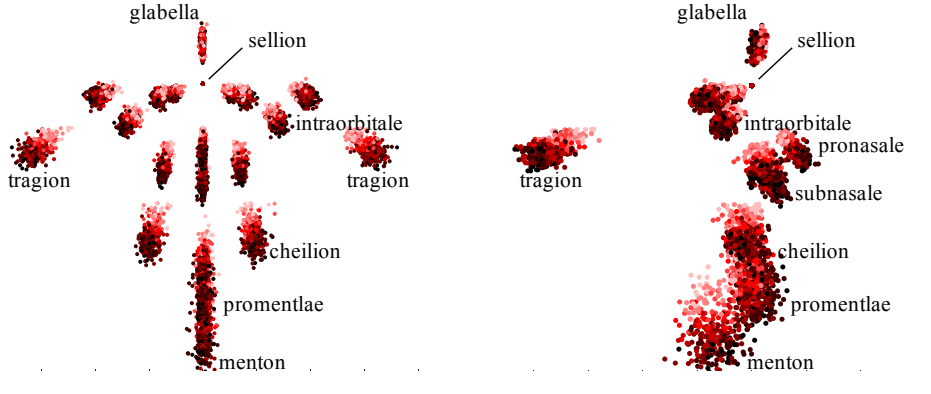

Figure 52 Variation of landmark positions of the sample (N=302) (front and right views) (W. Lee, Goto, Molenbroek, & Goossens, 2017)

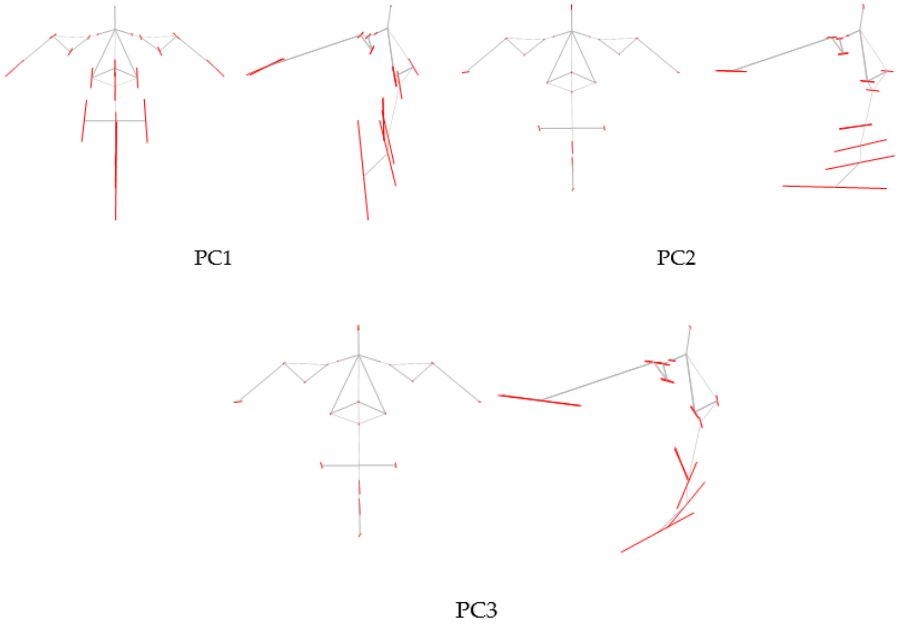

Figure 53 PCA applied to the x, y and z positions of all landmarks (front and right views). The red lines in the figure represent eigenvector × ± 10 SD applied to each landmark point. (W. Lee, Goto, Molenbroek, & Goossens, 2017)

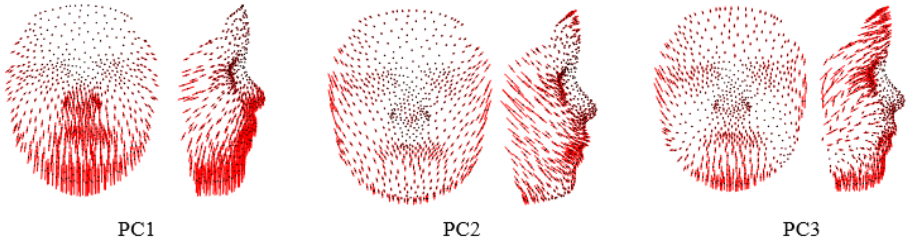

Figure 54 Visualisation of a PCA applied to x, y, z position of all vertex points on template-registered face models (front and right views). Red lines in the figure represent eigenvector × ± 20 SD applied to each vertex point. (W. Lee, Goto, Molenbroek, & Goossens, 2017)

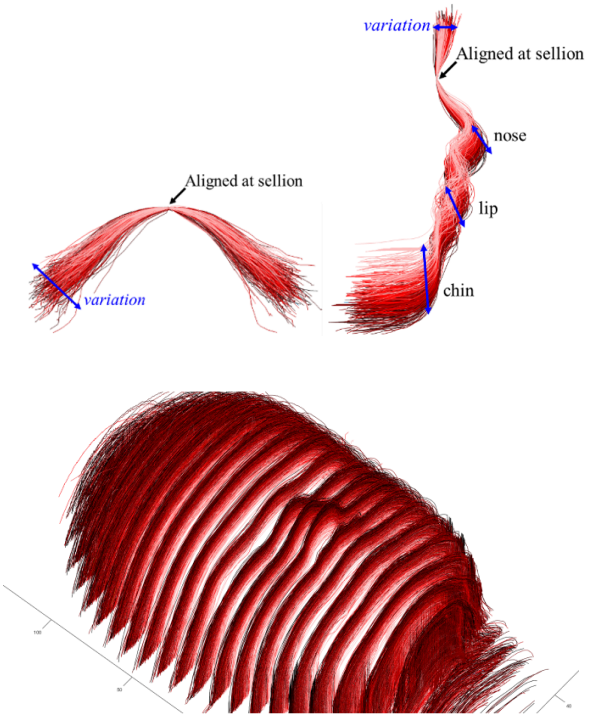

Figure 55 Variation of curvatures of (a) the nasal root curvatures between eyes, mid-saggital cross sections of the face (b) and horizontal cross sections of the face (c) (W. Lee, Goto, Molenbroek, & Goossens, 2017).

7.2.3 LIMITATIONS RELATED TO THIS DATASET AND OPPORTUNITIES FOR FUTURE RESEARCH

7.2.3.1 Representativeness and dataset expansion

In this thesis, the variation of heads and faces of Dutch children in terms of dimensions and shape was studied. The sample consisted of 302 children in total with varying number of children in each age group, ranging from 17 to 66. Children were recruited in the South Holland region and therefore it cannot be considered to be representative of the Netherlands. In order to conduct some verification of how these measurements compare to the national population, the traditional measurements of current dataset were compared with Steenbekkers dataset in chapter 2. However, the results did not show any clear trend and the significant differences that were found, were distributed throughout all age groups and different dimensions. In order to set up an anthropometric database

of a representative sample of children living in the Netherlands, ISO 15535 recommends to calculate the sample size with the following formula:

$$N = \left(\frac{1.96 \times CV}{a}\right)^2 \times 1.534$$

Where 1,96 is the critical value from a standard normal distribution for a 95% confidence interval (meaning that it ensures that the database 5th and 95th percentile estimates the true population 5th and 95th percentiles with 95 % confidence) and CV is the coefficient of variation of a relevant dimension that is part of the survey. For example, when using the CV of head height of 4-year-olds (Farkas, 1994), the calculation results in a sample size of 146 children per age group. Alternatively, when setting up a survey employing 3D surface scanners and subsequently set up a database consisting of scan extracted measurements, ISO 20685 recommends that at least 40 participants per age group per gender are included in the sample.

Also, the sample should be representative with respect to demographics such as sex, socio-economic variables, ethnical background and number of children in each region of the Netherlands, according to Steenbekkers (1993) these are variables that have a potential effect on growth. Because of limitations in time and resources, sampling this number for current dataset was not feasible but expanding current dataset based on the before mentioned calculations and variables would be beneficial considering the lack of 3D anthropometric data sets, especially of children.

7.2.3.2 Ethical considerations related to 3D face data

An important aspect of working with personally identifiable research data, which is often the case in anthropometric surveys, is setting up a data management plan and data storage en sharing strategy should be according to the European General Data Protection Regulation (GDPR). Personal identifiable information, such as name and email address is only used for administrative purposes and after anthropometric data collection, it is deleted in order to anonymise the data. All other individual data, such as measurements results, are often accessible in the form of tables and graphs and do not refer to an individual person. However, 3D scans of the face, especially including texture, is recognizable and is challenging to anonymise. Therefore, individual 3D scan data cannot be shared or published unless full consent is given by each participant. In videos and pictures, parts of the face (often the eyes) can be blurred out in order to make the person unrecognizable. But by blurring or smoothing out parts of the 3D image affects the

morphology of the face and by doing this, essential details of the face shape would gone missing.
One solution is generating statistical shape models that represent a certain sample. These mathematical models, as presented in this thesis as RFMs, can provide a solution for designers who want to study shape variation of a certain population or incorporate 3D shape information in their design. However, it is important to consider how these models reflect the variation of individuals, and whether there is still interesting or relevant information in the raw data. Can RFMs capture the subtle variation that is characteristic of individuals? Further research into the representativeness of these models is necessary.

7.3 DESIGN LEVEL

After developing an understanding on anthropometric level in terms of both the data and the processing the next step in the research was to develop a method to transform this data into meaningful and useful information for designers, which is reflected in the 2nd research question:

RQ 2: What are approaches/methods to integrate the use of 3D anthropometric data of the head and face in developing sizing systems of head related products?

With the following sub questions.

- What type of data is used and how is it processed?
- What information of the 3D head /face data is used in the sizing system development process?
- What considerations from a product development perspective are taken into account?
- How do 3D representative models (RM's), that are developed based on different sizing analysis methods differ and what are implications for the design and sizing of a ventilation mask?

In this phase we focused first on how 3D anthropometric head/face data has been applied in previous research and then set forth on exploring different anthropometric analysis methods and the development of representative models to determine the advantages and disadvantages of each.

Chapter 4 provided an overview of approaches for developing sizing systems based on 3D anthropometric head and face data. The review revealed that while there has been a growing trend of incorporating 3D shape information in sizing systems, a significant portion of the reviewed studies still rely primarily on 1D measurements that are

extracted from the 3D data. It also showed that incorporating shape information in sizing requires tailored sizing system development methods. 3D data enables diverse approaches for shape-oriented sizing, which rely solely on shape rather than key dimensions. However, these methods require skills in statistics, computer proficiency, and data science expertise which not every designer has.

Virtual representative models (RM) based on 3D data offer potential for sizing and design. These representative (design) models are commonly used to visualize the variability of the target population, allowing designers to use them in a CAD environment to virtually adjust their designs. Therefore, in chapter 5 we explore some approaches within the context of face mask development. In order to compare three anthropometric analysis methods for the development of sizing systems, representative face models (RFMs) and mask contours were generated based on each method and subsequently analysed. This resulted in the observation that by including more anthropometric information as input in the analysis, the quality of the generated RFM's increased in terms of representativeness per cluster.

During the literature research and subsequently applying different analysis methods, the following insights were developed both with respect to the specific topic area as well as the design process as a whole as will be explained in the following sections.

7.3.1 CONSIDERATIONS FOR INCORPORATING 3D SHAPE INFORMATION IN SIZING AND DESIGN

Apart from the many advantages that 3D anthropometric data can bring, there are some challenges to incorporate this type of data in sizing system development or product design. The motivation to incorporate 3D anthropometric data in the product development process can differ. This could depend on the type of product, the required fit and how the functioning of the product depends on the fit. But besides these product related considerations, there are other considerations from an implementation perspective such as data availability, complexity and financial resources which will be discussed below as well as presented in the flowchart (figure 56) in which these considerations are summarised.

7.3.1.1 The application of design/type of product

The choice to incorporate 3D data in design often depends on the application. In the development of a sizing system or design of a product that needs a close fit with the body, the 3D shape analysis of that specific part of the body might be necessary. Moreover, if this fit is more critical because the functioning of the product relies on it,

such as in protective gear or a medical product, a good fit is even more relevant and analysing the 3D shape variation has the potential to offer designers a richer information source. 3D shape data can be used to optimize the design or to conduct initial virtual fit testing to investigate how a new design could fit a certain target population.

7.3.1.2 The availability and accessibility of 3D anthropometric data (for design applications)

Depending on the target population, the first step is to evaluate whether relevant datasets are available. Over the past decades there is an increase in availability of 3D anthropometric data but publicly available 3D datasets, especially those of children, are still limited (Lacko, Huysmans, et al., 2017; Veitch & Robinette, 2006). And thus, anthropometrists and designers mostly rely on surveys, which are often initiated by (medical) research institutes, or larger commercial companies that have the time and financial resources to conduct these large-scale anthropometric projects (Bonin et al., 2022; Durá Gil et al., 2022). But often these datasets are not publicly available or expensive. And more importantly, they focus on specific populations such as the military, working population, or a specific nationality and might not be representative of the target population.

7.3.1.3 Complexity and quantity of the data

In order to be able to implement 3D data successfully into a sizing strategy, one relies on specific knowledge concerning data processing and analysis. 3D data is not ready to use immediately after collection given that the raw data needs formatting and processing. The complexity of the acquired 3D anthropometric data and the necessary iterations before one can use data in the sizing process can be seen as a multi-disciplinary effort and requires specific skills and knowledge. For example, statistical knowledge and programming skills are necessary to analyse, interpret and visualise the data. Also, procurement of specialized software and switching between platforms could offer potential challenges.

7.3.1.4 Financial resources and time

With decreasing costs of 3D scanners and advances in 3D data processing techniques, collecting the required data might be an option. And it is expected that more and more companies will establish 3D anthropometric databases for their own needs (Gupta, 2014). With the developments and increase in 3D scanning technologies there is a lower threshold to collect one's own data for a specific (product development) project in the form of small-scale tailored surveys. But even though collecting 3D anthropometric data could be a more efficient undertaking as compared to traditional surveys, one still need

to invest time, procure equipment and possibly hire personnel to compose the required multi-disciplinary team. This might not always be feasible for any design agency or company. Similarly, the processing of the data, analysis and use of the data and the required operations using specialized software are also often beyond the capabilities of the average designer and requires time investment, which is not always feasible for any design development trajectory.

For personalised products based on individual 3D scan data, the required operations and investments might be more relevant because these types of products are often categorised in a higher price range and find their application in for example medical products (protheses or implants) or high-end products such as tailored 3D scan-based suits or personalised bike helmets (Minnoye et al., 2022).

7.3.2 LIMITATIONS AND OPPORTUNITIES FOR FUTURE RESEARCH IN PRODUCT DESIGN

7.3.2.1 Towards a 3D anthropometric design tool

The methods presented in this thesis and other related work provide a wide array of possibilities for the application of 3D anthropometric data in product design and sizing. However, a method alone is not sufficient in order for anyone to use this type of data. There is a need for a tool to guide designers in the use of 3D anthropometric data and apply it in their design process (Ball, 2009; Lacko, Huysmans, et al., 2017; Niu & Li, 2012). This tool should, offer a platform that facilitates interaction and analysis of the complex data whilst giving room to a designer's creativity and preference and present 3D anthropometric data in a user-friendly way (Ball, 2009; A. Luximon et al., 2012; Wuhrer et al., 2012). Some have made efforts in that direction but further research is necessary in order to further develop the tool and make 3D anthropometric data more accessible (Huysmans et al., 2020; B. Lee et al., 2019; Li et al., 2022).

In order to further develop such a tool and tailor it to a designer's needs, one need to first investigate how designers currently use anthropometric data in different stages of the design process and record what type of resources they use in daily practice. Subsequently and based on that investigating, it is necessary to further investigate in which stages of the design process 3D anthropometric data would be beneficial and in what form. That should provide insight into how 3D anthropometric data could be best presented. Finally, one should enquire into how designers would want to interact with the data, providing insight into what features and functionalities the tool would need to provide.

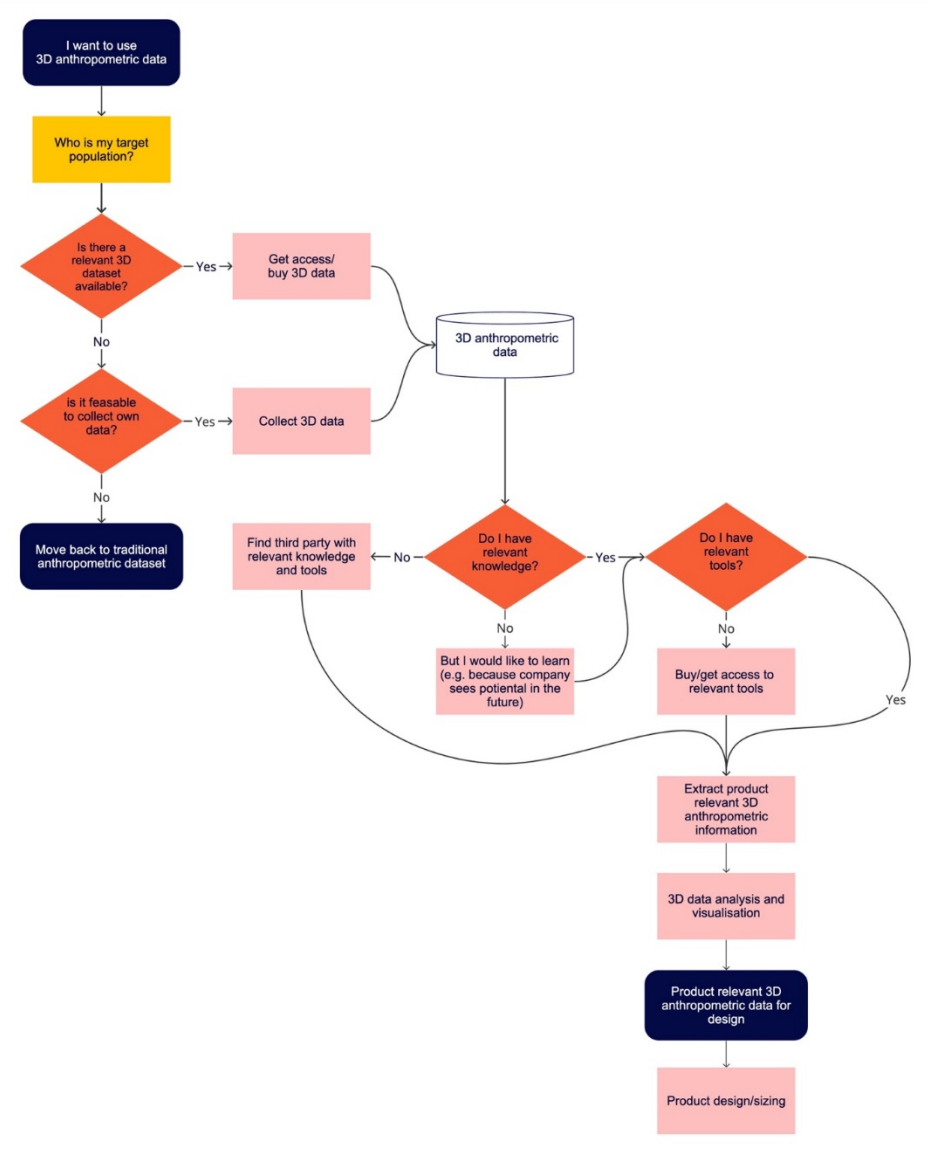

Figure 56 Flowchart summarizing the considerations for the use of 3D anthropometric data for design and sizing as discussed in section 7.3.1.

7.3.2.2 Does the use of 3D data result in better fitting products?

Studies have shown the potential of using 3D data by showing its effect on the quality of the sizing categories and product fit (Lacko, Huysmans, et al., 2017; Lacko, Vleugels, et al., 2017; W. Lee, Yang, et al., 2018). However, the question remains as to the use of 3D data compares to the use of traditional data with which most designers are used to work with and have been working with before the emergence of 3D anthropometric data and its effect on product fit. By comparing a product design and sizing process based on 3D anthropometric data and traditional data, the effect on the product fit could be verified. This could be done by providing designers with 3D anthropometric data in order to develop a product, for example, a ventilation mask for a specific age range, and by quantitively and qualitatively evaluating the fit comparing it with an existing product which was developed using traditional sizing schemes. It is also crucial to assess the design process in terms of how efficiently and effectively the 3D data can be implemented.

7.4 PRODUCT LEVEL

In the final stage of this thesis the knowledge developed on the anthropometric and design level was applied to a specific case in order to explore what the added value of 3D data would be for the designer during the design process for a specific product, in this case a ventilation mask for children. The research question was:

RQ 3: How can 3D anthropometric data be implemented in product design and sizing?

With the following sub questions.

- How can 3D face data of children be implemented in the design and sizing of ventilation masks?
- How does a ventilation mask, designed based on 3D representative face models (RFM's), fit the target population?

Chapter 6 presents a novel approach to mask design by applying computational methods to generate mask designs followed by virtual fit testing. By automating the process of tailoring mask designs to accommodate various facial shapes, specifically RFM's representing different clusters, the use of 3D face data was integrated in the design process. In this study, the accessibility for designers was prioritized by implementing the design and evaluation process through visual programming, making it accessible even for those without the required coding skills.

The study's findings reveal that increasing the number of RFMs that represent the sample leads to improved mask fit. However, it was observed that with three or more RFMs, further enhancements in fit were not significant. This could be related either to the design of the mask , the selected parameters and the parameter input on the on hand or on the other hand, it could also be the result of the mask fitting process, which was limited to 600 iterations for practical purposes, but could still be insufficient in consistently yielding the most optimal outcome, resulting in variability in quality even within a particular cluster. Visual inspections did indicate that poor fits within one, two, or three clusters primarily occurred around the eyes and mouth, clearly indicating sizing issues. Therefore, incorporating additional sizing categories would be necessary to address facial shape and size variations adequately. Nevertheless, regardless of the number of clusters, all clusters experienced fit issues in the nose-bridge region. This suggests that either the variation or morphology in this region is more challenging to fit compared to other areas or that the algorithm struggles to position the mask correctly in this region and needs optimization.

During the final phase of the research the following insights were developed and further applications of 3D face data in the development of ventilation masks will be presented in the following sections.

7.5 LIMITATIONS AND OPPORTUNITIES FOR FUTURE RESEARCH RELATED TO MASK DEVELOPMENT

In the study presented in chapter 6, the fit testing focused solely on evaluating the fit of the mask design's rim, providing a conceptual approach to assessing fit. However, defining an objective measure for fit that takes into account both comfort and performance posed a significant challenge. Achieving an appropriate fit involves finding the right balance, ensuring that the mask does not exert excessive pressure on the face while effectively sealing any potential gaps. It is important to note that material properties, certain crucial components such as straps, adjustable elements, and connectors to ventilation equipment were not considered in this particular study. Future research should expand the fit testing process to incorporate these elements and features, allowing for a more comprehensive understanding of mask effectiveness.

Moreover, including subjective measures such as user comfort, experience during prolonged use, and considering the impact of material properties and weight would further enhance mask design. Recent efforts by Smulders et al. (2023) have focused on mapping the sensitivity of various areas of the head, neck, and face, resulting in a 3D pressure discomfort threshold map that can guide the design of head and face-related

products. Integrating this information, along with the biomechanical properties of the face as demonstrated by Yang et al. (2022) and the development of Representative Face Models (RFMs) that incorporate these features, can contribute to a more realistic fit testing approach. By incorporating these advancements, it becomes possible to achieve more accurate and reliable assessments of mask fit, ultimately leading to improved designs that better meet the needs and preferences of users.

7.5.1.1 Biomechanical features

The final part of the research presented in this thesis focussed on the design of a ventilation mask based on 3D anthropometric data and subsequently evaluating the fit. For products for which a close fit is important more aspects are of importance which cannot be solved by using 3D data alone. Biomechanical features such as bony structures, fatty tissue, sensitiveness, and movement and flexibility of the facial tissue are not included, yet are important when striving for a perfect and comfortable fit. The fit was evaluated in an objective and quantified manner in the studies presented in this thesis. However, in order to achieve a good fit, further research is necessary into the anatomical and biomechanical aspects of the face and how that relates to the fit and comfort. The design and/or material properties can be adjusted accordingly to optimize the fit. The development of 3D shape models combined with finite element models to simulate biomechanical features and contact pressure as have been done with adults (Kwon et al., 2022; Yang et al., 2022).

7.5.1.2 Use and context

Finally, it is also important to take into account the product use and the context within it is used. For example, the ventilation mask is generally not worn in a static, upright way but more commonly in home ventilation, the mask is mostly worn during the night, while sleeping in a horizonal position. Movements during sleeping could cause dislocations of the mask or change of the pressure distribution on the face (e.g. when sleeping on side). In the context of the hospital PICU, the child would mostly be lying in bed. And even though these critically sick children would probably move less, there are other activities, such as airway hygiene procedures conducted by nurses, that can cause movement of the head and dislocation of the mask (Hovenier et al., 2022). Further research into the use of the mask and interaction with it in a real-life context is necessary to optimize the design.

7.6 FURTHER DEVELOPMENT AND RESEARCH RELATED TO THIS THESIS

The 3D dataset and insights generated during this thesis were utilized in the following projects, which were conducted in parallel to the research conducted in this thesis. The following sections briefly discuss the nature of these projects and their results.

Design and sizing of a ventilation mask for children

Based on current dataset, a sizing system was developed for a tailored non-invasive ventilation (NIV) mask for the paediatric intensive care unit (PICU) in collaboration with Amsterdam University Medical Centres (UMC). The project was part of a Master graduation project conducted at the faculty of Industrial design engineering at the technical university of Delft (Spijker, 2020). The project resulted in two design proposals for modular personalised NIV masks which both consisted of sized components and a personalised cushion (figure 57).

Figure 57 Two prototypes based on two design directions for a tailored modular ventilation mask (Spijker, 2020)

Current children's dataset served as input for the sizing system development process of the modular mask, and more specifically, the sizing of the holder and the frame (figure 58). Eight sizing categories for the mask frame were defined based on two dimensions: mouth width and face height for age group 0 to 7 years old. It was observed that especially for the youngest age group (> 1 years) more sizing categories were needed to accommodate the face size variation because of growth. The cushion of the modular mask was designed to be personalised based on a 3D scan of the patients face. In a follow

up study conducted as part of a collaborative project between Amsterdam UMC, the company Nsize (https://www.nsize.nl/) and the TU Delft fieldlab UPPS team (http://www.upps.nl), the sizing, design, materialisation and production of the different parts of the mask were further explored. Currently, as part of a separate PhD research, the mask sizing and design are being detailed and further optimized in order to develop a personalized ventilation mask to optimize the fit for each user.

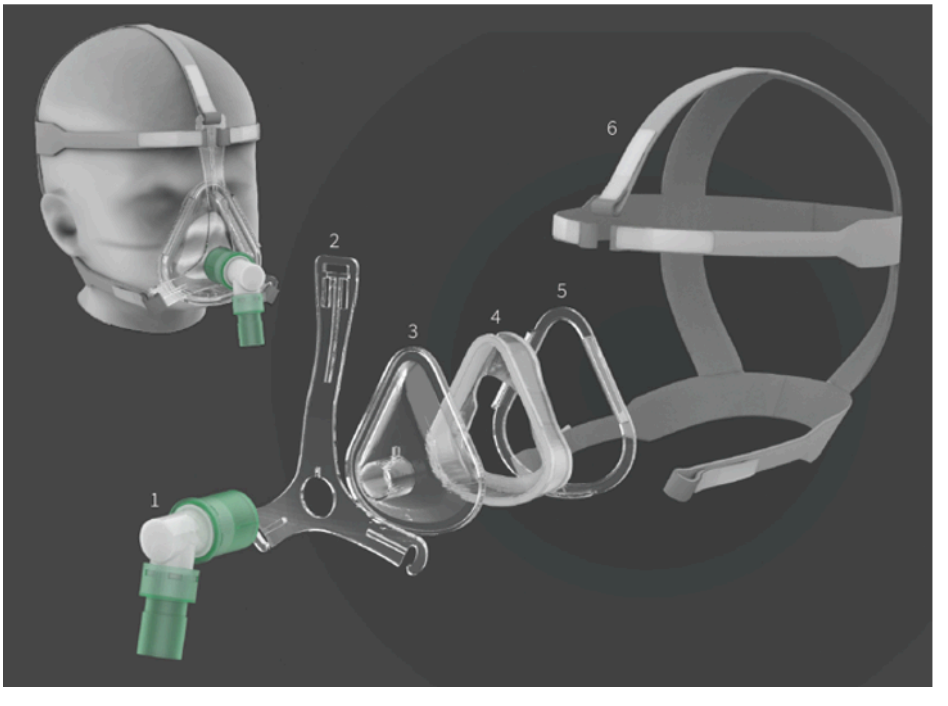

Figure 58 Parts of the Modular Mask, (1) swivel, (2) holder, (3) frame, (4) personalised cushion, (5) frame ring, and (6) headgear. (Spijker, 2020).

7.6.1 Anthropometric test model

As part of the above mentioned follow up project conducted at the Amsterdam UMC, a paediatric head-lung model was developed in order to simulate paediatric NIV and to investigate the effectiveness of NIV masks (Hovenier et al., 2022). For the design of the head model, a statistical shape model was developed based on current 3D anthropometric dataset of children's head and faces. A principal component analysis and regression model between age and the 3D head and face shape was conducted to generate a 3D model representing a 1-year-old child (figure 59). A future step would be to construct head models representing other age categories in order to test existing and new mask designs dedicated to children.

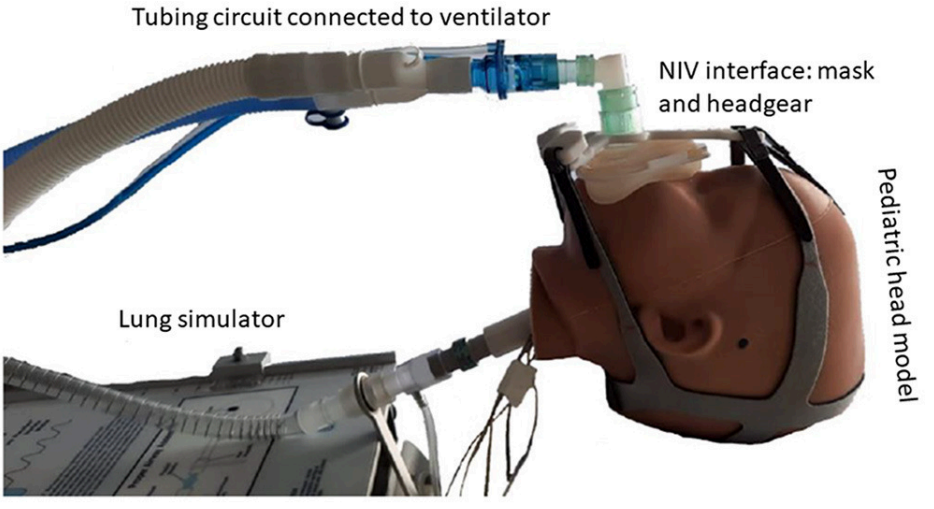

Figure 59 Paediatric head–lung model with a NIV interface mask connected to a lung simulator (Hovenier et al., 2022).

Both projects showcase practical examples of applications of the dataset in different phases of the design process, illustrating the potential and versatility of the dataset. By using scan extracted measurements for sizing, 3D face data for tailoring the mask cushion, 3D statistical models for mask design and presentation and finally, a physical model based on statistical shape analysis for mask testing.

7.6.2 ACCESSABILITY OF CURRENT DATASET

The 3D dataset was collected with the goal to provide detailed head and face measurements and shape information of Dutch children for the application of mask design. The presented research in this thesis focussed on the analysis of the variation of dimensions and shape in the area of the face that is considered relevant for mask design. However, the data presented could provide relevant information for other head and face related products as well. Since the 3D data remains accessible through a website, product relevant data can be extracted in the form of anthropometric measurements, scatterplots or 3D shape models through the Mannequin platform (Huysmans et al., 2020), all available at http://dined.io.tudelft.nl (figure 60). All can be used to analyse and visualise the (3D) variability of a certain product relevant area of the face or head and by providing a better understanding of the head and face shape variation of children in general.

Figure 60 Print screen of the DINED Mannequin tool (http://dined.io.tudelft.nl) where current dataset can be accessed.

7.7 CONCLUSION

This dissertation started with the generation of a 3D dataset of children's head and faces and based on this dataset presented further insights into the development of sizing systems as well as computational design methods for head-related products.

The generated dataset of more than 300 children's heads and faces, serves as a solid foundation for further expansion in order to provide researchers and designers with a larger and richer dataset. The dataset highlights the effect of growth in young children and the effect this has on the anthropometric measurements of their face and head. The analysis of the dataset revealed that overall face shape exhibits considerable variation, primarily in terms of length. Additionally, adjacent age groups often display significant overlap across various dimensions. Consequently, it is more relevant for designers to analyse face shape based on the face length as opposed to age, when developing head and face related products for children.

In parallel, this thesis presented an overview of approaches utilized in developing sizing systems based on 3D anthropometric head and face data. It provides insights into the

procedural steps involved in the process of collecting, processing and analysing the data. It also highlights the importance of incorporating shape information in the sizing process, which often come with tailored sizing system development methods. This overview can serve as reference for designers in determining their own strategy for using 3D anthropometric data. This thesis also showed that virtual representative models (RM) based on 3D data offer potential for sizing and design in providing researchers and designer with more detailed information as input for the design of products where fit is essential. These representative (design) models are commonly used to visualize the variability within a target population. By incorporating additional anthropometric information in the development of RFMs, ranging from bivariate and multivariate to shape-based data, the quality of the generated representative face models improves in terms of representativeness. This finding underscores the relevance of incorporating shape in the development of products that require a precise fit.

With the 3D dataset and these insights regarding different approaches for developing sizing systems as a foundation, this research presents a novel method for computational mask design and virtual fit testing. The study showcases the potential of integrating visual programming into the design and sizing of head-related products, enabling designers without the required coding skills to incorporate anthropometric shape information in their design process. This approach aligns with the working methods of designers, making 3D data more accessible to them which should ultimately lead to an improvement in the fit of the products they will be designing.

This study represents an important first step in the collection, analysis and utilization of 3D anthropometric data when designing products where high-quality fit is essential. The processes developed need further optimization and broader application, extending to other product categories in order for it to become a method to which designers can turn to regardless of the product or the part of the body for which the product is designed. By doing so, a more robust, universal and easily implementable process can be achieved, catering to the needs of designers. Additionally, expanding the research to include biomechanical features or 3D pressure discomfort threshold maps would enhance the process further ultimately leading to more effective and comfortable head-related products.

REFERENCES

Alemany, S., Olaso, J., Nacher, B., Gil, M., Hernández, A., Pizá, M., & Solves, C. (2012). A multidimensional approach to the generation of helmets' design criteria: A preliminar study. *Work*, *41*(SUPPL.1), 4031–4037. https://doi.org/10.3233/WOR-2012-0067-4031

Amin, R., Al Saleh, S., & Narang, I. (2016). Domiciliary Noninvasive Positive Airway Pressure Therapy in Children. *Pediatric Pulmonology*, *51*(4), 335–348. https://doi.org/10.1002/ppul.23353

Amirav, I., Luder, A. S., Halamish, A., Raviv, D., Kimmel, R., Waisman, D., & Newhouse, M. T. (2013). Design of aerosol face masks for children using computerized 3D face analysis. *Journal of Aerosol Medicine and Pulmonary Drug Delivery*. *26*(0), 1–7. https://doi.org/10.1089/jamp.2013.1069

Amirav, I., Masumbuko, C. K., Hawkes, M. T., Solomon, I., Aldar, Y., Margalit, G., Zvirin, A., Honen, Y., Sivasivugha, E. S., & Kimmel, R. (2019). 3D analysis of child facial dimensions for design of medical devices in low-middle income countries (LMIC). *PLoS ONE*, *14*(5), 1–12. https://doi.org/10.1371/journal.pone.0216548

Baek, S. Y., & Lee, K. (2012). Parametric human body shape modeling framework for human-centered product design. *CAD Computer Aided Design*, *44*(1), 56–67. https://doi.org/10.1016/j.cad.2010.12.006

Ball, R. M. (2009). 3-D Design Tools from the SizeChina Project. *Ergonomics in Design*. 8–13.

Ball, R. M. (2011). SizeChina: A 3D Anthropometric Survey of the Chinese Head. Doctoral Thesis. Delft University of Technology.

Ball, R. M., & Molenbroek, J. F. M. (2008). Measuring Chinese Heads and Faces. *Proceedings of the 9th International Congress of Physiological Anthropology, Human Diversity: Design for Life*, 150–155.

Ball, R. M., Shu, C., Pengcheng, X., Marc, R., Yan, L., & Molenbroek, J. F. M. (2010). A comparison between Chinese and Caucasian head shapes. *Applied Ergonomics*, *41*(6), 832–839.

Ballester, A., Valero, M., Nacher, B., Pierola, A., Piqueras, P., Sancho, M., Gargallo, G., Gonzalez, J. C., & Alemany, S. (2015). 3D Body Databases of the Spanish Population and its Application to the Apparel Industry. *Proceedings of the 6th*

International Conference on 3D Body Scanning Technologies, Lugano, Switzerland, 27-28 October 2015, 232–233. https://doi.org/10.15221/15.232

Barker, N., Willox, M., & Elphick, H. (2018). A Review of the Benefits, Challenges and the Future for Interfaces for Long Term Non-Invasive Ventilation in Children. *International Journal of Respiratory and Pulmonary Medicine*, *5*(1). https://doi.org/10.23937/2378-3516/1410077

Benjamini, Y., & Hochberg, Y. (1995). Controlling the False Discovery Rate : A Practical and Powerful Approach to Multiple Testing . *Journal of the Royal Statistical Society. Series B (Methodological)*, *57*(1), 289–300.

Blackwell, S., Robinette, K. M., Daanen, H. A. M., Boehmer, M., Fleming, S., Kelly, S., Brill, T., Hoeferlin, D., & Burnsides, D. (2002). Civilian American and European Surface Anthropometry Resource (CAESAR), Final Report, Volume II: Descriptions.

Bogin, B. (1988). *Patterns of human growth*. Cambridge University Press.

Bolkart, T., Bose, P., Shu, C., & Wuhrer, S. (2015). A general framework to generate sizing systems from 3D motion data applied to face mask design. *Proceedings - 2014 International Conference on 3D Vision, 3DV 2014*, 425–431. https://doi.org/10.1109/3DV.2014.43

Bolkart, T., & Wuhrer, S. (2013). Statistical analysis of 3D faces in motion. *Proceedings - 2013 International Conference on 3D Vision, 3DV 2013*, 103–110. https://doi.org/10.1109/3DV.2013.22

Bonin, D., Ackermann, A., Radke, D., Peters, M., & Wischniewski, S. (2022). Anthropometric dataset for the German working-age population using 3D body scans from a regional epidemiological health study and a weighting algorithm. *Ergonomics*. https://doi.org/10.1080/00140139.2022.2130440

Bradtmiller, B. (1996). Sizing Head Forms: Design and Development. In *SAE Technical Papers*. https://doi.org/10.4271/960455

Bradtmiller, B. (2022). 3D Scanning and Head-Mounted Products. *Ergonomics in Design* , 1–4. https://doi.org/https://doi.org/10.1177/10648046221083749

Bugaighis, I., Mattick, C. R., Tiddeman, B., & Hobson, R. (2013). Three-dimensional gender differences in facial form of children in the North East of England. *European Journal of Orthodontics*, *35*(3), 295–304. https://doi.org/10.1093/ejo/cjr033

Burdi, A. R., Huelke, D. F., Snyder, R. G., & Lowrey, G. H. (1969). Infants and Children in the adult Wold of Autmobile Safety Design: Pediatric and Anatomical Considerations for Design of Child Restraints. *Journal of Biomechanics*, *2*(3), 267–280. https://doi.org/10.1016/0021-9290(69)90083-9

Butler, K. M. (2007). *A Computational Model of an Outward Leak from a Closed-Circuit Breathing Device*. *25*, 41.

Capetillo-Cunliffe, L. (2007). Loni: Laboratory of Neuro Imaging.

Castro-Codesal, M. L., Olmstead, D. L., & MacLean, J. E. (2019). Mask interfaces for home non-invasive ventilation in infants and children. In *Paediatric Respiratory Reviews* (Vol. 32, pp. 66–72). W.B. Saunders Ltd. https://doi.org/10.1016/j.prrv.2019.03.004

Chamberland, A., Carrier, R., Forest, F., & Hachez, G. (1997). *1997 Anthropometric Survey of the Land Forces (DCIEM TR 98-CR-15)* .

Chen, W., Zhuang, Z., Benson, S., Du, L., Yu, D., Landsittel, D., Wang, L., Viscusi, D., Shaffer, R. E., & Chen W.a Zhuang, Z. b B. S. c D. L. a Y. D. a L. D. b d W. L. a V. D. b S. R. E. b. (2009). New respirator fit test panels representing the current chinese civilian workers. *Annals of Occupational Hygiene*, *53*(3), 297–305. https://doi.org/10.1093/annhyg/men089

Chen, X., Meiwu, S., Hong, Z., Xiting, W., & Zhou, G. (2002). The “Standard Head” for Sizing Military Helmet Based on Computerized Tomography and the Headform Sizing Algorithm. *Acta Armamentarii*, *23*(4), 476-480 (in Chinese).

Chinese Standard Institution. (2007). *CNS 2396, Protective helmets for motor cyclists*.

Chu, C.-H., Huang, S.-H., Yang, C.-K., & Tseng, C.-Y. (2015). Design customization of respiratory mask based on 3D face anthropometric data. *International Journal of Precision Engineering and Manufacturing*, *16*(3), 487–494. https://doi.org/10.1007/s12541-015-0066-5

Chu, C.-H., Wang, I.-J., Wang, J.-B., & Luh, Y.-P. (2017). 3D parametric human face modeling for personalized product design: Eyeglasses frame design case. *Advanced Engineering Informatics*, *32*, 202–223. https://doi.org/10.1016/j.aei.2017.03.001

Churchill, E., Laubach, L. L., Mcconville, J. T., & Tebbetts, I. (1978). *Anthropometric source book. Volume 1: Anthropometry for designers*. NASA, Houston, Tex., United States.

Coblentz, A., Mollard, R., & Ignazi, G. (1991). Three-dimensional face shape analysis of French adults, and its application to the design of protective equipment. *Ergonomics*, *34*(4), 497–517. https://doi.org/10.1080/00140139108967332

Conkle, J., Keirsey, K., Hughes, A., Breiman, J., Ramakrishnan, U., Suchdev, P. S., & Martorell, R. (2019). A collaborative, mixed-methods evaluation of a low-cost, handheld 3D imaging system for child anthropometry. *Maternal and Child Nutrition*, *15*(2), 1–12. https://doi.org/10.1111/mcn.12686

Cui, X., Jung, H., Lee, W., Kim, S. H., Yun, R. Y., Kim, S. Y., You, H., & Huh, S. (2022). Ergonomics and Personalization of Noninvasive Ventilation Masks. *Respiratory Care*, *67*(1), 87–101. https://doi.org/10.4187/respcare.08959

Daanen, H. a. M., & Ter Haar, F. B. (2013). 3D whole body scanners revisited. *Displays*, *34*(4), 270–275. https://doi.org/10.1016/j.displa.2013.08.011

Dainoff, M., Gordon, C., Robinette, K., & Strauss, M. (2004). *Guidelines for Using Anthropometric Data in Product Design - HFES 300 Commitee*.

Dianat, I., Molenbroek, J., & Castellucci, H. I. (2018). A review of the methodology and applications of anthropometry in ergonomics and product design. In *Ergonomics* (Vol. 61, Issue 12, pp. 1696–1720). Taylor and Francis Ltd. https://doi.org/10.1080/00140139.2018.1502817

Dirken, J. M. (1999). *Productergonomie - Ontwerpen voor gebruikers.* Delft University Press.

Du, L., Zhuang, Z., Guan, H., Xing, J., Tang, X., Wang, L., Wang, Z., Wang, H., Liu, Y., Su, W., Benson, S., Gallagher, S., Viscusi, D., & Chen, W. (2008). Head-and-face anthropometric survey of Chinese workers. *Annals of Occupational Hygiene*, *52*(8), 773–782. https://doi.org/10.1093/annhyg/men056

Durá Gil, J. V., Remon, A., Rodriguez, I. M., Pariente-Lobo, T., Salmeron-Majadas, S., Perrone, A., Ciuhu-Pijlman, C., Znamenskiy, D., Karavaev, K., Codina, J. O., Boura, L., Silva, L., Redon, J., Real, J., & Cipresso, P. (2022). 3D Human Big Data Exchange Between the Healthcare and Garment Sectors. In *Technologies and Applications for Big Data Value* (pp. 225–252). Springer International Publishing. https://doi.org/10.1007/978-3-030-78307-5_11

Dyke, R. M., Zhou, F., Lai, Y.-K., Rosin, P. . L., Guo, D., Li, K., Marin, R., & Yang, J. (2020). SHREC'20 : Non-rigid shape correspondence of physically-based deformations. In T. Schreck & T. Theoharis (Eds.), *Eurographics Workshop on*

3D Object Retrieval. The Eurographics Association. https://doi.org/10.2312/3dor.20201161

Ellena, T., Skals, S., Subic, A., Mustafa, H., & Pang, T. Y. (2017). 3D digital headform models of Australian cyclists. *Applied Ergonomics*, *59*, 11–18. https://doi.org/10.1016/j.apergo.2016.08.031

Ellena, T., Subic, A., Mustafa, H., & Pang, T. Y. (2016). The helmet fit index - an intelligent tool for fit assessment and design customisation. *Applied Ergonomics*, *55*, 194–207. https://doi.org/10.1016/j.apergo.2016.02.008

Ellena, T., Subic, A., Mustafa, H., & Yen Pang, T. (2018). A novel hierarchical clustering algorithm for the analysis of 3D anthropometric data of the human head. *Computer-Aided Design and Applications*, *15*(1), 25–33. https://doi.org/10.1080/16864360.2017.1353727

Facebase. (2013). 3D Facial Norms Technical Notes. https://www.facebase.org/facial_norms/notes/#landmarking_surfaces

Farkas, L. G. (1994). *Anthropometry of the head and face.* Raven Press.

Farkas, L. G. (1996). Accuracy of anthropometric measurements: Past, present, and future. *Cleft Palate-Craniofacial Journal*, *33*(1), 10–18.

Farkas, L. G., Katic, M. J., & Forrest, C. R. (2005). International anthropometric study of facial morphology in various ethnic groups/races. *Journal of Craniofacial Surgery*, *16*(4), 615–646. https://doi.org/10.1097/01.scs.0000171847.58031.9e

Farkas, L. G., & Posnick, J. C. (1992). Growth and development of regional units in the head and face based on anthropometric measurements. *Cleft Palate-Craniofacial Journal*, *29*(4), 301–302.

Farkas, L. G., Posnick, J. C., & Hreczko, T. M. (1992). Growth patterns of the face: A morphometric study. *Cleft Palate-Craniofacial Journal*, *29*(4), 308–314. https://doi.org/10.1597/1545-1569(1992)029<0308:GPOTFA>2.3.CO;2

Fauroux, B., Lavis, J.-F., Nicot, F., Picard, A., Boelle, P.-Y., Clément, A., & Vazquez, M.-P. (2005). Facial side effects during noninvasive positive pressure ventilation in children. *Intensive Care Medicine*, *31*(7), 965–969. https://doi.org/10.1007/s00134-005-2669-2

Fourie, Z., Damstra, J., Gerrits, P. O., & Ren, Y. (2011). Evaluation of anthropometric accuracy and reliability using different three-dimensional scanning systems.

Forensic Science International, *207*(1–3), 127–134. https://doi.org/10.1016/j.forsciint.2010.09.018

Fryar, C. D., Gu, Q., & Ogden, C. L. (2012). Anthropometric reference data for children and adults: United States, 2007-2010. *National Center for Health Statistics. Vital Health Stat*, *11(252)*, 1–40.

Godil, A. (2007). *Advanced Human Body and Head Shape*. *Digital Human Modeling*. 92–100.

Godil, A. (2009). Facial Shape Analysis and Sizing System. *Digital Human Modeling*, 29–35.

Gordon, C. C., Blackwell, C. L., Bradtmiller, B., Parham, J. L., Barrientos, P., Paquette, S. P., Corner, B. D., Carson, J. M., Venezia, J. C., Rockwell, B. M., Mucher, M., & Kristensen, S. (2014). 2012 Anthropometric Survey of U.S. Army Personnel: Methods and Summary Statistics. In *TECHNICAL REPORT NATICK/TR-15/007* (Issue April 2012).

Goto, L., Huysmans, T., Lee, W., Molenbroek, J. F. M., & Goossens, R. H. M. (2019). A comparison between representative 3D faces based on bi- and multi-variate and shape based analysis. *Proceedings of the 20th Congress of the International Ergonomics Association (IEA 2018) Volume VII*, *824*, 1355–1364. https://doi.org/10.1007/978-3-319-96071-5_137

Goto, L., Lee, W., Huysmans, T., Molenbroek, J. F. M., & Goossens, R. H. M. (2021). The variation in 3D face shapes of dutch children for mask design. *Applied Sciences (Switzerland)*, *11*(15). https://doi.org/10.3390/app11156843

Goto, L., Lee, W., Molenbroek, J. F. M., Cabo, A. J., & Goossens, R. H. M. (2019). Traditional and 3D scan extracted measurements of the heads and faces of Dutch children. *International Journal of Industrial Ergonomics*, *73*.

Goto, L., Lee, W., Song, Y., Molenbroek, J. F. M., & Goossens, R. H. M. (2015). Analysis of a 3D anthropometric data set of children for design applications. *Proceedings 19th Triennial Congress of the IEA*, *August*.

Goto, L., Molenbroek, J. F. M., & Goossens, R. H. M. (2013). 3D Anthropometric data set of the head and face of children aged 0.5-7 years for design applications. *In N D'Apuzzo (Ed.), Proceedings of the 4th International Conference on 3D Body Scanning Technologies Ascona, Switzerland: Hometrica Consulting.*, 157–165. https://doi.org/10.15221/13.157

Gower, J. C. (1975). Generalized procrustes analysis. *Psychometrika*, *40*(1), 33–51. https://doi.org/10.1007/BF02291478

Gupta, D. (2014). Anthropometry and the design and production of apparel: An overview. In *Anthropometry, Apparel Sizing and Design* (pp. 34–66). Elsevier Ltd. https://doi.org/10.1533/9780857096890.1.34

Hong, C., Choi, K., Kachroo, Y., Kwon, T., Nguyen, A., McComb, R., & Moon, W. (2017). Evaluation of the 3dMDface system as a tool for soft tissue analysis. *Orthodontics and Craniofacial Research*, *20*(Suppl 1), 119–124. https://doi.org/10.1111/ocr.12178

Hotzman, J., Gordon, C., Bradtmiller, B., Corner, B. D., Mucher, M., Kristensen, S., & Blackwell, C. L. (2011). Measurer's handbook: US Army and Marine Corps anthropometric surveys 2010-2011. In *Technical Report Natick/Tr-11/017*.

Hovenier, R., Goto, L., Huysmans, T., van Gestel, M., Klein-Blommert, R., Markhorst, D., Dijkman, C., & Bem, R. A. (2022). Reduced Air Leakage During Non-Invasive Ventilation Using a Simple Anesthetic Mask With 3D-Printed Adaptor in an Anthropometric Based Pediatric Head–Lung Model. *Frontiers in Pediatrics*, *10*. https://doi.org/10.3389/fped.2022.873426

HQL. (1997). *Japanese Body Size Data 1992-1994*. www.hql.jp/project/size1992/

Hsiao, H. (2013). Anthropometric procedures for protective equipment sizing and design. *Human Factors*, *55*(1), 6–35. https://doi.org/10.1177/0018720812465640

Hsiao, H., Whitestone, J., Kau, T.-Y., Whisler, R., Routley, J. G., & Wilbur, M. (2014). Sizing Firefighters: Method and Implications. *Human Factors*, *56*(5). https://doi.org/10.1177/0018720813516359

Huysmans, T., Goto, L., Molenbroek, J. F. M., & Goossens, R. H. M. (2020). DINED Mannequin: an Open Platform for 3D Anthropometry. *Tijdschrift Voor Human Factors*, *45*(1), 4–7.

Huysmans, T., Sijbers, J., & Brigitte, V. (2010). Automatic construction of correspondences for tubular surfaces. *IEEE Transactions on Pattern Analysis and Machine Intelligence*, *32*(4), 636–651. https://doi.org/10.1109/TPAMI.2009.93

Institute of Medicine (2007). Assessment of the NIOSH Head-and-Face Anthropometric Survey of U.S. Respirator Users. Washington, DC: The National Academies Press. https://doi.org/10.17226/11815.

ISO 7250-1. (2010). *Basic human body measurements for technological design - Part1: Body measurement definitions and landmarks*. European Committee for Standardization.

ISO 15535. (2007). *General requirements for establishing anthropometric databases*. European Committee for Standardization.

ISO 20685. (2010). *3-D scanning methodologies for internationally compatible anthropometric databases*. European Committee for Standardization.

Jollife, I. T., & Cadima, J. (2016). Principal component analysis: A review and recent developments. *Philosophical Transactions of the Royal Society A: Mathematical, Physical and Engineering Sciences*, *374*(2065). https://doi.org/10.1098/rsta.2015.0202

Kau, C. H., Zhurov, A., Richmond, S., Scheer, R., & Bouwman, S. (2004). The feasibility of measuring three-dimensional facial morphology in children. *Orthodontics and Craniofacial Research*, *7*(4), 198–204. https://doi.org/10.1111/j.1601-6343.2004.00289.x

Kim, H., Seo, H., Myong, J.-P., Yoon, J.-S., Song, Y., & Kim, C. (2016). Developing yellow dust and fine particulate masks for children. *Journal of Korean Society of Occupational and Environmental Hygiene*, *26*(3), 350–366. https://doi.org/10.15269/jksoeh.2016.26.3.350

Kolar, J. C., & Salter, E. M. (1997). *Craniofacial Anthropometry Practical Measurement of the Head and Face for Clinical, Surgical and Research Use.* Charles C Thomas Publisher.

Kouchi M., M. M., Kouchi, M., & Mochimaru, M. (2011). Errors in landmarking and the evaluation of the accuracy of traditional and 3D anthropometry. *Applied Ergonomics*, *42*(3), 518–527. https://doi.org/10.1016/j.apergo.2010.09.011

Kouchi, M., & Mochimaru, M. (2004). Analysis of 3D face forms for proper sizing and CAD of spectacle frames. *Ergonomics*, *47*(14), 1499–1516.

Kuo, C. C., Wang, M. J., & Lu, J. M. (2020). Developing sizing systems using 3D scanning head anthropometric data. *Measurement: Journal of the International Measurement Confederation*, *152*. https://doi.org/10.1016/j.measurement.2019.107264

Kwon, Y.-J., Kim, J.-G., & Lee, W. (2022). A framework for effective face-mask contact modeling based on finite element analysis for custom design of a facial

mask. *PLOS ONE*, *17*(7), e0270092. https://doi.org/10.1371/journal.pone.0270092

Lacko, D., Huysmans, T., Parizel, P. M., Bruyne, G. De, Verwulgen, S., Hulle, M. M. Van, & Sijbers, J. (2015). Evaluation of an anthropometric shape model of the human scalp. *Applied Ergonomics*, *48*, 70–85. https://doi.org/10.1016/j.apergo.2014.11.008

Lacko, D., Huysmans, T., Vleugels, J., De Bruyne, G., Van Hulle, M. M., Sijbers, J., & Verwulgen, S. (2017). Product sizing with 3D anthropometry and k-medoids clustering. *Computer Aided Design*, *91*, 60–74. https://doi.org/10.1016/j.cad.2017.06.004

Lacko, D., Vleugels, J., Fransen, E., Huysmans, T., Bruyne, G. De, Hulle, M. M. Van, Sijbers, J., & Verwulgen, S. (2017). Ergonomic design of an EEG headset using 3D anthropometry. *Applied Ergonomics*, *58*, 128–136. https://doi.org/10.1016/j.apergo.2016.06.002

Lee, B., Lee, W., Yang, X., Jung, K., & You, H. (2019). Development of a distributed representative human model generation and analysis system (DRHM-GAS): Application to optimization of flight suit and pilot oxygen mask sizing systems. *International Journal of Industrial Ergonomics*, *72*, 261–271. https://doi.org/10.1016/j.ergon.2019.06.005

Lee, W., Goto, L., Molenbroek, J. F. M., & Goossens, R. H. M. (2017). Analysis methods of the variation of facial size and shape based on 3D face scan images. *Proceedings of the Human Factors and Ergonomics Society*, *2017-Octob*, 1409–1413. https://doi.org/10.1177/1541931213601836

Lee, W., Goto, L., Molenbroek, J. F. M., Goossens, R. H. M., & Wang, C. C. C. (2017). A shape-based sizing system for facial wearable product design. In S. Wischniewski, D. Bonin, & T. Alexander (Eds.), *Proceedings of the 5th International Digital Human Modeling Symposium* (Issue June, pp. 150–158). Federal Institute for Occupational Safety and Health.

Lee, W., Jeong, J., Park, J., Jeon, E., Kim, H., Jung, D., Park, S., & You, H. (2013). Analysis of the facial measurements of Korean Air Force pilots for oxygen mask design. *Ergonomics*, *56*(9), 1451–1464. https://doi.org/10.1080/00140139.2013.816376

Lee, W., Jung, D., Park, S., Kim, H., & You, H. (2021). Development of a virtual fit analysis method for an ergonomic design of pilot oxygen mask. *Applied Sciences (Switzerland)*, *11*(12). https://doi.org/10.3390/app11125332

Lee, W., Lee, B., Kim, S., Jung, H., Bok, I., Kim, C., Kwon, O., & Choi, T. (2015). Development of Headforms and an Anthropometric Sizing Analysis System for Head-Related Product Designs. *59th Annual Meeting of the Human Factors and Ergonomics Society*, 1419–1422. https://doi.org/10.1177/1541931215591308

Lee, W., Lee, B., Yang, X., Jung, H., Bok, I., Kim, C., Kwon, O., & You, H. (2018). A 3D anthropometric sizing analysis system based on North American CAESAR 3D scan data for design of head wearable products. *Computers and Industrial Engineering*, *117*, 121–130. https://doi.org/10.1016/j.cie.2018.01.023

Lee, W., Lee, B., Yang, X., & You, H. (2022). A Method for Generation of a Sizing System and Representative Models for a Facial Mask Design. *Applied Sciences (Switzerland)*, *12*(23). https://doi.org/10.3390/app122312387

Lee, W., Yang, X., Jung, D., Park, S., Kim, H., & You, H. (2018). Ergonomic evaluation of pilot oxygen mask designs. *Applied Ergonomics*, *67*(June 2017), 133–141. https://doi.org/10.1016/j.apergo.2017.10.003

Lee, W., Yang, X., Jung, H., You, H., Goto, L., Molenbroek, J. F. M., & Goossens, R. H. M. (2016). Application of massive 3D head and facial scan datasets in ergonomic head-product design. *International Journal of the Digital Human*, *1*(4), 344. https://doi.org/10.1504/ijdh.2016.10005368

Lee, W., Yang, X., Yoon, S., Lee, B., Jeon, E., Kim, H., & You, H. (2017). Comparison of a semiautomatic protocol using plastering and three-dimensional scanning techniques with the direct measurement protocol for hand anthropometry. *Human Factors and Ergonomics In Manufacturing*, *27*(3), 138–146. https://doi.org/10.1002/hfm.20697

Li, Z., Deng, X., Lee, Y.-C., Jiang, L., Yu, G., & Fan, J. (2022). Establishment of open web platform based on 3D head model for product adaptability analysis and evaluation. *Heliyon*, e11732. https://doi.org/10.1016/j.heliyon.2022.e11732

Liu, H., Li, Z., & Zheng, L. (2008). Rapid preliminary helmet shell design based on three-dimensional anthropometric head data. *Journal of Engineering Design*, *19*(1), 45–54. https://doi.org/10.1080/09544820601186088

Liu, Y., Kau, C. H., Pan, F., Zhou, H., Zhang, Q., & Zacharopoulos, G. V. (2013). A 3-dimensional anthropometric evaluation of facial morphology among Chinese and Greek population. *Journal of Craniofacial Surgery*, *24*(4), e353–e358. https://doi.org/10.1097/SCS.0b013e3182902e5d

Lübbers, H.-T., Medinger, L., Kruse, A., Grätz, K. W., & Matthews, F. (2010). Precision and accuracy of the 3dMD photogrammetric system in craniomaxillofacial application. *The Journal of Craniofacial Surgery*, *21*(3), 763–767. https://doi.org/10.1097/SCS.0b013e3181d841f7

Lueder, R., & Berg Rice, V. J. (Eds.). (2008). *Ergonomics for Children - Designing products and places for toddlers to teens*. Taylor & Francis Group,.

Luximon, A., Zhang, Y., Luximon, Y., & Xiao, M. (2012). Sizing and grading for wearable products. *Computer-Aided Design*, *44*(1), 77–84. https://doi.org/10.1016/j.cad.2011.07.004

Luximon, Y., Ball, R. M., & Chow, E. H. C. (2016). A design and evaluation tool using 3D head templates. *Computer-Aided Design and Applications*, *13*(2), 153–161. https://doi.org/10.1080/16864360.2015.1084188

Luximon, Y., Ball, R. M., & Justice, L. (2010). The chinese face: A 3D anthropometric analysis. *Proceedings of the 8th International Symposium on Tools and Methods of Competitive Engineering, TMCE 2010*, *1*, 255–265. http://www.scopus.com/inward/record.url?eid=2-s2.0-79960499423&partnerID=40&md5=c95736fd6a566956d1f02074f23ed4fc

Luximon, Y., Ball, R. M., & Justice, L. (2012). The 3D Chinese head and face modeling. *Computer-Aided Design*, *44*(1), 40–47. http://www.scopus.com/inward/record.url?eid=2-s2.0-81855166641&partnerID=40&md5=e2c16acb400d684ce1fc94a67dec591b

Ma, Z., Drinnan, M., Hyde, P., & Munguia, J. (2018). Mask interface for continuous positive airway pressure therapy: selection and design considerations. *Expert Review of Medical Devices*, *15*(10), 725–733. https://doi.org/10.1080/17434440.2018.1525291

Martin, R. (1914). *Lehrbuch der Anthropologie in systematischer Darstellung*. Fischer.

Martin, R., & Knussmann, R. (1988). *Anthropologie: Handbuch der Vergleichenden Biologie des Menschen Band I: Wesen und Methoden der Anthropologie. 1. Teil:*

Wissenschaftstheorie, Geschichte, morphologische Methoden. Gustav Fischer Verlag.

Medialdea, L., Bazaco, C., D'Angelo del Campo, M. D., Sierra-Martínez, C., González-José, R., Vargas, A., & Marrodán, M. D. (2019). Describing the children's body shape by means of Geometric Morphometric techniques. *American Journal of Physical Anthropology*, *168*(4), 651–664. https://doi.org/10.1002/ajpa.23779

Mellies, U., Ragette, R., Dohna Schwake, C., Boehm, H., Voit, T., & Teschler, H. (2003). Long-term noninvasive ventilation in children and adolescents with neuromuscular disorders. *European Respiratory Journal*, *22*(4), 631–636. https://doi.org/10.1183/09031936.03.00044303a

Meunier, P., Shu, C., & Xi, P. (2009). Revealing the internal structure of human variability for design purposes. *Proceedings of the 17th World Congress on Ergonomics 2009*.

Meyer-Marcotty, P., Böhm, H., Linz, C., Kochel, J., Stellzig-Eisenhauer, A., & Schweitzer, T. (2014). Three-dimensional analysis of cranial growth from 6 to 12 months of age. *European Journal of Orthodontics*, *36*(5), 489–496. https://doi.org/10.1093/ejo/cjt010

Minnoye, A. L., Tajdari, F., Doubrovski, E. L., Wu, J., Kwa, F., Elkhuizen, W. S., Toon Huysmans, tudelftnl, & Song, Y. (2022). Personalized Product Design Through Digital Fabrication. *Proceedings of the ASME2022 International Design Engineering Technical Conferences and Computers and Informationin Engineering Conference*.

Molenbroek, J. F. M. (1994). *Made to Measure*. Delft University Press.

Molenbroek, J. F. M., & Bruin, R. De. (2005). Enhancing the use of anthropometric data. In *Human Factors in Design, Safety, and Management* (pp. 289–297).

Molenbroek J.F.M., & De Bruin, R. (2006). Anthropometry of a friendly rest room. *Assistive Technology*, *18*(2), 196–204. http://www.scopus.com/inward/record.url?eid=2-s2.0-33845246858&partnerID=40&md5=0670eced720ff7488f8f9c3730bd9927

Mortamet, G., Amaddeo, A., Essouri, S., Renolleau, S., Emeriaud, G., & Fauroux, B. (2017). Interfaces for noninvasive ventilation in the acute setting in children. In

Paediatric Respiratory Reviews (Vol. 23, pp. 84–88). W.B. Saunders Ltd. https://doi.org/10.1016/j.prrv.2016.09.004

Niu, J., & Li, Z. (2012). Using Three-Dimensional (3D) Anthropometric Data in Design. In *Handbook of Anthropometry: Physical Measures of Human Form in Health and Disease* (pp. 3001–3013). Springer New York. https://doi.org/10.1007/978-1-4419-1788-1

Niu, J., Li, Z., & Salvendy, G. (2009a). Multi-resolution description of three-dimensional anthropometric data for design simplification. *Applied Ergonomics*, *40*(4), 807–810. https://doi.org/10.1016/j.apergo.2008.05.005

Niu, J., Li, Z., & Salvendy, G. (2009b). Multi-resolution shape description and clustering of three-dimensional head data. *Ergonomics*, *52*(2), 251–269. https://doi.org/10.1080/00140130802334561

Niu, J., Li, Z. Z., & Xu, S. (2009). Block Division for 3D Head Shape Clustering. *Digital Human Modeling*, *5620 LNCS*, 64–71. http://www.springerlink.com/index/3m11v0m5347rx641.pdf

Nørregaard, O. (2002). Noninvasive ventilation in children. *European Respiratory Journal*, *20*(5), 1332–1342. https://doi.org/10.1183/09031936.02.00404802

Oestenstad, R. K., & Perkins, L. L. (1992). An assessment of critical anthropometric dimensions for predicting the fit of a half-mask respirator. *American Industrial Hygiene Association Journal*, *53*, 639–644. https://doi.org/10.1080/15298669291360283

Pedregosa, F., Varoquaux, G., Gramfort, A., Michel, V., Thirion, B., Grisel, O., Blondel, M., Prettenhofer, P., Weiss, R., Dubourg, V., Vanderplas, J., Passos, A., Cournapeau, D., Brucher, M., Perrot, M., & Duchesnay, É. (2011). Scikit-learn: Machine Learning in Python. *Journal of Machine Learning Research*, *12*, 2825–2830. http://scikit-learn.sourceforge.net.

Perret-Ellena, T., Skals, S. L., Subic, A., Mustafa, H., & Pang, T. Y. (2015). 3D anthropometric investigation of head and face characteristics of Australian cyclists. *Procedia Engineering*, *112*, 98–103. https://doi.org/10.1016/j.proeng.2015.07.182

Pheasant, S., & Haslegrave, C. M. (2006). *Bodyspace: Anthropometry, Ergonomics and the Design of Work*, Third Edition. Taylor & Francis.

Piotrowski, C. C., Warda, L., Pankratz, C., Dubberley, K., Russell, K., Assam, H., & Carevic, M. (2020). The perspectives of young people on barriers to and facilitators of bicycle helmet and booster seat use. *Child: Care, Health and Development*, *46*(5), 591–598. https://doi.org/10.1111/cch.12791

Ramirez, A., Delord, V., Khirani, S., Leroux, K., Cassier, S., Kadlub, N., Aubertin, G., Picard, A., & Fauroux, B. (2012). Interfaces for long-term noninvasive positive pressure ventilation in children. *Intensive Care Medicine*, *38*(4), 655–662. https://doi.org/10.1007/s00134-012-2516-1

Rivara, F. P., Astley, S. J., Clarren, S. K., Thompson, D. C., & Thompson, R. S. (1999). Fit of bicycle safety helmets and risk of head injuries in children. *Injury Prevention*, *5*(3), 194–197. https://doi.org/10.1136/ip.5.3.194

Robinette, K. M., Blackwell, S., Daanen, H. A. M., Boehmer, M., Fleming, S., Brill, T., Hoeferlin, D., & Burnsides, D. (2002). *Civilian American and European Surface Anthropometry Resource (CEASAR) Final Report, Volume I: Summary*.

Robinette, K. M., Daanen, H. A. M., & Paquet, E. (1999). The CAESAR project: a 3-D surface anthropometry survey. *Second International Conference on 3-D Digital Imaging and Modeling*, 380–386.

Robinette, K. M., & Hudson, J. A. (2006). Anthropometry. In *Handbook of Human Factors and Ergonomics* (3rd edition, pp. 322–339). John Wiley & Sons.

Roebuck, J. A., Kroemer, K. H. E., & Thomson, W. G. (1975). Engineering Anthropometry Methods. Wiley.

Samuels, M., & Boit, P. (2007). Non-invasive ventilation in children. *Paediatrics and Child Health*, *17*(5), 167–173. https://doi.org/10.1016/j.paed.2007.02.009

Schneider, L. W., Lehman, R. J., Pflug, M. A., & Owings, C. L. (1986). Size and shape of the head and neck from birth to four years. *Final Report to The Consumer Product Safety Commission*.

Schönbeck, Y., Talma, H., van Dommelen, P., Bakker, B., Buitendijk, S. E., HiraSing, R. a, & van Buuren, S. (2013). The world's tallest nation has stopped growing taller: the height of Dutch children from 1955 to 2009. *Pediatric Research*, *73*(3), 371–377. https://doi.org/10.1038/pr.2012.189

Schönbeck, Y., Talma, H., von Dommelen, P., Bakker, B., Buitendijk, S. E., HiraSing, R. A., & van Buuren, S. (2011). Increase in prevalence of overweight in dutch children and adolescents: A comparison of nationwide growth studies in 1980,

1997 and 2009. *PLoS ONE*, *6*(11), e27608. https://doi.org/10.1371/journal.pone.0027608

Schönbeck, Y., & van Buuren, S. (2010). Growth diagrams 2010, Netherlands fifth nation-wide survey. https://www.tno.nl/nl/aandachtsgebieden/gezond-leven/prevention-work-health/gezond-en-veilig-opgroeien/groeidiagrammen-in-pdf-formaat/

Schreinemakers, J. R. C., Oudenhuijzen, A. J. K., van Amerongen, P. C. G. M., & Kon, M. (2013). Oxygen Mask Fit Analysis in F-16 Fighter Pilots Using 3D Imaging. *Aviation, Space, and Environmental Medicine*, *84*(10), 1029–1033. https://doi.org/10.3357/ASEM.3611.2013

Seo, H., Song, Y., Kim, C., & Kim, H. (2016). Characteristics of Korean children's facial anthropometry evaluated by three-dimensional imaging. *Journal of the International Society for Respiratory Protection*, *33*(1), 23–38.

Seth M. Weinberg, MA, J. C. K. (2008). Three Dimensional Surface Imaging: Limitations and Considerations. The Journal of Craniofacial Surgery.

Shah, P., & Luximon, Y. (2018). Three-dimensional human head modelling: a systematic review. *Theoretical Issues in Ergonomics Science*, *19*(6), 658–672. https://doi.org/10.1080/1463922X.2018.1432715

Simonds, A. K., Ward, S., Heather, S., Bush, A., & Muntoni, F. (2000). Outcome of paediatric domiciliary mask ventilation in neuromuscular and skeletal disease. *European Respiratory Journal*, *16*(3), 476–481.

Sims, R. E., Marshall, R., Gyi, D. E., Summerskill, S. J., & Case, K. (2012). Collection of anthropometry from older and physically impaired persons: Traditional methods versus TC2 3-D body scanner. *International Journal of Industrial Ergonomics*, *42*(1), 65–72. https://doi.org/10.1016/j.ergon.2011.10.002

Skals, S., Ellena, T., Subic, A., Mustafa, H., & Pang, T. Y. (2016). Improving fit of bicycle helmet liners using 3D anthropometric data. *International Journal of Industrial Ergonomics*, *55*, 86–95. https://doi.org/10.1016/j.ergon.2016.08.009

Snyder, R. G., Schneider, L. W., Owings, C. L., Reynolds, H. M., Golomb, D. H., & Schork, M. A. (1977). *Anthropometry of infants, children and youths to age 18 for product safety design. Final report*.

Solves, C., Nácher, B., Benages, L., Marzo, R., Soriano, C., & Alemany, S. (2017). *Research on the existence and availability of anthropometric data of children. Internal report of Deutsches Institut für Normung.* Unpublished.

Spijker, J. (2020). *Tailored Non-Invasive Ventilation Masks for Paediatric Intensive Care.* Master's thesis, Delft University of Technology.

Statistics Netherlands (CBS). (2017). *CBS StatLine - Population; Key figures*. http://statline.cbs.nl/Statweb/publication/

Stavrakos, S.-K., & Ahmed-Kristensen, S. (2016). Methods of 3D data applications to inform design decisions for physical comfort. *Work*, *55*(2), 321–334. https://doi.org/10.3233/WOR-162399

Steenbekkers, L. P. A. (1993). *Child development, design implications and accident prevention.* Delft University Press.

Steenbekkers, L. P. A., & Molenbroek, J. F. M. (1990). Anthropometric data of children for non-specialist users. *Ergonomics*, *33*(4), 421–429. https://doi.org/10.1080/00140139008927146

The Canadian Institute of Child Health. (2007). Child anthropometry: A literature scan of national and international publications. https://doi.org/10.1201/9780203609163.ch3

Tutkuviene, J., Cattaneo, C., Obertová, Z., Ratnayake, M., Poppa, P., Barkus, A., Khalaj-Hedayati, K., Schroeder, I., & Ritz-Timme, S. (2015). Age- and sex-related growth patterns of the craniofacial complex in European children aged 3–6 years. *Annals of Human Biology*, *4460*(May 2016), 1–10. https://doi.org/10.3109/03014460.2015.1106584

Van Boeijen, A.G.C., Daalhuijzen, J.J., Zijlstra, J.J.M. (eds.), (2020, Rev. ed.). *Delft Design Guide: Perspectives-Models-Approaches-Methods.* Amsterdam:BISPublishers.

Van der Brand, C. L., Karger, L. B., Nijman, S. T. M., Valkenberg, H., & Jellema, K. (2020). Bicycle Helmets and Bicycle-Related Traumatic Brain Injury in the Netherlands. *Neurotrauma Reports*, *1*(1), 201–206. https://doi.org/10.1089/neur.2020.0010

Veitch, D. E., Caple, D., & Blewett, V. (2009). *Sizing up Australia: How contemporary is the anthropometric data Australian industrial designers use?* https://www.researchgate.net/publication/256706863

Veitch, D. E., & Robinette, K. (2006). World Engineering Anthropometry Resource (WEAR): A Review. *Human Factors & Ergonomics Society of Australia Inc*. https://www.researchgate.net/publication/256706869

Verwulgen, S., Lacko, D., Vleugels, J., Vaes, K., Danckaers, F., Bruyne, G. De, & Huysmans, T. (2018). A new data structure and work flow for using 3D anthropometry in the design of wearable products. *International Journal of Industrial Ergonomics*, *64*, 108–117. https://doi.org/10.1016/j.ergon.2018.01.002

Weinberg, S. M., Scott, N. M., Neiswanger, K., Brandon, C. A., & Marazita, M. L. (2004). Digital three-dimensional photogrammetry: Evaluation of anthropometric precision and accuracy using a Genex 3D camera system. *Cleft Palate-Craniofacial Journal*, *41*(5), 507–518. https://doi.org/10.1597/03-066.1

WHO Multicentre Growth Reference Study Group. (2009). *WHO Child Growth Standards: Growth velocity based on weight, length and head circumference: Methods and development*.

Wong, J. Y., Oh, A. K., Ohta, E., Hunt, A. T., Rogers, G. F., Mulliken, J. B., & Deutch, C. K. (2008). Validity and reliability of craniofacial anthropometric measurement of 3D digital photogrammetric images. *Palate-Craniofacial*, *45*(3), 232–239. https://doi.org/10.1597/06-175.1

World Health Organisation. (1995). Physical Status: The use and interpretation of Anthropometry.

Wortmann, T., Zuardin, A., Demin, D., & Waibel, C. (2023). *https://github.com/Tomalwo/FrOG*. https://github.com/Tomalwo/FrOG

Wu, Y. Y., Acharya, D., Xu, C., Cheng, B., Rana, S., & Shimada, K. (2018). Custom-Fit three-dimensional- printed BiPAP mask to improve compliance in patients requiring long-term noninvasive ventilatory support. *Journal of Medical Devices, Transactions of the ASME*, *12*(3). https://doi.org/10.1115/1.4040187

Wuhrer, S., Shu, C., & Bose, P. (2012). Automatically Creating Design Models From 3D Anthropometry Data. *Journal of Computing and Information Science in Engineering*, *12*(4), 041007. https://doi.org/10.1115/1.4007839

Xi, P., Lee, W.-S., & Shu, C. (2007). Analysis of Segmented Human Body Scans. *Graphics Interface* , 19–26.

Xi, P., & Shu, C. (2009). Consistent parameterization and statistical analysis of human head scans. *Visual Computer*, *25*, 863–871. https://doi.org/10.1007/s00371-009-0316-6

Yang, W., Wang, H., & He, R. (2022). Establishment of a finite element model based on craniofacial soft tissue thickness measurements and stress analysis of medical goggles. *Ergonomics*, *65*(2), 305–326. https://doi.org/10.1080/00140139.2021.1961023

Yin, L., Wei, X., Sun, Y., Wang, J., & Rosato, M. J. (2006). A 3D facial expression database for facial behavior research. *FGR 2006: Proceedings of the 7th International Conference on Automatic Face and Gesture Recognition*, *2006*, 211–216. https://doi.org/10.1109/FGR.2006.6

Young, J. W. (1966). Selected facial measurements of children for oxygen-mask design. *Office of Aviation Medicine, Federal Aviation Agency, Oklahoma City*, *Rep. No. AM66-9*.

Yu, Y., Benson, S., Cheng, W., Hsiao, J., Liu, Y., Zhuang, Z., & Chen, W. (2011). Digital 3-D headforms representative of Chinese workers. *Annals of Occupational Hygiene*, *56*(1), 113–122. https://doi.org/10.1093/annhyg/mer074

Zhang, J., Luximon, Y., Shah, P., & Li, P. (2023). 3D Statistical Head Modeling for Face/head-Related Product Design: A State-of-the-Art Review. In *CAD Computer Aided Design* (Vol. 159). Elsevier Ltd. https://doi.org/10.1016/j.cad.2023.103483

Zhang, J., Luximon, Y., Shah, P., Zhou, K., & Li, P. (2022). Customize My Helmet: A Novel Algorithmic Approach Based on 3D Head Prediction. *CAD Computer Aided Design*, *150*. https://doi.org/10.1016/j.cad.2022.103271

Zhuang, Z., Benson, S., & Viscusi, D. (2010). Digital 3-D headforms with facial features representative of the current us workforce. *Ergonomics*, *53*(5), 661–671. https://doi.org/10.1080/00140130903581656

Zhuang, Z., & Bradtmiller, B. (2005). Head-and-face anthropometric survey of U.S. respirator users. *Journal of Occupational and Environmental Hygiene*, *2*(11), 567–576. https://doi.org/10.1080/15459620500324727

Zhuang, Z., Bradtmiller, B., & Shaffer, R. E. (2007). New respirator fit test panels representing the current U.S. civilian work force. *Journal of Occupational and Environmental Hygiene*, *4*(9), 647–659.

Zhuang, Z., Coffey, C. C., & Ann, R. B. (2005). The effect of subject characteristics and respirator features on respirator fit. *Journal of Occupational and Environmental Hygiene*, *2*(12), 641–649. https://doi.org/10.1080/15459620500391668

Zhuang, Z., Landsittel, D., Benson, S., Roberge, R., & Shaffer, R. (2010). Facial anthropometric differences among gender, ethnicity, and age groups. *Annals of Occupational Hygiene*, *54*(4), 391–402.

Zhuang, Z., Shu, C., Xi, P., Bergman, M., & Joseph, M. (2013). Head-and-face shape variations of U.S. civilian workers. *Applied Ergonomics*, *44*(5), 775–784.

Zhuang, Z., Slice, D. E., Benson, S., Lynch, S., & Viscusi, D. J. (2010). Shape analysis of 3D head scan data for U.S. respirator users. *EURASIP Journal on Advances in Signal Processing*, *2010*, 1–10.

APPENDIX

2.1 SUMMARY STATISTICS

Summary statistics of face and head measurements (Mean and Standard Deviation) of Dutch children (gender combined). Traditional measurements and 3D image derived measurements*(mm).

	Stature									
	Male + Female									
Age	N	Mean	SD	Min	5th	25th	50th	75th	95th	Max
0	17	730.1	40.1	655.0	655.8	720.0	735.0	760.0	780.0	800.0
1	28	821.8	45.4	720.0	766.8	799.3	818.0	840.0	876.5	976.0
2	23	938.4	75.1	810.0	842.0	893.0	932.0	967.0	1057.2	1154.0
3	32	1003.8	40.6	894.0	944.2	980.0	1009.5	1038.0	1058.5	1080.0
4	54	1094.2	41.2	1015.0	1034.0	1061.0	1093.0	1127.0	1162.4	1185.0
5	64	1154.2	55.3	1020.0	1066.1	1124.8	1153.5	1188.5	1246.4	1292.0
6	66	1217.8	50.4	1108.0	1139.5	1177.5	1214.0	1254.0	1296.8	1331.0
7	17	1250.8	47.3	1185.0	1189.0	1211.0	1255.0	1269.0	1338.0	1338.0

	Head Circumference									
	Male + Female									
Age	N	Mean	SD	Min	5th	25th	50th	75th	95th	Max
0	17	453.5	13.8	430.0	434.8	440.0	454.0	467.0	472.4	474.0
1	27	473.7	15.9	448.0	450.0	463.0	475.0	481.0	501.5	505.0
2	22	488.0	11.3	467.0	472.1	483.0	490.0	493.0	499.9	518.0
3	32	503.1	20.6	468.0	475.1	488.8	498.5	514.5	542.3	550.0
4	54	508.5	13.1	479.0	490.0	500.0	507.5	517.5	531.4	540.0
5	64	510.6	13.9	475.0	490.0	502.8	510.5	520.0	531.0	553.0
6	66	513.1	15.9	467.0	487.8	501.5	515.5	522.8	539.5	543.0
7	17	514.7	13.9	493.0	496.2	500.0	517.0	525.0	533.4	535.0

	Weight									
	Male + Female									
Age	N	Mean	SD	Min	5th	25th	50th	75th	95th	Max
0	17	8.8	1.0	6.6	6.9	8.5	9.1	9.6	10.0	10.3
1	28	10.9	1.4	8.0	8.8	10.1	11.0	11.6	13.1	13.2
2	23	13.8	1.9	11.3	11.4	12.1	13.6	14.7	17.3	18.5
3	32	15.5	1.6	11.0	13.4	14.3	15.5	16.7	18.0	19.1
4	54	18.9	2.4	12.0	15.1	17.5	19.0	20.5	22.6	23.5
5	64	20.9	2.7	16.0	17.1	19.0	20.5	23.0	25.9	29.5
6	66	22.7	2.7	17.5	18.6	21.0	22.3	25.0	26.8	31.0
7	17	24.6	2.4	21.0	21.0	23.0	24.5	26.0	27.8	29.0

	Head Height									
	Male + Female									
Age	N	Mean	SD	Min	5th	25th	50th	75th	95th	Max
0	13	158.2	9.9	143.0	145.4	150.0	156.0	168.0	170.8	172.0
1	16	168.8	7.6	157.0	158.5	164.5	168.5	172.0	179.5	187.0
2	22	174.9	12.9	137.0	161.0	170.3	176.0	183.3	192.0	195.0
3	32	181.6	12.6	150.0	168.1	173.0	179.5	188.3	203.9	209.0
4	54	188.0	10.1	165.0	175.0	183.0	187.0	192.8	208.4	221.0
5	64	190.9	9.4	166.0	177.2	184.8	192.0	196.0	206.9	216.0
6	66	193.8	10.4	170.0	179.0	187.0	193.0	200.0	207.8	230.0
7	17	193.4	9.6	177.0	181.8	187.0	191.0	202.0	207.6	210.0

	Head Breadth									
	Male + Female									
Age	**N**	**Mean**	**SD**	**Min**	**5th**	**25th**	**50th**	**75th**	**95th**	**Max**
0	15	124.1	5.1	115.0	117.1	120.0	125.0	127.5	130.9	133.0
1	20	132.3	8.5	118.0	121.8	128.8	131.5	135.0	151.2	154.0
2	22	135.7	7.1	122.0	124.3	131.3	134.5	141.0	147.9	150.0
3	32	137.8	6.3	124.0	126.6	134.3	139.5	143.0	144.0	148.0
4	54	140.1	5.8	130.0	132.0	135.3	140.0	144.5	149.4	152.0
5	64	141.8	6.8	131.0	132.3	136.0	142.0	146.0	153.7	163.0
6	66	144.0	7.3	130.0	134.0	138.5	143.5	148.8	156.0	163.0
7	17	145.5	7.1	135.0	137.4	142.0	144.0	149.0	154.2	167.0

	Face Width									
	Male + Female									
Age	**N**	**Mean**	**SD**	**Min**	**5th**	**25th**	**50th**	**75th**	**95th**	**Max**
0	15	99.6	5.0	93.0	93.7	96.5	98.0	103.0	107.1	112.0
1	21	103.1	7.4	90.0	91.0	100.0	102.0	107.0	116.0	116.0
2	22	103.7	5.6	91.0	93.2	100.3	104.0	107.0	111.9	113.0
3	32	106.6	4.7	98.0	98.6	103.0	107.0	110.0	113.0	116.0
4	54	108.1	5.5	100.0	101.0	103.3	107.0	111.0	118.7	123.0
5	64	108.6	5.8	100.0	101.0	104.0	108.0	112.0	120.6	123.0
6	66	110.7	6.9	99.0	100.3	106.0	111.0	114.0	123.0	129.0
7	17	111.0	6.8	99.0	102.2	108.0	110.0	114.0	121.2	126.0

	Head Length									
	Male + Female									
Age	**N**	**Mean**	**SD**	**Min**	**5th**	**25th**	**50th**	**75th**	**95th**	**Max**
0	13	151.7	7.9	136.0	141.4	147.0	152.0	158.0	162.4	163.0
1	20	162.8	7.8	147.0	151.8	156.8	161.5	168.5	172.3	177.0
2	22	165.5	10.5	132.0	150.3	163.3	168.0	172.8	177.0	179.0
3	32	172.1	7.7	160.0	161.7	167.8	170.0	176.0	183.3	197.0
4	54	175.9	6.6	162.0	166.0	171.0	176.0	179.0	187.4	192.0
5	64	177.8	6.8	159.0	167.3	174.8	177.0	182.0	188.9	194.0
6	66	177.8	8.1	155.0	165.3	173.0	178.0	183.0	190.8	194.0
7	17	178.6	7.4	167.0	168.6	172.0	179.0	183.0	190.4	192.0

	Face Height*									
	Male + Female									
Age	**N**	**Mean**	**SD**	**Min**	**5th**	**25th**	**50th**	**75th**	**95th**	**Max**
0	17	74.7	3.9	66.8	69.3	71.8	74.3	77.5	80.6	81.3
1	29	80.0	4.1	72.4	74.2	76.8	80.0	83.3	86.1	87.9
2	23	83.7	3.9	76.5	78.7	80.6	83.4	86.6	90.6	90.8
3	32	87.9	3.7	79.8	83.8	85.4	87.4	89.5	94.0	95.0
4	54	92.9	4.0	83.9	87.6	90.4	92.9	95.3	99.9	104.5
5	64	94.9	4.8	84.2	87.7	91.4	94.4	98.6	102.3	104.9
6	66	96.2	4.4	85.9	88.7	93.4	95.9	99.4	102.8	106.6
7	17	97.8	5.0	84.2	90.5	95.5	98.0	100.8	104.5	105.6

	Lower Face Height*									
	Male + Female									
Age	N	Mean	SD	Min	5th	25th	50th	75th	95th	Max
0	17	47.0	3.2	39.8	42.1	45.0	48.1	49.5	50.4	51.7
1	29	50.7	3.0	45.3	46.1	48.1	50.5	52.7	56.0	56.8
2	23	52.4	2.6	47.2	48.4	50.1	53.0	54.1	55.8	56.4
3	32	54.6	3.2	46.8	49.0	52.9	54.5	56.5	58.8	61.3
4	54	57.3	3.7	48.9	51.9	55.2	57.3	59.0	63.1	67.8
5	64	58.3	3.7	50.3	52.4	55.8	57.8	61.1	63.9	67.7
6	66	58.5	3.4	51.6	53.4	55.7	58.1	61.1	63.5	66.9
7	17	59.1	3.8	49.5	52.8	57.6	60.4	61.3	63.1	65.1

	Nasal Root Breadth*									
	Male + Female									
Age	N	Mean	SD	Min	5th	25th	50th	75th	95th	Max
0	17	19.4	1.4	17.8	17.8	18.6	19.2	20.1	21.2	23.4
1	29	19.4	2.2	14.4	15.6	18.6	19.1	21.3	22.4	23.4
2	23	19.7	2.0	14.8	15.7	18.8	20.0	21.2	21.8	23.0
3	32	20.7	1.3	17.0	18.6	19.8	21.1	21.9	22.2	22.8
4	54	21.3	1.8	17.4	18.6	20.1	21.1	22.5	24.6	26.0
5	64	21.1	1.7	16.9	17.8	20.3	21.1	22.4	23.3	24.5
6	66	21.4	1.9	17.0	18.9	20.1	21.3	22.7	24.4	26.8
7	17	21.7	2.1	16.6	19.4	20.7	21.5	22.4	25.1	26.2

	Height of Chin*									
	Male + Female									
Age	N	Mean	SD	Min	5th	25th	50th	75th	95th	Max
0	17	17.4	2.1	13.6	14.3	15.8	17.5	18.3	20.9	21.2
1	29	19.9	2.6	15.4	16.0	18.3	19.5	21.2	24.6	25.4
2	23	21.6	2.3	16.9	17.8	20.3	22.0	22.7	24.8	26.1
3	32	24.0	2.9	19.4	20.3	21.8	23.9	25.4	27.9	33.0
4	54	24.9	2.8	19.3	20.6	22.8	24.7	26.7	29.3	32.0
5	64	25.3	2.4	20.6	21.5	23.4	25.5	26.9	29.1	32.0
6	66	26.2	2.5	20.5	21.6	24.7	26.4	27.6	30.0	33.7
7	17	25.8	2.6	20.7	22.3	24.0	25.9	27.6	29.1	31.7

	Nose Length*									
	Male + Female									
Age	N	Mean	SD	Min	5th	25th	50th	75th	95th	Max
0	17	27.6	1.9	24.8	25.4	26.7	27.2	28.4	30.9	31.5
1	29	29.3	1.8	25.9	26.2	28.2	29.4	30.4	32.0	33.5
2	23	31.2	2.7	25.9	26.6	30.2	31.1	32.9	34.9	36.4
3	32	33.2	2.2	28.5	30.0	31.5	33.4	34.7	36.6	38.0
4	54	35.6	2.1	31.4	32.3	34.0	35.9	36.7	38.7	40.4
5	64	36.6	2.3	31.8	33.4	34.9	36.4	38.0	40.6	42.7
6	66	37.8	2.6	31.1	33.0	35.9	37.8	39.7	41.6	43.0
7	17	38.8	2.6	34.7	35.7	36.4	38.7	40.4	43.0	44.5

	Nasal Tip Protrusion*									
	Male + Female									
Age	**N**	**Mean**	**SD**	**Min**	**5th**	**25th**	**50th**	**75th**	**95th**	**Max**
0	17	11.5	1.0	9.6	9.9	10.9	11.6	12.1	12.8	13.0
1	29	11.6	0.9	10.4	10.5	10.8	11.4	12.4	13.0	13.5
2	23	12.5	1.6	9.8	10.4	11.0	12.4	13.7	14.7	15.4
3	32	13.2	1.4	10.4	11.4	12.2	13.3	14.1	15.5	15.9
4	54	14.2	1.2	11.0	12.3	13.5	14.0	15.2	16.1	16.4
5	64	14.7	1.2	12.0	12.9	13.9	14.6	15.6	16.5	18.1
6	66	15.2	1.3	12.6	13.2	14.3	15.4	15.9	17.2	19.0
7	17	15.4	1.3	13.5	14.0	14.5	15.3	16.0	17.5	18.9

	Mouth width*									
	Male + Female									
Age	**N**	**Mean**	**SD**	**Min**	**5th**	**25th**	**50th**	**75th**	**95th**	**Max**
0	16	32.7	3.8	26.8	27.8	29.7	33.1	35.4	38.0	38.8
1	28	34.2	2.5	30.1	30.8	32.0	34.1	35.6	37.8	40.1
2	22	35.6	2.2	29.7	32.9	34.3	35.7	37.0	39.1	39.4
3	32	36.7	2.9	31.6	32.6	34.2	36.2	39.1	41.1	42.1
4	54	37.4	2.8	32.7	33.6	35.2	37.2	39.2	41.9	44.7
5	64	38.6	3.5	29.9	33.0	36.6	38.7	41.8	43.8	44.0
6	66	39.7	3.1	32.2	34.7	37.5	39.5	41.9	44.9	45.9
7	17	40.9	3.5	33.1	36.2	38.2	41.4	43.0	45.1	47.3

	Nose width*									
	Male + Female									
Age	**N**	**Mean**	**SD**	**Min**	**5th**	**25th**	**50th**	**75th**	**95th**	**Max**
0	17	25.3	1.4	23.3	23.8	24.2	25.2	25.9	27.4	28.5
1	29	26.2	1.7	23.6	24.0	24.9	26.1	26.7	29.6	30.1
2	23	26.9	1.9	24.3	24.5	25.6	26.8	27.4	30.0	32.4
3	32	27.9	2.2	24.3	25.5	26.4	27.8	28.6	32.2	34.7
4	54	28.1	1.6	25.1	25.8	26.6	27.9	29.2	31.1	31.5
5	64	28.3	1.5	24.6	26.1	27.3	28.2	29.1	30.9	32.5
6	66	28.9	1.6	25.7	26.1	27.9	28.9	30.1	31.1	32.3
7	17	29.5	1.4	27.1	27.4	28.6	29.3	30.6	31.1	32.5

2.2 BAR CHARTS

Bar charts showing mean values (mm) and standard deviations per age group for head circumference, head height, head breadth, head length, face width, face height and mouth width.

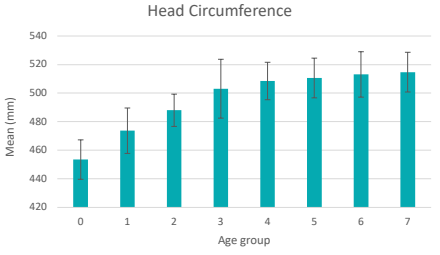

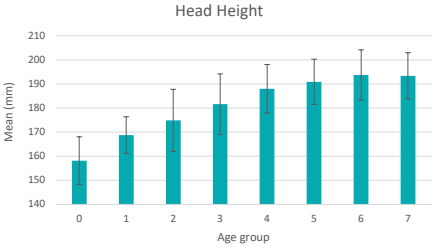

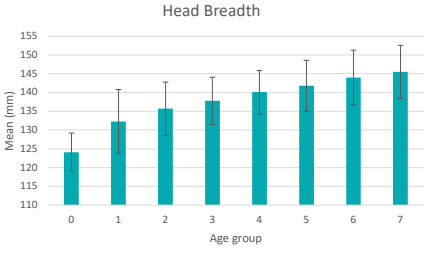

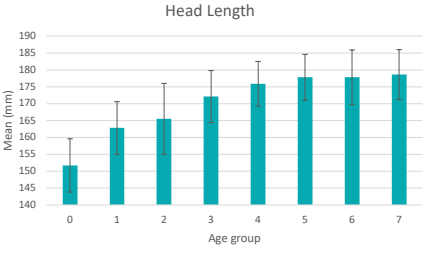

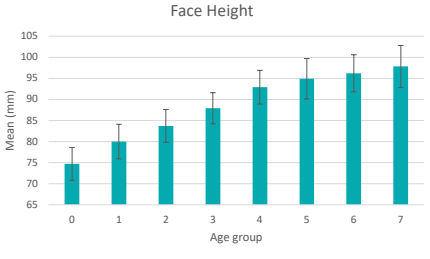

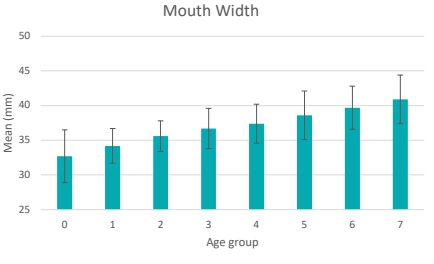

2.3 CROSS SECTIONAL GROWTH CURVES (STEENBEKKERS AND GOTO)

Cross sectional growth curves of the mean measurements per age group for this dataset and the dataset of L.P.A. Steenbekkers (1993).

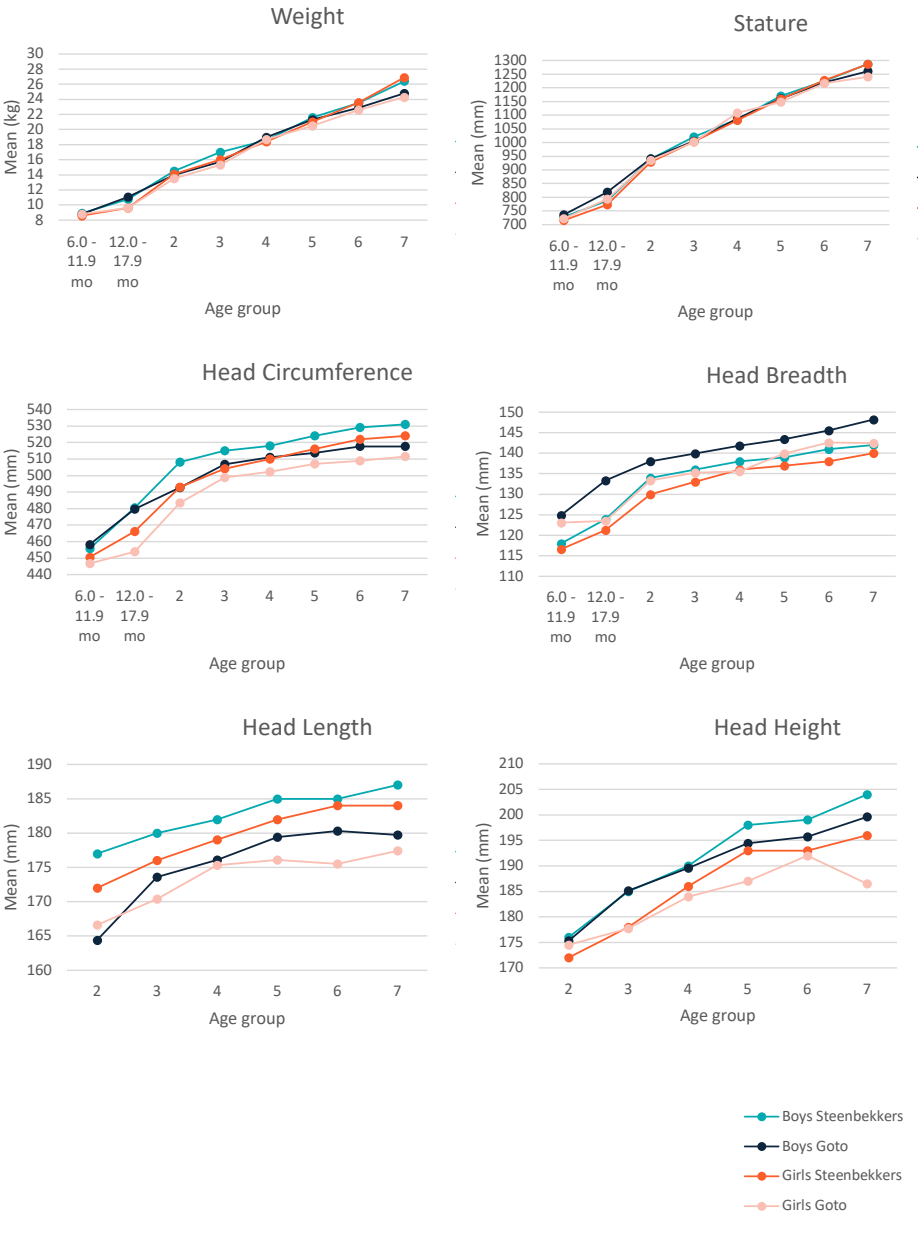

2.4 CROSS SECTIONAL GROWTH CURVES (FARKAS AND GOTO)

Cross sectional growth curves of the mean face and head measurements per age group for this dataset and the dataset of L.G. Farkas (1994).

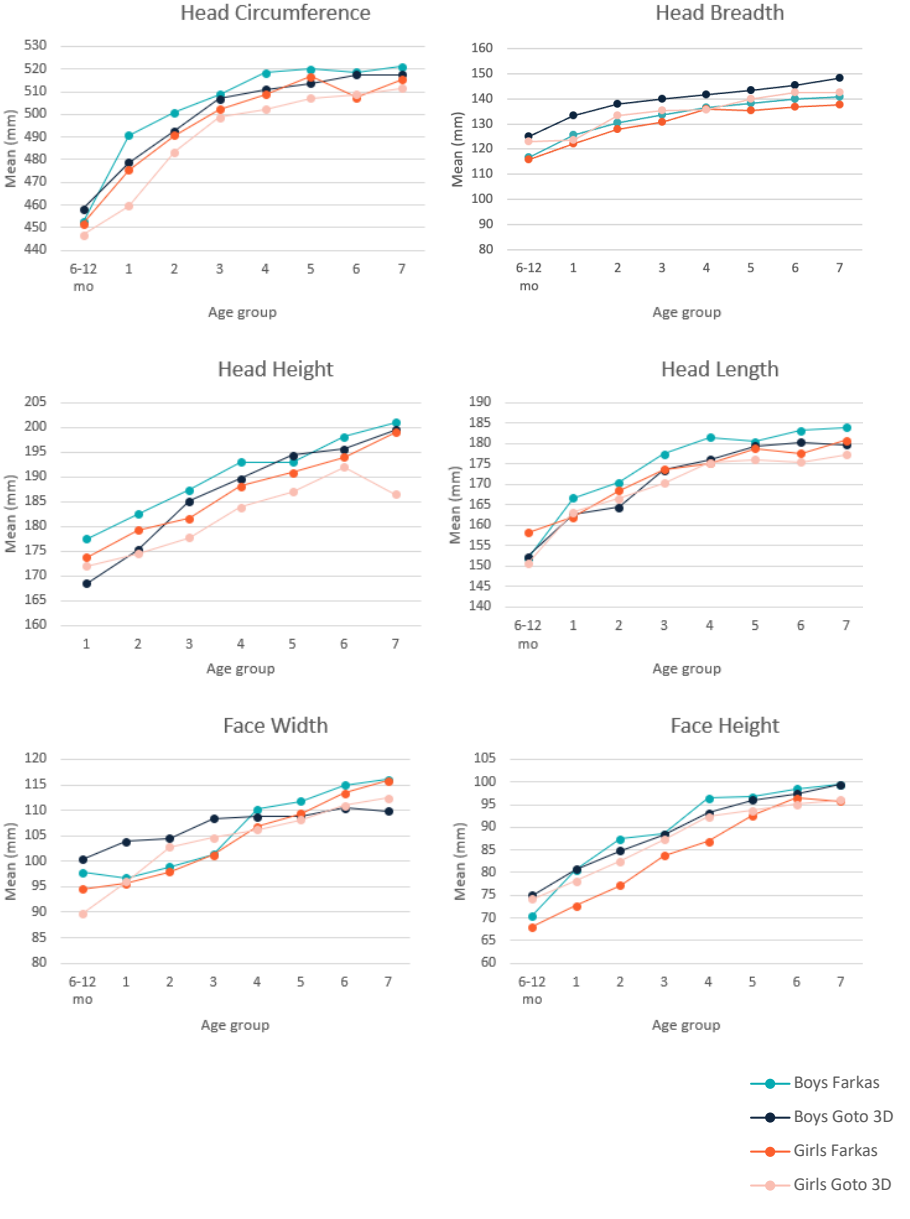

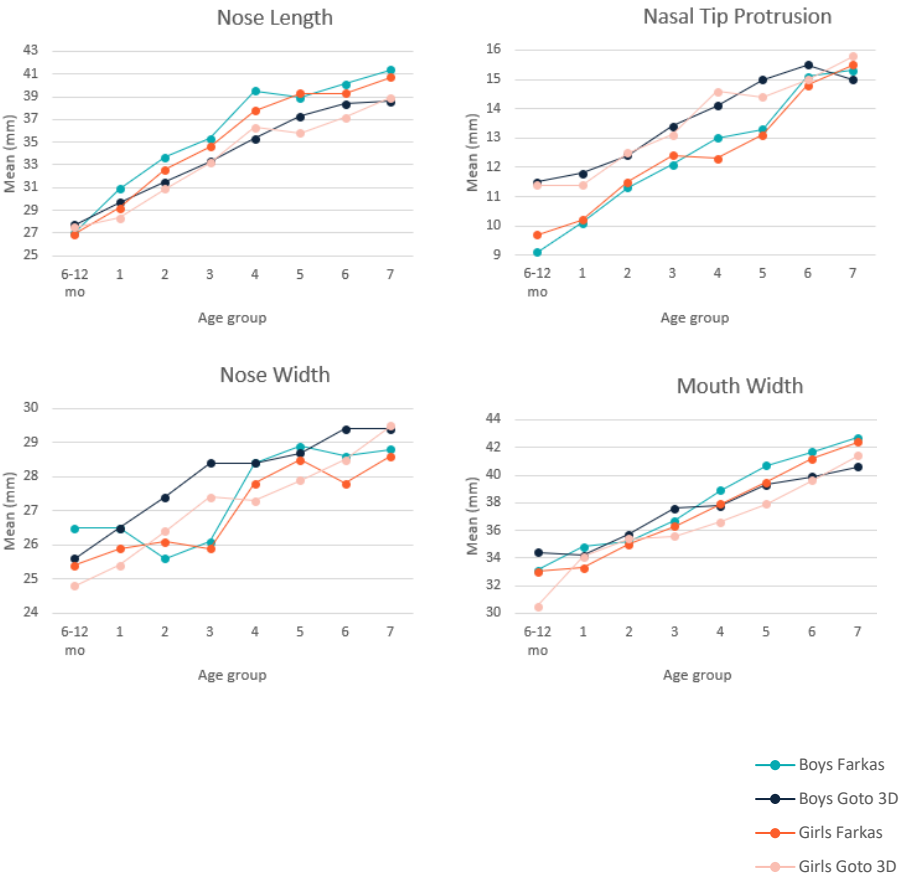
Nose Length
Mean (mm)
43
41
39
37
35
33
31
29
27
25
6-12 mo
1
2
3
4
5
6
7
Age group
Nasal Tip Protrusion
Mean (mm)
16
15
14
13
12
11
10
9
6-12 mo
1
2
3
4
5
6
7
Age group
Nose Width
Mean (mm)
30
29
28
27
26
25
24
6-12 mo
1
2
3
4
5
6
7
Age group
Mouth Width
Mean (mm)
44
42
40
38
36
34
32
30
6-12 mo
1
2
3
4
5
6
7
Age group
Boys Farkas
Boys Goto 3D
Girls Farkas
Girls Goto 3D

“And once the storm is over you won’t remember how you made it through, how you managed to survive. You won’t even be sure, in fact, whether the storm is really over. But one thing is certain. When you come out of the storm you won’t be the same person who walked in. That’s what this storm’s all about.”

— Haruki Murakami

ACKNOWLEDGEMENTS

This PhD journey has undeniably been a long and winding road with times of achievement and times of struggle, marked by its fair share of life-altering events, both joyous and sorrowful. However, it is the multitude of encounters with individuals, each contributing in their unique way, that made this journey worthwhile and propelled me forward.

First of all, I want to express my heartfelt thanks to Michel Holper for his dedication and concern as a student, and to Johan Molenbroek for their joint efforts in securing funding from the Prinses Beatrix Spierfonds. Their initiative gave me the chance to explore home ventilation for children with respiratory illnesses and 3D children's anthropometry, without them this project would not have been possible. Johan, thank you for offering me the opportunity to become part of this project. You have been an invaluable source of knowledge, generously sharing your extensive expertise in anthropometry, from the practical aspects of measuring people to its application in design. Your unwavering positivity, encouragement, and willingness to help have been invaluable to me. I am happy that we can continue our collaboration in the KidsCAN project.

Richard, your role in my academic journey, from my master's thesis to my junior researcher position, and eventually as my promotor, has been truly invaluable. Despite your jam-packed schedule, you always made time for me, adjusting to my deadlines with flexibility. While scribbling down your illegible notes you were always able to swiftly grasp the essence of my questions and challenges and help me move forward. Thank you for your infinite patience, ever-positive encouragement, and optimistic attitude. These qualities, particularly during the tougher times, have been invaluable in helping me through. And maybe someday, I'll also find someone to mentor who is born on the fourth of November ;).

Thank you, committee members for your time and effort in reviewing this dissertation and providing me with valuable feedback to further improve my research. I am honoured that you are taking part in my defence!

Wonsup, you arrived at the perfect moment. After I had collected the 3D data, we were in search of someone who could share their experience and knowledge about analysing and processing 3D data. You joined our department, and not only did you contribute to valuable in-depth discussions and offer much-appreciated advice for my research, but you also introduced your wonderful family into our lives. I am deeply grateful to you and sincerely hope that our paths will cross once again in the future.

Toon, without you, my research wouldn't have reached the depth it did, and the exploration wouldn't have extended as far. With your computer science expertise, you

have the ability to provide insight into complex data and transform it into beautiful visuals that resonate with a designer's visual-oriented mind. Despite the many black boxes in this process, you taught me so much during our collaboration. I appreciate your calm nature and want to thank you especially for your endless patience in explaining these processes. Also, thank you for the trust in including me in the KidsCAN team; This opportunity has allowed me to further immerse myself in the research field, gaining valuable experience and knowledge in a practical and enjoyable manner. I am thankful for our collaboration.

Miriam and Trudi, you introduced me to the world of home ventilation for children with great care and passion for your profession. My visits to you at the “Centrum voor Thuis Beademing” were always invaluable, motivating me, and despite your demanding work, I always felt welcome. You consistently radiated cheerfulness, even in the face of the serious cases you were handling. Time has caught up with me regarding the design of the specific mask foreseen at the beginning of this project, but thankfully other options presented themselves over time which were of even greater benefit for the children you care for. Your input and expertise are interwoven into this research indirectly benefiting so many other children.

De 3D dataset is mede dankzij jou tot stand gekomen, Bertus. Samen zijn we meer dan 30 dagen op pad geweest in de regio Delft om kinderkopjes te verzamelen. Hoewel dat al even geleden is, herinner ik me die dagen nog goed. Jouw relaxte omgang met de kinderen, je flauwe grappen - het maakte de hele ervaring voor de kinderen leuk en heeft bijgedragen aan hun bereidheid om mee te werken aan de metingen.

Lieve paranimphs Boudewijn and Charlotte, I am so grateful to have you by my side. Boudewijn, during our rides to the university, I could prepare for the day and cool down on the way back. Our like-mindedness immediately set the tone from the beginning. I cherish the friendship that has grown from this and consider it one of the positive side effects of pursuing a PhD. Another positive side effect is you Charlotte, you were the first person I talked to about pursuing a PhD. We'll leave out the details, but I'm thankful for your support throughout these years. Knowing that you're proud of me now that I've completed it means a lot to me!

My special colleagues and friends, Patty and Chen, it has been quite a roller-coaster ride, and I've thoroughly enjoyed sharing it with both of you! Patty, being born on the same day, we share so much in common, making our connection so effortless. I am so grateful to have had you by my side for the last stretch. Your unwavering support and encouragement have meant the world to me. You are truly the most considerate and selfless person I know. Chen, thank you so much for always showing support for me. I admire your optimism and the way you've organized your life. I'm hoping you can impart some of that wisdom, perhaps during our upcoming trip to Japan as we continue to plan

our post-PhD dreams ;) Dear Patty and Chen, I treasure our friendship and eagerly anticipate many more coffee sessions and delicious meals as we reflect on life together.

I'd like to extend my gratitude to all the wonderful children who participated in my research. I initially thought measuring you might be a challenging task, but it turned out to be anything but. Your curiosity and openness to new experiences made the measurements a pleasure. I'd also like to thank the schools that played a crucial role in recruiting the children and opening their doors for the measurements. CBS Ackerweide, Deltse Montessori School, Mariaschool, Het Spectrum, and Anke, thank you for facilitating contact with your school and helping with logistical planning. A big thank you to all the TU Delft colleagues who participated with their children in the research. Also, my appreciation goes to JGZ Zuid-Holland West, particularly Karin Verheijen, for their invaluable assistance in organizing our presence at various JGZ locations.

Throughout various stages of my research, several students have contributed to the project. Veerle, Joeri, Matthijs, the AED Team Flow (Emilie, Sahil, Linde, Mark, Romee, Marjolein), and Jip, your work was indispensable, and your dedication and passion for the topic were truly inspiring to me. I want to extend special thanks to Mathijs; it's thanks to you that we were able to carry out the final study.

Furthermore, I had the pleasure of being a part of one of the nicest sections of the faculty. I'd like to extend my gratitude to all my AED colleagues for the camaraderie, stimulating discussions, and the open atmosphere we shared. A special thanks goes out to Sonja, who was the first to introduce me to the world of research at IO. Marijke, you provided me with the opportunity to further develop as a teacher, allowing me to rediscover my passion for medical design. I did this with great pleasure, and it was a welcomed distraction alongside my thesis work. Daan, it's largely thanks to you that I've been able to channel and further develop my experience and knowledge within the UPPS projects. I never anticipated I'd be heading in a direction so closely aligned with my PhD research. Together with the kidsCAN project, it feels like all the pieces of the puzzle are coming together. I greatly appreciate the trust and the room you've afforded me to complete my thesis.

I consider myself incredibly fortunate to be a part of the Studiolab community. This diverse and vibrant group of people, the countless coffee corner chats, lunches at the picnic table, dinners, and parties have all infused me with so much energy over the years. Aadjan and Ianus, thank you for creating such an incredible workspace.

I'd also wish to thank Martin for the nice random chats, and Haian, Siyuan, Cehao for sharing your food and thoughts with me, Xueliang, for your support and numerous amazing sketches, Abhigyan, Maria Luce, Froukje, Susanne, Stella, Valentijn, Natalia, Marina, Susanne, Nico, Tomasz, Deger, Caiseal, Evert, Iohanna, Anna, Mahan,

Zhuochao, Eliv, Tingting, Adriaan, Nynke, Marieke, Nazli, Timothy, Marco, Alev, Dajung, Willem, Sam, Paula, Hannah, Laura, Razieh, Jasper, Charlie, and Pepper, you've all brought positive vibes and made my journey richer. And to the former Studiolabbers, Hester, Makiko, Berit, Marian, Mailin, Lenny, Anna, Fenne, Marierose, Bob, Tessa, Steven, thank you for the wonderful conversations. Others within the faculty, Daphne, Denise, Jessica, and Amanda, your patience and willingness to assist me during my numerous visits and questions over the years have been greatly appreciated. Helen, Wolf, Maxim, Farzam, JC, Duygu, Matthijs, and the many others whose names escape me at the moment, thank you for all the pleasant chats during our shared research and teaching journeys! Thanks also to Cecile, Annemarie and Ana-Laura, for sharing the first steps in research at this faculty and how we tackled the challenges and celebrated the joys of being new moms while juggling our research commitments.

Liefste familie, broer en schone zus, dank voor jullie aanmoedigingen gedurende al die jaren. Vaak gepaard met de heerlijkste maaltijden. Zelfs in de moeilijkere tijden, met de drukte van vier kinderen, waren jullie altijd bereid om te helpen en mee te denken over zowel de emotionele als praktische kanten van het leven. Lieve Yuna en Maeko, zonder dat jullie je het echt realiseren zijn jullie mijn muzes voor dit werk. Dank jullie wel voor jullie mooie kopjes ;)

Lieve Frans en Heleen, dank jullie wel voor alles. Jullie steun hebben mijn PhD-reis mede mogelijk gemaakt, en dat waardeer ik enorm. Jullie zijn de beste opa en oma die de kindjes maar kunnen wensen.

Lieve Mam, zonder jou was ik nooit zo ver gekomen. Jouw onvoorwaardelijke liefde en zorg (ook voor Alex en de kleintjes), ik ben je zo dankbaar. Het is zo fijn om jou dichtbij te hebben. Dit is nu af, één zorg minder ;)

Lieve Yuki en Kenta, eindelijk is het klaar! Jullie kusjes en ontelbare knuffels hebben me super veel kracht gegeven om door te gaan en door te zetten. Ik kijk er zo naar uit om proefschrift-vrije weekendjes en gezellige avondjes met jullie te hebben.

Liefste Alex, jij hebt zo'n belangrijke rol gespeeld, bedankt voor jouw oneindige geduld. Jij bent mijn personal coach, sparringpartner, editor, co-author, super househusband, maar vooral mijn rots in de branding en de beste vriend die ik me kan wensen. Ik ben je ontzettend veel verschuldigd, zonder jou zou het nooit zijn gelukt.

ABOUT THE AUTHOR

Lyè Goto was born in The Hague, the Netherlands. In 2007, Lyè obtained her Industrial Design Engineering Master's degree with a specialisation in the design of medical products (Medisign). Her thesis involved designing a universal backpack for people who depend on enteral feeding. Here, Lyè got her first real taste of Design for Healthcare which really sparked her curiosity for the medical field further. After working at the marketing department of Olympus Medical Systems and as a freelance graphic designer she came to realise that she wanted to be more closely involved in the product development process of healthcare innovations and especially on the research side. In 2010, she became a researcher on the Laparoscopic Surgery Skills Programme for the European Association for Endoscopic Surgery. In 2012, she started her PhD at Delft University of Technology at the department Human-Centred-Design. Her research focusses on the integration of 3D Anthropometric data of children's heads and faces into the design of a ventilation mask. In 2017, she started a position as a part-time teacher at the department of Human Centred Design where she was mainly involved in courses for the master's specialization of Medisign. Starting 2022 she is working as a researcher for the Ultra Personalized Products project (http://www.upps.nl/en/) whereby she coordinates projects together with companies interested in this field, and the KidsCAN project (http://kidscan.tudelft.nl) which will run for the next two years with the goal of measuring and 3D scanning 1800 children between the ages of 0 and 16 year olds in the Netherlands as part of a larger European Project.

LIST OF PUBLICATIONS

Poot, C.C., de Boer J., **Goto L.**, van de Hei, S.J., Chavannes, N.H., Visch, V.T., Meijer, E. (in press). The design of a persuasive game to motivate people with asthma in adherence to their maintenance medication. *Patient Preference and Adherence.*

Hovenier, R., **Goto, L.**, Huysmans, T., van Gestel, M., Klein-Blommert, R., Markhorst, D., Dijkman, C., Bem, R.A., 2022. Reduced Air Leakage During Non-Invasive Ventilation Using a Simple Anesthetic Mask With 3D-Printed Adaptor in an Anthropometric Based Pediatric Head–Lung Model. *Frontiers in Pediatrics* 10. https://doi.org/10.3389/fped.2022.873426

Goto, L., Lee, W., Huysmans, T., Molenbroek, J. F. M., & Goossens, R. H. M. (2021). The Variation in 3D Face Shapes of Dutch Children for Mask Design. *Applied Sciences* 2021 (1).

Goto, L., Lee, W., Molenbroek, J. F. M., Cabo, A. J., & Goossens, R. H. M. (2019). Traditional and 3D Scan Extracted Measurements of the Heads and Faces of Dutch Children. *International Journal of Industrial Ergonomics*, 73. https://doi.org/10.1016/j.ergon.2019.102828

Goto, L., Huysmans, T., Lee, W., Molenbroek, J. F. M., & Goossens, R. H. M. (2019). A Comparison Between Representative 3D Faces Based on Bi- and Multi-variate and Shape Based Analysis. *Proceedings of the 20th Congress of the International Ergonomics Association (IEA 2018) Volume VII. Vol. 824*. 1355–1364. https://doi.org/10.1007/978-3-319-96071-5_137

Goto, L., Lee, W., Song, Y., Molenbroek, J. F. M., & Goossens, R. H. M. (2015). Analysis of a 3D Anthropometric Data Set of Children for Design Applications. *Proceedings 19th Triennial Congress of the International Ergonomics Association* (IEA 2015). Melbourne.

Goto, L., Molenbroek, J. F. M., & Goossens, R. H. M. (2013). 3D Anthropometric Data Set of the Head and Face of Children Aged 0.5-7 Years for Design Applications. *In N D'Apuzzo (Ed.), Proceedings of the 4th International Conference on 3D Body Scanning Technologies* Ascona, Switzerland: Hometrica Consulting. 157–165. https://doi.org/10.15221/13.157

Huysmans, T., **Goto, L.,** Molenbroek, J. F. M., & Goossens, R. H. M. (2021). Dined Mannequin: an Open Platform for 3D Anthropometry. *Tijdschrift Voor Human Factors*, 45(1).

Lee, W., **Goto, L**., Molenbroek, J. F. M., & Goossens, R. H. M. (2017). Analysis Methods of the Variation of Facial Size and Shape based on 3D Face Scan Images. *Proceedings of the Human Factors and Ergonomics Society*, 2017. 1409–1413. https://doi.org/10.1177/1541931213601836

Lee, W., **Goto, L**., Molenbroek, J. F. M., Goossens, R. H. M., & Wang, C. C. C. (2017). A Shape-based Sizing System for Facial Wearable Product Design. In S. Wischniewski, D. Bonin, & T. Alexander (Eds.), *Proceedings of the 5th International Digital Human Modeling Symposium.* 150–158. Federal Institute for Occupational Safety and Health.

Molenbroek, J.F.M. & **Goto, L**. (2016), The Application of 3D Scanning as an Educational Challenge. *Proceedings of the 19th Triennial Congress of the IEA*. Lindgaard, G. & Moore, D. (eds.). International Ergonomics Association. 1–77.

Lee, W., Yang, X., Jung, H., You, H., **Goto, L.**, Molenbroek, J. F. M., Goossens, R.H.M. (2016). Application of Massive 3D Head and Facial Scan Datasets in Ergonomic Head-Product Design. *International Journal of the Digital Human*, 1(4). 344. https://doi.org/10.1504/ijdh.2016.10005368

Book chapters

Lee, W., Molenbroek, J. F. M., **Goto, L**., Jellema, A., Song, Y., & Goossens, R. H. M. (2019). Application of 3D scanning in design education. S. Scataglini & G. Paul (Eds.), *DHM and Posturography*. 721–731. Elsevier. https://doi.org/10.1016/B978-0-12-816713-7.00056-8

de Bruin, R., Molenbroek, J. F. M., & **Goto, L.** (2016). Past het niet, print het dan! Kinderbeademingsmaskers dankzij 3D-Technologie. I. Geesink, M. Heerings, & S. van Egmond (Eds.). *De Meetbare Mens.* 109–127. Den Haag: Rathenau Instituut.

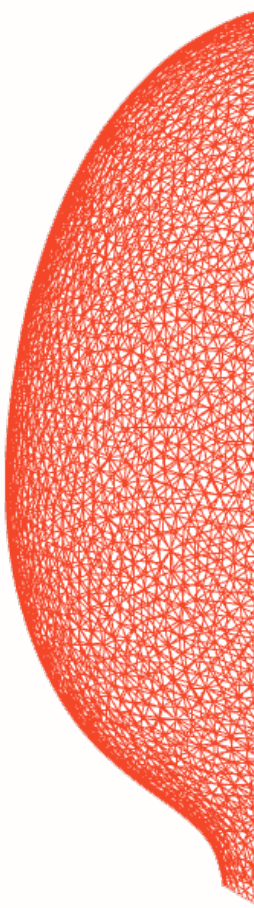

TU Delft Delft University of Technology